U.S. DEPARTMENT OF COMMERCE
National Technical Information Service

PB-260 586

Particulate Collection Study EPA/TVA Full-Scale Dry Limestone Injection Tests

Cottrell Environmental Systems, Inc, Bound Brook, N J

Prepared for

National Environmental Research Center, Research Triangle Park, N C
Control Systems Lab

Jun 74

327106

EPA-650/2-74-053

JUNE 1974

PB 260 586

Environmental Protection Technology Series

PARTICULATE COLLECTION STUDY, EPA/TVA FULL-SCALE DRY LIMESTONE INJECTION TESTS

REPRODUCED BY
NATIONAL TECHNICAL
INFORMATION SERVICE
U. S. DEPARTMENT OF COMMERCE
SPRINGFIELD, VA. 22161

Office of Research and Development
U.S. Environmental Protection Agency
Washington, DC 20460

20

BIBLIOGRAPHIC DATA SHEET

1. Report No. EPA-650/2-74-053

2.

3. Recipient's Accession No.

4. Title and Subtitle
Particulate Collection Study EPA/TVA Full-Scale
Dry Limestone Injection Tests

5. Report Date June 1974

6.

7. Author(s)
R. F. Brown

8. Performing Organization Rept. No.

9. Performing Organization Name and Address
Cottrell Environmental Systems, Inc.
Division of Research-Cottrell, Inc.
Bound Brook, N.J.

10. Project/Task/Work Unit No.

11. Contract/Grant No.
CPA 22-69-139

12. Sponsoring Organization Name and Address
U.S. Environmental Protection Agency
Office of Research and Development
Washington DC

13. Type of Report & Period Covered

14.

15. Supplementary Notes
Environmental Protection Technology Series

16. Abstracts

A particulate control system consisting of a mechanical cyclone-electrostatic precipitator combination has been evaluated on a full-scale boiler without and with limestone injection (dry) into the boiler for sulfur oxide removal. The main objective of the study was to determine the effects of dry additive injection on the particulate control equipment and evaluate system modification alternatives including a cost benefit analysis that will maintain stack particulate emissions with injection equivalent to about 2.8% sulfur and 15.5% ash coal-firing without injection.

17. Key Words and Document Analysis. 17a. Descriptors

17b. Identifiers/Open-Ended Terms

17c. COSATI Field/Group

18. Availability Statement

19. Security Class (This Report) UNCLASSIFIED

20. Security Class (This Page UNCLASSIFIED

21. No. of Pages 209

22. Price $7.75-3.00

EPA-650/2-74-053

PARTICULATE COLLECTION STUDY, EPA/TVA FULL-SCALE DRY LIMESTONE INJECTION TESTS

by

R.F. Brown

Cottrell Environmental Systems, Inc.
Division of Research-Cottrell, Inc.
P. O. Box 750
Bound Brook, N. J. 08805

Contract No. CPA 22-69-139
ROAP No. 21ACY-16
Program Element No. 1AB013

EPA Project Officer: R.D. Stern

Control Systems Laboratory
National Environmental Research Center
Research Triangle Park, North Carolina 27711

Prepared for

OFFICE OF RESEARCH AND DEVELOPMENT
U.S. ENVIRONMENTAL PROTECTION AGENCY
WASHINGTON, D.C. 20460

June 1974

This report has been reviewed by the Environmental Protection Agency and approved for publication. Approval does not signify that the contents necessarily reflect the views and policies of the Agency, nor does mention of trade names or commercial products constitute endorsement or recommendation for use.

ABSTRACT

A particulate control system consisting of a mechanical cyclone-electrostatic precipitator combination has been evaluated on a full-scale boiler without and with limestone injection (dry) into the boiler for sulfur oxide removal.

The main objective of the study was to determine the effects of dry additive injection on the particulate control equipment and evaluate system modification alternatives including a cost benefit analysis that will maintain stack particulate emissions with injection equivalent to about 2.8% sulfur and 15.5% ash coal-firing without injection.

Two separate test programs by Cottrell Environmental Systems were conducted, one in December, 1969 which quantified the collection system on coal-firing only to serve as a performance baseline and the other in July, 1971 in which coal sulfur and flue gas temperature, along with limestone particle size and amount injected were studied at two levels. A third more comprehensive test program without limestone injection by the Tennessee Valley Authority in the summer of 1970 has been used to establish the baseline conditions for the electrostatic precipitator and boiler flue gas. Mechanical collector performance did not vary substantially whether fly ash alone was collected or in combination with coarse or fine limestone. Efficiencies measured were in the 50 to 60% range depending upon pressure loss across the collector. Therefore, the overall efficiency of the dust collection equipment was a significant function of the precipitator performance and inlet loading only. In general, as expected, the electrostatic precipitator performance was adversely affected by limestone injection. It was found that the precipitation rate parameter without and with limestone injection was mainly a function of corona power density input, and that the power level and therefore the performance reached without excessive sparking was lower in the limestone injection cases.

The average particulate emission rate and flue gas conditions found on #10 boiler at Shawnee Station of TVA with the presently installed dust collection equipment were 412 lbs/hr and 570,000 cfm at 309°F. Cost estimates for size modification to the presently installed precipitator to maintain baseline emission with limestone injection have been considered for flue gas temperatures into the precipitator of 250 and 309. Other options such "hot" precipitator, gas

conditioning and precipitator energization modifications have been discussed but since actual performance data for these alternatives was beyond the scope of this experimental program, only speculative comments have been made as to expected results. For coarse limestone injection, the present precipitator on boiler #10 at 309F would have to be increased in size about 45% in order to maintain the desired emission level stipulated above. If it is feasible to reduce the gas temperature to about 250F, the size increase required would only be 17%. On the other hand with fine limestone injection, the size increases at 309 and 250F would be 225% and 56% respectively.

For the grassroots plant, the evaluation shows a cold precipitator (250F) as the best option on a cost basis.

SUMMARY

The Environmental Protection Agency is sponsoring a variety of programs to develop technically feasible and economic means for removing sulfur oxides from stack gases of fossil fuel-fired boilers. One such means is the injection of dry limestone into the hot gas zone of the boiler where the gaseous sulfur oxides react with the finely dispersed additive to form solid sulfur-additive compounds which can be removed from the flue gas in mechanical and/or electrostatic precipitator collectors.

This report presents solid collection system performance results obtained from 37 test runs on a full-scale plant firing pulverized coal and having a dry additive injection system. The major variables studied include flue gas temperature into the dust collecting equipment, coal sulfur, and additive stoichiometry and particle size. Two levels of each variable were investigated. These tests and data from other pertinent sources have been analyzed and correlated. The results are summarized as follows:

(1) The performance of the mechanical collector was relatively insensitive to all test conditions of injection or non-injection ranging between 50 and 60% efficiency. On the other hand, the overall efficiency of the dust collection system varied broadly between 72 and 99% depending significantly on the electrostatic precipitator performance. Without limestone injection, flue gas temperature and volume, and coal sulfur were the critical variables while with injection, the particle size of the additive was another important parameter.

(2) The precipitation rate parameter was a significant semi-logrithmic function of the corona power input density.

$W = 0.47+0.16\ln P_A$ (No Injection)

$W = 0.52+0.12\ln P_A$ (Coarse Additive Injection)

$W = 0.46+0.14\ln P_A$ (Fine Additive Injection)

where,

W = precipitation rate parameter (FPS)

P_A = corona power input density (kilowatts/1000 ft^2 of collecting surface)

In general, the precipitator performance was poorer with limestone injection because the maximum corona input power density attainable was lower, particularly when fine limestone was injected.

(3) A correlation of use in sizing electrostatic precipitators was found by examining the affects of the parameters of limestone particle size, flue gas temperature, coal sulfur and limestone injection rate on corona power input density. The correlation resulted in the following equations:

(coarse)

$$P_A = -1.435 - 0.336S + \frac{10.0}{L} + \frac{3.87}{T}$$

(fine)

$$P_A = -0.990 + 0.199S - \frac{0.694}{L} + \frac{2.74}{T}$$

where,

S = coal sulfur fired (tons/hr)

L = limestone injected (tons/hr)

T = flue gas temperature ($°F \times 10^{-2}$)

By use of these equations and the correlation between precipitation rate parameter and power density shown above, and standard design equations, it is possible to size a precipitator within the following limiting conditions:

Coal Sulfur Fired (S)
1.0 to 3.2 tons/hr

Limestone Feedrate (L)
5.3 to 16.8 tons/hr.

Flue Gas Temperature (T)
$(240 \text{ to } 315)(10^{-2})°F$.

Stoichiometry 0.28(L/S) = 1.0 to 4.0

(4) Mechanical collector fractional efficiency curves based on Bahco analysis of collected samples for fly ash ash alone and fly ash plus additive reaction products were essentially the same ranging from 25% on the 5 micron size to 90 to 95% on the greater than 25 micron size. However,

the electrostatic precipitator fractional efficiency curve on fly ash alone was nearly constant over a particle size range from 2 to 30μ, i.e. 80 to 90%. With limestone injection, the electrostatic precipitator showed decreasing collection efficiency as particle size increased. The fly ash alone had an average mean size by weight of 19 microns at the mechanical collector inlet while with both coarse and fine limestone injection, the mean size was about 9 microns.

The average particulate loading at the mechanical outlet-precipitator inlet varied linearly with limestone injection rate ranging from 1.5 grains per scf at 0 feedrate to about 4.0 grains at 16 tons/hr.

(5) Laboratory particle resistivity measurements, in general, were higher than in-situ resistivities on samples from the same test both with and without limestone injection.

The criticality of coal sulfur and moisture on particle resistivity was verified by in-situ measurements without limestone injection, particularly at the lower gas temperatures.

With limestone injection, the effect of sulfur appeared to be random, but moisture conditioning at lower temperatures was still evident.

(6) The precipitation rate parameter degradation as a function of particle resistivity was demonstrated. However, the critical range of resistivity seemed to be occurring in the 10^{11} to 10^{13} ohm-cm range which is somewhat higher than published figures. A possible explanation is the "in-situ" resistivity measuring technique.

(7) There was no obvious correlation between the chemical composition of the particulate and the performance of the precipitator.

(8) An optical sensor installed on the precipitator outlet duct provided a good qualitative indication of boiler and dust collecting equipment operation. There appeared to be a linear relationship between outlet particulate loading and sensor output voltage. However, the necessity for maintaining clean lenses was evident.

(9) Using a baseline of 412 pounds emitted/hr and 570,000 cfm of flue gas at 309F, estimated costs of the fly ash only electrostatic precipitator (installed) at 309F was compared with one at 600F. In addition, size modifications and costs for electrostatic precipitators with coarse and fine limestone injection (2 x stoichiometry) were compared at 250, 309, and 600F.

The following summarizes the results:

Electrostatic Precipitator Cost and Size Factors		250F*	309F*	309F**	600F**	(See pgs. 171 and 172)
Cost Installed	($/Kilowatt)					
No	Injection	-	2.21	2.99	5.85	
Coarse	Injection	2.58	3.21	3.95	7.10	
Fine	Injection	3.44	7.20	8.89	7.10	
Size Factor	(x no injection at 309F = 1.0)					
No	Injection	-	1.0	1.35	2.44	
Coarse	Injection	1.17	1.45	1.79	2.96	
Fine	Injection	1.56	3.25	4.02	2.96	

* Follows Mechanical Collector
** Straight Precipitator

Coarse limestone at a flue gas temperature around 250F emerged as the best alternative for the limestone injection cases when only considering precipitator size modification.

However, the present Shawnee boiler flue gas is about 300F and would require cooling in order to take advantage of the 250F result. This added cost could offset the difference between coarse limestone at 309F at $3.21/KW and $2.59/KW at 250F. With fine limestone injection, the precipitator size requirements at 250F are still at a minimum but as above, extra cost for gas cooling would be required. With fine limestone injection, the requirements at 309F and 600F are for all practical purposes equivalent.

It is of interest to compare a straight hot precipitator at 600F with a straight 309F precipitator on fine limestone injection.

The size factors are 2.96 and 4.02 respectively with the installed $/KW being $7.10 and $8.89 respectively. Clearly, the hot precipitator is advantageous for this case.

TABLE OF CONTENTS

page

TITLE PAGE i
ABSTRACT iii
SUMMARY v

I. INTRODUCTION 1
II. TECHNICAL APPROACH 3
III. TEST METHODS 6
  1. Gas Velocity Measurements 6
  2. Moisture Content 7
  3. Particulate Sampling 8
  4. Test Sections 11
  5. In-Situ Resistivity 13
  6. Laboratory Resistivity 13
  7. Skeletal or True Density 22
  8. Particle Size 24
  9. Stack Opacity 26
  10. Coal Analysis 26
IV. TEST CONDITIONS AND PROCEDURES 28
V. TEST RESULTS AND SAMPLE ANALYSES 38
  1. Test Data 38
  2. Coal Analyses 38
  3. Particle Size Analyses 39
  4. Resistivities 39
  5. Chemical Analyses 39
VI. ANALYSIS AND DISCUSSION OF TEST RESULTS 70
  1. Electrostatic Precipitator Performance 70
    A. Theoretical Considerations of Electrostatic Performance As A Function of Corona Power . . 72
    B. Correlation of Precipitator Performance With Corona Power Input 77
    C. Correlation of Precipitator Corona Power Input With Process Variables 91
  2. Performance of The Combination Mechanical-Electrostatic Dust Collector 97
    A. Correlation of Particle Size And Dust Collector Performance 99
  3. Discussion of Particle Resistivity Data 129
    A. Correlation of In-Situ And Laboratory Measurements 129
    B. Relationship of Particle Resistivity, Flue Gas Temperature, and Coal Sulfur (No Limestone Injection) 140
    C. Relationship of Particle Resistivity, Flue Gas Temperature, and Coal Sulfur (With Limestone Injection) 140
    D. Relationship Between Precipitation Rate Parameter and Particle Resistivity 143

TABLE OF CONTENTS (Continued)

page

4. Discussion of Chemical Analyses Results 147
   - A. Relationship of Calcium Compounds at Electrostatic Precipitator Inlet With Limestone Feedrate 147
   - B. Examination of Particle Resistivity At The Precipitator Inlet As A Function of Calcium Oxide/Sulfur Ratio for High and Low Temperature Flue Gas 151

5. Review of Optical Sensor Data 153

VII. TECHNO-ECONOMIC EVALUATION OF VARIOUS ALTERNATIVES FOR MAINTAINING THE STACK EMISSION RATE WITH LIMESTONE INJECTION EQUIVALENT TO A BASELINE CONDITION OF NO LIMESTONE INJECTION 166

1. Size Modification of The Presently Installed Dust Collecting System 168
2. Installation of A "Hot" Precipitator 171
3. Gas Cooling Ahead of The Dust Collection System . . 173
4. Gas Conditioning Ahead of The Dust Collecting System 173
5. Electrical Energization of The Precipitator 175

VIII. RECOMMENDATIONS 184

BIBLIOGRAPHY 186

TECHNICAL DATA/ABSTRACT SHEET. 188

TABLE OF CONTENTS (Continued)

LIST OF FIGURES

page

FIGURE 1 - EQUIPMENT FOR MAKING GAS VELOCITY MEASUREMENTS AND TAKING PARTICULATE SAMPLES 9

FIGURE 2 - SCHEMATIC DIAGRAM OF BOILER #10 SHAWNEE STATION, TVA 12

FIGURE 3 - DETAILS OF MECHANICAL COLLECTOR INLET SAMPLING STATION 14

FIGURE 4 - DETAILS OF MECHANICAL COLLECTOR OUTLET - ELECTROSTATIC PRECIPITATOR INLET SAMPLING STATION 15

FIGURE 5 - DETAILS OF ELECTROSTATIC PRECIPITATOR OUTLET SAMPLING STATION 16

FIGURE 6 - IN-SITU RESISTIVITY APPARATUS 17

FIGURE 7 - POINT-PLANE RESISTIVITY CELL 18

FIGURE 8 - LABORATORY RESISTIVITY MEASURING APPARATUS . . . 19

FIGURE 9 - SCHEMATIC DIAGRAM OF LABORATORY RESISTIVITY MEASURING APPARATUS 20

FIGURE 10 - CROSS-SECTION DIAGRAM OF MEASURING CELL USED IN LABORATORY RESISTIVITY APPARATUS 21

FIGURE 11 - SCHEMATIC OF ELECTRIC CIRCUIT FOR LABORATORY RESISTIVITY APPARATUS 21

FIGURE 12 - APPARATUS FOR MEASURING SKELETAL OR TRUE DENSITY OF PARTICULATE 23

FIGURE 13 - BAHCO CENTRIFUGAL PARTICLE CLASSIFIER 25

FIGURE 14 - FUNCTIONAL DIAGRAM OF THE OPTICAL SENSOR 27

FIGURE 15 - SCHEMATIC DIAGRAM OF ELECTROSTATIC PRECIPITATOR ARRANGEMENT AND ELECTRICAL HOOK-UP 29

FIGURE 16 - REPRESENTATIVE TEMPERATURE AND VELOCITY TRAVERSE AT THE MECHANICAL COLLECTOR INLET ("B" SIDE) 33

FIGURE 17 - REPRESENTATIVE TEMPERATURE AND VELOCITY TRAVERSE AT THE MECHANICAL COLLECTOR OUTLET - PRECIPITATOR INLET SAMPLE STATION ("B" SIDE) . . 34

FIGURE 18 - REPRESENTATIVE TEMPERATURE AND VELOCITY TRAVERSE AT THE PRECIPITATOR OUTLET SAMPLING STATION ("B" SIDE) 35

FIGURE 19 - PRECIPITATION RATE PARAMETER AS A FUNCTION OF CORONA POWER DENSITY FOR TESTS WITHOUT LIMESTONE INJECTION 78

TABLE OF CONTENTS (Continued)

LIST OF FIGURES

page

FIGURE 20 - COMPARISON OF DATA FROM FIGURE 19 WITH PUBLISHED DATA OF SOUTHERN RESEARCH INSTITUTE FOR VARIOUS FLY ASH PRECIPITATOR INSTALLATIONS - REF. (11) 82

FIGURE 21 - LOSS IN COLLECTION EFFICIENCY AS A FUNCTION OF POWER RATE FOR TESTS WITHOUT LIMESTONE INJECTION 84

FIGURE 22 - COMPARISON OF DATA FROM FIGURE 21 WITH PUBLISHED DATA OF SOUTHERN RESEARCH INSTITUTE FOR VARIOUS FLY ASH PRECIPITATOR INSTALLATIONS - REF. (11) 85

FIGURE 23 - PRECIPITATION RATE PARAMETER AS A FUNCTION OF CORONA POWER DENSITY FOR TESTS WITH LIMESTONE INJECTION 87

FIGURE 24 - LOSS IN COLLECTION EFFICIENCY AS A FUNCTION OF POWER RATE FOR TESTS WITH LIMESTONE INJECTION 89

FIGURE 25 - PRECIPITATION RATE PARAMETER AS A FUNCTION OF POWER DENSITY FOR TESTS WITH LIMESTONE INJECTION (GAS TEMPERATURE AND LIMESTONE PARTICLE SIZE ARE IDENTIFIED SEPARATELY). . . . 92

FIGURE 26 - PARTICLE SIZE ANALYSES OF LIMESTONE FEED SAMPLES USED IN SECOND CES TEST SERIES 95

FIGURE 27 - PARTICLE SIZE ANALYSES OF MECHANICAL COLLECTOR INLET SAMPLES WITHOUT LIMESTONE INJECTION (TESTS 1A, 1B, 3A, 4A, 5A, 5B). . . . 101

FIGURE 28 - PARTICLE SIZE ANALYSES OF ELECTROSTATIC PRECIPITATOR INLET SAMPLES WITHOUT LIMESTONE INJECTION (TESTS 3A, 4A, 4B, 5A, 5B) 102

FIGURE 29 - PARTICLE SIZE ANALYSES OF ELECTROSTATIC PRECIPITATOR OUTLET SAMPLES WITHOUT LIMESTONE INJECTION (TESTS 2A, 3A, 3B, 4B). 103

FIGURE 30 - PARTICLE SIZE ANALYSES OF MECHANICAL HOPPER SAMPLES WITHOUT LIMESTONE INJECTION (TESTS 1A, 1B, 2A, 3A, 4A, 5A, 5B) 104

FIGURE 31 - PARTICLE SIZE ANALYSES OF ELECTROSTATIC PRECIPITATOR HOPPER SAMPLES WITHOUT LIMESTONE INJECTION (TESTS 1A, 1B, 2A, 3A, 4A, 5A, 5B). . 105

TABLE OF CONTENTS (Continued)

LIST OF FIGURES

page

FIGURE 32 - PARTICLE SIZE ANALYSES OF ELECTROSTATIC PRECIPITATOR INLET SAMPLES WITHOUT LIMESTONE INJECTION (TESTS 16, 19, 20, 21, 22) 106

FIGURE 33 - PARTICLE SIZE ANALYSES OF ELECTROSTATIC PRECIPITATOR HOPPER SAMPLES WITHOUT LIMESTONE INJECTION (TESTS 16, 21, 22) 107

FIGURE 34 - PARTICLE SIZE ANALYSES MECHANICAL COLLECTOR INLET SAMPLES WITH COARSE LIMESTONE INJECTION (TESTS 14, 15, 32, 33) 108

FIGURE 35 - PARTICLE SIZE ANALYSES OF ELECTROSTATIC PRECIPITATOR INLET SAMPLES WITH COARSE LIMESTONE INJECTION (TESTS 10, 11, 14, 15, 25, 32, 33). 109

FIGURE 36 - PARTICLE SIZE ANALYSIS OF ELECTROSTATIC PRECIPITATOR OUTLET SAMPLES WITH COARSE LIMESTONE INJECTION (TESTS 11, 14) 110

FIGURE 37 - PARTICLE SIZE ANALYSES OF MECHANICAL COLLECTOR HOPPER SAMPLES WITH COARSE LIMESTONE INJECTION (TESTS 14, 15, 32, 33) 111

FIGURE 38 - PARTICLE SIZE ANALYSES OF ELECTROSTATIC PRECIPITATOR HOPPER SAMPLES WITH COARSE LIMESTONE INJECTION (TESTS 14, 15) 112

FIGURE 39 - PARTICLE SIZE ANALYSES OF MECHANICAL COLLECTOR INLET SAMPLES WITH FINE LIMESTONE INJECTION (TESTS 2, 3, 5, 6, 8). 113

FIGURE 40 - PARTICLE SIZE ANALYSES OF ELECTROSTATIC PRECIPITATOR INLET SAMPLES WITH FINE LIMESTONE INJECTION (TESTS 2, 3, 4, 5, 6, 8, 17, 18, 23, 24, 26, 27, 28, 29, 30) 114

FIGURE 41 - PARTICLE SIZE ANALYSES OF ELECTROSTATIC PRECIPITATOR OUTLET SAMPLES WITH FINE LIMESTONE INJECTION (TESTS 2, 3, 4, 5, 6, 23, 24, 26). 115

FIGURE 42 - PARTICLE SIZE ANALYSES OF MECHANICAL COLLECTOR HOPPER SAMPLES WITH FINE LIMESTONE INJECTION (TESTS 2, 3, 5, 6, 8). 116

TABLE OF CONTENTS (Continued)

LIST OF FIGURES

page

FIGURE 43 - PARTICLE SIZE ANALYSIS OF ELECTROSTATIC PRECIPITATOR HOPPER SAMPLES WITH FINE LIMESTONE INJECTION (TESTS 17, 18, 23, 24) . . . 117

FIGURE 44 - FRACTIONAL EFFICIENCY CURVE FOR MECHANICAL COLLECTOR 122

FIGURE 45 - FRACTIONAL EFFICIENCY CURVES FOR ELECTROSTATIC PRECIPITATOR 123

FIGURE 46 - ELECTROSTATIC PRECIPITATOR PARTICULATE INLET LOADING AS A FUNCTION OF LIMESTONE FEEDRATE . . 128

FIGURE 47 - IN-SITU RESISTIVITIES OBTAINED ON FULL-SCALE AND PILOT SCALE PULVERIZED COAL-FIRING BOILERS WITHOUT LIMESTONE INJECTION 131

FIGURE 48 - IN-SITU RESISTIVITIES OBTAINED ON FULL SCALE AND PILOT SCALE PULVERIZED COAL FIRING BOILERS WITH LIMESTONE INJECTION 132

FIGURE 49 - IN-SITU RESISTIVITY DATA OBTAINED BY K.J. McLEAN AT TVA SHAWNEE STATION, BOILER #10 DURING THE CES SECOND TEST SERIES 134

FIGURE 50 - RESISTIVITY OF FLY ASH SAMPLES FROM VARIOUS COALS FIRED IN PILOT PLANT OF B&W 136

FIGURE 51 - IN-SITU AND LABORATORY RESISTIVITIES FOR REACTED ADDITIVE-FLY ASH SAMPLES FROM B&W PILOT PLANT 136

FIGURE 52 - IN-SITU AND LABORATORY RESISTIVITIES FOR REACTED ADDITIVE-FLY ASH MIXTURES FROM B&W PILOT PLANT 137

FIGURE 53 - IN-SITU AND LABORATORY RESISTIVITIES FOR REACTED ADDITIVE-FLY ASH MIXTURES FROM B&W PILOT PLANT 137

FIGURE 54 - LABORATORY RESISTIVITY MEASUREMENTS OF PRECIPITATOR INLET SAMPLES AS A FUNCTION OF GAS TEMPERATURE WITHOUT LIMESTONE INJECTION . . 138

FIGURE 55 - LABORATORY RESISTIVITY MEASUREMENTS ON PRECIPITATOR INLET SAMPLES AS A FUNCTION OF GAS TEMPERATURE WITH LIMESTONE INJECTION 139

FIGURE 56 - IN-SITU RESISTIVITY VS. TEMPERATURE RELATIONSHIP FOR VARIOUS COAL SULFUR (NO LIMESTONE INJECTION) 142

TABLE OF CONTENTS (Continued)

LIST OF FIGURES

page

FIGURE 57 - IN-SITU RESISTIVITY VS. TEMPERATURE RELATIONSHIP FOR VARIOUS COAL SULFURS (WITH LIMESTONE INJECTION) 144

FIGURE 58 - APPROXIMATE PRECIPITATION RATE PARAMETER VS. RESISTIVITY RELATIONSHIP WITHOUT AND WITH LIMESTONE INJECTION 145

FIGURE 59 - CALCIUM OXIDE AT ELECTROSTATIC INLET AS A FRACTION OF LIMESTONE FEEDRATE TO THE BOILER . . 150

FIGURE 60 - PARTICLE RESISTIVITY AS A FUNCTION OF THE CaO/S RATIO AT THE PRECIPITATOR INLET 152

FIGURE 61 - SIMPLIFIED SYSTEM DIAGRAM OF THE RESEARCH COTTRELL, INC. PROPRIETARY OPTICAL SENSOR . . . 154

FIGURE 62 - DATA OBTAINED ON PARTICULATE LOADING USING AN OPTICAL MONITOR 157

FIGURE 63 - TYPICAL OPTICAL SENSOR CHART ON SHAWNEE #10 BOILER ("B" SIDE) WITH AND WITHOUT LIMESTONE INJECTION 159

FIGURE 64 - TYPICAL PRECIPITATOR VOLTAGE VS. CURRENT CHARACTERISTIC 177

FIGURE 65 - TYPICAL PRECIPITATOR ENERGIZATION ARRANGEMENTS . 182

TABLE OF CONTENTS (Continued)

LIST OF TABLES

page

TABLE I COMPLETED TESTS (FIRST CAMPAIGN) CONTRACT CPA 22-69-139 36

TABLE II COMPLETED TESTS (SECOND CAMPAIGN) CONTRACT CPA 22-69-139 MODIFICATIONS 6 AND 7 37

TABLE III SUMMARY OF THE TEST DATA FROM THE COTTRELL ENVIRONMENTAL SYSTEM'S FIRST TEST SERIES . . . 40

TABLE IV SUMMARY OF TEST DATA FROM THE COTTRELL ENVIRONMENTAL SYSTEM'S FIRST TEST SERIES . . . 41

TABLE V SUMMARY OF TEST DATA FROM THE COTTRELL ENVIRONMENTAL SYSTEM'S FIRST TEST SERIES . . . 42

TABLE VI SUMMARY OF TEST DATA FROM THE COTTRELL ENVIRONMENTAL SYSTEM'S SECOND TEST SERIES . . 43

TABLE VII SUMMARY OF TEST DATA FROM THE COTTRELL ENVIRONMENTAL SYSTEM'S SECOND TEST SERIES . . 44

TABLE VIII SUMMARY OF TEST DATA FROM TVA'S FIRST TEST SERIES 45

TABLE IX SUMMARY OF TEST DATA FROM TVA'S FIRST TEST SERIES 46

TABLE X SUMMARY OF TEST DATA FROM TVA'S SECOND TEST SERIES 47

TABLE XI SUMMARY OF TEST DATA FROM TVA'S SECOND TEST SERIES 48

TABLE XII SUMMARY OF TEST DATA FROM TVA'S SECOND TEST SERIES 49

TABLE XIII SUMMARY OF TEST DATA FROM TVA'S SECOND TEST SERIES 50

TABLE XIV SUMMARY OF TEST DATA FROM TVA'S SECOND TEST SERIES 51

TABLE XV SUMMARY OF TEST DATA FROM TVA'S SECOND TEST SERIES 52

TABLE XVI COAL ANALYSES FOR BOTH COTTRELL ENVIRONMENTAL SYSTEM'S TEST SERIES 53

TABLE XVII COAL ANALYSES FOR TVA'S FIRST TEST SERIES . . 54

TABLE XVIII COAL ANALYSES FOR BABCOCK AND WILCOX PILOT TEST PROGRAM 55

TABLE OF CONTENTS (Continued)

LIST OF TABLES

page

TABLE XIX PARTICLE SIZE ANALYSES FOR COTTRELL ENVIRONMENTAL SYSTEM'S FIRST TEST SERIES 56

TABLE XX PARTICLE SIZE ANALYSES FOR COTTRELL ENVIRONMENTAL SYSTEM'S SECOND TEST SERIES . . . 57

TABLE XXI PARTICLE SIZE ANALYSES FOR COTTRELL ENVIRONMENTAL SYSTEM'S SECOND TEST SERIES . . . 58

TABLE XXII PARTICLE SIZE ANALYSES FOR COTTRELL ENVIRONMENTAL SYSTEM'S SECOND TEST SERIES . . . 59

TABLE XXIII LABORATORY AND IN-SITU RESISTIVITY MEASUREMENTS FOR COTTRELL ENVIRONMENTAL SYSTEM'S FIRST TEST SERIES 60

TABLE XXIV LABORATORY AND IN-SITU RESISTIVITY MEASUREMENTS FOR COTTRELL ENVIRONMENTAL SYSTEM'S SECOND TEST SERIES 61

TABLE XXV LABORATORY AND IN-SITU RESISTIVITY MEASUREMENTS FOR COTTRELL ENCIRONMENTAL SYSTEM'S SECOND TEST SERIES 62

TABLE XXVI LABORATORY AND IN-SITU RESISTIVITY MEASUREMENTS FOR BABCOCK AND WILCOX PILOT TEST PROGRAM . . . 63

TABLE XXVII SUMMARY OF CHEMICAL ANALYSES PERFORMED ON SAMPLES TAKEN DURING THE FIRST CES TEST SERIES . 64

TABLE XXVIII SUMMARY OF CHEMICAL ANALYSES PERFORMED ON SAMPLES TAKEN DURING THE SECOND TEST SERIES. . . 65

TABLE XXIX CHEMICAL ANALYSES OF LIMESTONE USED DURING SECOND CES TEST SERIES 69

TABLE XXX SUMMARY OF TEST DATA USED IN CORRELATIONS . . . 94

TABLE XXXI FRACTIONAL EFFICIENCY OF DUST COLLECTORS - FLY ASH ONLY 119

TABLE XXXII FRACTIONAL EFFICIENCY OF DUST COLLECTORS - FINE LIMESTONE 120

TABLE XXXIII FRACTIONAL EFFICIENCY OF DUST COLLECTORS - COARSE LIMESTONE 121

TABLE XXXIV SUMMARY OF PARTICLE SIZE ANALYSES ON SAMPLES FROM BOTH CES TEST SERIES 125

TABLE XXXV IN-SITU RESISTIVITY DATA OBTAINED BY SOUTHERN RESEARCH INSTITUTE AT TVA SHAWNEE STATION, BOILER #10 DURING THE CES SECOND TEST SERIES . . 133

TABLE OF CONTENTS (Continued)

LIST OF TABLES

page

TABLE XXXVI DATA SUMMARY - FULL SCALE DOLOMITE INJECTION TEST RESULTS OBTAINED BY RESEARCH COTTRELL, INC. AT A LARGE MIDWEST UTILITY 135

TABLE XXXVII DATA USED FOR RELATIONSHIP BETWEEN PRECIPITATION RATE PARAMETER AND PARTICULATE RESISTIVITY 146

TABLE XXXVIII SUMMARY OF DATA USED IN SECTION ON CHEMICAL ANALYSES (PPS. 147-153) 148

TABLE XXXIX DATA TAKEN FROM THE OPTICAL SENSOR RECORDER CHARTS 156

TABLE XL SUMMARY OF 1970 TVA TEST RESULTS USED IN ESTABLISHING BASELINE BOILER AND PARTICULATE COLLECTOR OPERATING PARAMETERS FOR NO LIMESTONE INJECTION 167

TABLE XLI SUMMARY OF ELECTROSTATIC PRECIPITATOR SIZE MODIFICATIONS AND COSTS FOR THE PRESENTLY INSTALLED DUST COLLECTING SYSTEM REQUIRED TO MAINTAIN A STACK EMISSION RATE EQUIVALENT TO BASELINE NO LIMESTONE INJECTION 170

TABLE XLII SUMMARY OF THE "HOT" PRECIPITATOR SIZING AND COSTING FOR SHAWNEE STATION BOILER #10 WITH AND WITHOUT LIMESTONE INJECTION (STRAIGHT PRECIPITATOR) 172

TABLE XLIII SUMMARY OF GAS COOLING AS AN OPTION FOR COARSE OR FINE LIMESTONE INJECTION 174

I. INTRODUCTION

This report is submitted as a partial fulfillment of the requirements for Environmental Protection Agency (EPA) Contract CPA 22-69-139 and presents the results of a full-scale study to quantify the operation of a combination mechanical collector electrostatic precipitator dust collection system with and without dry limestone injection. This study is part of the overall program being undertaken at the Shawnee power generating station of the Tennessee Valley Authority for the control of sulfur oxide emissions from a full-scale utility boiler. Definition of the effects of dry additive injection on the particulate control equipment operation and the recommended system modifications, including cost benefit data to maintain stack particulate emissions with injection equivalent to that of 2.7% sulfur and 10% ash coal-firing without injection are the primary requirements of this study. A further requirement is to recommend investigative programs to be considered for future study.

Two test campaigns were conducted by Cottrell Environmental Systems, Inc. during this study:

> The first occurred in December, 1969 and related to the quantification of the dust collection system performance _without_ additive injection. The main purpose of the data acquisition was for use as a baseline in defining the effects of subsequent additive injection;

The second was in July, 1971 during limestone injection and consisted of controlling four parameters at two levels which included two boiler variables (coal sulfur and flue gas temperature), and two limestone injection variables (amount and particle size).

The data and samples from these tests and other pertinent sources,(1-5)* i.e. Tennessee Valley Authority, Southern Research Institute, Research-Cottrell, Inc., Babcock and Wilcox, Co., and Dr. K. J. McLean, EPA visiting associate from Wollongong University, Australia, have been analyzed and correlated. The results are contained in subsequent sections of this report.

---

* The numbers in superscript refer to the bibliography at the end of the text.

II. TECHNICAL APPROACH

Because of the chemical and physical properties of the injected additive material, the characteristics as well as the quantity of particulate to be collected will vary substantially. These variations, including the degree of affect on the operating parameters of the dust collection system, must be monitored and evaluated in order to size and cost the system. The changes in particulate loading, specific gravity and particle size distribution will affect the performance of the mechanical colelctors which precede the electrostatic precipitator. This in turn will vary the quantity and nature of the dust entering the precipitator, resulting in operational changes. Of particular significance will be the change in the electrical conductivity of the dust caused mainly by the removal of sulfur trioxide from the flue gas by the alkaline additive and the higher bulk resistance of limestone.

In the collection of fly ash-limestone reaction products by an electrostatic precipitator, the most critical parameter is the bulk electrical resistivity of the particulate. Values above 10^{10} to 10^{11}ohm-cm result in reduced electrical power to the precipitator and poor performance. This particular subject has been treated extensively in the literature(6-9) and will be covered in more detail in subsequent sections of this report. A comparison of present results with past experience will also be discussed.

The main operational parameters that were monitored during the test program include:

1. Particulate Characteristics (Fly Ash, Fly Ash-Limestone Reaction Products)
    - (a) Specific Gravity
    - (b) Particle Size Analysis (Bahco and Sieve)
    - (c) Bulk Electrical Resistivity (Laboratory)
    - (d) In-Situ Electrical Resistivity
    - (e) Chemical Analysis
        - (1) Loss on Ignition
        - (2) S_iO_2, Al_2O_3, Fe_2O_3, CaO, MgO, TiO_2 Na_2O, K_2O, $SO_4^=$, $SO_3^=$, $S^=$

2. Collector Variables
    - (a) Particulate Loadings Inlet and Outlet (ESP and MC)
    - (b) Pressure Drop of Mechanical Collector
    - (c) Current-Voltage Characteristics of ESP
    - (d) Sparking Rate of ESP
    - (e) Particulate Collection Efficiency (ESP and MC)

3. Boiler Variables
    - (a) Flue Gas Analysis (O_2, SO_2, H_2O)
    - (b) MW Load, Steam, Air
    - (c) Flue Gas Temperature, Pressure
    - (d) Gas Volume
    - (e) Coal-Firing Rate
    - (f) Limestone Addition Rate

4. Additive Characteristics
   - (a) Particle Size Analysis (Bahco and Sieve)
   - (b) Electrical Resistivity (Laboratory)
   - (c) Chemical Analysis
     - (1) CaO, MgO, Fe_2O_3, SiO_2

5. Coal Analysis
   - (a) Sulfur
     - (1) Pyritic
     - (2) Organic
     - (3) Sulfate
   - (b) Ash
   - (c) Moisture

The objective of the test program was to provide an assessment of the particulate collecting system with and without additives for use in establishing the additional gas cleaning equipment required to maintain stack particulate emissions at levels associated with 2.8% sulfur 15.5% ash coal-firing. In addition, other alternatives such as gas cooling, hot precipitator, gas conditioning, and type of electrical energization were evaluated.

III. TEST METHODS

The test methods used were in compliance with the ASME-PTC 27 and ASME-PTC 28 with regard to determining gas volume, particulate loading and analyzing the collected material.

1. Gas Velocity Measurements are required to obtain the necessary data for determining:
   - (a) Total gas volume being treated by the dust collector.
   - (b) Distribution and flow pattern of gas entering the collector.
   - (c) The sampling rates required to obtain representative particulate loadings entering and leaving the collector.

The equipment used to make these measurements during the test program reported herein is shown schematically in Figure 1(a). It consisted of a Stauscheibe pitot tube with inclined draft gauge for velocity head readings, plus a thermocouple and potentiometer for simultaneous temperature measurements.

The gas velocity was calculated from the equation:

$$v = 15.6\ k_p \left[\frac{T_D\ h}{P}\right]^{\frac{1}{2}} = 13.37\ \left[\frac{T_D\ h}{P}\right]^{\frac{1}{2}} \qquad (1)$$

Where,

v = Gas Velocity - FPS

T_D = Duct Temp. °F + 460-°R

h = Velocity Head - "H_2O

P = Duct Pressure - "Hg

= Barometric pressure $\pm \frac{\text{Duct Static Pressure ("}H_2O)}{13.6}$

k_p = 0.855 = Stauscheibe pitot tube factor

15.6 = Constant for flue gas from pulverized coal combustion.

The total gas volume was calculated from the equation:

$$V = 60\, A\bar{v} \qquad (2)$$

Where,

V = Total Gas Volume - ACFM

A = Flue Cross-Sectional Area Where Velocity Traverse Made - Ft^2

$\bar{v}$ = Average gas velocity obtained from traverse - FPS

60 = seconds/minute

2. Moisture Content of the gas was determined by hot-gas psychrometry which involves determining the wet and dry bulb temperatures of the gas. The following equations are used to calculate the moisture content:

$$e = e^1 - 0.01\,(t_d - t_w), \text{ and} \qquad (3)$$

$$M = \left(\frac{e}{B \pm S_f}\right)\left(100\right) \qquad (4)$$

Where,

e = Vapor pressure of gas - "Hg
e^1 = Vapor pressure of saturated gas at t_w - "Hg
t_d = Dry bulb temperature - °F
t_w = Wet bulb temperature - °F
M = Moisture in gas - %
B = Barometric pressure - "Hg
S_f = Flue pressure - "Hg

3. Particulate Sampling was done by means of the large volume Aerotec sampling equipment which is shown schematically in Figure 1(b). The equipment consists of a sample nozzle and probe connected to the dust separating elements which include a high efficiency cyclone with a glass jar hopper and a filter bag (both predried and weighed) followed by a fan for drawing the gas through the sampling train. The gas flow rate is monitored by measuring the pressure drop across the calibrated cyclone and can be varied to maintain isokinetic sampling by means of a valve located at the filter bag outlet. The gas temperature is measured at the cyclone outlet with a dial thermometer and the gas pressure is assumed to be the same as the main duct pressure which is determined by barometer and a static pressure measurement.

FIGURE 1

EQUIPMENT FOR MAKING GAS VELOCITY MEASUREMENTS AND TAKING PARTICULATE SAMPLES

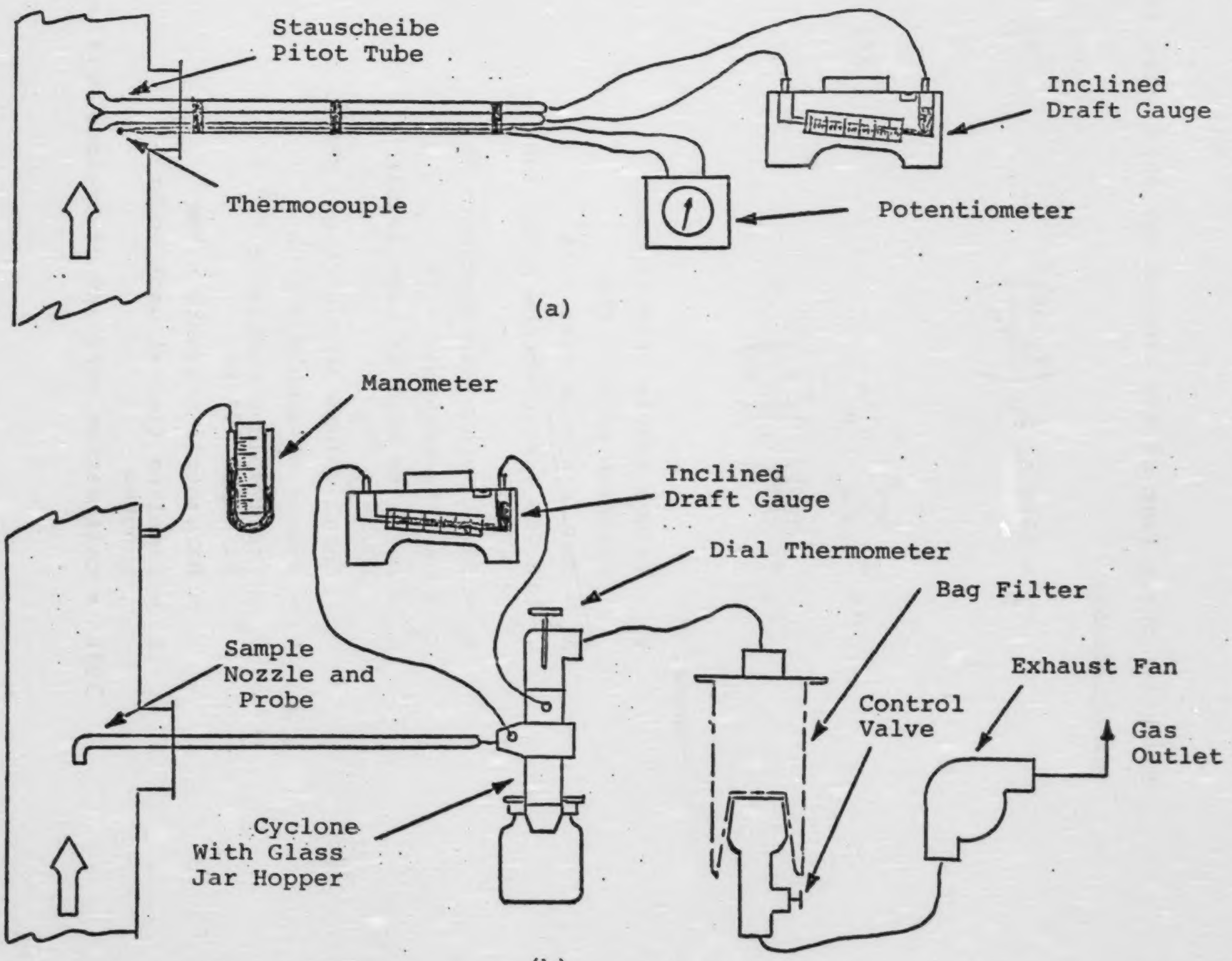
Stauscheibe Pitot Tube
Thermocouple
Inclined Draft Gauge
Potentiometer
(a)
Manometer
Inclined Draft Gauge
Dial Thermometer
Bag Filter
Sample Nozzle and Probe
Control Valve
Exhaust Fan
Gas Outlet
Cyclone With Glass Jar Hopper
(b)

The total cubic feet of gas sampled was calculated from the equations:

$$V_p = 3930\ A_n\ k_p \left(\frac{T_s\ hp}{T_D}\right)^{\frac{1}{2}} \qquad (5)$$

$$V_t = \sum_{0}^{N} V_p\text{'s} \qquad (6)$$

$$V_S = \left(\frac{530B}{30}\right)\left(V_t\right)\left(\frac{1}{T_s}\right)^{\frac{1}{2}}\ t \qquad (7)$$

Where,

V_p = Volume sample rate at each traverse point - CFM

A_n = Sample nozzle area - Ft^2

k_p = 0.855 = Stauscheibe pitot tube factor

T_S = Sample train temperature - °R

T_D = Duct temperature - °R

h_p = Velocity head at each sample point - "H_2O

V_t = Total volume sample rate - CFM

N = Number of sample points

V_S = Total volume sampled - Ft^3 @ 70 F and 30" Hg

B = Barometric pressure - "Hg

t = Sampling time at each point - minutes

3930 = Calibration constant of cyclone orifice

The amount of particulate collected was determined by drying and reweighing the cyclone sampler jar and filter bag. The particulate loading was calculated using the equation:

$$D = \frac{(D_C)(15.43)}{V_S} \qquad (8)$$

Where,

D = Particulate loading - grains/Ft^3 @ 70 F and 30"Hg
D_C = Net weight of particulate collected - grams
V_S = Total volume sampled - Ft^3 @ 70 F and 30 "Hg
15.43 = Conversion factor, grams to grains

The efficiency of the collector was determined by the equation:

$$E = \left(\frac{D_I - D_O}{D_I}\right)\left(100\right) \qquad (9)$$

Where,

E = Efficiency - %
D_I = Inlet particulate loading - grains/Ft^3
D_O = Outlet particulate loading - grains/Ft^3

4. Test Sections were located in areas of reasonably straight runs of duct work and free of interference from nearby equipment. Figure 2 is a schematic diagram of the boiler,

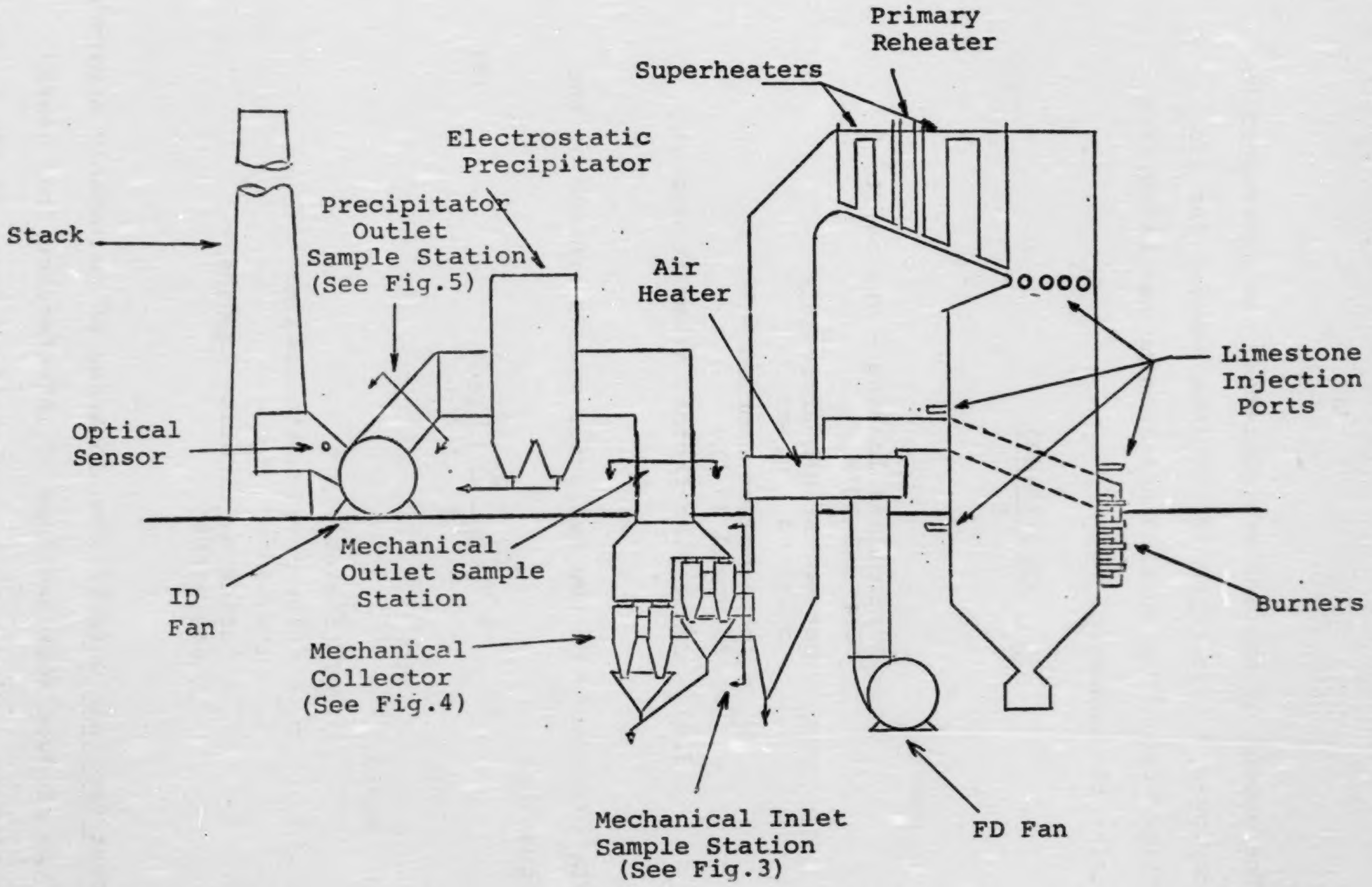
Primary
Reheater
Superheaters
Electrostatic
Precipitator
Precipitator
Outlet
Sample Station
(See Fig.5)
Stack
Air
Heater
Limestone
Injection
Ports
Optical
Sensor
Mechanical
Outlet Sample
Station
ID
Fan
Burners
Mechanical
Collector
(See Fig.4)
Mechanical Inlet
Sample Station
(See Fig.3)
FD Fan

FIGURE 2

SCHEMATIC DIAGRAM OF BOILER #10 SHAWNEE STATION, TVA collectors, and associated equipment showing the location of the sampling areas. Figures 3 through 5 detail the actual dimensions and number of sample points used at the mechanical collector inlet and the electrostatic precipitator inlet and outlet.

5. In-Situ Resistivity measurements were made using a portable apparatus (Figure 6) designed and supplied by Research-Cottrell, Inc. The apparatus measures the electrical resistance of a layer of dust precipitated from flue gas under actual operating conditions. It consists of a small electrostatic point-plane precipitator (Figure 7), an iron constantan thermocouple located near the plane, and a control unit for supplying power and measuring voltage and current.

6. The Laboratory Resistivity measurements were made in apparatus shown photographically and schematically in Figures 8 and 9. The cell shown in Figure 10 is mounted in an electrically heated and thermostatically controlled chamber capable of reaching temperatures in the 650°F range. In addition, humidity can be controlled from bone dry up to 30 or 40% by volume. The schematic electrical circuitry is shown in Figure 11.

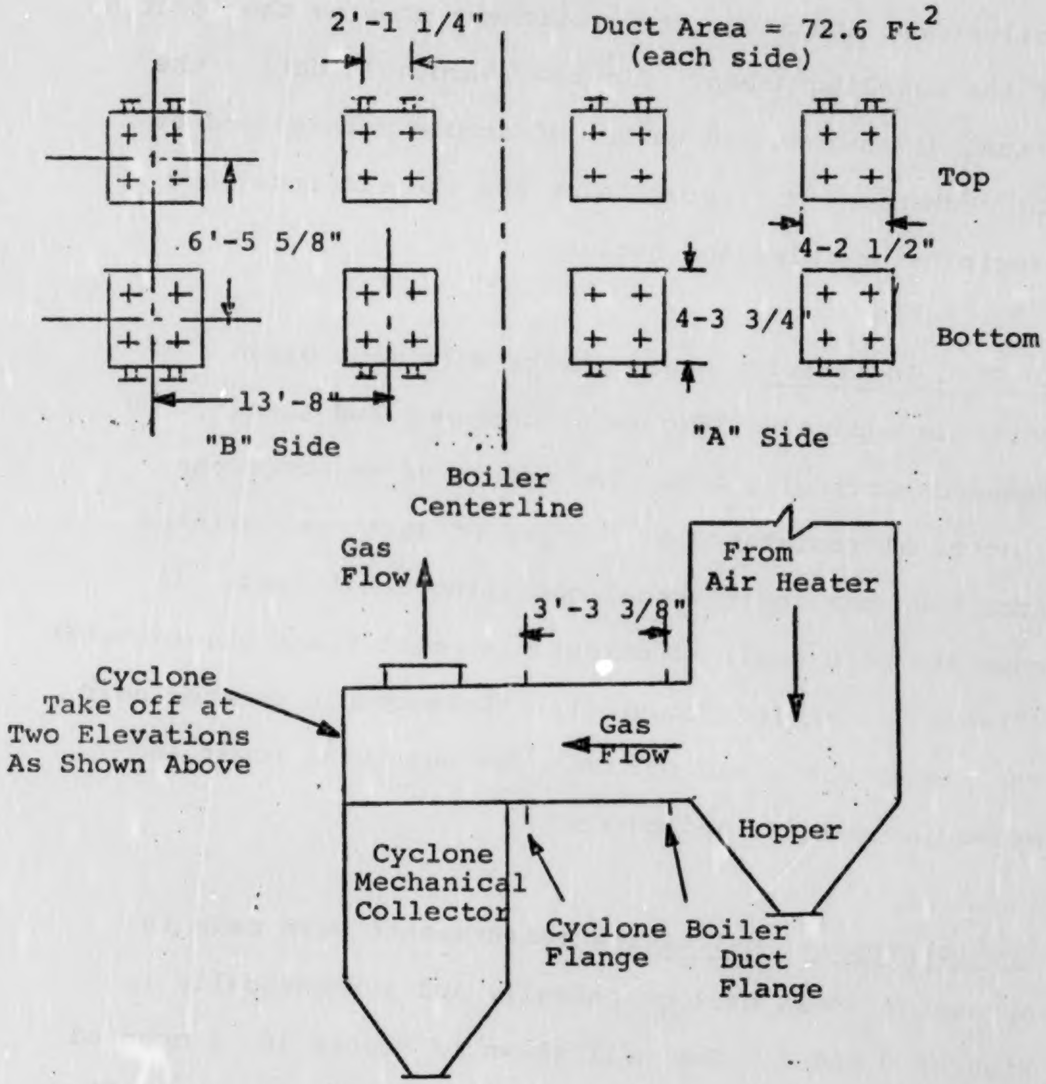
2'-1 1/4"
Duct Area = 72.6 Ft^2
(each side)
Top
6'-5 5/8"
4-2 1/2"
4-3 3/4"
Bottom
13'-8"
"B" Side
"A" Side
Boiler
Centerline
Gas
Flow
From
Air Heater
3'-3 3/8"
Cyclone
Take off at
Two Elevations
As Shown Above
Gas
Flow
Hopper
Cyclone
Mechanical
Collector
Cyclone
Flange
Boiler
Duct
Flange

FIGURE 3

DETAILS OF MECHANICAL COLLECTOR
INLET SAMPLING STATION

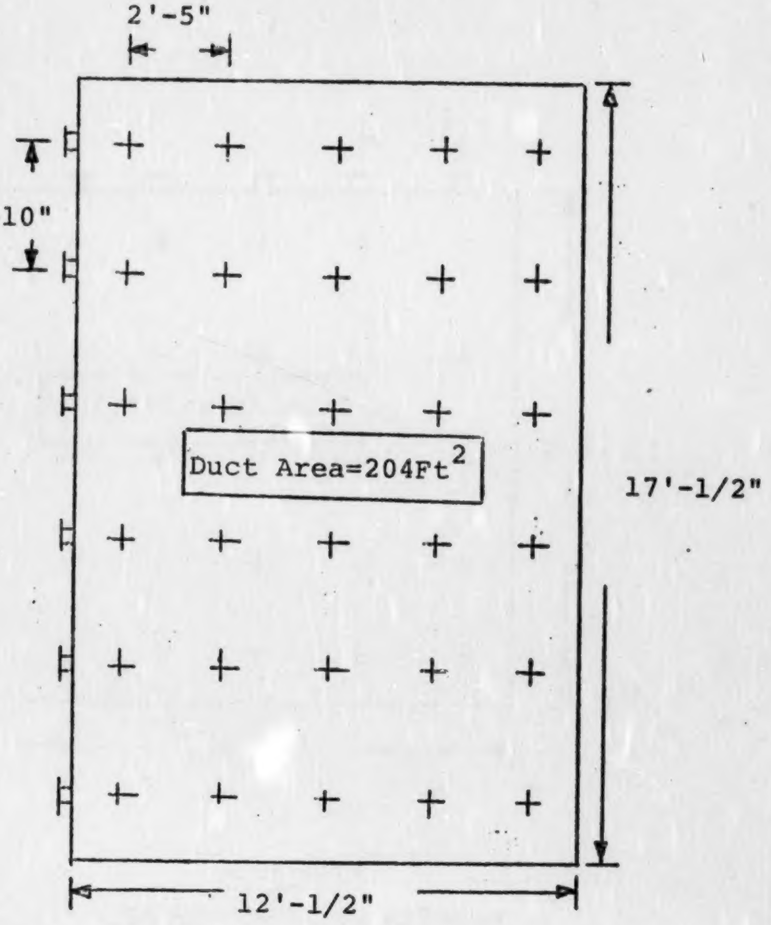
2'-5"
2'-10"
Duct Area=204Ft^2
17'-1/2"
12'-1/2"

FIGURE 4

DETAILS OF MECHANICAL COLLECTOR
OUTLET - ELECTROSTATIC PRECIPITATOR INLET
SAMPLING STATION

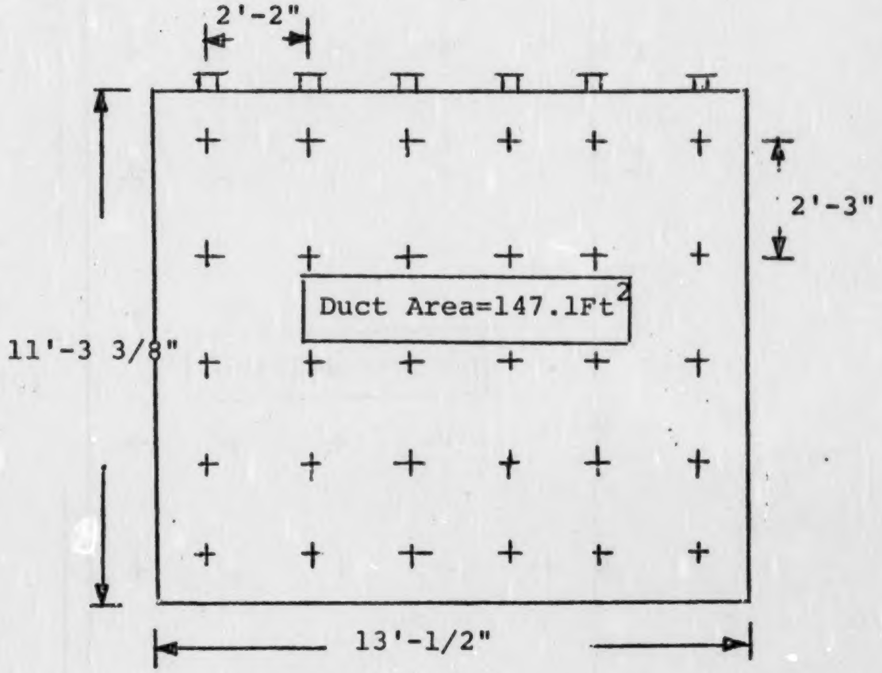
2'-2"
2'-3"
Duct Area=147.1Ft²
11'-3 3/8"
13'-1/2"

FIGURE 5

DETAILS OF ELECTROSTATIC

PRECIPITATOR OUTLET SAMPLING STATION

FIGURE 6

IN-SITU RESISTIVITY APPARATUS

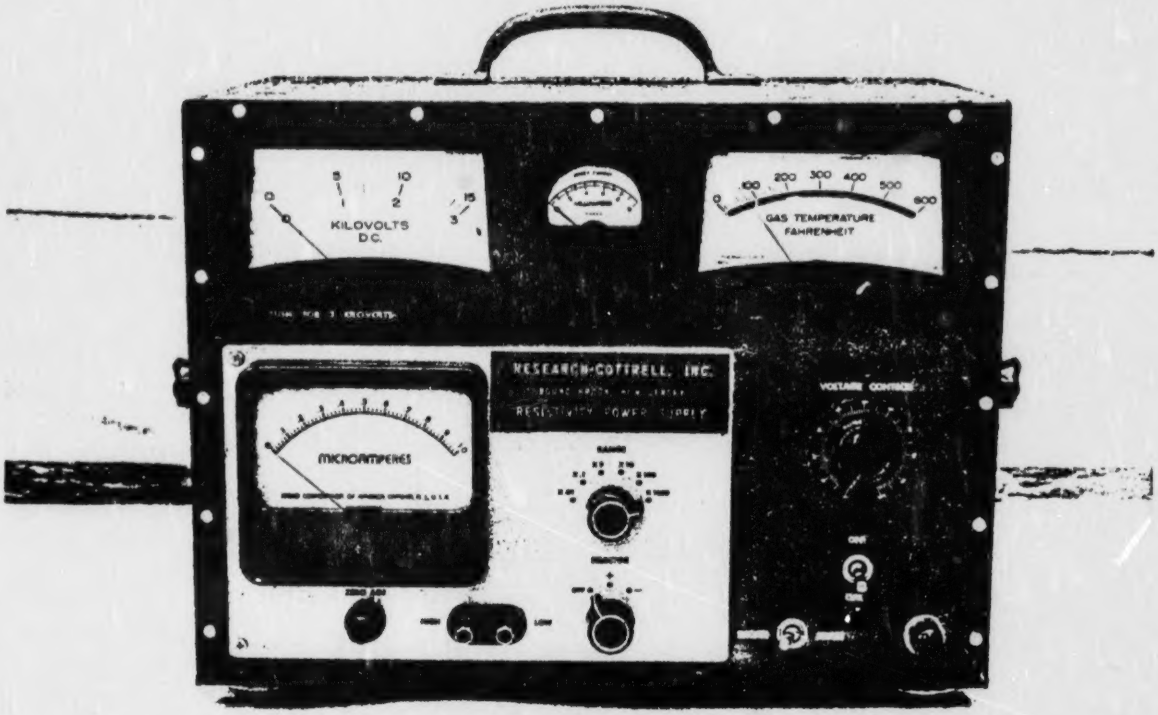
0
5
10
15
0
1
2
3
KILOVOLTS
D.C.
0
100
200
300
400
500
600
GAS TEMPERATURE
FAHRENHEIT
MICROAMPERES
RESEARCH-COTTRELL, INC.
RESISTIVITY POWER SUPPLY
VOLTAGE CONTROL

POWER SUPPLY AND METERING UNIT

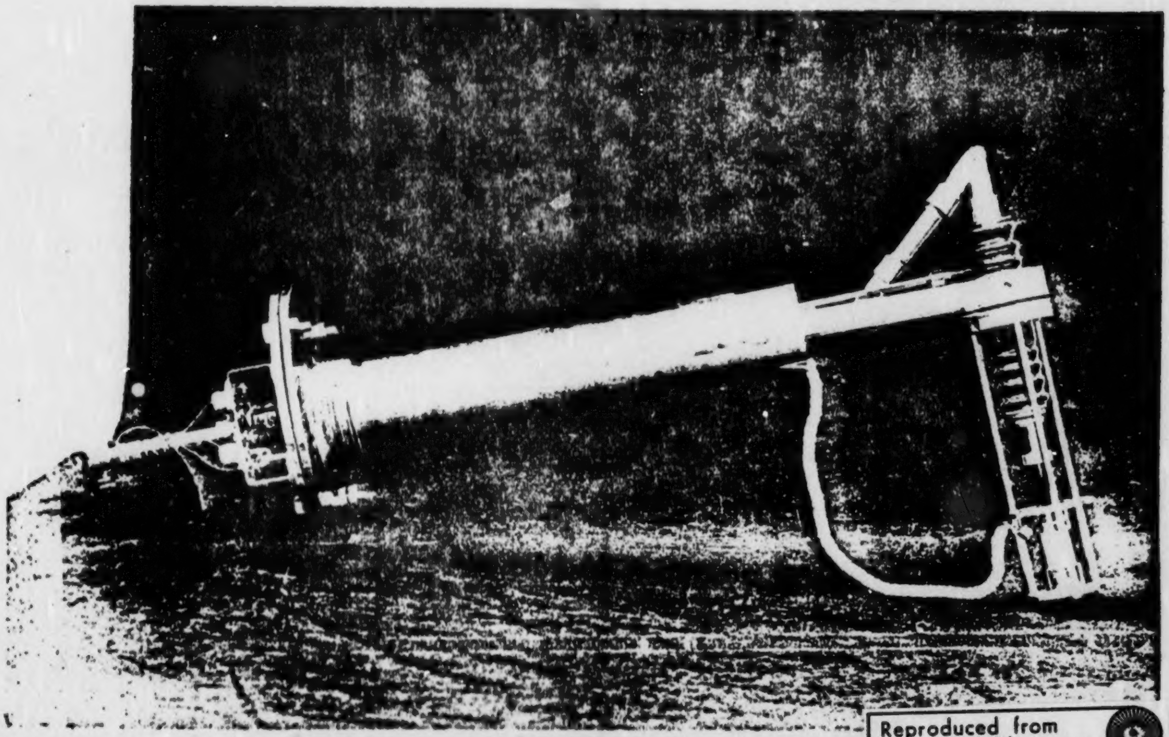

PROBE AND POINT-PLANE CELL

Reproduced from
best available copy.

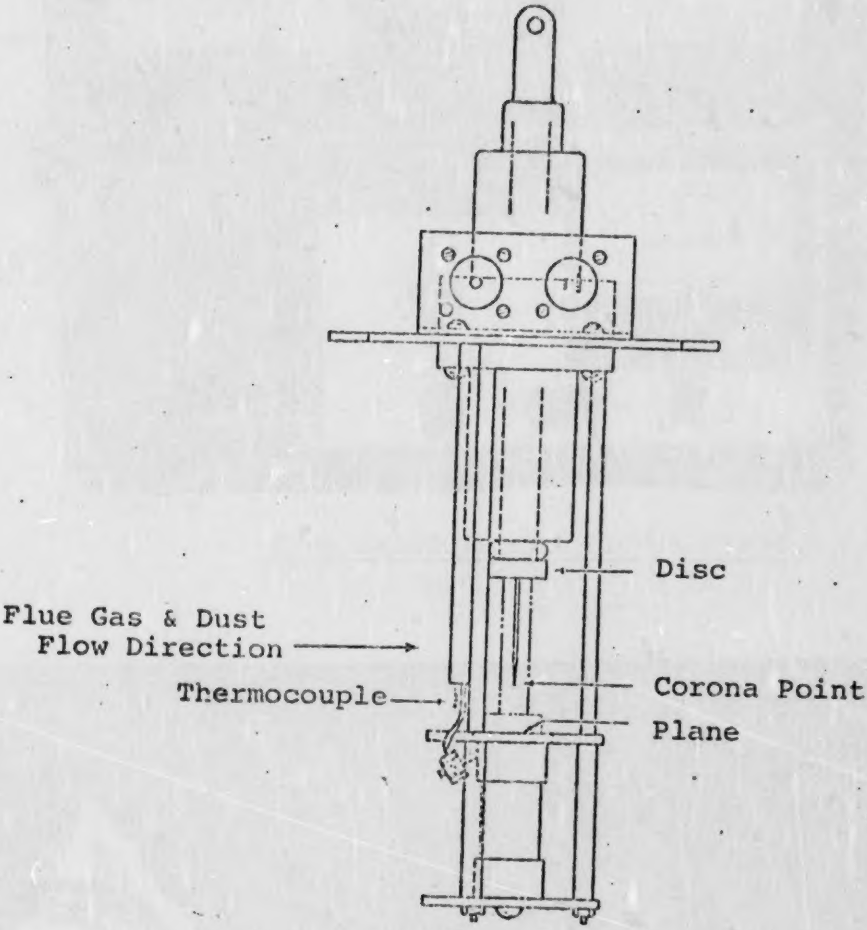
Disc
Flue Gas & Dust Flow Direction
Thermocouple
Corona Point
Plane

FIGURE 7

POINT-PLANE RESISTIVITY CELL

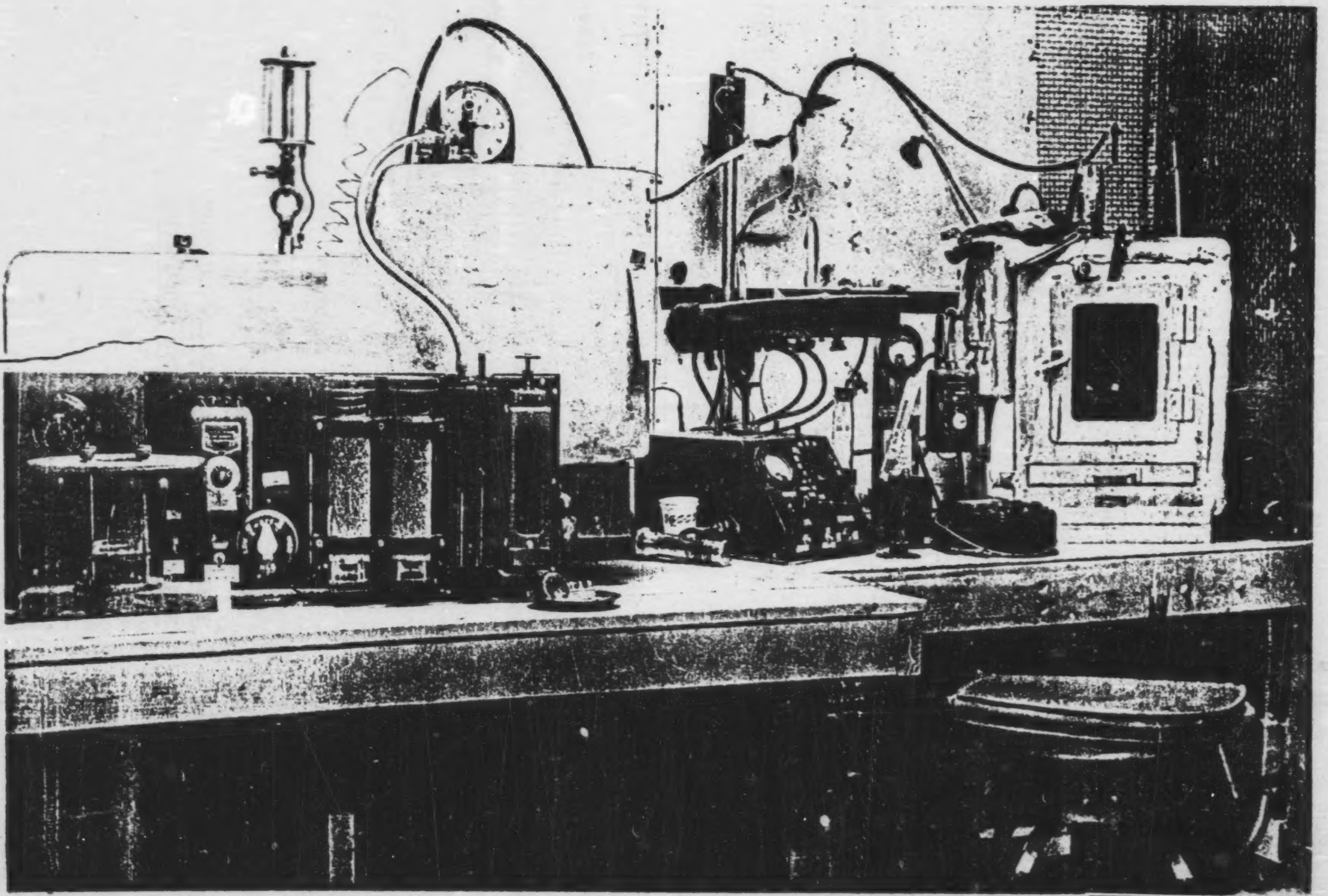

Reproduced from best available copy.

FIGURE 8 - LABORATORY RESISTIVITY MEASURING APPARATUS

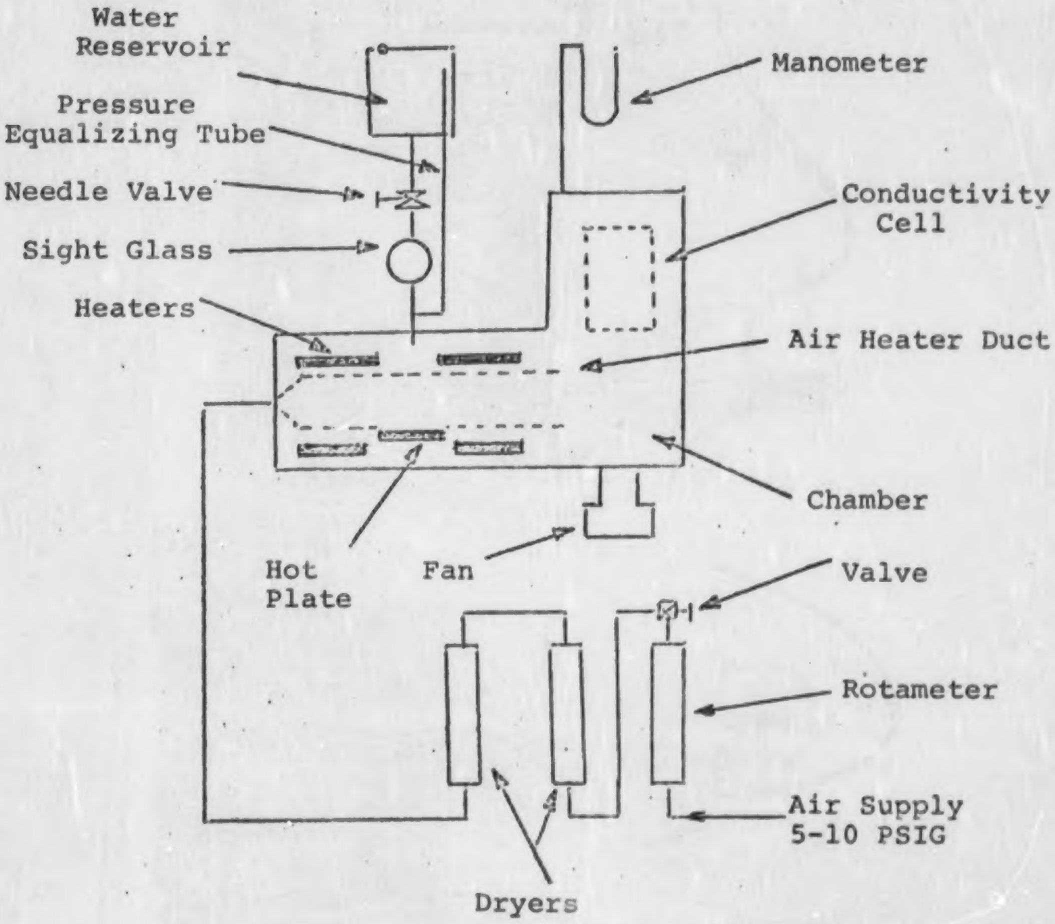
Water Reservoir
Manometer
Pressure Equalizing Tube
Needle Valve
Conductivity Cell
Sight Glass
Heaters
Air Heater Duct
Chamber
Hot Plate
Fan
Valve
Rotameter
Air Supply 5-10 PSIG
Dryers

FIGURE 9

SCHEMATIC DIAGRAM OF LABORATORY RESISTIVITY MEASURING APPARATUS

FIGURE 10

CROSS-SECTION DIAGRAM OF MEASURING CELL USED IN LABORATORY RESISTIVITY APPARATUS

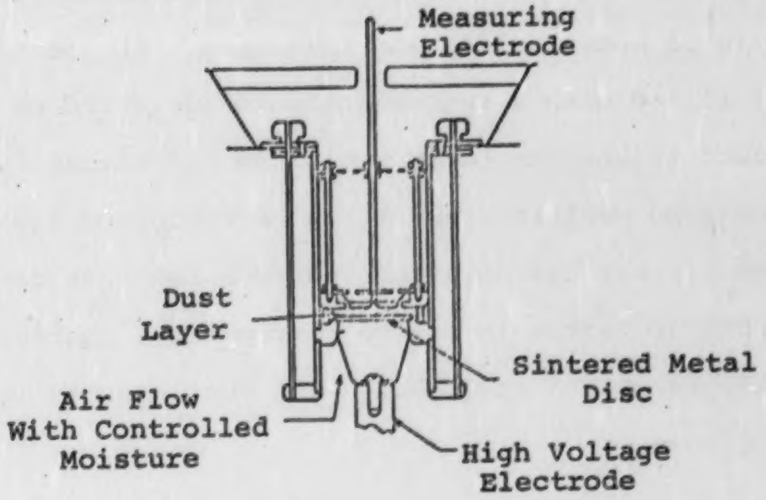
Measuring Electrode
Dust Layer
Sintered Metal Disc
Air Flow With Controlled Moisture
High Voltage Electrode

FIGURE 11

SCHEMATIC OF ELECTRIC CIRCUIT FOR LABORATORY RESISTIVITY APPARATUS

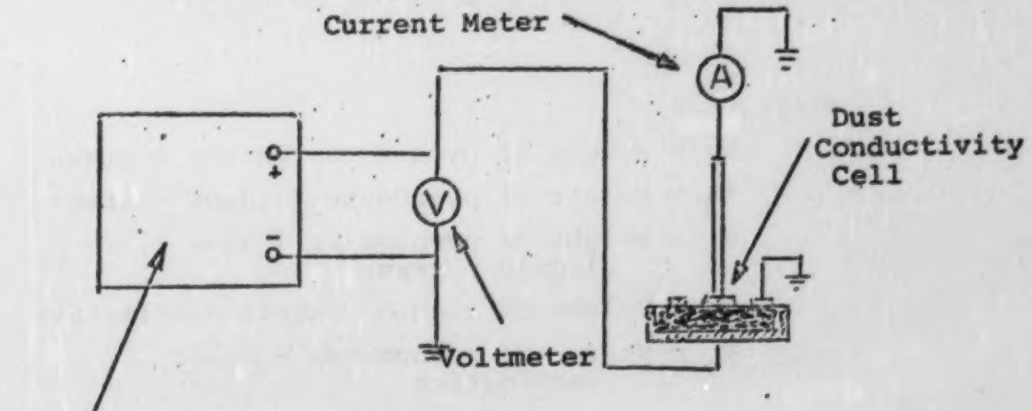
Current Meter
A
Dust Conductivity Cell
+
-
V
Voltmeter
H-V Rectifier 0-15KV

7. The skeletal or true density of the particulate samples was determined by the pycnometer method. Approximately a 5-gram sample is transferred to a weighed pycnometer bottle of known volume and reweighed. The bottle is half filled with a suitable liquid (selected on the basis of dust solubility being a minimum) and placed in a dessicator-type container which can be evacuated (see Figure 12). After all air has been removed from the dust sample, the pycnometer bottle is filled to capacity, thermally equilibrated and reweighed. The dust density is calculated as follows:

$$V_1 = \frac{W_3 - W_2}{d_1} \qquad (10)$$

$$d_p = \frac{W_2 - W_1}{V_p - V_1} \qquad (11)$$

Where,

W = Weight of pycnometer bottle - grams

W_2 = Weight of pycnometer + dust - grams

W_3 = Weight of pycnometer + dust + liquid - grams

V_1 = Volume of liquid - cubic centimeters

V_p = Volume of pycnometer - cubic centimeters

d_1 = Density of liquid - grams/cubic centimeters

d_p = True density of dust - grams/cubic centimeters

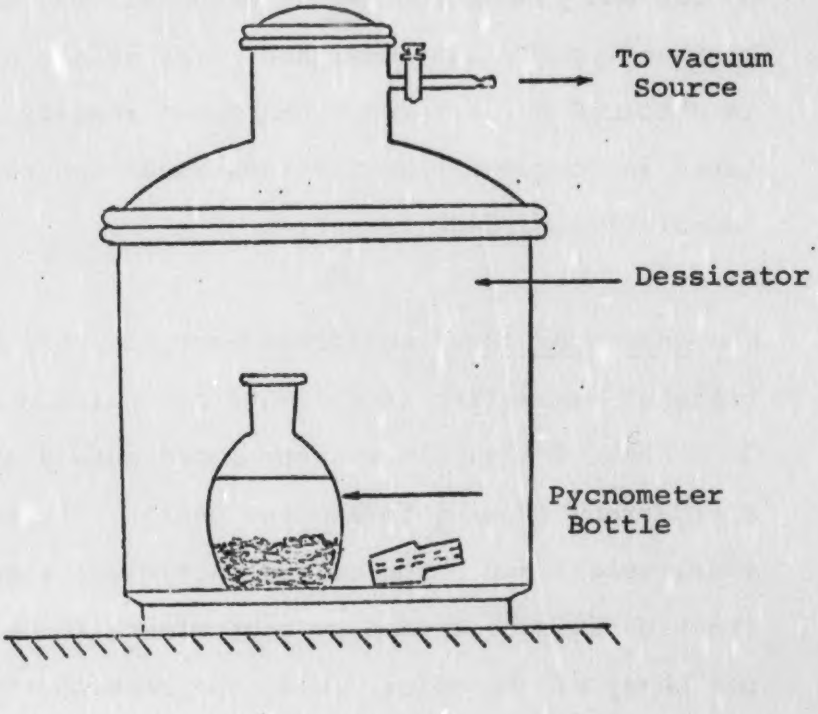
To Vacuum Source
Dessicator
Pycnometer Bottle

FIGURE 12

APPARATUS FOR MEASURING SKELETAL OR TRUE DENSITY OF PARTICULATE

8. The particle size distributions were made by sieve and Bahco methods. A set of 3 inch U.S. Standard sieves and pan are weighed. The sieves are then nested reading 50-mesh (297 microns), 100-mesh (149 microns), 200-mesh (74 microns), 325-mesh (44 microns) and pan from top to bottom. About a 2 gram sample of dried dust is placed on the top sieve and covered. The set of sieves is then placed in a Ro-tap and shaken for twenty minutes. The sieves are brushed lightly and reweighed. The weight of fractions is obtained by difference and final results are calculated as "percent fraction separated" and reported as "cumulative percent finer".

The Bahco method of sub-sieve particle sizing uses a centrifugal classifier (see Figure 13) which operates at 3500 RPM. The sample is introduced into a spiral-shaped air current flowing toward the center. Depending on the size, weight and shape of the particles, a certain fraction is accelerated by centrifugal force toward the periphery of the whirl, while the remainder is carried toward the center. By varying flow through the use of throttles, the dust sample can be divided into a number of fractions between about 2 and 30 microns. This particular method is not absolute but must be calibrated with a standard sample of known distribution based on an absolute method.

FIGURE 13

BAHCO CENTRIFUGAL PARTICLE CLASSIFIER

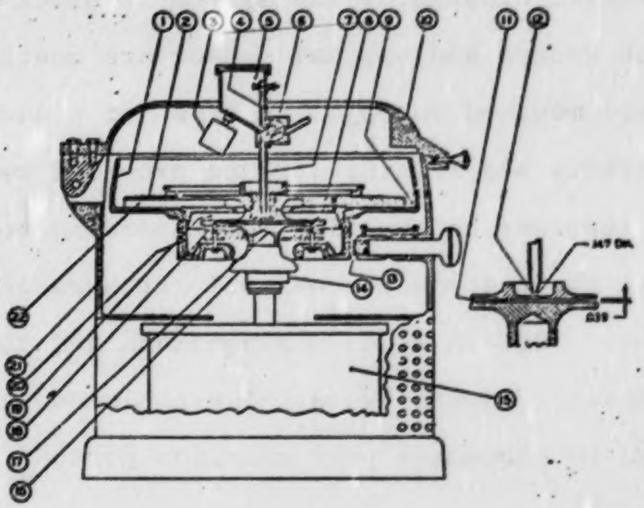

1 Rotor Casting
2 Fan
3 Vibrator
4 Adjustable Slide
5 Feed Hopper
6 Revolving Brush
7 Feed Tube
8 Feed Slot
9 Fan Wheel Outlet
10 Cover
11 Rotary Duct
12 Feed Hole
13 Brake
14 Throttle Spacer
15 Motor - 3520 RPM
16 Grading Member
17 Threaded Spindle
18 Symmetrical Disc
19 Sifting Chamber
20 Catch Basin
21 Housing
22 Radial Vanes

9. The stack opacity was monitored by means of an optical sensor designed and supplied by Research-Cottrell, Inc. A schematic diagram of the system is shown in Figure 14. A light source and optical sensor are contained in sealed housings mounted on opposite sides of a duct. Sufficient sensitivity and flexibility are provided to permit full scale recorder calibration corresponding to 20 up to 100% optical obscuration for aerosol paths ranging from 6 to 30 feet. (20% is a No. 1 Ringelmann and 100% a No. 5 Ringelmann). Normally, a 0-5 Ringelmann scale calibration is used to encompass peak emission periods such as sootblowing.

   A clean gas reference signal is continually compared with the dirty gas signal by means of a differential signal amplifier whose signal is recorded continually as optical density readout.

10. Coal Analyses were provided by Smith, Rudy and Company, chemists in Philadelphia, Pennsylvania while other chemical analyses of particulate samples were performed by the TVA laboratory chemists located in Chattanooga, Tennessee.

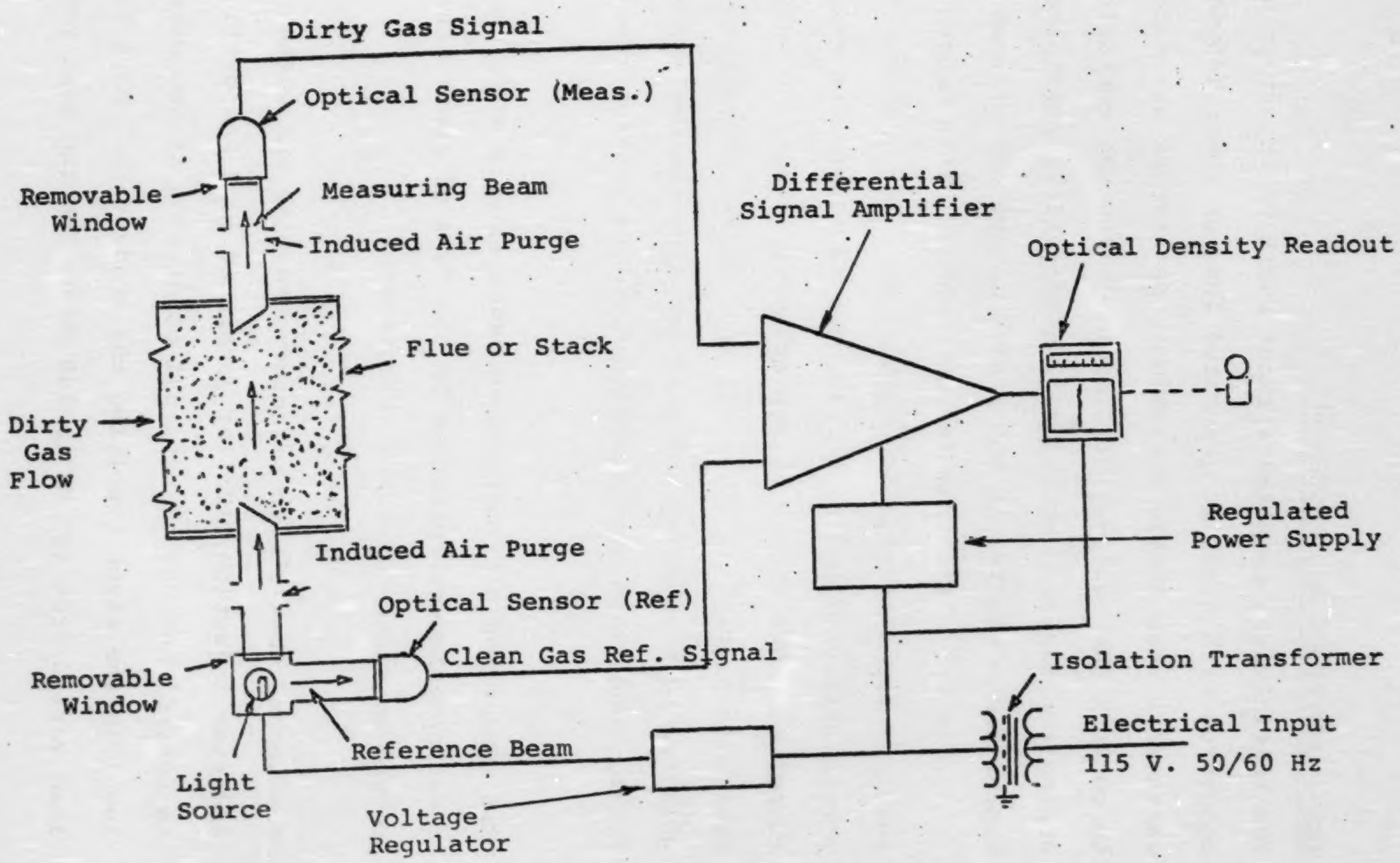
Dirty Gas Signal
Optical Sensor (Meas.)
Removable Window
Measuring Beam
Induced Air Purge
Flue or Stack
Dirty Gas Flow
Induced Air Purge
Optical Sensor (Ref)
Clean Gas Ref. Signal
Removable Window
Reference Beam
Light Source
Voltage Regulator
Differential Signal Amplifier
Optical Density Readout
Regulated Power Supply
Isolation Transformer
Electrical Input
115 V. 50/60 Hz

FIGURE 14

FUNCTIONAL DIAGRAM OF THE OPTICAL SENSOR

IV. TEST CONDITIONS AND PROCEDURES

The initial test campaign without additive injection was conducted with a boiler generated load of about 140 megawatts with very little variation. No attempt was made to control the coal sulfur. Soot-blowing was curtailed during the tests. Mechanical and electrical precipitator hoppers were emptied at the beginning and end of each test period at which time samples were taken. This procedure ensured representative hopper samples. Both "A" and "B" precipitators of boiler No. 10 were tested during this campaign. (See Figure 15 for schematic diagram of electrostatic precipitator). Coal feed rates and samples were obtained by monitoring and grab-sampling the coal feeders. Boiler conditions were recorded from the control room panels.

Main operating difficulties encountered were with the electrostatic precipitators in the form of short circuits caused by broken discharge electrodes.

The second test series was conducted with and without additive injection. Boiler generated load was difficult to control because of external conditions of low water level in the river supplying the condensers. As a result, load varied from 125 MW to 148 MW during the test period.

FIGURE 15

SCHEMATIC DIAGRAM OF ELECTROSTATIC PRECIPITATOR ARRANGEMENT AND ELECTRICAL HOOK-UP

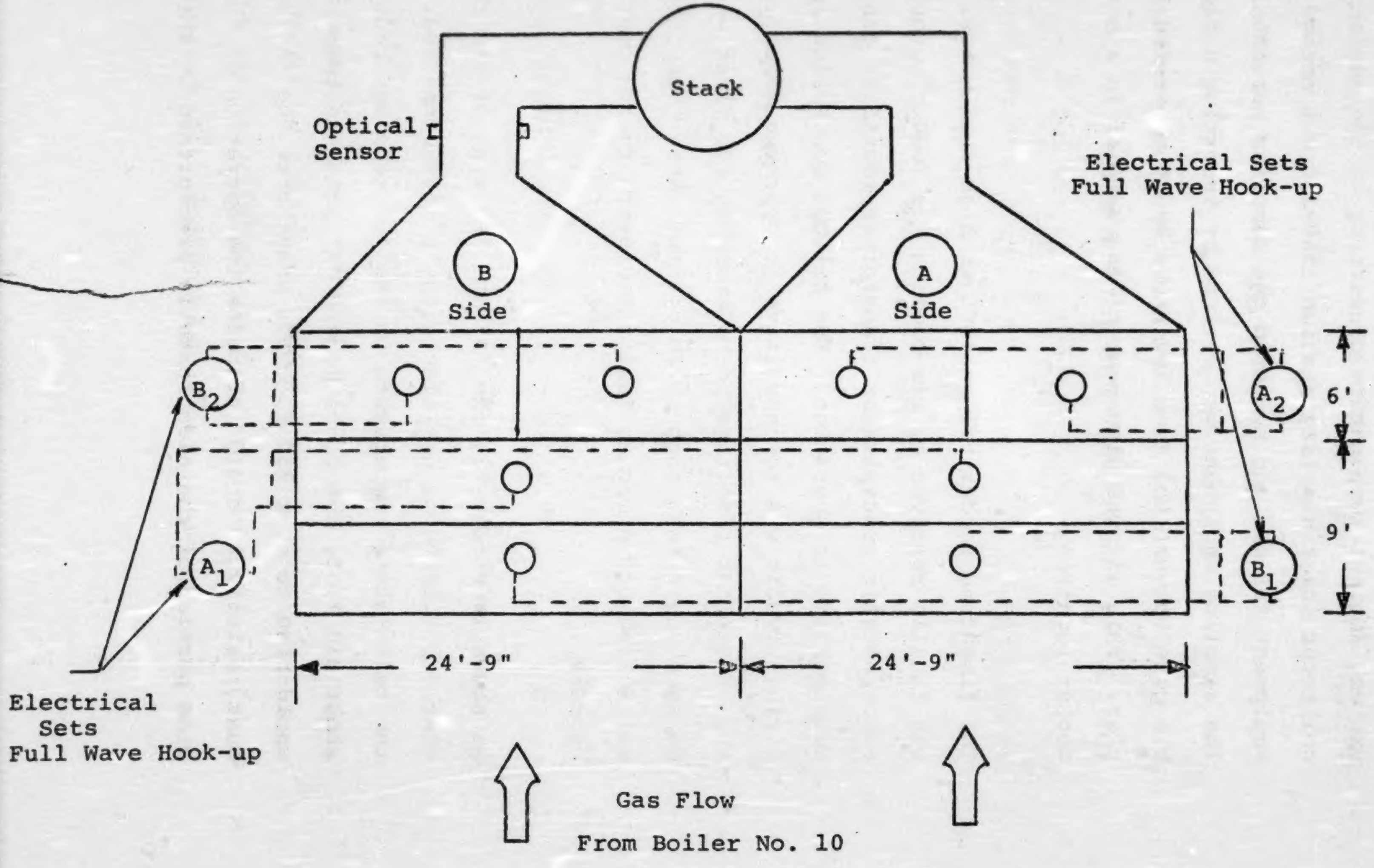
Stack
Optical Sensor
B Side
A Side
Electrical Sets Full Wave Hook-up
B2
A1
A2
B1
6'
9'
24'-9"
24'-9"
Electrical Sets Full Wave Hook-up
Gas Flow
From Boiler No. 10

Extreme ambient temperature conditions at the mechanical collector inlet sampling station (160-180 F.) caused equipment failure and hampered the sampling personnel. The sampling equipment was revised by inserting a flexible hose between the sampling probe and the Aerotec Sampler. This allowed placement of the sampler in a somewhat cooler location.

The limestone feeder tripped-off at high feed rates. This was finally resolved by air-cooling the feeder motor. The electrostatic precipitator transformer-rectifier controls were erratic in operation. The silicon controlled rectifier firing circuit was too sensitive to sparking which caused the precipitator voltage to be lowered at the first occurence of sparking rather than at an optimum rate. The problem was solved by replacing faulty resistors in the control circuit.

As shown in Figure 15, the "A" and "B" side of the electrostatic precipitator are electrically interconnected. For the tests where temperature on the "B" side was reduced to about 250 F. by fan biasing, the "A" side gas temperature would rise to over 350 F. This meant that the "A" side dust resistivity could influence the operation of the "B" side portion of the electrostatic precipitator. This interference was corrected by deenergizing the "A" side and using the electrical sets to energize only the "B" side.

Soot blowing, condenser repairs, and hopper enptying took more time than originally anticipated and modifications in test and operating procedures were instituted. In order to complete as much of the statistically designed test program as possible within reasonable cost and schedule constraints, the following changes in procedure were agreed upon:

1. The velocity and temperature traverses before each test were eliminated. The gas temperature and pressure drop of the mechanical collector were adjusted by fan biasing to give the desired test conditions at the electrostatic precipitator inlet. Previous velocity and temperature traverses at similar mechanical collector conditions (temperature within 5°F and pressure drop within 10%)were then used to obtain isokinetic sampling. Figures 16 to 18 are representative temperature and velocity traverses for the three sampling stations.

2. Elimination of sampling at the mechanical inlet for most tests allowed the use of these two samplers, one each, on the ESP inlet and outlet or a total of three samplers at each of these locations. Time per test was thus reduced to 50 minutes from 75 minutes thereby improving test scheduling without reducing the amount of dust collected.

Tables I and II list the completed tests for both campaigns.

FIGURE 16

REPRESENTATIVE TEMPERATURE AND VELOCITY TRAVERSE AT THE MECHANICAL COLLECTOR INLET ("B" SIDE)

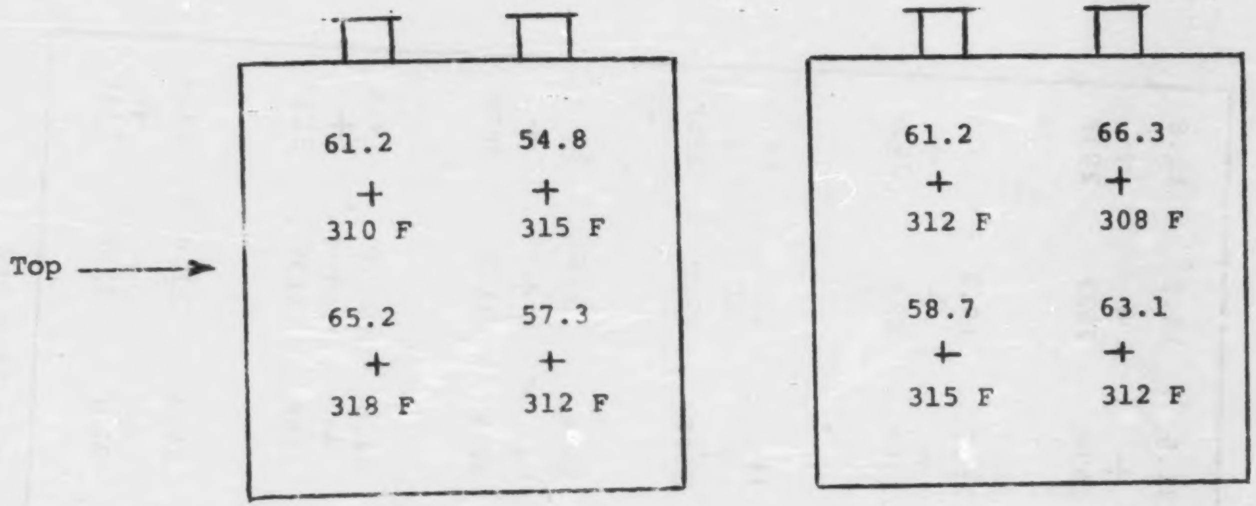
Top
61.2
310 F
54.8
315 F
65.2
318 F
57.3
312 F
61.2
312 F
66.3
308 F
58.7
315 F
63.1
312 F

Avg. Velocity = 60.4 FPS
Avg. Temperature =
ACFM of Gas = (60.4)(72.6)(60) = 263,157

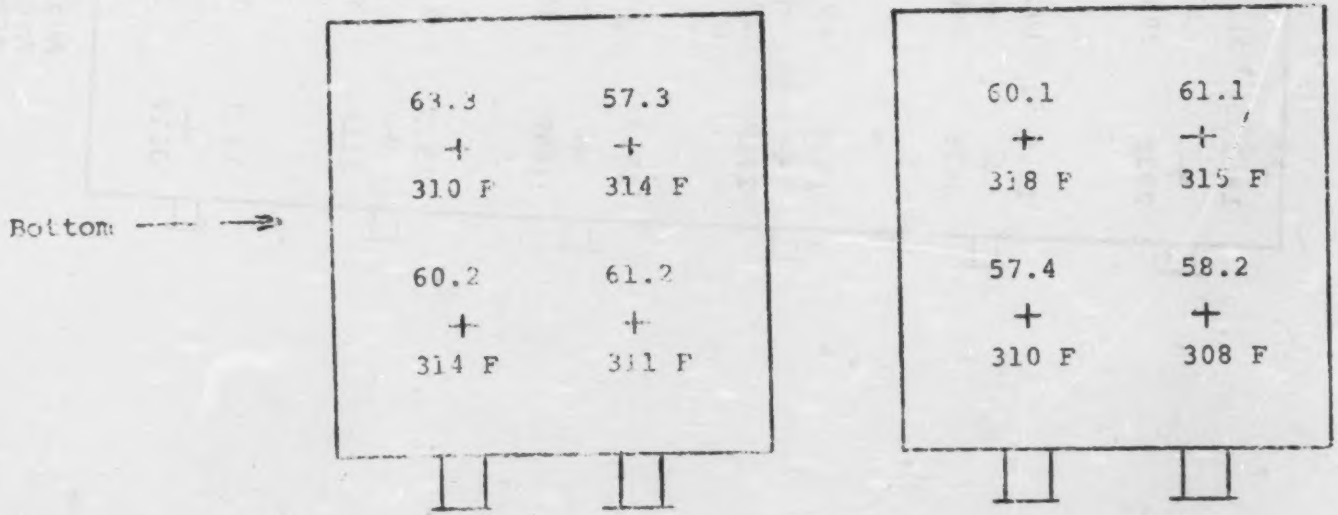
Bottom
63.3
310 F
57.3
314 F
60.2
314 F
61.2
311 F
60.1
318 F
61.1
315 F
57.4
310 F
58.2
308 F

FIGURE 17

REPRESENTATIVE TEMPERATURE AND VELOCITY TRAVERSE AT THE MECHANICAL OUTLET - PRECIPITATOR INLET SAMPLE STATION ("B" SIDE)

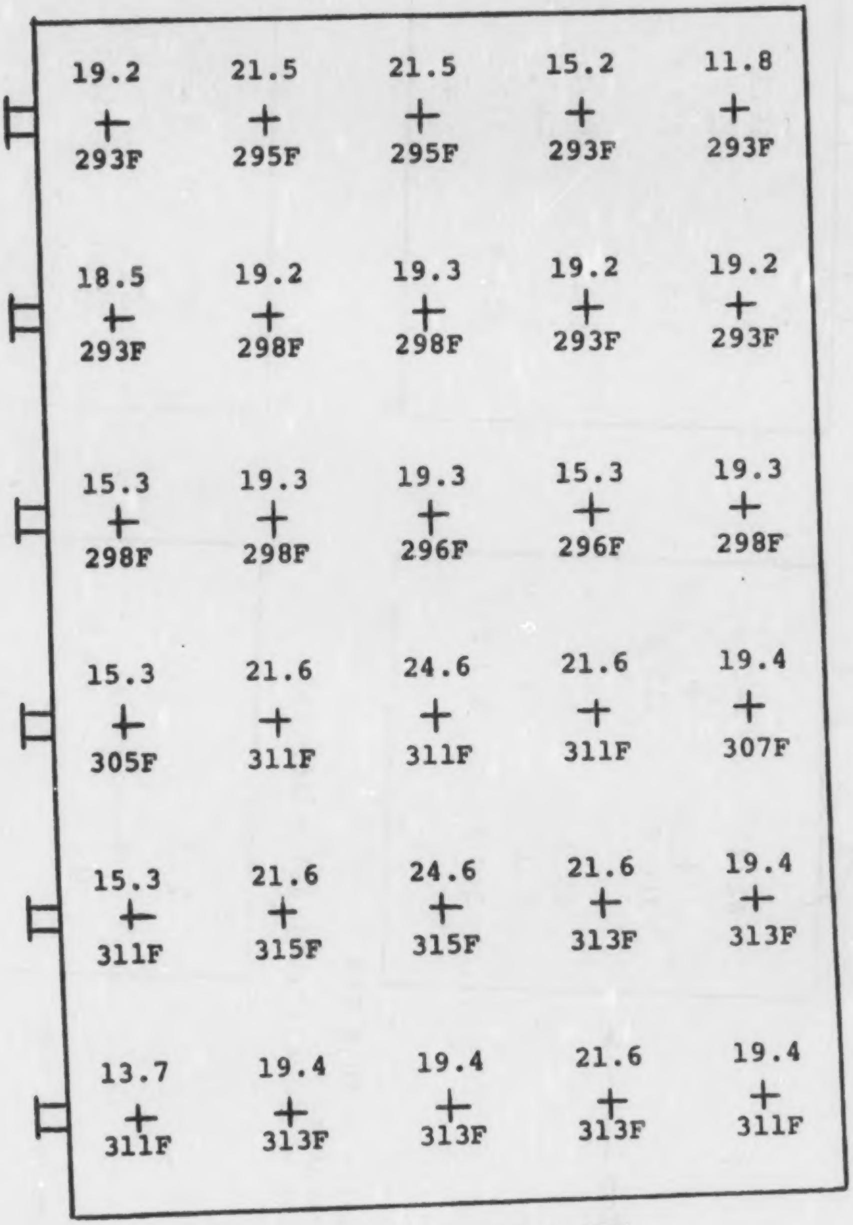

19.2 293F	21.5 295F	21.5 295F	15.2 293F	11.8 293F
18.5 293F	19.2 298F	19.3 298F	19.2 293F	19.2 293F
15.3 298F	19.3 298F	19.3 296F	15.3 296F	19.3 298F
15.3 305F	21.6 311F	24.6 311F	21.6 311F	19.4 307F
15.3 311F	21.6 315F	24.6 315F	21.6 313F	19.4 313F
13.7 311F	19.4 313F	19.4 313F	21.6 313F	19.4 311F

Avg. Velocity = 19.1 FPS
Avg. Temperature = 303F
ACFM of Gas = (19.1)(204)(60) = 233,784

FIGURE 18

REPRESENTATIVE TEMPERATURE AND VELOCITY TRAVERSE AT THE PRECIPITATOR OUTLET SAMPLING STATION ("B" SIDE)

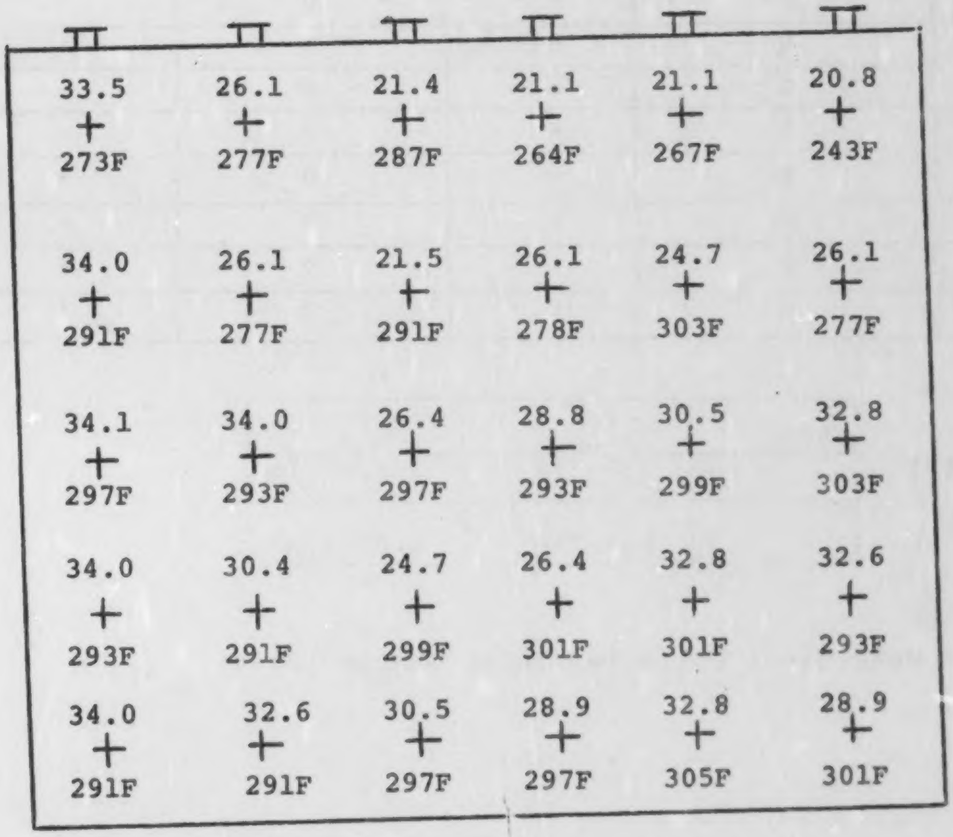

33.5 273F	26.1 277F	21.4 287F	21.1 264F	21.1 267F	20.8 243F
34.0 291F	26.1 277F	21.5 291F	26.1 278F	24.7 303F	26.1 277F
34.1 297F	34.0 293F	26.4 297F	28.8 293F	30.5 299F	32.8 303F
34.0 293F	30.4 291F	24.7 299F	26.4 301F	32.8 301F	32.6 293F
34.0 291F	32.6 291F	30.5 297F	28.9 297F	32.8 305F	28.9 301F

Avg. Velocity = 28.6 FPS
Avg. Temperature = 289F
ACFM of Gas = (28.6)(147.1)(60) = 252,424

TABLE I

COMPLETED TESTS (FIRST CAMPAIGN)

CONTRACT CPA 22-69-139

Test Number	Additive Stoich. X_1	Gas Temp. X_2	Particle Size X_3	% S in Coal X_4	Date Performed
1A*	0	+	0	+	12/11/69
1B*	0	+	0	+	12/11
2A	0	+	0	+	12/12
3A*	0	+	0	-	12/14
3B*	0	+	0	-	12/13
4A*	0	+	0	+	12/14
4B*	0	+	0	-	12/13
5A*	0	+	0	+	12/15
5B*	0	+	0	+	12/15

KEY:

LEVEL	X_2	X_4
+	289-318	2.30-4.10
-	238-256	1.00-2.29

* Mechanical Collector Inlet Sample Taken

TABLE II

COMPLETED TESTS (SECOND CAMPAIGN)

CONTRACT CPA 22-69-139 MODIFICATIONS 6 & 7

Test Number	Additive Stoich. X_1	Gas Temp. X_2	Particle Size X_3	% S in Coal X_4	Date Performed
1	0	+	0	+	7/9/71
2*	-	+	-	+	7/10
3*	-	-	-	+	
4*	+	+	-	-	7/12
5*	-	-	-	+	
6*	+	+	-	+	7/13
8*	-	-	-	+	7/14
9	0	-	0	-	7/15
10	+	-	+	-	
11	+	+	+	-	
25	-	-	+	-	7/19
19	0	-	0	≤0.8	7/20
20	0	+	0	≤0.8	
21	0	-	0	≤0.8	
22	0	+	0	≤0.8	
23	-	+	-	≤0.8	
24	+	+	-	≤0.8	
28	-	+	-	+	7/21
29	-	-	-	+	
30	-	+	-	+	
16	0	-	0	-	7/22
17	+	-	-	-	
18	+	+	-	-	
26	-	+	-	-	7/23
27	-	-	-	-	
14*	+	+	+	+	7/24
15*	+	-	+	-	
32*	-	+	+	+	7/26
33*	-	-	+	+	

KEY:

LEVEL	X_1	X_2	X_3	X_4
+	2.0-4.0	289-318°F	COURSE (50%-400M)	2.30-4.10
-	0.5-2.0	238-256°F	FINE (80%-400M)	1.00-2.29

* Mechanical Collector Inlet Sample Taken

NOTE: All tests were run on "B" side. However, first five tests had electrical equipment energizing both "A" and "B" sides. Test six on had only "B" side energized, one set per section (fullwave).

V. TEST RESULTS AND SAMPLE ANALYSES

1. Test Data

Tables III through XV summarize the data from both the CES test programs, and the TVA test programs. All runs were made on Boiler No. 10 at Shawnee Station. However, the TVA tests were conducted on the "A" precipitator while the first CES test program was on both "A" and "B" precipitators and the second was on the "B" only. (See Figure 15).

Since the flue gas and particulate to both "A" and "B" precipitators came from the same boiler, there is no obvious reason to expect any significant difference in results due to the side tested, and for analysis purposes the test data can be considered comparable. The only exception is the optical sensor data which was recorded on the "B" side and a quantitative analysis requires test data from the "B" side. However, a qualitative evaluation of the data can include "A" side tests as well.

2. Coal Analyses

Tables XVI through XVIII summarize coal sample analyses for both the CES and TVA programs, and the Babcock and Wilcox pilot plant work at Alliance, Ohio.

3. **Particle Size Analyses** (Bahco, sieve and specific gravity)

   Tables XIX through XXII summarize the Bahco and sieve analyses of samples obtained during the CES test programs. Included are limestone feed samples, fly ash samples and reacted limestone fly ash mixtures.

4. **Resistivities**

   Tables XXIII through XXV summarize all laboratory and in-situ resistivity measurements made on samples from the CES programs. Table XXVI shows resistivities obtained on fly ash from various coals used in the Babcock and Wilcox pilot program.

5. **Chemical Analyses**

   Tables XXVII through XXIX summarize all the chemical analyses obtained on the particulate samples from both of the CES test programs. These analyses were performed by TVA personnel at their Chattanooga, Tennessee laboratory.

TABLE III

SUMMARY OF THE TEST DATA FROM THE COTTRELL ENVIRONMENTAL SYSTEM'S FIRST TEST SERIES

(December, 1969)

Test No.	Feed Rate Tons/Hr.		Bar. Press. "Hg	Duct Press. ID Fan in "H_2O	In-Situ Resistivity Pptr. Inlet		Elec. Pptr.		
	Coal	Limestone			Temp. °F	OHM-CM	Inlet T °F	Gas Vol. MACFM	Vel. FPS
1A	57.0	0	29.61	-13.90	—	—	—	275	6.2
1B	57.0	0	29.75	-13.25	—	—	—	255	5.7
2A	56.0	0	29.71	-13.60	293	4.8×10^{9}	293	275	6.2
3A	58.0	0	29.75	-13.30	318	2.1×10^{10}	318	273	6.1
3B	59.0	0	29.91	-12.75	293	2.6×10^{11}	293	237	5.3
4A	58.0	0	29.88	-13.10	312	4.7×10^{10}	312	270	6.1
4B	59.0	0	29.75	-12.75	302	3.0×10^{11}	302	230	5.2
5A	57.0	0	29.98	-13.30	—	—	—	276	6.2
5B	57.0	0	29.96	-12.75	—	—	—	230	5.2

(a)

Test No.	Unit Load	Steam M Lbs. Per Hr.	Air M Lbs. Per Hr.	Flue Gas % by Volume		MC Inlet Temp. °F	ΔP "H_2O		
				O_2	H_2O		AH	MC	Pptr.
1A	140	970	1030	3.0-5.0	—	295	2.3	4.40	0.3
1B	140	965	1020	2.3-4.0	—	300	2.3	3.80	0.3
2A	137-144	940-1000	1000-1030	3.0-5.0	8.3	297	2.3	4.20	0.3
3A	140	960	1020	2.0-4.0	—	300	2.2	4.30	0.3
3B	140	960	1010	2.0-4.0	—	303	2.3	3.80	0.3
4A	141	962	1020	2.0-4.0	9.1	300	2.3	4.00	0.3
4B	141	965	1020	2.0-4.0	7.7	310	2.2	3.80	0.3
5A	140	970	1020	3.2-5.0	—	290	2.2	4.30	0.3
5B	140	960	1020	3.2-3.9	—	290	2.2	3.75	0.3

(b)

TABLE IV

SUMMARY OF TEST DATA FROM THE COTTRELL ENVIRONMENTAL SYSTEM'S FIRST TEST SERIES

(December, 1969)

Test No.	T-R Set B2 - Outlet Section					T-R Set A2 - Outlet Section				
	Spks Min.	Volts AC	Amps AC	KVolts DC	Amps DC	Spks Min.	Volts AC	Amps AC	KVolts DC	Amps DC
1A	—	—	—	—	—	0	305	70	34.4	0.30
1B	78	300	73	33.8	.26	—	—	—	—	—
2A	—	—	—	—	—	3	310	79	34.9	.32
3A	—	—	—	—	—	100	200	50	22.5	.26
3B	143	233	50	26.2	.14	—	—	—	—	—
4A	—	—	—	—	—	200	250	50	28.2	.24
4B	145	229	50	25.8	.13	—	—	—	—	—
5A	—	—	—	—	—	15	330	50	37.2	.24
5B	130	300	80	33.8	.32	—	—	—	—	—

(a)

Test No.	T-R Set B1 - Inlet Section					T-R Set A1 - Center Section				
	Spks Min.	Volts AC	Amps AC	KVolts DC	Amps DC	Spks Min.	Volts AC	Amps AC	KVolts DC	Amps DC
1A	150	330	60	37.2	.28	150	315	60	35.5	.33
1B	148	345	63	38.8	.30	145	330	73	37.2	.40
2A	85	355	75	40.0	.34	95	350	88	39.4	.50
3A	150	250	40	28.2	.12	150	278	50	31.2	.24
3B	160	233	35	26.2	.105	158	283	65	31.8	.35
4A	150	250	30	28.2	.12	150	265	50	29.8	.24
4B	160	228	34	25.6	.10	158	268	57	30.2	.28
5A	70	350	80	39.4	.40	118	330	90	37.2	.46
5B	85	305	73	34.4	.33	140	305	80	34.4	.44

(b

TABLE V

SUMMARY OF TEST DATA FROM THE COTTRELL ENVIRONMENTAL SYSTEM'S FIRST TEST SERIES

(December, 1969)

Test No.	Power		Grain Loading @ 70°F & 30 "Hg-Gr/Ft^3			Removal Efficiency %			Migration Vel. W FPS/CMPS
	Watts/1000 ACFM	Watts/1000 Ft^2	MC Inlet	MC Outlet Pptr. Inlet	Pptr. Outlet	MC	ESP	Overall	
1A	78	720	3.17	—	.036	—	—	98.7	—
1B	89	740	3.09	—	—	—	—	—	—
2A	102	940	—	—	—	—	—	—	—
3A	38	360	3.22	1.45	—	55.0	—	—	—
3B	40	360	3.14	1.37	0.227	56.4	83.5	92.6	.190/5.8
4A	42	410	2.73	1.19	—	56.5	—	—	—
4B	34	300	3.31	1.20	0.328	63.8	72.8	91.5	.18/5.5
5A	91	850	3.20	1.42	0.112	55.7	92.8	96.5	.41/12.5
5B	113	1000	2.95	1.26	0.045	57.3	96.4	98.3	.43/13.1

TABLE VI

SUMMARY OF TEST DATA FROM THE COTTRELL ENVIRONMENTAL SYSTEM'S SECOND TEST SERIES

(July, 1971)

Test No.	Unit Load MW	Steam M Lbs Per Hr.	Air M Lbs Per Hour	Flue Gas O_2 % by Vol.	Flue Gas H_2O % by Vol.	MC Inlet T. °F.	Δp "H_2O			Feed Rate Tons/Hr.		Bar. Press "Hg	Duct Press. ID Fan In. "H_2O	Elec. Precipitator		
							AH	MC	Pptr	Coal	Limestone			Inlet T. °F.	Gas Vol. M ACFM	Vel. FPS
1	134	975	1050	—	—	314	2.7	3.8	0.5	60.9	0	29.97	-13.5	293	299	6.7
2	126	990	1020	5.0	8.0	334	2.6	3.5	0.5	57.9	7.55	29.87	-13.2	314	292	6.6
3	127	920	980	4.4	5.8	270	2.2	2.8	0.3	55.5	8.50	29.79	-10.3	251	254	5.7
4	142	1060	1145	3.0	11.1	327	3.2	4.3	0.6	72.3	9.50	29.85	-14.8	305	337	[illegible]
5	140	1005	1095	—	6.2	265	2.4	3.2	0.4	64.6	4.75	29.83	-11.9	246	256	5.7
6	144	1040	1100	4.2	9.0	322	2.8	3.8	0.5	—	11.60	29.83	-13.5	301	302	6.9
8	142	1020	1100	3.2	7.0	276	2.6	3.5	0.5	62.3	11.15	29.76	-12.3	256	274	6.2
9	133	1010	1090	4.5	6.3	265	2.5	3.3	0.5	66.8	0	29.73	-11.5	246	264	5.9
10	143	1010	1100	3.1	8.0	270	2.5	3.3	0.5	67.5	15.75	29.69	-12.0	251	262	5.9
11	132	1010	1050	2.7	7.2	311	2.6	3.5	0.5	66.3	15.25	29.67	-12.5	290	234	6.4
14	138	980	1070	4.3	6.3	310	2.9	3.5	0.5	59.5	14.10	29.72	-12.6	289	285	6.4
15	132	1000	1070	4.4	7.3	263	2.5	3.2	0.4	62.6	14.45	29.71	-11.7	244	256	5.7
16	135	980	1040	4.2	5.8	260	2.5	3.3	0.5	58.5	0	29.89	-11.0	241	259	5.8
17	139	980	1035	5.3	5.6	262	2.4	3.2	0.4	57.2	9.70	29.90	-11.1	243	256	5.7
18	138	1000	1065	4.0	4.8	310	2.6	3.5	0.5	58.9	9.15	29.86	-12.0	289	282	6.3
19	137	980	1100	6.2	5.1	257	2.5	3.3	0.5	62.0	0	29.84	-12.0	238	259	5.8
20	140	999	1080	5.0	5.4	310	2.8	3.6	0.5	62.2	0	29.83	-12.8	289	288	6.5
21	140	980	1115	5.3	4.9	260	2.5	3.4	0.5	61.2	0	29.87	-12.0	241	264	5.9
22	139	980	1020	6.2	4.7	310	2.6	3.5	0.5	62.1	0	29.85	-12.1	289	282	6.3
23	134	980	1080	—	5.5	314	2.6	3.5	0.5	63.6	1.80	29.82	-12.2	292	284	6.4
24	140	980	1030	5.8	5.4	318	2.5	3.5	0.5	66.3	3.45	29.82	-12.1	296	284	6.4
25	136	960	1060	4.3	6.2	273	2.5	3.4	0.5	62.5	10.55	29.68	-11.8	253	268	6.0
26	141	973	1070	4.6	6.1	310	2.6	3.6	0.5	57.8	7.05	29.78	-12.1	289	286	6.4
27	139	980	1050	4.2	5.6	261	2.5	3.4	0.5	61.8	6.45	29.75	-11.7	242	265	6.0
28	133	1000	1065	5.2	4.7	311	2.7	2.7	0.5	61.2	11.15	29.90	-12.1	290	292	6.6
29	137	1000	1050	—	5.4	260	2.3	3.3	0.5	62.1	6.25	29.90	-11.1	241	259	5.8
30	139	1000	1064	4.8	6.1	309	2.7	3.7	0.5	62.6	5.30	29.89	-12.1	288	292	6.6
32	96	650	780	5.5	6.9	310	2.6	3.6	0.5	45.7	8.50	29.70	-10.0	289	288	6.5
33	136	980	1080	5.0	6.3	260	2.4	3.2	0.5	56.4	7.85	29.70	-11.2	241	259	5.8

TABLE VII

SUMMARY OF TEST DATA FROM THE COTTRELL ENVIRONMENTAL SYSTEM'S SECOND TEST SERIES

(July, 1971)

Reproduced from best available copy.

Test No.	T-R Set B1--Inlet Section					T-R Set A1--Center Section					T-R Set B2--Outlet Section					Power		Grain Loading @ 70F & 30 "Hg-Gr/Ft.^{3}			Removal Efficiency, %			Migration Vel., w
	Spks/ Min.	Volts AC	Amps AC	K Volts DC	Amps DC	Spks/ Min.	Volts AC	Amps AC	K Volts DC	Amps DC	Spks/ Min.	Volts AC	Amps AC	K Volts DC	Amps DC	Watts/ 1000 ACFM	Watts/ 1000 Ft^2	MC Inlet	MC Outlet Pptr. Inlet	Pptr. Outlet	MC	LSP	Overall	FPS/CMPS
1	59	192	<10	22.9	.031	25	275	43	33.0	0.203	55	174	<10	20.8	.060	18.5	186	No Sample	Wet Sample	0.33	—	—	—	—
2	95	199	<20	23.8	.032	73	192	<10	21.75	0.083	100	187	<10	22.35	.040	9.5	93.3	5.46	1.95	0.44	64.3	77.4	91.9	0.24/7.3
3	113	159	<10	18.5	.061	70	172	<10	20.6	0.059	100	180	<5	21.5	.040	8.4	72.2	5.18	2.27	1.57	56.2	30.8	69.7	0.05/1.6
4	100	122	<10	22.9	.070	70	177	<5	21.2	0.060	105	154	<5	18.4	.014	4.7	57.1	3.23	2.21	1.63	31.6	26.2	49.6	0.06/1.8
5	103	168	<5	20.1	.070	70	188	<5	22.5	0.063	100	190	<5	21.5	.020	8.0	69.2	3.22	1.74	1.21	46.1	30.5	62.4	0.05/1.6
6	103	134	<5	23.2	.060	55	174	<5	20.8	0.060	110	167	<5	20.0	.011	9.5	96.2	6.37	2.36	1.95	62.8	17.4	69.3	0.03/1.0
8	57	269	33	31.1	.120	59	231	23	27.6	.114	100	242	50	28.9	.225	49.3	469	7.23	3.34	0.35	53.8	89.5	95.2	0.35/11.0
9	95	238	30	29.4	.120	73	221	17	26.4	.095	100	285	73	34.1	.330	64.0	569	—	1.23	0.12	—	90.2	—	0.34/10.4
10	95	244	28	29.2	.110	75	210	10	25.1	.080	100	263	45	31.4	186	42.2	377	—	2.18	0.12	—	94.5	—	0.43/13.1
11	100	191	17	23.1	.066	69	174	<5	20.8	.060	107	217	17	25.9	.081	17.1	164	—	3.78	0.75	—	80.2	—	0.26/7.9
14	102	191	<5	22.8	.061	70	174	<5	20.0	.060	29	203	<5	24.3	.061	14.5	139	8.25	3.93	0.93	51.8	76.3	88.6	0.33/10.1
15	59	232	18	28.4	.075	70	274	25	32.7	.028	0	237	25	25.3	.100	21.9	275	6.97	3.75	0.520	46.2	86.7	92.8	0.29/8.8
16	100	225	27	26.9	0.10	75	215	<5	25.0	.076	22	234	25	29.0	.103	25.2	254	—	1.43	0.390	—	72.65	—	0.19/5.7
17	100	220	25	26.3	0.08	75	203	<5	24.3	.060	20	235	24	28.1	.100	25.5	220	—	2.80	0.214	—	92.35	—	0.37/11.25
18	103	195	10	22.1	0.06	75	168	<5	20.1	.043	30	198	10	23.7	.048	11.8	112	—	2.395	0.847	—	64.9	—	0.165/5.0
19	93	316	71	37.8	0.44	53	270	58	32.3	0.327	0	256	84	31.8	.413	156.6	1366	—	3.10	0.19	—	93.9	—	0.41/12.5
20	95	265	58	31.7	0.27	55	271	56	32.4	0.28	0	264	77	31.5	.358	101.3	982	—	4.42	0.12	—	97.3	—	0.58/17.7
21	95	258	59	30.4	0.29	59	244	49	29.2	0.26	0	263	80	32.9	.389	99.8	867	—	2.48	0.13	—	94.8	—	0.44/13.4
22	93	214	43	25.5	0.17	67	231	14	25.2	0.11	27	239	65	28.6	0.30	55.1	524	—	2.81	0.29	—	89.7	—	0.36/11.0
23	99	189	57	22.5	0.24	69	171	<5	20.4	0.09	28	206	51	24.6	0.22	44.3	423	—	2.82	1.28	—	54.7	—	0.13/4.0
24	100	192	61	22.4	0.27	68	173	<5	20.6	0.09	30	195	43	23.5	0.15	42.0	402	—	2.92	1.17	—	60.0	—	0.15/4.4
25	95	237	54	29.3	0.25	59	220	37	26.3	0.16	0	245	66	29.3	0.30	74.7	674	—	3.59	0.13	—	96.4	—	0.50/15.3
26	101	174	13	23.2	0.07	75	173	<5	20.7	0.05	30	199	<5	23.3	0.05	13.4	179	—	2.20	0.74	—	66.2	—	0.17/5.3
27	99	247	22	29.5	0.11	69	245	10	29.3	0.09	21	236	15	28.2	0.10	33.2	296	—	2.44	0.42	—	82.8	—	0.26/8.0
28	100	215	25	25.7	0.10	64	190	12	22.7	0.11	24	215	43	25.7	0.19	33.9	334	—	3.27	0.56	—	82.9	—	0.29/8.8
29	100	211	25	25.2	0.08	75	201	<5	24.0	0.06	21	224	25	28.9	0.10	24.4	213	—	3.22	0.51	—	84.3	—	0.27/8.2
30	102	174	27	22.0	0.09	77	168	<5	20.1	0.05	30	193	29	23.7	0.11	20.3	199	—	3.49	1.15	—	67.0	—	0.18/5.5
32	99	222	23	25.5	0.11	69	214	10	25.6	0.10	8	253	51	30 2	0.21	40.9	396	9.23	4.61	0.24	50.3	94.8	97.4	0.48/14.5
33	95	275	46	32.3	0.19	60	253	35	30.2	0.17	<5	263	67	31.4	0.30	81.2	708	8.13	3.42	0.18	57.9	94.67	97.8	0.43/13.0

TABLE VIII

SUMMARY OF TEST DATA FROM TVA'S FIRST TEST SERIES

(July-August, 1969)

Test No.	Gas Flow M ACFM	Unit Load MW	Pptr. Eff. %	Pptr. Gas Temp. °F	Lime-stone Rate Tons/Hr	WATTS / 10^3 ACFM	WATTS / 10^3 FT^2	MIGRATION VELOCITY W FT/SEC.	MIGRATION VELOCITY W CM/SEC.	GRAIN LOADING @32°F-29.92"Hg OUTLET grs./ft^3
4	258	140	95.8	303	0	94.3	818	0.46	13.9	0.0712
5	252	142	95.6	303	0	98.9	839	0.44	13.4	0.0697
7	200	134	97.2	308	0	132.2	890	0.40	12.2	0.0491
16	227	130	98.0	312	0	108.8	831	0.50	15.2	0.0309
24	282	144	94.9	304	0	101.4	963	0.47	14.3	0.0952
25	302	143	94.4	304	0	92.9	945	0.49	14.9	0.1284
27	250	125	96.7	271	0	102.0	858	0.48	14.6	0.0496
28	241	124	97.6	271	0	130.1	1056	0.50	15.4	0.0393
30	216	139	97.8	268	0	210.9	1534	0.46	14.1	0.0266
31	221	141	98.4	268	0	202.4	1506	0.51	15.6	0.0215
33	235	137	96.6	272	0	108.3	930	0.48	14.7	0.0455
34	237	137	95.7	272	0	100.1	866	0.45	13.8	0.0559
36	295	138	93.7	323	0	87.9	873	0.46	13.9	0.0792
38	327	137	95.8	317	0	136.0	1498	0.58	17.7	0.0596
39	324	136	94.0	317	0	104.4	1139	0.51	15.6	0.0839
41	340	137	94.9	308	0	108.9	1247	0.57	17.3	0.0837
42	373	136	95.0	308	0	88.2	1108	0.63	19.1	0.076

TABLE IX

SUMMARY OF TEST DATA FROM TVA'S FIRST TEST SERIES

(July-August, 1969)

Test No.	T-R SET 1A (FULL WAVE)					T-R SET 1A (FULL WAVE)					T-R SET 3A (FULL WAVE				
	Spks/Min	PRI Volts AC	PRI Amps AC	SEC. Amps DC	KV Avg.	Spks/Min	PRI Volts AC	PRI Amps AC	SEC. Amps DC	KV Avg.	Spks/Min	PRI Volts AC	PRI. Amps AC	SEC. Amps DC	KV Avg.
4	154	335	84	0.22	40.	129	341	86	0.215	40.8	148	269	51	0.21	32.1
5	195	342	86	0.22	40.8	150	360	83	0.215	43.0	145	267	46	0.21	31.9
7	214	335	97	0.25	40.0	193	327	92	0.22	39.1	141	285	50	0.23	34.0
16	329	345	90	0.22	41.2	105	358	65	0.21	42.8	148	278	50	0.20	33.2
24	27	360	89	0.245	43.0	12	372	83	0.205	44.5	143	268	59	0.28	32.0
25	40	363	93	0.26	43.4	14	377	86	0.22	45.1	145	262	50	0.22	31.3
27	140	329	90	0.235	39.3	121	348	78	0.20	41.6	143	266	48	0.25	31.8
28	291	284	87	0.22	33.9	139	317	72	0.195	37.9	167	337	78	0.41	40.3
30	78	342	102	0.29	40.9	63	358	94	0.255	42.8	1	318	105	0.60	38.0
31	132	320	98	0.29	38.2	100	326	94	0.24	38.9	2	328	106	0.62	39.2
33	167	324	89	0.24	38.7	130	344	80	0.21	41.1	140	280	62	0.29	33.5
34	177	348	88	0.235	41.6	132	332	75	0.195	39.7	142	265	48	0.26	31.7
36	69	333	93	0.255	39.8	47	372	81	0.20	44.5	143	275	47	0.21	32.9
38	15	350	111	0.325	41.8	15	350	111	0.325	41.8	123	315	84	0.46	37.6
39	16	351	112	0.33	41.9	16	351	112	0.33	41.9	145	245	48	0.21	29.3
41	28	336	112	0.325	40.2	28	336	112	0.325	40.7	135	286	64	0.32	34.7
42	92	322	106	0.2[illegible]	38.5	92	322	106	0.29	38.5	138	296	65	0.30	35.4

BLE X

SUMMARY OF TEST DATA FROM TVA'A SECOND TEST SERIES

(June-July, 1970)

Test No.	Gas Flow- M ACFM	Unit Load- MW	Pptr. Eff. %	Pptr. Gas Temp-°F	Ultimate Coal Analysis (Dry) Ash %	Ultimate Coal Analysis (Dry) Sulphur %	Ash / Sulphur Ratio	Lime-stone Rate Tons/Hr.	Coal Rate Tons/Hr.
4	286	140	89.4	309	14.4	2.0	7.2	0	62.5
5	255	140	73.4	309	15.0	1.4	10.7	11.0	62.5
8	247	142	83.3	303	14.2	2.2	6.5	9.5	64
10	234	127	86.8	315	13.3	2.9	4.6	0	56.5
11	239	130	70.3	315	13.9	4.1	3.4	9.0	58
13	271	140	84.3	315	14.3	2.9	4.9	0	62.5
14	266	141	70.9	315	19.9	2.4	8.3	5.0	63
15	269	144	70.9	315	23.8	2.5	9.5	9.5	68
17	277	140	81.4	317	16.7	2.7	6.2	0	62.5
18	278	143	61.2	317	23.7	2.6	9.1	5.0	66.5
19	250	145	47.0	317	28.6	2.4	11.9	10.0	69
21	283	141	73.3	320	14.5	2.1	6.9	0	63
23	301	143	85.7	311	19.2	2.4	8.0	0	66.5
24	290	141	68.7	311	16.6	3.4	4.9	10	63
26	296	141	92.3	311	16.7	3.1	5.4	0	63
27	300	142	68.8	311	16.3	2.6	6.3	5.5	64
28	302	142	67.9	311	15.1	2.4	6.3	9.5	64
30	279	134	94.7	313	18.9	3.3	5.7	0	59.5
31	277	134	78.8	313	17.3	2.9	6.0	5.15	59.5
32	279	134	81.8	313	18.5	3.0	6.2	10.0	59.5
34	298	140	83.8	316	21.8	2.5	8.7	5.0	62.5
35	289	141	76.3	316	15.3	3.0	5.1	10.0	63
36	289	140	86.3	316	15.7	2.9	5.4	0	62.5
38	314	143	85.8	314	18.3	2.7	6.8	5.5	66.5
39	311	144	78.2	314	15.4	3.0	5.1	10.0	68
40	311	144	79.8	314	15.3	2.8	5.5	0	68
42	306	142	91.3	316	17.7	3.4	5.2	0	64
43	306	143	82.7	316	16.1	3.0	5.4	4.5	66.5

TABLE XI

SUMMARY OF TEST DATA FROM TVA'S SECOND TEST SERIES

(June-July, 1970)

Test No.	WATTS / 10^3 ACFM	WATTS / 10^3 FT^2	MIGRATION VELOCITY W, ft/sec	MIGRATION VELOCITY W, cm/sec	GRAIN LOADING @ 32°F and 29.92"Hg OUTLET grs/ft^3
4	35.9	346	0.36	10.9	0.153
5	27.3	262	0.21	6.4	0.448
8	44.1	367	0.24	7.5	0.294
10	35.7	281	0.26	8.1	0.195
11	10.10	81	0.16	4.9	0.652
13	27.4	250	0.28	8.5	0.167
14	10.7	96	0.18	5.6	0.522
15	8.3	75	0.18	5.6	0.648
17	15.6	146	0.26	7.9	0.364
18	9.7	91	0.14	4.5	0.675
19	7.0	66	0.10	3.0	1.139
21	14.7	140	0.21	6.3	0.362
23	48.8	494	0.32	10.0	0.211
24	32.2	324	0.19	5.9	0.674
26	88.6	883	0.42	12.9	0.135
27	23.1	234	0.19	5.9	0.431
28	23.3	237	0.19	5.8	0.516
30	149.8	1407	0.46	14.0	0.0728
31	34.4	321	0.24	7.3	0.386
32	20.6	193	0.26	8.1	0.377
34	69.8	700	0.30	9.2	0.299
35	41.10	399	0.23	7.1	0.477
36	50.5	491	0.32	9.8	0.237
38	53.2	563	0.34	10.4	0.270
39	47.8	500	0.26	8.1	0.410
40	53.9	564	0.27	8.5	0.258
42	67.3	693	0.41	12.7	0.126
43	40.7	420	0.30	9.1	0.264

TABLE XII

SUMMARY OF TEST DATA FROM TVA'S SECOND TEST SERIES

(June-July, 1970)

Test No.	T-R SET 1A (FULL WAVE) SPKS Min.	PRI Volts AC	PRI Amps AC	Sec. Amps DC	KV Avg.	T-R SET 2A (FULL WAVE) SPKS Min.	PRI Volts AC	PRI Amps AC	SEC. Amps DC	KV Avg.	T-R SET 3A (FULL WAVE) SPKS Min.	PRI Volts AC	PRI Amps AC	SEC. Amps DC	KV Avg.
4	0	285	65	0.15	34.0	120	250	30	0.08	29.8	155	233	50	0.10	27.8
5	0	275	70	0.155	32.8	[illegible]	225	22	0.05	26.8	160	190	125	0.06	22.7
6	0	250	38	0.06	29.8	[illegible]	250	43	0.105	29.8	500	250	40	0.20	29.8
10	185	250	35	0.05	29.8	160	255	45	0.09	30.4	180	200	15	0.16	23.9
11	210	200	0	0.03	23.9	170	220	20	0.05	26.2	190	160	0	0.02	19.1
13	180	260	30	0.065	31.0	145	255	55	0.135	34.0	185	170	16	0.04	20.5
14	195	190	10	0.01	22.7	[illegible]	220	27	0.05	26.2	195	180	12	0.04	21.5
15	180	162	0	0.015	19.3	[illegible]	200	42	0.02	23.9	215	205	25	0.06	21.4
17	215	230	15	0.06	27.1	[illegible]	240	70	0.08	28.6	190	165	0	0.02	19.7
18	215	205	10	0.03	24.4	[illegible]	220	10	0.06	26.2	185	165	0	0.02	19.7
19	215	200	10	0.03	23.9	[illegible]	210	10	0.05	25.0	190	135	0	0	16.1
21	205	220	20	0.035	26.2	[illegible]	260	35	0.085	31.0	185	170	15	0.03	20.3
23	140	255	40	0.035	30.1	[illegible]	250	34	0.075	29.8	150	330	50	0.25	39.4
24	145	225	35	0.06	26.8	[illegible]	220	25	0.06	26.2	155	225	45	0.24	[illegible]
26	150	330	75	0.18	39.4	[illegible]	300	63	0.155	35.8	150	325	60	0.35	38.8
27	165	225	23	0.06	26.9	[illegible]	220	20	0.06	26.2	155	210	22	0.15	25.0
28	165	220	20	0.05	26.2	[illegible]	220	20	0.06	26.2	160	205	20	0.17	24.4
30	30	385	115	0.3	46.0	[illegible]	295	74	0.23	35.2	142	370	55	0.45	44.2
31	165	235	38	0.085	28.0	[illegible]	250	42	0.105	29.8	155	240	32	0.14	28.6
32	165	230	33	0.075	27.4	[illegible]	230	29	0.075	27.4	160	195	17	0.07	23.3
34	590	270	65	0.16	32.2	[illegible]	230	70	0.20	33.4	500	250	45	0.30	29.8
35	490	250	60	0.12	[illegible]	[illegible]	260	55	0.14	31.0	500	220	40	[illegible]	26.9
36	485	280	60	0.14	33.4	[illegible]	275	52	0.145	32.8	500	240	40	0.18	28.8
38	490	270	58	0.135	[illegible]	[illegible]	285	69	0.20	34.0	500	245	40	0.19	29.2
39	495	265	53	0.125	31.6	[illegible]	270	67	0.205	32.2	500	225	32	0.16	26.8
40	480	290	60	0.145	34.6	[illegible]	295	67	0.195	35.2	500	240	37	0.17	28.8
42	150	310	80	0.145	37.0	[illegible]	300	65	0.185	35.8	155	320	60	0.24	35.5
43	160	270	60	0.11	32.2	175	285	45	0.125	31.6	210	260	40	0.16	32.0

Reproduced from best available copy.

TABLE XIII

SUMMARY OF TEST DATA FROM TVA'S SECOND TEST SERIES

(June-July, 1970)

Test No.#	Gas Flow M ACFM	Unit Load MW	Pptr. Eff. %	Pptr. Gas Temp. °F	Ultimate Coal Analysis (Dry) Ash %	Ultimate Coal Analysis (Dry) Sulphur %	Ash/Sulphur Ratio	Limestone Rate Tons/Hr.	Coal Rate Tons/Hr.
44	299	144	85.3	316	15.9	2.7	5.9	9.5	68
46	295	142	92.6	306	17.1	2.7	6.3	0	64
47	283	139	77.3	306	15.8	2.7	5.9	5.0	62
48	280	140	83.4	306	15.7	3.0	5.2	10.0	62.5
50	239	142	93.7	307	14.0	2.7	5.2	0	64
51	237	142	91.1	313	14.0	2.8	5.0	5.0	64
52	239	143	89.6	320	14.3	3.0	4.8	10.0	66.5
54	285	140	89.8	310	13.7	2.7	5.1	0	62.5
55	285	141	71.3	310	13.6	2.8	4.9	3.3	63
56	280	141	79.3	310	13.7	2.8	4.9	2.25	63
58	279	142	94.9	304	14.0	2.8	5.0	0	64
59	279	142	88.3	304	13.2	2.7	4.9	2.3	64
60	283	144	82.0	304	12.9	2.5	5.2	1.25	68
61	302	141	91.6	304	13.8	2.6	5.3	0	63
62	296	143	81.3	304	14.0	2.6	5.4	1.2	66.5
64	294	142	93.4	310	14.2	3.1	4.6	0	64
65	293	142	82.6	310	13.6	2.8	4.9	5.0	64
66	290	142	74.0	310	13.6	2.6	5.2	10.5	64
68	287	140	85.6	309	14.8	2.5	5.9	0	62.5
69	275	140	78.6	309	16.3	2.4	6.8	1.4	62.5
70	273	142	78.8	309	15.8	2.4	6.6	5.5	64
72	227	139	88.5	311	20.2	2.5	8.1	0	62
73	222	140	88.0	311	14.0	2.4	5.8	1.3	62.5
74	223	143	87.2	311	16.2	2.4	6.8	5.5	66.5

TABLE XIV

SUMMARY OF TEST DATA FROM TVA'S SECOND TEST SERIES

(June-July, 1970)

Test No. #	WATTS / 10^3 ACFM	WATTS / 10^3 FT^2	MIGRATION VELOCITY		GRAIN LOADING @ 32°F and 29.92"Hg
			W ft/sec	W cm/sec	OUTLET grs/ft^3
44	21.7	219	0.32	9.8	0.319
46	62.7	623	0.43	13.1	0.1022
47	19.7	187	0.23	7.2	0.311
48	18.1	171	0.28	8.6	0.329
50	72.3	582	0.37	11.3	0.0990
51	33.8	269	0.32	9.8	0.145
52	29.5	237	0.30	9.2	0.228
54	57.1	548	0.36	11.1	0.149
55	21.6	207	0.20	6.1	0.362
56	20.5	193	0.24	7.5	0.334
58	63.2	593	0.46	14.2	0.0870
59	27.1	255	0.33	10.2	0.246
60	22.1	211	0.27	8.3	0.279
61	59.6	606	0.42	12.8	0.0965
62	34.6	345	0.27	8.5	0.243
64	94.1	931	0.44	13.6	0.0941
65	30.7	302	0.28	8.8	0.362
66	22.1	216	0.21	6.6	0.418
68	41.4	400	0.31	9.5	0.214
69	24.3	225	0.23	7.2	0.319
70	21.7	199	0.23	7.2	0.352
72	61.5	470	0.27	8.4	0.129
73	34.4	257	0.26	8.0	0.162
74	32.4	243	0.25	7.8	0.214

TABLE XV

SUMMARY OF TEST DATA FROM TVA'S SECOND TEST SERIES

(June-July, 1970)

Test No. #	T-R SET 1A (FULL WAVE)					T-R SET 2A (FULL WAVE)					T-R SET 3A (FULL WAVE)				
	SPKS/Min	PRI Volts AC	PRI Amps AC	SEC Amps DC	KV Avg.	SPKS/Min.	PRI Volts AC	PRI Amps AC	SEC. Amps DC	KV Avg.	SPKS/Min	PRI Volts AC	PRI Amps AC	SEC. Amps DC	KV Avg.
44	170	235	35	0.07	28.083	170	240	30	0.06	28.680	270	215	25	0.110	25.6
46	155	295	55	0.145	35.253	160	290	57	0.155	34.655	160	280	45	0.24	33.4
47	165	230	30	0.065	27.485	180	230	30	0.07	27.485	170	195	25	0.08	23.3
48	170	225	30	0.065	26.888	185	225	27	0.065	26.888	170	190	25	0.07	22.7
50	160	320	60	0.14	38.240	165	230	56	0.135	33.460	160	270	50	0.23	32.2
51	165	240	35	0.08	28.680	180	245	33	0.085	29.278	165	225	29	0.12	26.8
52	165	230	31	0.07	27.485	180	235	30	0.08	28.083	165	220	24	0.11	26.2
54	160	255	40	0.085	30.473	165	290	60	0.14	34.655	160	285	45	0.26	34.0
55	165	240	30	0.07	28.680	180	230	30	0.08	27.485	165	205	20	0.08	24.4
56	165	235	30	0.065	28.083	180	230	30	0.08	27.485	168	205	20	0.07	24.4
58	160	290	47	0.105	34.655	170	250	47	0.11	31.070	155	295	60	0.30	35.2
59	165	260	30	0.075	31.070	180	240	28	0.08	28.680	163	225	20	0.11	26.8
60	165	235	30	0.07	28.083	180	235	30	0.075	28.083	165	205	20	0.09	24.4
61	155	310	70	0.15	37.645	140	300	60	0.17	35.850	160	280	40	0.19	33.4
62	160	290	50	0.10	34.655	165	265	45	0.115	31.668	165	220	27	0.12	26.2
64	150	315	70	0.175	37.643	145	300	61	0.175	35.850	120	335	67	0.37	40.0
65	165	240	37	0.08	28.680	170	240	35	0.085	28.680	180	210	23	0.17	25.0
66	158	230	30	0.07	27.485	170	235	31	0.08	28.083	182	210	19	0.09	25.0
68	160	285	50	0.105	34.058	160	275	50	0.13	32.863	175	260	29	0.13	30.0
69	165	250	37	0.08	29.875	170	240	32	0.09	28.680	180	205	20	0.07	24.4
70	165	250	35	0.07	29.875	170	240	30	0.085	28.680	180	195	20	0.06	23.3
72	160	310	60	0.13	37.045	155	270	50	0.13	32.265	175	260	37	0.16	32.0
73	162	255	35	0.075	30.473	175	245	32	0.08	29.278	180	230	25	0.11	27.4
74	165	240	37	0.065	28.680	175	245	32	0.08	29.278	180	230	27	0.11	27.4

TABLE XVI

COAL ANALYSES FOR BOTH COTTRELL ENVIRONMENTAL SYSTEM'S TEST SERIES

(December, 1969 & July, 1971)

Run(1) No.	Moisture	Vol. Comb. Matter	Fixed Carbon	Ash	Sulfur				Ash/Sulfur
					Pyritic	Organic	Sulfate	Total	
1A&1B	10.10	33.93	44.52	11.45	1.44	1.32	0.04	2.80	4.2
2A	5.90	36.10	45.89	12.11	2.24	1.44	0.04	3.72	3.3
3A	9.90	35.66	45.89	10.78	1.25	0.88	0.02	2.15	5.0
3B	10.40	34.59	43.86	11.15	0.82	1.06	0.02	1.90	5.9
4A	9.40	35.53	45.90	9.17	1.16	1.52	0.03	2.71	3.4
4B	8.80	34.93	43.83	12.44	0.94	0.92	0.03	1.89	6.6
5A&5B	8.00	36.43	45.79	9.78	1.67	1.52	0.03	3.22	3.0
1	10.30	30.69	45.62	13.39	1.39	0.88	0.10	2.37	5.6
2	11.00	31.92	43.06	14.02	1.41	1.01	0.13	2.55	5.5
3	9.30	32.93	44.35	13.42	1.47	0.96	0.12	2.55	5.3
4	10.90	29.40	41.28	18.42	0.66	0.67	0.04	1.37	13.5
5	10.80	31.96	42.64	14.60	1.59	0.96	0.14	2.69	5.4
6	8.70	31.74	41.55	18.01	1.64	0.91	0.08	2.63	6.9
8	10.90	32.39	42.60	14.11	1.48	1.00	0.11	2.59	5.4
9	10.50	32.39	41.06	16.05	0.78	0.77	0.07	1.62	9.9
10	10.80	32.61	40.20	16.39	0.77	0.79	0.04	1.60	10.2
11	11.10	30.92	41.57	16.41	0.82	0.80	0.06	1.68	9.8
14	9.20	35.06	41.73	14.01	1.55	1.08	0.06	2.69	5.2
15	10.10	32.59	44.16	13.15	1.27	0.89	0.06	2.22	5.9
16	8.30	32.87	45.34	13.49	0.72	0.70	0.03	1.45	9.3
17	8.40	31.99	45.48	14.13	0.92	0.67	0.03	1.62	8.7
18	8.60	30.81	46.80	13.79	1.24	0.84	0.05	2.13	6.5
19	7.90	29.13	43.08	19.89	0.22	0.59	0.03	0.84	23.7
20	8.20	29.22	42.71	19.87	0.24	0.57	0.04	0.85	23.4
21	7.20	30.32	43.89	18.59	0.25	0.58	0.03	0.86	21.6
22	6.90	30.28	43.63	19.19	0.30	0.63	0.02	0.95	20.2
23	8.90	28.82	41.13	21.15	0.35	0.68	0.04	1.07	19.8
24	8.90	28.86	40.09	22.15	0.36	0.80	0.06	1.22	18.1
25	7.40	32.92	41.18	18.50	1.07	0.87	0.06	2.00	9.3
26	8.70	31.92	46.08	13.30	1.28	0.94	0.05	2.27	5.9
27	8.20	36.36	42.59	12.85	1.04	0.65	0.04	1.73	7.4
28	7.20	34.81	39.76	18.23	1.74	1.46	0.14	3.34	5.5
29	10.20	33.00	41.70	15.10	1.18	1.02	0.10	2.30	6.6
30	8.50	33.26	42.45	15.79	1.36	1.22	0.08	2.66	5.9
32	10.90	34.69	37.44	16.97	2.70	1.26	0.10	4.06	4.2
33	5.60	36.47	37.99	19.94	2.25	1.57	0.22	4.04	4.9

TABLE XVII

COAL ANALYSES FOR TVA'S FIRST TEST SERIES

(July-August, 1969)

TVA TEST NO.	MOISTURE	VOL. COMB. MATTER	FIXED CARBON	ASH	TOTAL SULFUR	HEATING VALUE BTU/LB.	ASH / SULFUR
4	11.9	34.62	42.99	10.48	2.73	11,189	3.8
5	12.2	33.80	42.85	11.15	3.16	10,993	3.5
7	13.0	32.80	42.72	11.48	3.39	10,823	3.4
16	9.2	35.05	42.77	12.98	2.63	11,168	4.9
24	9.4	34.34	43.94	12.32	3.08	11,298	4.0
25	9.6	33.99	44.93	11.48	2.44	11,327	4.7
27	11.4	31.36	43.50	13.73	2.04	10,738	6.7
28	10.9	32.34	43.93	12.83	2.41	10,968	5.3
30	9.9	35.50	44.42	10.18	2.70	11,533	3.8
31	10.3	34.44	44.67	10.58	2.69	11,401	3.9
33	10.7	32.24	45.63	11.43	2.14	11,171	5.3
34	10.9	31.90	45.98	11.26	1.69	11,191	6.7
36	8.8	34.11	44.41	12.68	3.01	11,300	4.2
38	8.3	34.39	45.57	11.74	3.39	11,545	3.5
39	8.3	34.85	44.75	12.10	3.76	11,527	3.2
41	7.9	33.89	45.04	13.17	3.59	11,448	3.7
42	8.3	34.00	46.07	11.33	3.02	11,580	3.8

TABLE XVIII

COAL ANALYSES FOR BABCOCK AND WILCOX PILOT TEST PROGRAM

(1967-1969)

	STANDARD TEST COALS COLBERT STEAM PLANT			TVA TEST COALS				LIGNITE COAL	HIGH SULFUR COAL
	B-22791 1st Shipment	C-13167 2nd Shipment 1st Box	C-13331 2nd Shipment 2nd Box	C-13273 Orient #3 Mine	C-13274 Atkinson Mine	C-13279 Old Ben #24 Mine	C-13319 Little Joe Mine	C-13376 North Dakota Lignite	C-13378 Peabody Coal Company
Proximate Analysis % Dry									
Volatile Matter	37.4	38.8	37.6	33.5	34.4	38.8	37.0	43.3	32.4
Fixed Carbon	47.4	48.2	47.9	49.8	46.7	50.2	46.9	48.0	55.0
Ash	15.2	13.0	14.5	16.7	18.9	11.0	16.1	8.7	12.6
BTU/lb Dry	12,150	12,560†	--	12,150	11,360	12,760	11,980	11,020	9.330
Ultimate Analysis % Dry									
Carbon	67.5	68.7	--	--	--	--	--	65.6	69.0
Hydrogen	4.6	4.9	--	--	--	--	--	4.5	3.7
Nitrogen (Calculated)	1.3	1.4	--	--	--	--	--	1.6	1.0
Sulfur	4.3	4.2	--	--	--	--	--	0.7	13.2
Ash	15.2	12.8	--	--	--	--	--	8.7	12.6
Oxygen (Difference)	7.1	8.0	--	--	--	--	--	19.1	0.5
Sulfur Forms % Dry gas Sulfur*									
Pyritic	2.7	1.4	--	0.8	2.6	1.3	1.9	0.1	10.9
Sulfate	0.1	0.9	--	<0.1	0.2	<0.1	0.1	<0.1	0.3
Organic (Difference)	1.5	1.9	--	0.6	1.2	1.3	1.6	0.6	2.0
Total	4.3	4.2	4.2	1.4	4.0	2.6	3.6	0.7	13.2
Chlorine % Dry	0.02	0.07	--	--	--	--	0.03	--	--
Ash Composition %									
SiO_2	39.	36.	--	52.	42.	45.	31.	25.	30.
Al_2O_3	16.	13.	--	24.	17.	22.	24.	8.	18.
Fe_2O_3	27.	28.	--	9.0	18.	17.	18.	11.	45.
TiO_2	0.5	0.4	--	0.6	0.6	0.5	0.5	0.4	0.4
CaO	9.0	9.0	--	6.0	13.	6.0	1.0	24.	1.0
MgO	0.3	0.5	--	2.0	0.9	1.0	1.0	9.0	0.4
Na_2O	0.6	0.6	--	1.4	0.8	1.3	0.5	3.0	0.3
K_2O	2.2	2.3	--	1.9	1.6	1.7	2.4	0.4	1.9
SO_3 (Gravimetric)	3.4	12.9	--	--	--	--	--	--	--
Ash Fusion Temperature °F*									
Atmosphere	Red. Oxid.	Red. Oxid.	Red. Oxid.	Red. Oxid.	Red. Oxid.	Red. Oxid.	Red. Oxid.	Red. Oxid.	Red. Oxid.
IT	1940 2240	1950 2250	-- --	2070 2200	1950 2160	2070 2270	1990 2440	2270 2280	1990 2370
SS	1990 2300	2000 2340	-- --	2270 2410	1990 2220	2140 2360	2170 2480	2350 2320	2070 2510
SH	2060 2340	2040 2380	-- --	2330 2460	2020 2250	2180 2410	2240 2500	2380 2340	2110 2550
FT 1/16	2340 2460	2310 2500	-- --	2740 2670	2270 2440	2650 2670	2680 2710	2450 2370	2460 2570
FT (flat)	2370 2510	2390 2540	-- --	2880 2860	2480 2540	2780 2750	2710 2800	2550 2430	2510 2580

†Calc. Btu (DuLong)
*ASTM Designations

TABLE XIX

PARTICLE SIZE ANALYSES FOR COTTRELL ENVIRONMENTAL SYSTEM'S FIRST TEST SERIES

(December, 1969)

Reproduced from best available copy.

Run No.	Cumulative Per Cent By Weight Less Than Indicated Particle Diameter									SP.GR. gm/cc	Sample Source
	Bahco					Sieve					
	2μ	5μ	10μ	20μ	30μ	44μ	74μ	149μ	297μ		
1A	5.8	18.0	30.0	41.0	48.0	66.2	74.0	95.2	98.6	2.17	Mech. Inlet
1B	10.2	28.0	42.2	62.0	71.8	69.0	97.0	97.9	99.8	2.65	Mech. Inlet
2A	6.4	17.0	28.6	43.0	53.0	74.0	84.0	95.0	99.4	2.16	Mech. Inlet
4A	2.8	12.2	26.0	44.4	46.0	87.0	92.8	98.0	99.7	2.31	Mech. Inlet
4B	4.8	13.0	28.0	49.2	62.4	86.2	87.2	95.4	99.7	2.58	Mech. Inlet
5A	3.0	13.8	26.2	42.0	51.0	77.8	84.8	92.2	95.6	2.41	Mech. Inlet
5B	4.2	16.8	30.2	35.6	54.0	84.0	85.0	92.4	96.0	2.26	Mech. Inlet
2A	6.9	37.0	68.8	89.6	95.5	86.2	90.4	95.0	97.8	2.40	Pptr. Inlet
3A	11.9	48.0	74.2	90.4	95.0	89.0	92.4	95.8	98.0	2.16	Pptr. Inlet
3B	10.6	46.6	76.6	93.2	97.2	91.2	94.2	97.0	98.3	2.24	Pptr. Inlet
4A	12.5	49.4	78.	93.6	97.4	92.0	96.8	98.6	99.1	2.40	Pptr. Inlet
4B	12.0	49.2	78.0	93.6	97.4	90.0	95.2	97.9	99.0	2.41	Pptr. Inlet
5A	9.2	43.6	75.6	94.2	98.2	89.4	93.6	97.0	98.8	2.34	Pptr. Inlet
5B	11.5	46.0	76.2	94.0	98.0	92.4	95.2	97.8	99.1	2.53	Pptr. Inlet
2A	13.8	50.0	73.8	89.2	94.2	86.0	88.0	93.5	97.8	1.97	Pptr. Outlet
3A	25.4	48.4	76.0	93.8	96.8	82.0	88.8	95.8	98.0	1.71	Pptr. Outlet
3B	9.0	40.6	81.8	92.5	94.8	73.4	83.8	91.5	95.6	2.05	Pptr. Outlet
4B	13.6	52.6	79.0	92.0	95.0	86.5	89.8	94.0	97.0	2.20	Pptr. Outlet
1A&1B	2.2	8.2	20.8	40.6	50.4	86.2	89.6	98.9	99.7	1.64	Mech. Coll. Hopper & Catch
2A	3.8	10.8	24.0	45.4	59.8	78.0	94.2	97.8	99.4	—	Mech. Pptr.
3A&3B	2.2	7.4	17.0	34.0	47.4	82.5	87.2	98.0	99.6	2.38	Mech. Coll. Hopper & Catch
3A&4A	3.4	10.8	24.2	41.0	48.2	86.0	89.0	98.7	99.78	2.38	Mech. Coll. Hopper & Catch
5A&5B	3.4	9.8	20.2	37.8	50.0	86.5	89.8	97.8	99.72	2.37	Mech. Pptr. Hopper
1A&1B	17.5	58.0	81.5	93.2	96.8	38.0	91.5	98.6	99.6	2.15	Electrostatic Collector
2A	13.0	49.6	78.0	94.0	97.8	89.0	94.5	99.0	99.6	2.26	Elect. Pptr. Hopper
3A&4A	13.0	48.0	86.0	93.0	97.2	68.0	96.8	99.5	99.9	1.64	Elect. Pptr. Hopper & Catch
5A&5B	14.8	51.0	79.8	95.0	98.2	63.0	93.0	98.2	99.5	2.21	Elect. Pptr. Hopper & Catch

TABLE XX

PARTICLE SIZE ANALYSES FOR COTTRELL ENVIRONMENTAL SYSTEM'S SECOND TEST SERIES

(July, 1971)

Run No.	Cumulative Per Cent By Weight Less Than Indicated Particle Diameter									SP.GR. gm/cc	Sample Source
	Dahco					Sieve					
	2µ	5µ	10µ	20µ	30µ	44µ	74µ	149µ	297µ		
6	16.5	42.0	61.5	75.0	79.5	92.8	97.5	100.0	100.0	2.68	Limestone Feed Tank
8	19.2	47.5	67.5	79.0	82.0	94.3	99.1	100.0	100.0	2.61	Limestone Feed Tank
14	10.8	28.0	42.0	49.0	52.0	62.5	64.4	79.2	94.0	2.60	Limestone Feed Tank
23	15.5	44.0	65.0	77.0	81.5	97.1	99.2	99.9	100.0	2.51	Limestone Feed Tank
24	15.0	43.0	65.0	76.0	80.0	96.0	97.9	99.9	100.0	2.34	Limestone Feed Tank
32	10.0	28.0	43.5	52.0	55.0	64.5	82.2	85.6	96.0	2.54	Limestone Feed Tank
33	9.7	27.5	42.5	51.0	54.5	62.4	78.5	82.4	95.5	2.50	Limestone Feed Tank
2	8.2	33.5	55.8	76.0	84.8	92.9	97.1	99.41	99.78	2.85	Mech. Inlet
2	9.0	36.0	83.0	95.5	96.9	93.6	94.6	95.8	97.6	2.80	Pptr. Inlet
2	10.8	50.0	82.5	93.6	94.9	90.6	91.6	93.2	96.9	2.75	Pptr. Outlet
3	7.0	32.4	54.0	74.0	83.0	90.4	96.2	99.3	99.7	2.49	Mech. Inlet
3	6.4	38.4	71.0	92.8	97.4	99.25	99.5	99.8	99.9	2.48	Pptr. Inlet
3	3.6	18.1	41.0	67.0	80.0	90.0	94.6	99.15	99.76	2.36	Pptr. Outlet
4	7.8	46.0	81.2	95.5	97.4	98.3	98.6	99.04	99.1	3.07	Pptr. Inlet
4	9.0	40.8	72.4	92.4	97.2	93.5	94.3	95.4	97.9	2.56	Pptr. Outlet
5	4.4	20.2	44.0	70.0	82.0	88.9	92.1	95.5	98.3	1.89	Mech. Inlet
5	7.0	39.8	74.0	94.0	98.2	95.4	95.8	97.2	98.9	3.11	Pptr. Inlet
5	7.0	38.0	72.0	90.0	94.2	39.1	59.1	76.2	87.0	2.86	Pptr. Outlet
6	5.2	22.4	46.0	71.0	83.8	92.1	94.4	98.9	99.6	2.70	Mech. Inlet
6	6.8	40.0	75.8	95.0	98.6	97.3	98.3	98.8	99.2	2.30	Pptr. Inlet
6	4.0	34.4	68.4	88.2	93.0	99.4	99.7	99.9	99.96	1.38	Pptr. Outlet
8	5.2	21.6	44.0	68.4	80.5	89.0	95.6	98.1	98.8	2.39	Mech. Inlet
8	8.2	47.0	79.6	95.0	98.0	99.3	99.5	99.87	99.92	2.66	Pptr. Inlet
8	—	—	—	—	—	65.7	89.3	97.8	99.1	—	Pptr. Outlet
9	—	—	—	—	—	68.5	94.1	96.2	99.4	2.31	Pptr. Inlet
10	5.0	31.0	65.8	88.8	95.0	96.4	97.2	97.5	97.8	2.63	Pptr. Inlet
11	6.0	38.8	75.0	94.8	97.5	98.3	99.2	99.8	99.9	2.50	Pptr. Inlet
11	9.8	31.2	71.8	91.5	96.6	96.6	97.6	99.9	99.99	3.19	Pptr. Outlet
14	4.8	20.0	41.0	65.2	77.6	86.2	92.9	95.5	98.6	2.53	Mech. Inlet
14	9.2	46.0	79.8	96.0	98.9	99.5	99.5	99.7	99.7	2.91	Pptr. Inlet
14	5.5	29.6	60.0	85.5	93.6	99.5	99.5	99.5	99.94	2.91	Pptr. Outlet
15	7.4	25.0	46.4	69.6	80.5	91.6	95.1	98.9	99.4	2.48	Mech. Inlet
15	3.8	32.0	70.0	93.5	98.2	98.7	98.9	99.0	99.2	2.55	Pptr. Inlet
16	3.5	28.6	65.0	91.0	97.0	98.3	98.8	99.5	99.5	2.50	Pptr. Inlet

TABLE XXI

PARTICLE SIZE ANALYSES FOR COTTRELL ENVIRONMENTAL SYSTEM'S SECOND TEST SERIES

Reproduced from best available copy.

(July, 1971)

Run No.	Cumulative Per Cent By Weight Less Than Indicated Particle Diameter									SP.GR. gm/cc	Sample Source
	Bahco					Sieve					
	2μ	5μ	10μ	20μ	30μ	44μ	74μ	149μ	297μ		
17	5.0	29.8	62.0	87.8	95.0	98.0	98.5	99.4	99.8	2.47	Pptr. Inlet
18	6.5	33.0	73.0	93.6	98.0	97.9	98.3	99.3	99.6	2.09	Pptr. Inlet
19	—	—	—	—	—	95.9	96.6	98.6	99.6	—	Pptr. Outlet
19	11.0	42.0	63.8	81.0	88.0	92.2	97.9	99.1	99.77	2.37	Pptr. Inlet
20	6.5	30.0	52.0	73.6	91.6	65.9	93.0	99.0	99.77	2.51	Pptr. Inlet
21	13.6	52.0	82.0	96.2	98.8	98.6	99.0	99.45	99.64	2.62	Pptr. Inlet
22	13.0	51.8	82.0	96.4	99.0	98.2	98.9	99.4	99.7	2.63	Pptr. Inlet
23	16.0	56.0	85.0	97.2	99.4	98.3	98.8	99.2	99.4	2.67	Pptr. Inlet
23	15.0	55.6	84.0	94.2	96.2	98.3	98.9	99.5	99.9	2.21	Pptr. Outlet
24	14.0	57.2	84.5	96.0	98.3	97.6	97.9	98.6	98.8	2.75	Pptr. Inlet
24	13.2	52.2	79.8	93.0	96.0	98.2	98.8	99.4	99.8	2.76	Pptr. Outlet
25	8.8	44.6	77.0	93.2	96.5	98.8	99.1	99.5	99.7	2.71	Pptr. Inlet
26	11.2	51.8	83.0	96.0	98.4	98.1	98.6	99.0	99.4	4.33	Pptr. Inlet
26	7.8	38.0	69.6	89.8	94.2	93.2	96.6	97.6	98.8	2.63	Pptr. Outlet
27	4.4	25.6	61.0	88.2	95.8	98.6	99.1	99.5	99.8		Pptr. Inlet
27	—	—	—	—	—	—	—	—	—	—	Pptr. Outlet
28	18.2	59.6	85.6	96.2	98.2	98.0	98.4	98.9	99.2	2.89	Pptr. Inlet
28	—	—	—	—	—	96.6	97.1	99.1	99.6	2.83	Pptr. Outlet
29	5.0	37.8	78.4	94.5	97.4	97.9	98.1	98.7	99.1	2.37	Pptr. Inlet
30	—	—	—	—	—	90.9	98.3	99.1	99.5	2.66	Pptr. Outlet
30	10.6	50.4	79.6	93.8	98.0	98.6	99.0	99.3	99.6	3.02	Pptr. Inlet
30	22.2	70.0	90.2	96.5	97.8	98.4	98.9	99.5	99.7	3.93	Pptr. Outlet
32	9.6	31.6	42.0	71.4	79.6	93.3	94.8	98.2	99.8	2.62	Mech. Inlet
32	9.8	48.0	80.4	95.4	98.2	99.4	99.7	99.8	99.9	2.69	Pptr. Inlet
33	18.2	44.0	64.0	78.2	84.0	95.6	97.5	99.3	99.7	3.11	Mech. Inlet
33	10.0	48.4	90.8	95.8	98.6	98.8	99.2	99.6	99.9		Pptr. Inlet
2	4.8	14.6	28.2	48.0	60.2	88.3	94.7	99.7	99.99	2.85	← Mechanical Hoppers "B" Side 1, 2, 5, 6 →
3	4.4	14.2	27.6	45.0	56.0	84.1	95.7	99.9	100.00	2.98	
5	3.5	12.5	26.0	44.0	56.0	88.1	91.1	99.4	99.99	2.52	
6	2.8	10.2	22.2	39.6	51.0	79.7	87.8	99.2	99.93	2.49	
8	3.6	13.0	27.0	46.0	58.0	90.5	93.5	99.5	99.92	2.71	
14	2.8	11.8	22.4	36.8	46.0	64.9	87.0	96.1	99.5	2.83	
15	2.2	11.6	23.0	38.0	48.0	64.7	87.6	94.0	99.6	3.04	
32	2.8	12.6	24.2	40.2	50.2	83.2	82.2	96.3	99.7	2.74	
33	3.0	10.8	23.0	40.0	51.8	79.5	87.0	97.3	99.7	2.80	

TABLE XXII

PARTICLE SIZE ANALYSES FOR COTTRELL ENVIRONMENTAL SYSTEM'S SECOND TEST SERIES

(July, 1971)

Run No.	Cumulative Per Cent By Weight Less Than Indicated Particle Diameter										
	Bahco					Sieve				SP.GR. gm/cc	Sample Source
	2μ	5μ	10μ	20μ	30μ	44μ	74μ	149μ	297μ		
15	17.8	60.4	88.2	98.2	99.58	99.9	99.9	100.00	100.00	2.63	Electrical Pptr. Hoppers "B" Side 1, 2, 5, 6
16	16.8	58.0	86.0	97.4	99.3	99.8	99.94	99.96	100.00	2.29	
14	15.8	59.6	87.0	97.2	99.1	99.8	99.3	99.95	99.95	2.43	
17	16.2	61.6	88.0	97.8	99.2	99.5	99.6	99.7	100.00	2.65	
18	17.2	62.0	88.2	98.1	99.5	99.9	99.99	100.00	100.00	2.75	
21	14.0	54.0	89.0	92.6	94.5	96.9	97.6	99.6	99.95	2.16	
22	17.5	61.8	86.0	96.2	98.4	98.3	98.7	99.5	99.8	2.46	
23	17.5	57.8	82.8	95.0	97.9	98.1	98.8	99.8	99.91	2.55	
24	18.0	53.0	82.8	94.2	96.9	97.3	99.2	99.7	100.00	2.56	

TABLE XXIII

LABORATORY AND IN-SITU RESISTIVITY MEASUREMENTS FOR COTTRELL ENVIRONMENTAL SYSTEM'S FIRST TEST SERIES

(December, 1969)

Run No.	Sample Source	Lab Rdsistivity - OHM CM (6% Moisture in Gas)					Temp °F	In-Situ Resistivity
		250°F.	350°F.	450°F.	550°F.	650°F.		
1A	AH Inlet						509	1.4×10^{10}
1B	AH Inlet						510	4.3×10^{10}
3A	AH Inlet						520	1.3×10^{10}
4A	AH Inlet						520	1.2×10^{10}
5A	AH Inlet						634	3.7×10^{9}
5B	AH Inlet						638	1.1×10^{10}
1A	MC	1.1×10^{13}	1.4×10^{12}	1.6×10^{11}	1.1×10^{10}	1.1×10^{9}		
1B	MC	1.4×10^{14}	1.5×10^{13}	1.6×10^{12}	1.8×10^{11}	1.2×10^{10}		
3A	MC	1.4×10^{13}	2.5×10^{12}	2.3×10^{11}	1.2×10^{10}	9.0×10^{8}		
4A	MC	2.1×10^{12}	9.0×10^{11}	6.8×10^{10}	9.0×10^{9}	9.0×10^{8}		
4B	MC	9.0×10^{12}	1.4×10^{13}	1.1×10^{12}	1.2×10^{11}	1.8×10^{10}		
5A	MC	1.9×10^{12}	1.7×10^{11}	4.5×10^{10}	6.8×10^{9}	1.2×10^{9}		
5B	MC	5.4×10^{12}	1.3×10^{12}	1.1×10^{12}	3.4×10^{11}	6.8×10^{10}		
2A	Pptr. Inlet	1.2×10^{12}	9.0×10^{11}	5.4×10^{11}	4.5×10^{10}	6.8×10^{9}	293	4.8×10^{9}
3A	Pptr. Inlet	1.4×10^{12}	5.4×10^{11}	5.4×10^{10}	6.8×10^{9}	9.0×10^{8}	318	2.1×10^{10}
3B	Pptr. Inlet	1.6×10^{12}	9.0×10^{11}	1.1×10^{11}	9.0×10^{10}	5.4×10^{8}	293	2.6×10^{11}
4A	Pptr. Inlet	1.6×10^{12}	6.8×10^{11}	9.0×10^{10}	6.8×10^{9}	9.0×10^{8}	312	4.7×10^{10}
4B	Pptr. Inlet	2.5×10^{12}	1.8×10^{12}	2.7×10^{11}	1.8×10^{10}	1.5×10^{9}	302	3.0×10^{11}
5A	Pptr. Inlet	9.0×10^{12}	1.6×10^{12}	1.7×10^{11}	9.0×10^{9}	1.1×10^{9}		
5B	Pptr. Inlet	5.4×10^{12}	1.5×10^{12}	1.6×10^{11}	9.0×10^{9}	1.4×10^{9}		
2A	Pptr. Outlet	6.8×10^{12}	1.4×10^{12}	1.7×10^{11}	1.1×10^{10}	1.1×10^{9}		
3A	Pptr. Outlet	1.2×10^{12}	3.9×10^{11}	1.5×10^{11}	1.4×10^{10}	1.3×10^{9}		
3B	Pptr. Outlet	1.0×10^{12}	5.4×10^{11}	1.4×10^{11}	1.5×10^{10}	1.2×10^{9}		
4B	Pptr. Outlet	1.4×10^{11}	2.7×10^{11}	6.8×10^{10}	6.8×10^{9}	6.8×10^{8}		
5B	Pptr. Outlet	1.1×10^{12}	4.5×10^{11}	1.6×10^{10}	3.9×10^{9}	6.8×10^{8}		

TABLE XXIV

LABORATORY AND IN-SITU RESISTIVITY MEASUREMENTS FOR COTTRELL ENVIRONMENTAL SYSTEM'S SECOND TEST SERIES

(July, 1971)

Run No.	Source Sample	Lab Resistivity - OHM-CM (6% Moisture in Gas)							Temp. °F	In-Situ Resistivity
		200°F.	250°F.	300°F.	350°F.	400°F.	500°F.	600°F.		
19	Pptr. Inlet	3.4×10^{13}	5.4×10^{13}	4.5×10^{13}	3.9×10^{13}	5.4×10^{12}	3.4×10^{11}	1.9×10^{10}	260	2.8×10^{10}
20	Pptr. Inlet	4.5×10^{10}	2.1×10^{13}	2.7×10^{13}	2.3×10^{13}	9.0×10^{12}	5.4×10^{11}	5.4×10^{10}	330	1.8×10^{11}
21	Pptr. Inlet	9.0×10^{12}	1.4×10^{14}	2.3×10^{13}	1.4×10^{13}	4.5×10^{12}	2.1×10^{11}	1.3×10^{10}	260	1.4×10^{11}
22	Pptr. Inlet	1.8×10^{13}	5.4×10^{13}	2.7×10^{13}	2.7×10^{13}	9.0×10^{12}	1.4×10^{12}	1.1×10^{11}	322	1.8×10^{11}
23	Pptr. Inlet	6.8×10^{12}	6.8×10^{13}	4.5×10^{13}	3.9×10^{13}	2.7×10^{13}	2.7×10^{12}	9.0×10^{11}	323	3.7×10^{12}
24	Pptr. Inlet	9.0×10^{12}	2.7×10^{14}	1.4×10^{14}	9.0×10^{13}	6.8×10^{13}	9.0×10^{13}	1.4×10^{13}	328	2.9×10^{12}
28	Pptr. Inlet	3.0×10^{12}	--	9.0×10^{13}	--	1.4×10^{14}	3.4×10^{13}	1.4×10^{13}	320	5.9×10^{12}
32	Pptr. Inlet	3.0×10^{11}	--	6.8×10^{13}	--	1.4×10^{14}	1.4×10^{14}	6.8×10^{13}	325	8.3×10^{11}
33	Pptr. Inlet	2.7×10^{12}	--	3.9×10^{13}	--	5.4×10^{13}	3.9×10^{13}	6.8×10^{12}	260	9.1×10^{11}
1	Pptr. Inlet								315	1.1×10^{11}
2	Pptr. Inlet								312	1.2×10^{12}
3	Pptr. Inlet								250	5.7×10^{10}
4	Pptr. Inlet								325	1.6×10^{11}
5	Pptr. Inlet								268	2.1×10^{11}
6	Pptr. Inlet								323	5.6×10^{11}
8	Pptr. Inlet								285	1.6×10^{11}
9	Pptr. Inlet								280	3.8×10^{11}
10	Pptr. Inlet								260	6.7×10^{11}
11	Pptr. Inlet								320	6.5×10^{11}
14	Pptr. Inlet								320	8.9×10^{11}
15	Pptr. Inlet								262	1.4×10^{11}
16	Pptr. Inlet								270	2.9×10^{12}
17	Pptr. Inlet								262	2.3×10^{11}
18	Pptr. Inlet								310	5.6×10^{11}
25	Pptr. Inlet								270	1.4×10^{12}
26	Pptr. Inlet								326	2.4×10^{11}
27	Pptr. Inlet								272	1.5×10^{11}
29	Pptr. Inlet								265	4.3×10^{11}
30	Pptr. Inlet								320	9.0×10^{12}

Reproduced from best available copy.

TABLE XXV

LABORATORY AND IN-SITU RESISTIVITY MEASUREMENTS FOR COTTRELL ENVIRONMENTAL SYSTEM'S SECOND TEST SERIES

(July, 1971)

Run No.	Source Sample	Lab Resistivity - OHM-CM (6% Moisture in Gas)						Temp. °F.	In-Situ Resistivity
		200°F	300°F	400°F	500°F	600°F	650°F		
4	Pptr. Inlet	$2.7x10^{9}$	$6.8x10^{11}$	$2.5x10^{12}$	$1.6x10^{12}$	$2.7x10^{11}$	$1.4x10^{11}$	325	$1.6x10^{11}$
9	Pptr. Inlet	$4.5x10^{6}$	$2.7x10^{9}$	$9.0x10^{10}$	$1.3x10^{10}$	$3.0x10^{9}$	$1.8x10^{9}$	280	$3.8x10^{11}$
10	Pptr. Inlet	$3.3x10^{10}$	$9.0x10^{11}$	$1.3x10^{13}$	$3.4x10^{12}$	$2.5x10^{11}$	$9.0x10^{10}$	260	$6.7x10^{11}$
25	Pptr. Inlet	$4.5x10^{12}$	$3.9x10^{13}$	$9.0x10^{13}$	$2.7x10^{13}$	$5.4x10^{12}$	$3.9x10^{12}$	270	$1.4x10^{12}$
30	Pptr. Inlet	$3.9x10^{12}$	$3.4x10^{13}$	$4.5x10^{13}$	$1.8x10^{13}$	$3.0x10^{12}$	$1.8x10^{12}$	320	$9.0x10^{12}$

TABLE XXVI

LABORATORY AND IN-SITU RESISTIVITY MEASUREMENTS FOR BABCOCK AND WILCOX PILOT TEST PROGRAM

(1967-1969)

Legend	Test No.	Coal No.	Laboratory Resistivity, ohm-cm			In Situ Resistivity, ohm-cm	
			300 F	600 F	At In Situ Temp	Temp, F	Resistivity
●	67-7-1	B-22791	3.2×10^{12}	6.7×10^{10}	-	-	-
	68-4-1		4.0×10^{12}	2.0×10^{10}	9.0×10^{10}	505	1.0×10^{10}
	68-7-10		1.8×10^{13}	3.9×10^{11}	1.8×10^{13}	299	2.7×10^{10}
	68-4-11		-	-	-	460	1.6×10^{10}
	68-5-2		-	-	-	425	4.3×10^{9}
	69-2-11		-	-	-	300	1.9×10^{11}
○	69-4-2	C-13167	2.5×10^{12}	8.4×10^{9}	1.0×10^{12}	270	1.7×10^{11}
	69-4-4		3.4×10^{12}	6.8×10^{9}	2.5×10^{12}	310	1.6×10^{11}
	69-4-5		2.7×10^{13}	6.8×10^{11}	2.7×10^{13}	300	2.6×10^{10}
	69-4-6		2.7×10^{12}	3.9×10^{10}	2.5×10^{12}	305	2.6×10^{10}
	69-4-8		-	-	-	300	1.3×10^{11}
▲	69-4-13	C-13273	1.2×10^{12}	6.8×10^{9}	1.0×10^{12}	310	1.1×10^{11}
	69-4-15		-	-	-	310	1.8×10^{11}
△	69-4-19	C-13274	2.1×10^{12}	4.5×10^{9}	2.1×10^{12}	300	3.4×10^{11}
	69-4-21		-	-	-	320	4.4×10^{10}
⬢	69-4-25	C-13279	4.5×10^{11}	6.8×10^{9}	4.0×10^{11}	310	4.6×10^{11}
	69-5-1		-	-	-	305	3.1×10^{11}
	69-5-5		-	-	-	355	7.2×10^{10}
⬡	69-7-7	C-13319	4.5×10^{12}	6.8×10^{9}	4.0×10^{12}	313	5.7×10^{10}
■	69-11-11	C-13376	1.5×10^{11}	1.4×10^{9}	1.3×10^{11}	400	3.2×10^{10}
	69-11-13		-	-	-	365	6.2×10^{9}
□	69-12-5	C-13378	8.4×10^{12}	5.4×10^{9}	8.0×10^{12}	295	1.4×10^{12}

● ○ Standard Test Coal
Colbert Steam Plant (TVA)
▲ Orient #3 Mine (TVA)
△ Ackinson Mine (TVA)
⬢ Old Ben #24 Mine (TVA)
⬡ Little Joe Mine (TVA)

TABLE XXVII

SUMMARY OF CHEMICAL ANALYSES PERFORMED ON SAMPLES TAKEN DURING THE FIRST CES TEST SERIES

Test Date	Sample Identification	CES Test No.	TVA Lab No.	% SiO_2	% Al_2O_3	% Fe_2O_3	% CaO	% MgO	% TiO_2	% Na_2O	% K_2O	% $SO_4^=$	% Loss on Ignition
12-11-69	MC Inlet	1A	C-34	46.8	20.9	16.7	7.0	1.0	0.7	0.8	2.2	1.3	2.2
12-11	MC Hopper	–	C-48	46.3	20.2	16.9	7.1	1.0	0.9	0.6	1.7	1.6	2.6
12-11	ESP Hopper	–	C-53	49.9	23.2	10.6	4.7	1.2	1.1	0.8	2.0	2.8	2.7
12-11	MC Inlet	1B	C-35	46.8	20.1	16.3	6.4	1.1	0.9	0.7	2.2	1.8	3.9
12-12	MC Outlet	2A	C-41	48.0	20.7	14.2	5.4	1.0	1.0	0.6	2.3	2.5	2.8
12-12	MC Hopper	–	C-49	45.6	20.0	18.2	6.7	1.1	0.9	0.5	1.7	1.5	2.3
12-12	ESP Hopper	–	C-54	47.4	21.4	13.6	5.3	1.2	1.1	0.6	1.9	2.5	2.8
12-13	MC Outlet	3B	C-43	49.8	24.1	9.7	4.5	1.3	1.0	1.0	2.3	1.2	3.1
12-13	MC Inlet	4B	C-38	46.5	20.9	13.6	6.7	1.0	0.7	0.9	2.0	1.0	4.6
12-13	MC Outlet	4B	C-45	50.1	23.7	10.1	4.5	1.4	0.9	1.0	2.1	1.2	2.7
12-13	MC Hopper	–	C-51	46.0	20.6	14.6	7.7	1.1	1.0	0.6	1.7	1.1	3.1
12-14	MC Inlet	3A	C-36	47.6	21.9	16.4	6.6	1.0	0.7	0.7	2.0	0.9	2.2
12-14	MC Outlet	3A	C-42	50.1	24.5	10.1	4.0	1.5	1.0	0.9	2.3	1.6	2.3
12-14	MC Inlet	4A	C-37	47.3	21.1	16.0	6.3	0.9	0.7	0.8	2.0	1.1	2.4
12-14	MC Outlet	4A	C-44	50.6	24.0	10.2	4.1	1.2	1.0	1.0	2.2	1.5	2.1
12-14	MC Hopper	–	C-50	45.6	19.9	17.9	6.9	1.0	0.8	0.5	1.4	0.8	4.0
12-14	ESP Hopper	–	C-55	50.3	24.0	10.1	4.2	1.3	1.1	0.8	1.9	1.7	2.8
12-15	MC Inlet	5A	C-39	43.4	19.8	25.1	3.5	1.0	0.8	0.4	1.8	0.9	3.2
12-15	MC Outlet	5A	C-46	50.1	23.4	14.1	2.4	1.2	1.0	0.5	2.0	1.6	2.6
12-15	MC Inlet	5B	C-40	42.6	19.3	22.0	3.8	0.9	0.9	0.4	1.8	0.7	5.0
12-15	MC Outlet	5B	C-47	49.6	23.0	14.1	2.9	1.3	1.0	0.5	1.9	1.3	3.0
12-15	MC Hopper	–	C-52	43.6	18.5	24.0	4.6	1.0	0.9	0.3	1.4	0.8	3.1
12-15	ESP Hopper	–	C-56	49.8	22.9	12.6	3.1	1.4	1.1	0.6	1.9	1.6	2.5
-	AH Inlet	–	C-57	47.4	21.0	13.5	5.9	1.2	1.1	0.7	1.7	2.2	3.2

TABLE XXVIII

SUMMARY OF CHEMICAL ANALYSES PERFORMED ON SAMPLES TAKEN DURING THE SECOND CES TEST SERIES

Test Date	Sample Identification	CES Test No.	TVA Lab No.	% $S^=$	% $SO_4^=$	% $SO_3^=$	Total %S	% CaO
7-10-71	MC Inlet	2	C-883	<0.1	6.4	6.7	4.8	30.8
"	MC Outlet	2	C-881		7.8	10.8	6.9	28.6
"	ESP Outlet	2	C-882		6.3	2.0	2.9	19.9
"	MC Hopper	2	C-774		4.9	0.1	1.7	32.5
"	ESP Hopper	2	C-773		6.7	0.1	2.3	24.2
7-13-71	MC Inlet	6	C-895		4.8	7.8	4.7	33.0
"	MC Outlet	6	C-893		5.6	10.5	6.1	30.0
"	ESP Outlet	6	C-894		4.0	3.0	2.5	30.2
"	MC Hopper	6	C-790		2.6	0.3	1.0	22.0
"	ESP Hopper	6	C-789		4.6	1.1	2.0	32.5
7-14-71	MC Inlet	8	C-898		5.3	9.6	5.6	33.3
"	MC Outlet	8	C-896		6.6	12.3	7.1	31.4
"	ESP Outlet	8	C-897		5.0	8.5	5.1	22.1
"	MC Hopper	8	C-794		4.4	0.2	1.6	37.5
"	ESP Hopper	8	C-793		4.7	0.5	1.7	24.1
7-15-71	MC Outlet	9	C-899		4.4	<0.1	1.5	4.5
"	MC Outlet	10	C-901		4.5	11.7	6.2	23.5
"	MC Outlet	11	C-903		5.2	7.9	4.9	31.6
7-24-71	MC Inlet	14	C-907		5.4	8.2	5.1	35.6
"	MC Outlet	14	C-905		7.3	7.9	5.6	33.9

TABLE XXVIII (continued)

SUMMARY OF CHEMICAL ANALYSES PERFORMED ON SAMPLES TAKEN DURING THE SECOND CES TEST SERIES

Test Date	Sample Identification	CES Test No.	TVA Lab No.	% $S^=$	% $SO_4^=$	% $SO_3^=$	Total %S	% CaO
7-24-71	ESP Outlet	14	C-906	<0.1	5.6	5.0	3.9	28.0
"	MC Hopper	14	C-814		4.5	0.5	1.7	46.5
"	ESP Hopper	14	C-813		5.2	0.9	2.1	24.6
7-24-71	MC Inlet	15	C-910		5.6	7.7	5.0	36.7
"	MC Outlet	15	C-908		6.9	10.8	6.6	34.7
"	ESP Outlet	15	C-909		5.5	5.5	4.0	26.6
"	MC Hopper	15	C-817		4.3	0.6	1.7	49.3
"	ESP Hopper	15	C-816		6.0	1.1	2.4	31.4
7-22-71	--	17	C-912		4.4	6.5	4.0	26.9
7-22-71	MC Outlet	18	C-915		5.5	7.5	4.8	33.6
7-20-71	MC Outlet	19	C-917		0.8	0.3	0.4	1.4
"	ESP Outlet	19	C-918		4.4	3.7	2.9	9.8
"	ESP Hopper	19	C-830		0.6	0.1	0.3	1.7
"	MC Outlet	20	C-919		0.8	0.9	0.6	2.2
"	ESP Outlet	20	C-920		7.2	4.4	4.2	13.4
"	ESP Hopper	20	C-832		0.8	<0.0	0.3	2.2
7-20-71	MC Outlet	21	C-921		0.8	0.2	0.4	1.1
"	ESP Outlet	21	C-922		5.3	3.0	2.9	11.8
"	ESP Hopper	21	C-835		0.8	<0.1	0.3	1.4
"	MC Outlet	22	C-923		1.6	0.6	0.8	5.6

TABLE XXVIII (continued)

SUMMARY OF CHEMICAL ANALYSES PERFORMED ON SAMPLES TAKEN DURING THE SECOND CES TEST SERIES

Test Date	Sample Identification	CES Test No.	TVA Lab No.	% $S^=$	% $SO_4^=$	% $SO_3^=$	Total %S	% CaO
"	ESP Outlet	22	C-924	<0.1	3.7	1.1	1.7	6.2
"	ESP Hopper	22	C-838		0.7	<0.1	0.3	2.8
"	MC Outlet	23	C-925		1.9	1.1	1.1	5.9
"	ESP Outlet	23	C-926		2.5	1.4	1.4	16.2
"	ESP Hopper	23	C-842		1.6	<0.1	0.6	9.8
"	MC Outlet	24	C-927		4.0	1.9	2.1	18.8
"	ESP Outlet	24	C-928		3.7	1.4	1.8	17.6
"	ESP Hopper	24	C-846		3.0	<0.1	1.0	15.1
7-19-71	MC Outlet	25	C-929		5.9	8.6	5.4	26.0
7-23-71	MC Outlet	26	C-931		6.0	7.6	5.0	30.8
"	MC Outlet	27	C-934		5.3	8.5	5.2	28.8
7-21-71	MC Outlet	28	C-936		8.4	2.8	3.9	38.6
"	MC Outlet	29	C-938		6.9	4.1	3.9	28.8
"	MC Outlet	30	C-940		6.7	5.0	4.2	27.2
7-26-71	MC Inlet	32	C-944		6.5	4.5	4.0	27.7
"	MC Outlet	32	C-942		8.7	9.7	6.8	27.7
"	ESP Outlet	32	C-943		7.2	10.6	6.6	23.5
"	MC Hopper	32	C-873		4.5	0.4	1.7	29.7
"	ESP Hopper	32	C-872		7.1	0.3	2.5	24.9

TABLE XXVIII (continued)

SUMMARY OF CHEMICAL ANALYSES PERFORMED ON SAMPLES TAKEN DURING THE SECOND CES TEST SERIES

Test Date	Sample Identification	CES Test No.	TVA Lab No.	% $S^=$	% $SO_4^=$	% $SO_3^=$	Total %S	% CaO
7-26-71	MC Inlet	33	C-947	<0.1	6.0	6.7	4.7	25.5
"	MC Outlet	33	C-945	↓	8.3	7.9	5.9	26.3
"	ESP Outlet	33	C-946	↓	6.4	10.8	6.4	21.0
"	MC Hopper	33	C-877	↓	4.6	0.3	1.6	31.6
"	ESP Hopper	33	C-876	↓	8.8	0.2	3.0	26.6

TABLE XXIX

CHEMICAL ANALYSES OF LIMESTONE USED DURING SECOND CES TEST SERIES

Test Date	Sample Identification	CES Test No.	TVA Lab No.	% H_2O (105°C)	% CaO	% MgO	% $CO_3^=$
7-10-71	Limestone 98% Gyroclass (Fine)	2	C-772	0.1	54.9	0.2	55.6
7-24-71	Limestone 20% Gyroclass (Coarse)	14	C-812	<0.1	54.9	0.2	55.7
7-26-71	Limestone 20% Gyroclass (Coarse)	32	C-871	<0.1	55.0	0.2	55.0

VI. ANALYSIS AND DISCUSSION OF TEST RESULTS

The main sources of data used in the analysis and correlation of the test results are two CES test programs at Shawnee (December, 1969 and July, 1971), two TVA test programs (July-August, 1969 and June-July, 1970), SRI test program at Shawnee during July, 1971, Research-Cottrell, Inc. tests at a midwest power station during limestone injection tests (February, 1967) and Babcock and Wilcox pilot plant study (1967-1970).

1. Electrostatic Precipitator Performance

The precipitator is a Research-Cottrell, Inc. design installed on the unit 10 steam generator at TVA Shawnee Station, Paducah, Kentucky. The boiler is a B&W pulverized coal, front-fired unit rated at 175 megawatts designed to produce one million pounds of steam per hour at 1800 psig and 1000/1000°F. The dust collecting equipment is a Buell mechanical cyclone designed for 65% efficiency followed by the Research-Cottrell, Inc. precipitator designed for 95% efficiency. (Overall design efficiency is 98%).

The boiler is fired with about 60 tons per hour of coal containing an average of 10% ash and 2.7% sulfur. Combustion of this fuel produces about

585,000 cfm of flue gas at 300°F containing 2200 ppm by volume SO_2 and about 3 grains of fly ash per standard cubic foot.

The precipitator shown in Figure 15 consists of two units ("A" and "B") each including three sections as follows:

Inlet Section of 33 opzel plate ducts each 9" x 30" high x 4.5' long.
Center Section of 33 opzel plate ducts each 9" x 30' high x 4.5' long.
Outlet Section of 33 opzel plate ducts each 9" x 30' high x 6.0' long.

There are 20 magnetic impulse-gravity impact rappers per precipitator and 4 electrical sets with automatic control rated at 70 KV_{peak} 750 ma each.

The total collecting area of the precipitator is 59,400 ft^2. The cross-sectional area is 1,485 ft^2. The secondary electrical readings without limestone injection, i.e. those at the precipitator can be estimated from the following expression using the transformer primary readings:

$$\text{Sec. } KV_{avg.} = (0.1195)(\text{primary voltage}_{AC\ Volts}) \qquad (12)$$

$$\text{Sec. } I_{ma} = \left[(5.96)(\text{primary current}_{\text{AC amps}}) - 77.2\right] \qquad (13)$$

The first basis for analysis of precipitator performance was a function of corona power input. A brief look at theoretical considerations of this approach follows.

A. Theoretical Considerations of Electrostatic Precipitator Performance As A Function of Corona Power

$$1-E = Q = \varepsilon^{-\frac{A}{V}W} \qquad (14)$$

$$W = \frac{d_p E_o E_p}{4 \pi \eta} \qquad (15)$$

where,

E = Fractional efficiency of precipitator
Q = Fractional loss from precipitator
A = Collecting electrode area of precipitator
V = Gas flow rate through precipitator
W = Precipitation rate parameter
d_p = Particle diameter
E_o = Charging field in precipitator
E_p = Precipitating field in precipitator
η = Gas viscosity

Combining equations (14) and (15) gives:

$$\ln Q = \left(-\frac{A}{V}\right)\left(\frac{d_p E_o E_p}{4 \pi \eta}\right) \qquad (16)$$

Reproduced from best available copy.

The precipitator total corona power normally is a function of the applied voltage, precipitator size, electrode geometry, and gas and particulate characteristics.

It is generally known from the literature(6,11) that as a useful first approximation, the precipitation rate parameter is related linearly to the corona power/ft^2 of collecting electrode area as shown below. However, there has been some conflict between this approach and experimental results obtained during this study. A more detailed discussion of this matter is contained in subsequent sections.

$$P_c = \alpha A \, E_o \, E_p \qquad (17)$$

where,

P_c = Precipitator corona power input

α = Precipitation parameter dependent upon gas and particle characteristics, and precipitator electrode geometry to a minor extent.

Equation (16) can be rewritten as:

$$\ln Q = - \frac{d_p}{4 \pi \eta \alpha} \; \frac{P_c}{V} \qquad (18)$$

Thus, for similar particle size, and gas and particle characteristics, Equation (18) shows that:

$$\ln Q = -k \frac{P_c}{V} = - \frac{A}{V} W \qquad (19)$$

From which is obtained the relationship that:

$$\frac{P_c}{A} = \frac{W}{k} \text{ , or} \qquad (20)$$

W is directly proportional to precipitator corona power/ft^2 of collecting electrode, which means that by doubling the corona power to precipitator designed for 90% efficiency, one can theoretically increase the efficiency to about 99%. However, for practical considerations, the attainment of the corona power in a precipitator necessary to obtain the design efficiency requires the examination of factors which determine and affect corona power.

(a) Particle Characteristics

(1) Particle Size - This can reduce corona power by suppressing corona current at a given voltage through space charge phenomena. However, sub-micron particles of fairly high loadings are necessary in order to produce a significant affect.

(2) Electrical Resistivity - When the ash resistivity exceeds about 10^{10} to 10^{11} ohm-cm, the effective corona power is reduced. Generally, the first effect is increased sparking requiring a voltage reduction in order to hold a preselected sparkrate. Lower corona current and power input results causing a decrease in collection efficiency. In order to compensate for the lower power, it becomes necessary to enlarge the precipitator until the total power requirements for the

desired efficiency are met. Note that the corona power per unit area of precipitator is lower, but increased area, increases the total corona power to the desired level.

With very high dust resistivity, a condition known as "back corona" sets in, characterized by very high currents, low voltages and no sparking. Precipitation practically stops and can only be restored by lowering the dust resistivity.

On the other hand, extremely conductive particles of less than about 10^4 ohm-cm may be reentrained and escape collection.

(b) Gas Characteristics

(1) Temperature - Increase in gas temperature reduces gas density and reduces sparkover potential and increases the rate of rise of current with voltage. The result is that for increased gas temperature, at least up to levels of approximately 1000°F, higher temperature operation allows increase in power density. The affect of this increase in power density is to elevate the precipitation rate parameter, W.

(2) Pressure - Small increases in gas pressure raise the precipitator sparking voltage proportionately while the corona current decreases at a fixed voltage. Again, the corona current at sparking is not significantly changed, so that the net effect is to increase corona power as gas pressure increases and vice versa.

(3) Composition - Determines the kind of gas ions formed in corona. Electronegative and high molecular weight gases tend to form low mobility ions, reducing corona current and raising sparking voltage.

Gases such as sulfur trioxide and water vapor condition the ash by affecting its electrical resistivity. Sulfur trioxide is a critical factor which depends mainly on the amount of sulfur in the coal. However, excess air, residence time of sulfur dioxide in an optimum temperature zone, catalytic materials in the ash such as iron oxide, etc. can also influence the amount of sulfur trioxide present. Generally, moisture is not effective as a conditioning agent until low gas temperatures are reached, e.g. 200-225°F, and even then large amounts (percents) are required, while concentrations on the order of parts per million by volume of sulfur trioxide can radically change precipitator performance.

B. Correlation Of Precipitator Performance With Corona Power Input

The data used for this analysis are taken from Tables III through XV. The corona power inputs shown in these Tables were calculated by the use of Equation 12 and the secondary currents taken from the electrical set panels. The sparking rate of the precipitator was maintained between 50 and 200 sparks/min. in an attempt to control the power input to sparking a constant for all tests.

In order to establish a baseline operating condition of corona power input and precipitator performance, only tests without limestone injection have been used for the first correlation. In Figure 19, the precipitation rate parameter W in ft/sec is plotted as a function of corona power input expressed as a density parameter, i.e. kilowatts/1000 ft^2 of precipitator collecting surface. From equation 20, expectations are that the correlation will be a linear one. However, it is of interest to note that the data appear

FIGURE 19

PRECIPITATION RATE PARAMETER AS A FUNCTION OF CORONA POWER DENSITY FOR TESTS WITHOUT LIMESTONE INJECTION

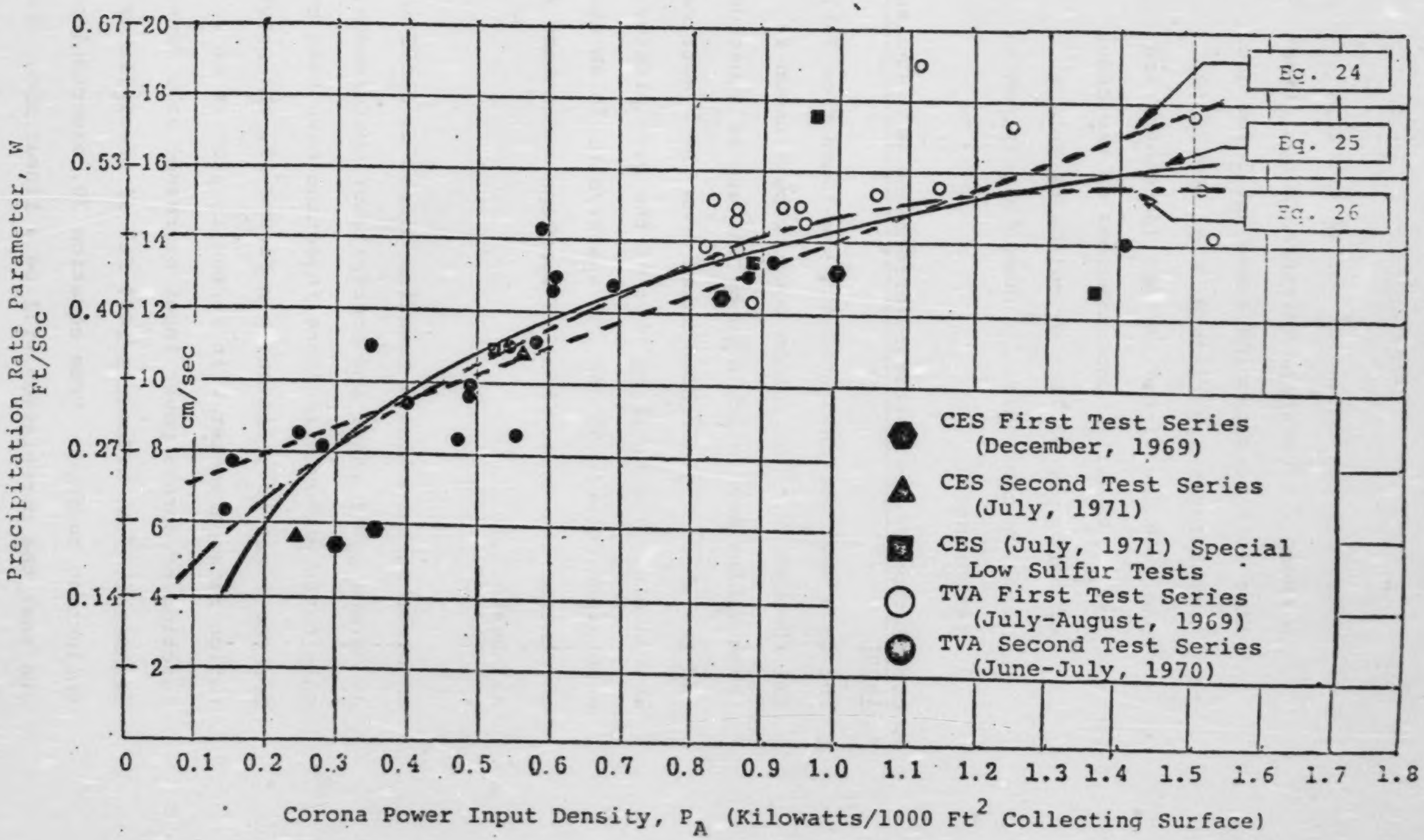

to fit a curved function rather than the linear one predicted by theoretical considerations. The precipitation rate parameter is leveling off or even decreasing at the higher power densities where the value of the rate parameter is in the range of 0.5 to 0.6 ft/sec. This is somewhat higher than the typical average value of 0.4 to 0.5 ft/sec for fly ash precipitators. There may be some level of power input above which a diminishing benefit is derived and other factors such as gas distribution, particle size, rapping losses, electrostatic reentrainment, etc. become the over-riding considerations in precipitator performance. In fact, experimental work(10) with an electrostatic precipitator on high pressure pipeline natural gas containing oil contaminant has shown that at very high electrical field strengths (five to ten times normal), a decrease in the precipitation rate parameter occurs due to electrostatic force reentrainment from the collecting surface.

Regression analyses of the data (42 sets) using the equation forms,

$$y = a + bx \tag{21}$$

$$y = a + b \ln x \tag{22}$$

$$y = a + bx + cx^2 \tag{23}$$

where,

y = precipitation rate parameter, W (FPS)

x = corona power input density, P_A (KW/1000 Ft^2)

were performed with a GE Mark I computer. The 4 sets of special low sulfur coal tests, although plotted in Figure 19, have been excluded from the regression analyses.

The following results were obtained:

$$W = 0.21 + 0.25\ P_A \qquad (24)$$

Correlation Coefficient = 0.84
F - Ratio Test Statistic = 98

$$W = 0.47 + 0.16\ \ln P_A \qquad (25)$$

Correlation Coefficient = 0.87
F - Ratio Test Statistic = 120

$$W = 0.11 + 0.57\ P_A - 0.20\ P_A^2 \qquad (26)$$

Correlation Coefficient = 0.89
F - Ratio Test Statistic = 75

These equations are limited to corona power density data falling in the range of 0.15 to 1.5 kilowatts per 1000 ft^2 of collecting surface which encompasses the normal operating range of fly ash precipitators. All three equations are reasonably good representations of the data with the quadratic form of equation (23) producing the best fit.

Previously published data(11) by Southern Research Institute for a variety of fly ash installations is contained in Figure 20 along with a plot of the data from Figure 19. Although there is considerable scatter in the data points, it is quite apparent that there is a strong relationship between the precipitation rate parameter and the corona power input density. In the range of 0.1 to 1.2 kilowatts/1000 ft^2 of collecting surface, there is fair agreement between the published data and the results of this report. It is postulated that the flue gas temperature and coal sulfur which affect the particulate conductivity are the main parameters causing the data scatter. These variables will be examined in subsequent sections of this report.

Another way of analyzing precipitator performance is to plot the loss in particulate collection efficiency as a semi-logarithmic function of the corona input power expressed as a rate i.e. watts per 1000 actual cubic feet of flue gas per minute. (See equation 19).

The same no limestone injection tests as analyzed above were used for this correlation and the data are plotted in Figure 21. A regression analysis was performed using the form of equation 21 where,

FIGURE 20

COMPARISON OF DATA FROM FIGURE 19 WITH PUBLISHED DATA OF SOUTHERN RESEARCH INSTITUTE FOR VARIOUS FLY ASH PRECIPITATOR INSTALLATIONS REF (11)

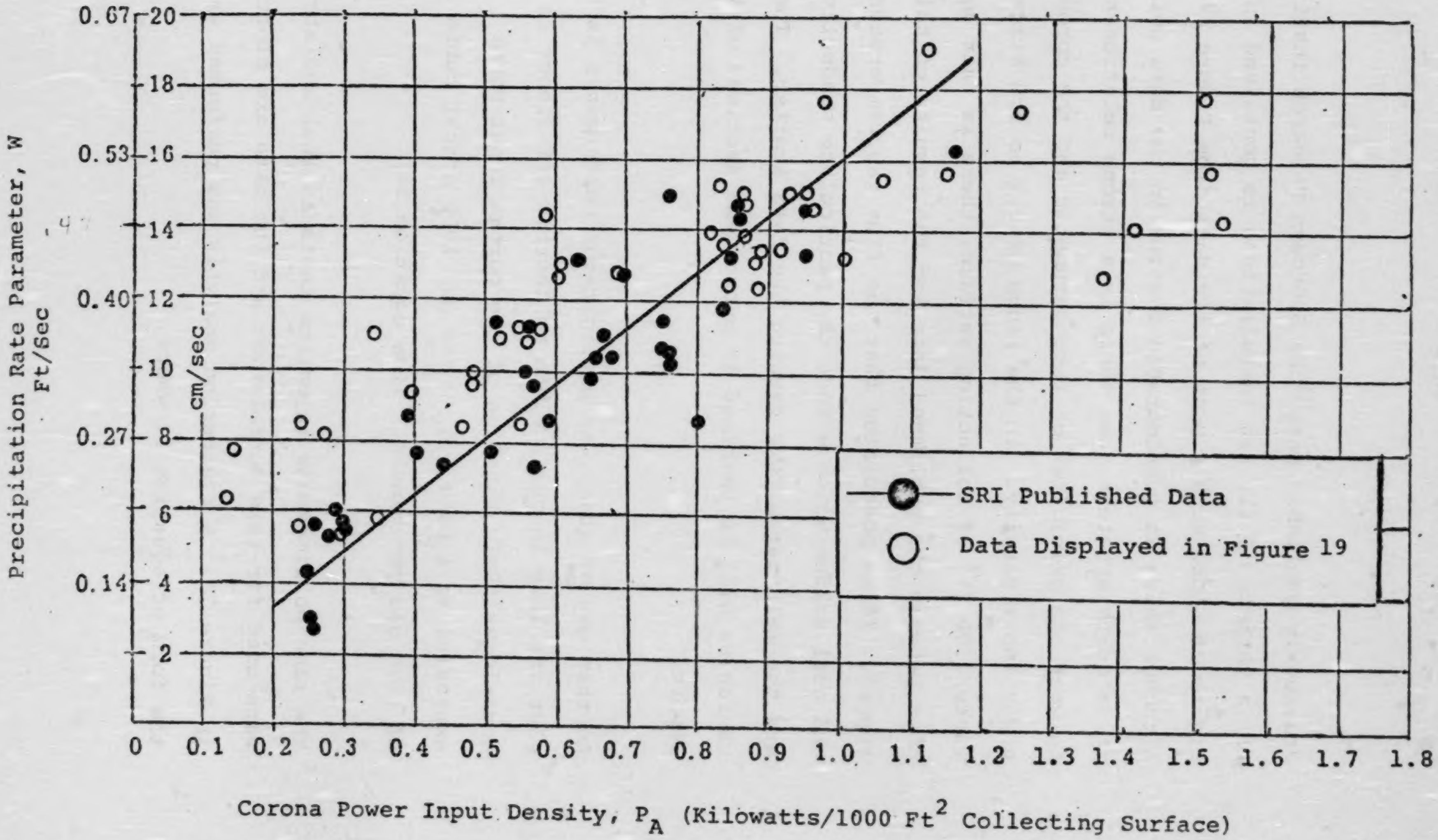

y = ln of the loss in precipitator collection efficiency Q expressed as a fraction

x = precipitator corona input power, P_V (watts/1000 ACFM of flue gas)

The following equation resulted:

$$\ln Q = -1.507 - 0.0138\ P_V \tag{27}$$

Correlation Coefficient = 0.85
F-Ratio Test Statistic = 112

Equation 27 is limited to values of precipitator corona input power rates in the range of 15 to 215 watts per 1000 ACFM of flue gas which encompasses the normal operating range of fly ash precipitators. In Figure 22 the previously published data(11) of Southern Research Institute is plotted along with the results from this report shown in Figure 21. Again the data points are scattered. However, the dependence of precipitator performance on corona power input rate in watts per 1000 ACFM of flue gas treated is obvious. There is fair agreement between the published data and results contained in this report. A resolution of the scatter in data requires a more detailed examination of such variables as gas temperature, coal sulfur, particulate size, gas velocity, rapping mode, etc. which all affect corona power input and precipitator performance. A

FIGURE 21

LOSS IN COLLECTION EFFICIENCY AS A FUNCTION OF POWER RATE FOR TESTS WITHOUT LIMESTONE INJECTION

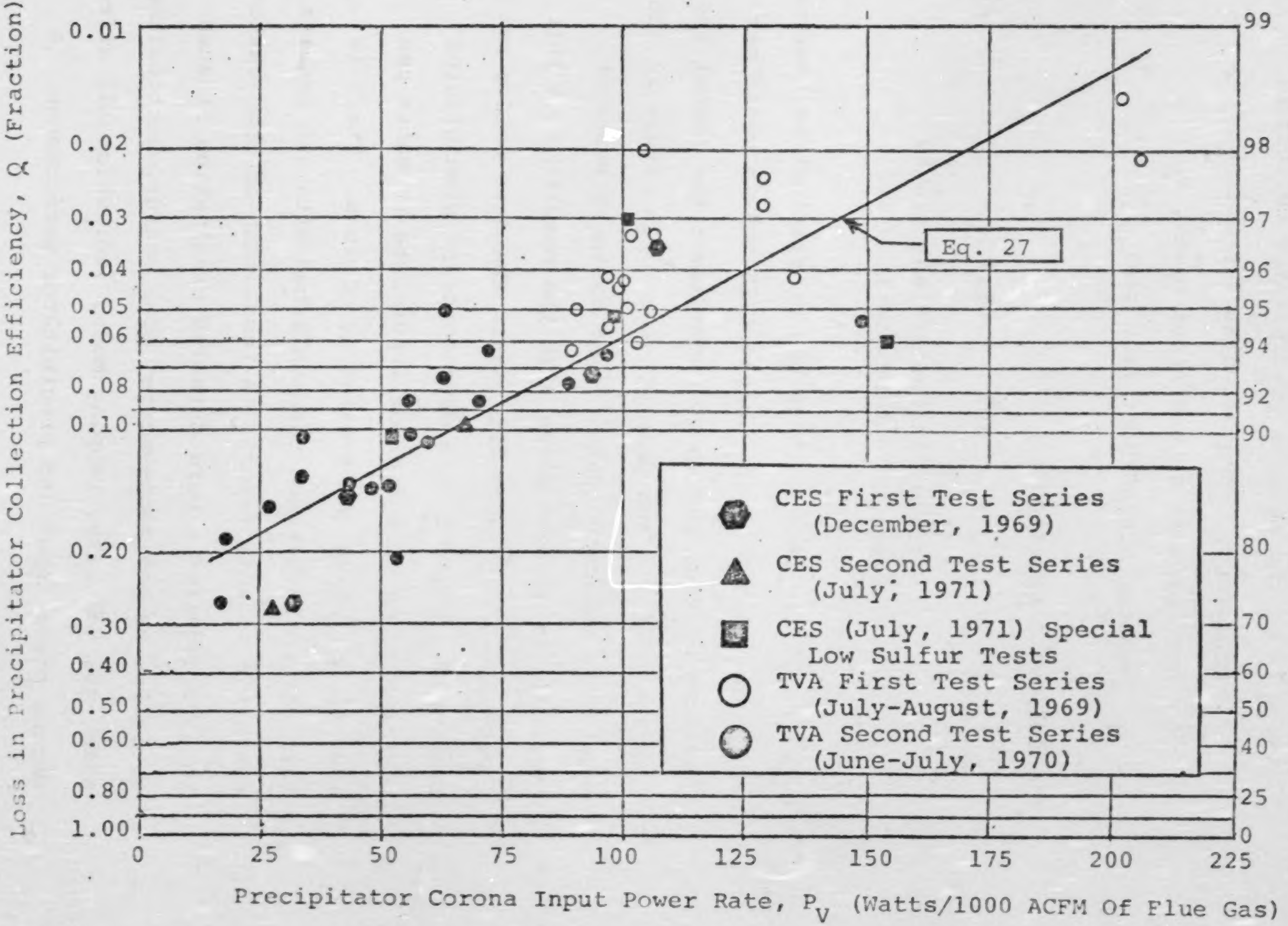

FIGURE 22

COMPARISON OF DATA FROM FIGURE 21 WITH PUBLISHED DATA OF SOUTHERN RESEARCH INSTITUTE FOR VARIOUS FLY ASH PRECIPITATOR INSTALLATIONS - REF. (11)

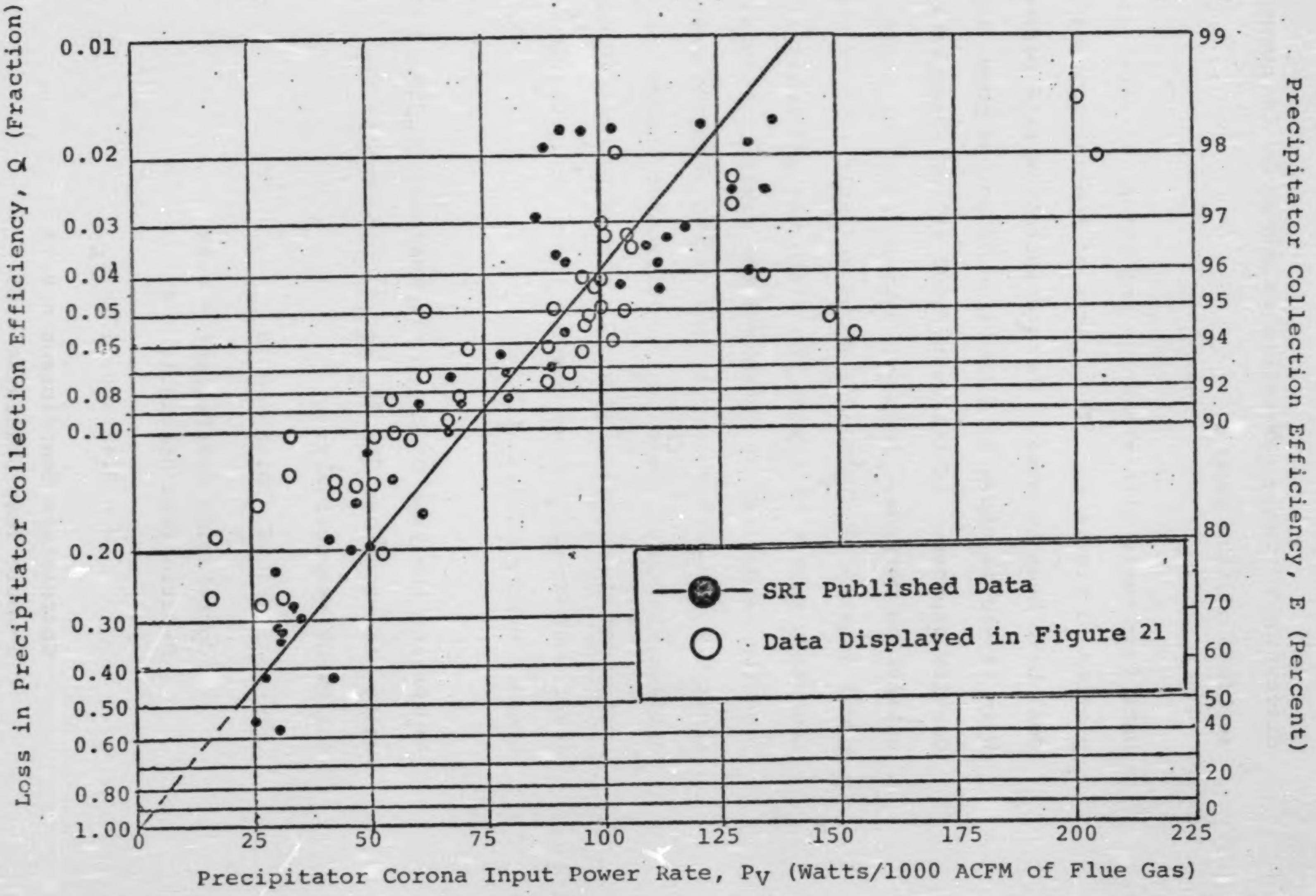

discussion of these parameters is contained in subsequent sections of this report.

Data from tests with limestone injection (51 sets) are plotted in Figure 23. The 2 sets of special low sulfur coal have been omitted. The precipitation rate parameter W in ft/sec is shown as a function of corona power input density expressed in kilowatts/1000 ft^2 of precipitator collecting surface. Note the maximum level of input power density attainable is about one-half that of the No Limestone injection tests. As discussed previously, the limestone additive has increased the electrical resistivity of the particulate to the extent that the preset optimum sparking rate of the precipitator chosen for the test program, i.e. 50-150 sparks/min is reached at much lower voltage and corona current input resulting in decreased corona power.

Regression analyses of the data presented in Figure 20 using the equations 21, 22, and 23 resulted in the following respectively:

$$W = 0.15 + 0.40\ P_A \qquad (28)$$

Correlation Coefficient = 0.68
F-Ratio Test Statistic = 42

$$W = 0.42 + 0.11\ \ln P_A \qquad (29)$$

Correlation Coefficient = 0.73
F-Ratio Test Statistic = 55

FIGURE 23

PRECIPITATION RATE PARAMETER AS A FUNCTION OF CORONA POWER DENSITY FOR TESTS WITH LIMESTONE INJECTION

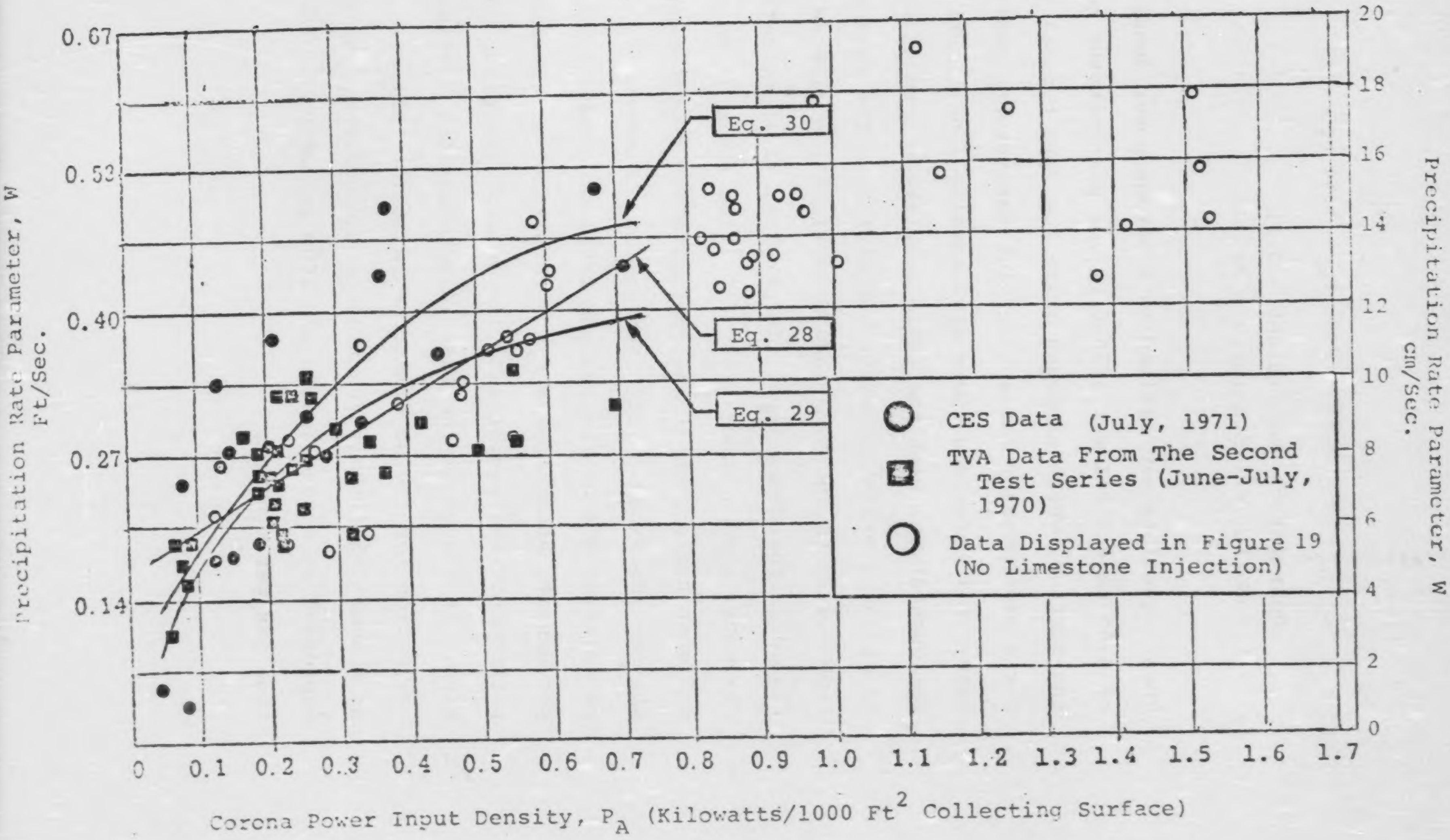

$$W = 0.10 + 0.78\ P_A - 0.54\ P_A^{\ 2} \tag{30}$$

Correlation Coefficient = 0.71
F-Ratio Test Statistic = 24

These equations are limited to a corona power density range of 0.05 to 0.7 kilowatts/1000 Ft^2 of precipitator collecting surface, which although quite low, are typical values for a precipitator collecting high resistivity particulate. All three equations give equally significant data representations with the semi-logarithmic form of equation 22 giving a slightly better correlation. The data points from Figure 19 (No Limestone injection) are plotted on Figure 23 for comparison. In general, it appears that for equal corona power input densities there is no significant difference in the precipitation rate parameter whether limestone is injected or not. However, it should be reiterated that the maximum level of corona power input density attainable and the resultant precipitator performance is significantly lower with limestone injection. In Figure 24 the loss in precipitator particulate collection for the No Limestone injection tests is plotted as a semi-logarithmic function of the corona input power expressed as a rate (watts per 1000 actual cubic feet of flue gas per minute).

FIGURE 24

LOSS IN COLLECTION EFFICIENCY AS A FUNCTION OF POWER RATE FOR TESTS WITH LIMESTONE INJECTION

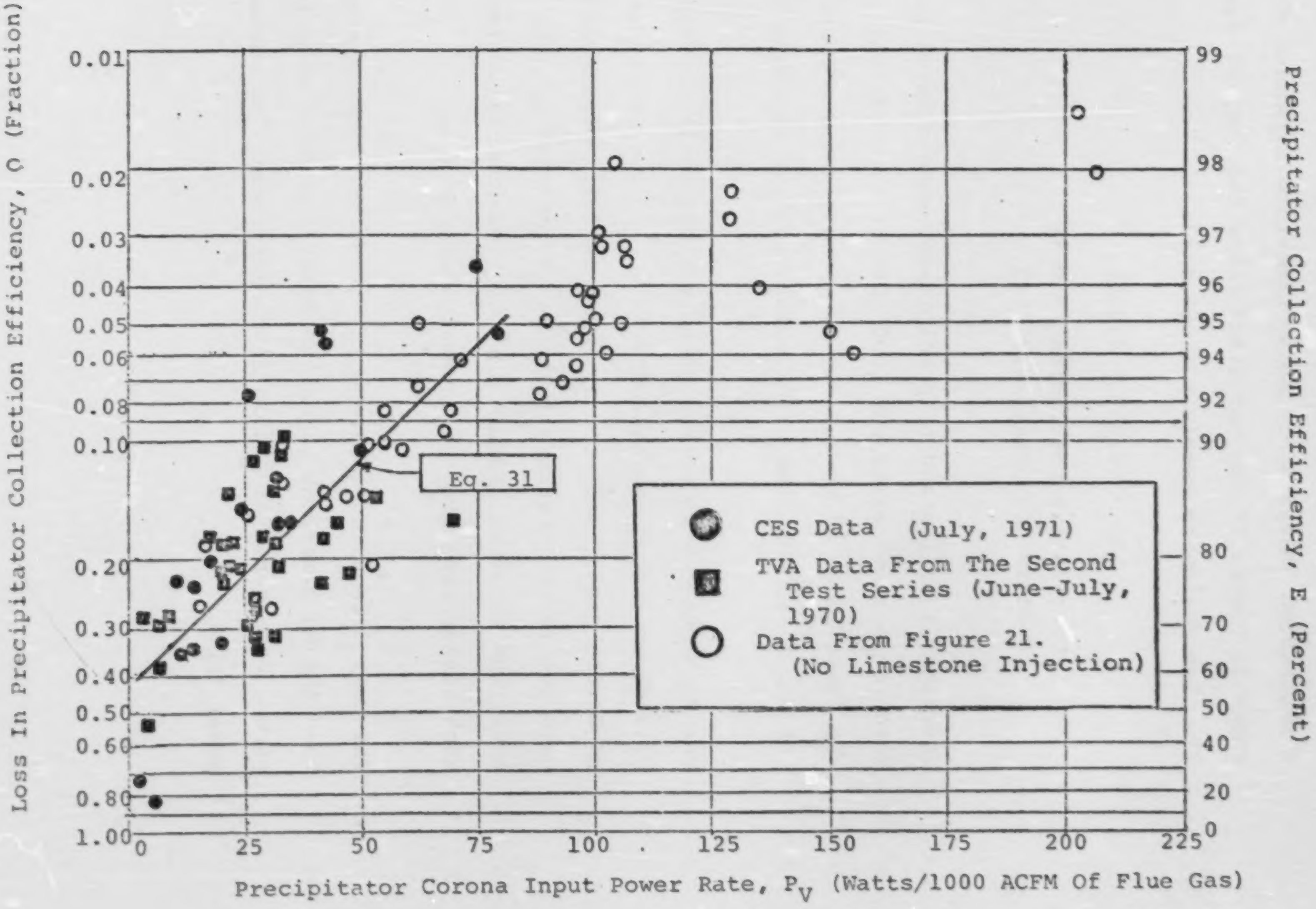

A regression analysis of the No Limestone injection data shown in Figure 24 was performed using the form of equation 21. The following result was obtained:

$$\ln Q = -0.868 - 0.026P_V \qquad (31)$$

Correlation Coefficient = 0.66
F-Ratio Test Statistic = 43

Equation 31 is limited to precipitator corona input power rates of 5 to 80 watts per 1000 ACFM of flue gas which is the lower range of normal fly ash precipitator operation but still typical when high resistivity ash is encountered.

The No Limestone injection data from Figure 21 are also plotted on Figure 24 for comparison. In comparable ranges of corona power input rates, there is fair correlation of data regardless whether limestone is injected or not. However, the rates attainable with No Limestone injection are much higher resulting in increased performance.

The test data with limestone injection are more scattered than the No Limestone injection data, but still show the strong dependence of precipitator performance on corona power input.

C. Correlation of Precipitator Corona Power Input With Process Variables

In order to make the results of the test program more useful for predicting precipitator performance and sizing with limestone injection, a more detailed analysis has been made using only the test results from the Cottrell Environmental System's second test series (July, 1971) in which a statistically designed experiment investigated four variables at two levels, i.e. limestone particle size, flue gas temperature, coal sulfur and limestone to sulfur stoichiometry. Other variables such as precipitator sparking rate and rapping mode were held essentially constant. The four variables have been correlated with corona power input density which in turn allows estimating the precipitation rate parameter from Figure 25 with subsequent sizing of the electrostatic precipitator for any gas volume and collection efficiency specified. A summary of pertinent data used for this analysis is contained in Table XXX. In Figure 25, the precipitation rate and corona power input data (Table XXX) have been plotted so as to be able to identify the injected limestone particle size and flue gas temperature for each point. Note that the coarse limestone injection generally resulted in higher precipitation rates at equivalent corona power input, and the lower gas temperatures allowed increased corona power input. (As indicated earlier, this latter result

FIGURE 25

PRECIPITATION RATE PARAMETER AS A FUNCTION OF CORONA POWER DENSITY FOR TESTS WITH LIMESTONE INJECTION

(GAS TEMPERATURE AND LIMESTONE PARTICLE SIZE ARE IDENTIFIED SEPARATELY)

(Data Points From Table XXX)

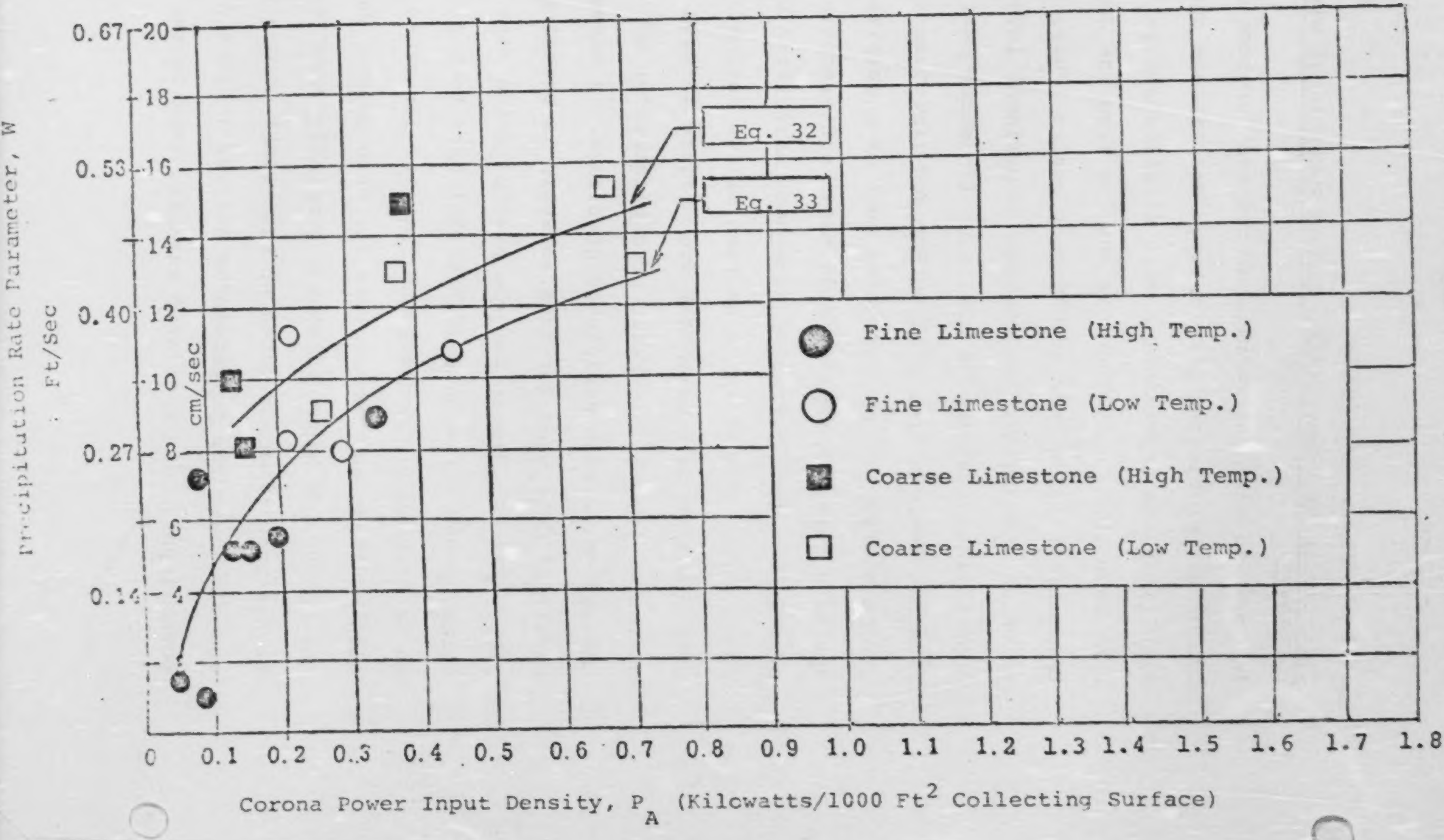

can be explained on the basis of lower particulate resistivity at the decreased gas temperature resulting in higher voltage and corona current input before the preset spark limitation). Using the simpler form of Equation 22 which is nearly as good a fit as Equation 23, a separate regression analysis on the coarse and fine limestone test results was performed involving 7 and 11 sets of data, respectively.

The following equations were obtained:

(Coarse) $$W = 0.522 + 0.121 \ln P_A \qquad (32)$$

Correlation Coefficient = 0.80
F-Ratio Test Statistic = 16

(Fine) $$W = 0.46 + 0.136 \ln P_A \qquad (33)$$

Correlation Coefficient = 0.81
F-Ratio Test Statistic = 9

Equations 32 and 33 are limited to values of precipitator corona input power densities in the range of 0.05 to 0.70 kilowatts per 1000 Ft^2 of collecting surface. The coarse and fine limestone particle size distributions from randomly selected tests (Table XXX) are shown in Figure 26. Separate regression analyses on coarse and fine limestone injection correlating the corona input power density to the four process variables tested were performed. (See Table XXX for data used). From theoretical considerations and

TABLE XXX

SUMMARY OF TEST DATA USED IN CORRELATIONS

(CES Limestone Injection Tests, July 1971)

Test No.	Flue Gas Temp., °F	Limestone Particle Size	Limestone Ton/Hr Feed	Sulfur Ton/Hr Fired	Stoichio-metry CaO/SO_2 (3)	Precipitation Rate Parameter FPS	Power Density Watts/Ft^2
2	314	F (1)	7.55	1.47	1.44	0.24	0.093
4	305	F	9.50	0.99	2.69	0.06	0.057
6	301	F	11.60	1.79	1.81	0.03	0.096
8	256	F	11.15	1.63	1.92	0.35	0.460
10	251	C (2)	16.75	1.08	4.34	0.43	0.372
11	290	C	15.25	1.11	3.85	0.26	0.164
14	289	C	14.10	1.60	2.47	0.33	0.139
15	244	C	14.45	1.39	2.91	0.29	0.275
17	243	F	9.70	0.93	2.92	0.37	0.220
18	289	F	9.15	1.25	2.05	0.17	0.112
25	253	C	10.55	1.25	2.36	0.50	0.674
26	289	F	7.05	1.31	1.51	0.17	0.129
27	242	F	6.45	1.07	1.69	0.26	0.296
28	290	F	11.15	2.04	1.53	0.29	0.334
29	241	F	6.25	1.43	1.22	0.27	0.213
30	288	F	5.30	1.67	0.89	0.18	0.199
32	289	C	8.50	1.85	1.29	0.48	0.396
33	241	C	7.85	2.28	0.96	0.43	0.708

(1) F - Fine (80%-400 Mesh)
(2) C - Coarse (50%-400 Mesh)
(3) Assumes limestone is 100% $CaCO_3$ and all sulfur in the coal appears in the flue gas as SO_2

FIGURE 26

PARTICLE SIZE ANALYSES OF LIMESTONE FEED SAMPLES
USED IN SECOND CES TEST SERIES

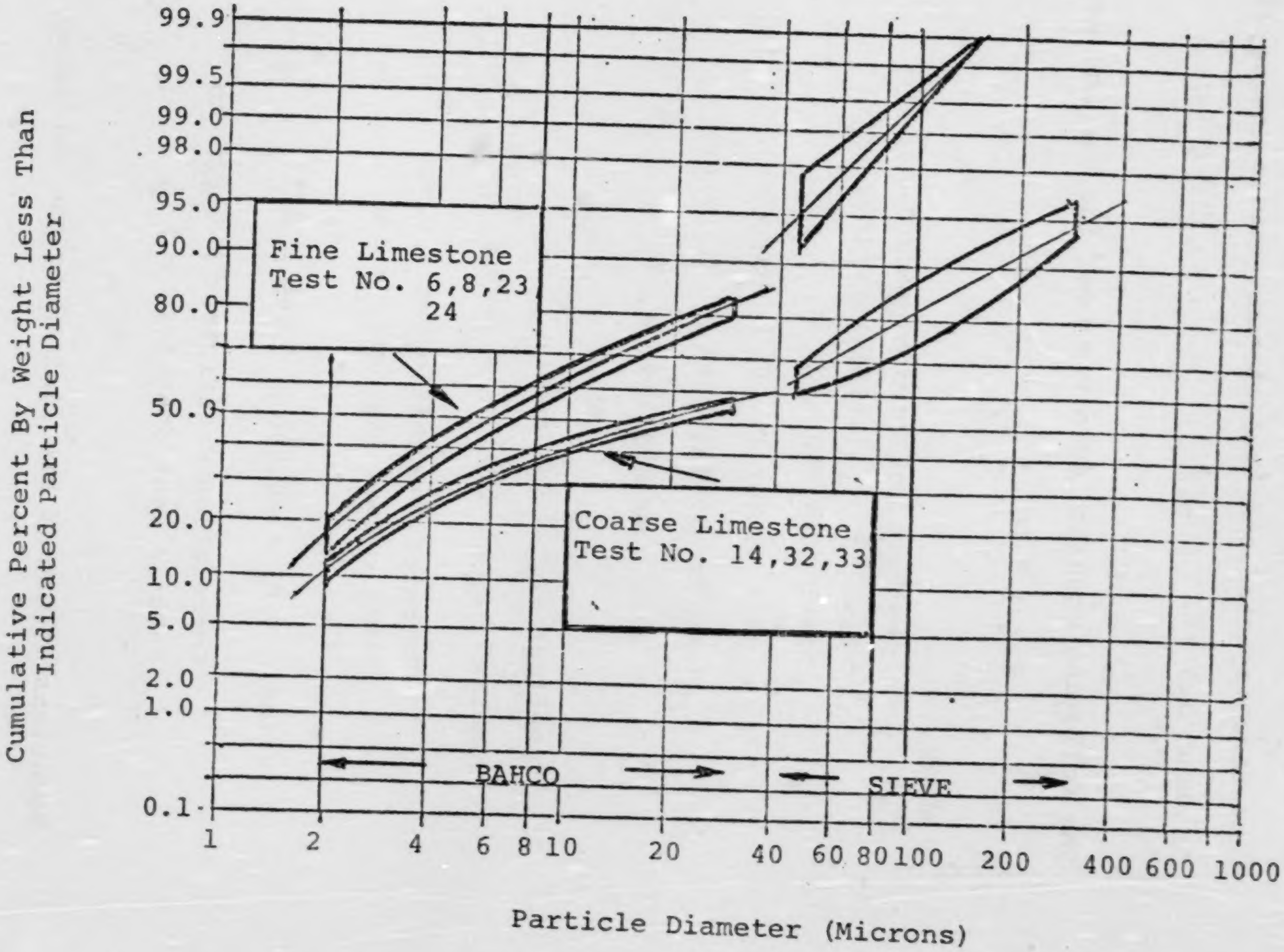

past operational experience, expectations were that the corona power input would vary directly with the amount of sulfur in the coal, and inversely with the amount of limestone injected and the gas temperature (range 240 to about 325 F).

The following equation form was used for the analyses:

$$y = a + bx_1 + \frac{c}{x_2} + \frac{d}{x_3} \tag{34}$$

where,

y = precipitator corona power input density, P_A (killowatts/1000 Ft^2 collecting surface).

x_1 = coal sulfur fired, S (tons/hr)

x_2 = limestone injected, L (tons/hr)

x_3 = flue gas temperature, T (°F x 10^{-2})

The resultant equations were:

$$\text{(Coarse)} \quad P_A = -1.435 - 0.336S + \frac{10.0}{L} + \frac{3.87}{T} \tag{35}$$

Correlation Coefficient = 0.96
F-Ratio Test Statistic = 12

$$\text{(Fine)} \quad P_A = -0.990 + .199S - \frac{0.694}{L} + \frac{2.74}{T} \tag{36}$$

Correlation Coefficient = 0.83
F-Ratio Test Statistic = 5

Equations 35 and 36 are limited to the following ranges representing actual test conditions which are realistic in practice:

Coal Sulfur Fired (S)	1.0 to 3.2 tons/hr
Limestone Feedrate (L)	5.3 to 16.8 tons/hr
Flue Gas Temperature (T)	(240 to 315)(10^{-2})°F
Stoichiometry 0.28 (L/S)	1.0 to 4.0

The ratio of limestone feedrate (L) to coal sulfur fired (S) is a function of stoichiometry and if the assumption is made that the limestone is 100% $CaCO_3$ and all the coal sulfur fired appears in the flue gas as sulfur oxides, the following relationship is established:

$$\text{Stoichiometry } \frac{CaO}{SO_2} = 0.28 \frac{L}{S} \tag{37}$$

By using equations 32, 33, 35, and 36, it is possible to predict precipitator corona power input and performance with limestone injection based on the process variables of limestone size, injection rate, coal sulfur and flue gas temperature provided the equation limitations indicated are met.

2. Performance of the Combination Mechanical-Electrostatic Dust Collector

The dust collecting equipment on Shawnee, Boiler No. 10 (see Figure 2) is a combination multitube mechanical collector followed by an electrostatic precipitator. In early years, when 90% collection efficiency was satisfactory, the economics were against combination units. However, demands for high efficiency changed this, resulting in utilization of combination unit principles where advantageous, as discussed below.

> Technical advantages cited for the combination unit are the complementary affects, e.g. mechanical efficiency drops off with lower gas throughput while precipitator efficiency increases with higher collecting area to volume ratios. Conversely, mechanical efficiency increases with high throughput while precipitator performance decreases. Furthermore, grit collection is more readily done with a mechanical while fine particulate is more effectively removed with a precipitator. With a combination unit, electrical failure of the precipitator or other outage still permits some collection with a mechanical. Removal of grit particulate ahead of the precipitator can reduce erosion losses. A multiple tube mechanical preceding the electrostatic in a close couple will also improve gas distribution as well as reduce the dust loading allowing the use of a smaller precipitator.

Disadvantages of the combination unit are the high draft loss of the mechanical collector which represents a higher operating cost (typically, about 0.25 KW per thousand CFM per inch of draft loss), and also higher capital costs for fans, flues, etc. With mechanical collectors as primary units, discharge electrode rappers are a necessity and plate rapping may also be more difficult because of compaction of the finer dust. Abrasion and plugging of the mechanical tubes can be a consideration.

In the present case where dry limestone is injected into the boiler for sulfur oxide removal, all the technical advantages cited above are favored and the use of a combination collector is desirable, particularly in the case of coarse limestone.

A. Correlation of Particle Size and Dust Collector Performance

The most important parameters in determining the performance of a mechanical collector are dust particle size and specific gravity. Normally, maximum performance is obtained when pressure loss across the collector is between 2.5 and 4 inches of water. On the other hand, the electrical properties of the dust and level of applied electrical power are critical parameters in an electrostatic precipitator with particle size of lesser importance.

A critique of particle size as it is related to dust collector performance on Shawnee Boiler No. 10 follows:

A plot of the particle size analyses contained in Table XIX through XXII are shown graphically in Figures 26 through 43.

Figure 26 shows particle size distributions of the raw limestone feed for both the coarse and fine grinds. Note that the grind was very uniform with the fine having a geometric mean size by weight of about 6 microns and the coarse 17 microns.

Size distributions for fly ash obtained during no limestone injection tests (both CES test series) are shown in Figures 27 through 33. Figures 34 through 43 present particle size distributions of samples taken during the limestone injection runs (second CES test series).

Using the average distribution curves from the above figures, fractional efficiency curves were calculated for both the mechanical and electrostatic collectors. Differences in

FIGURE 27

PARTICLE SIZE ANALYSES OF MECHANICAL COLLECTOR INLET SAMPLES WITHOUT LIMESTONE INJECTION (TESTS 1A,1B,3A,4A,5A,5B)

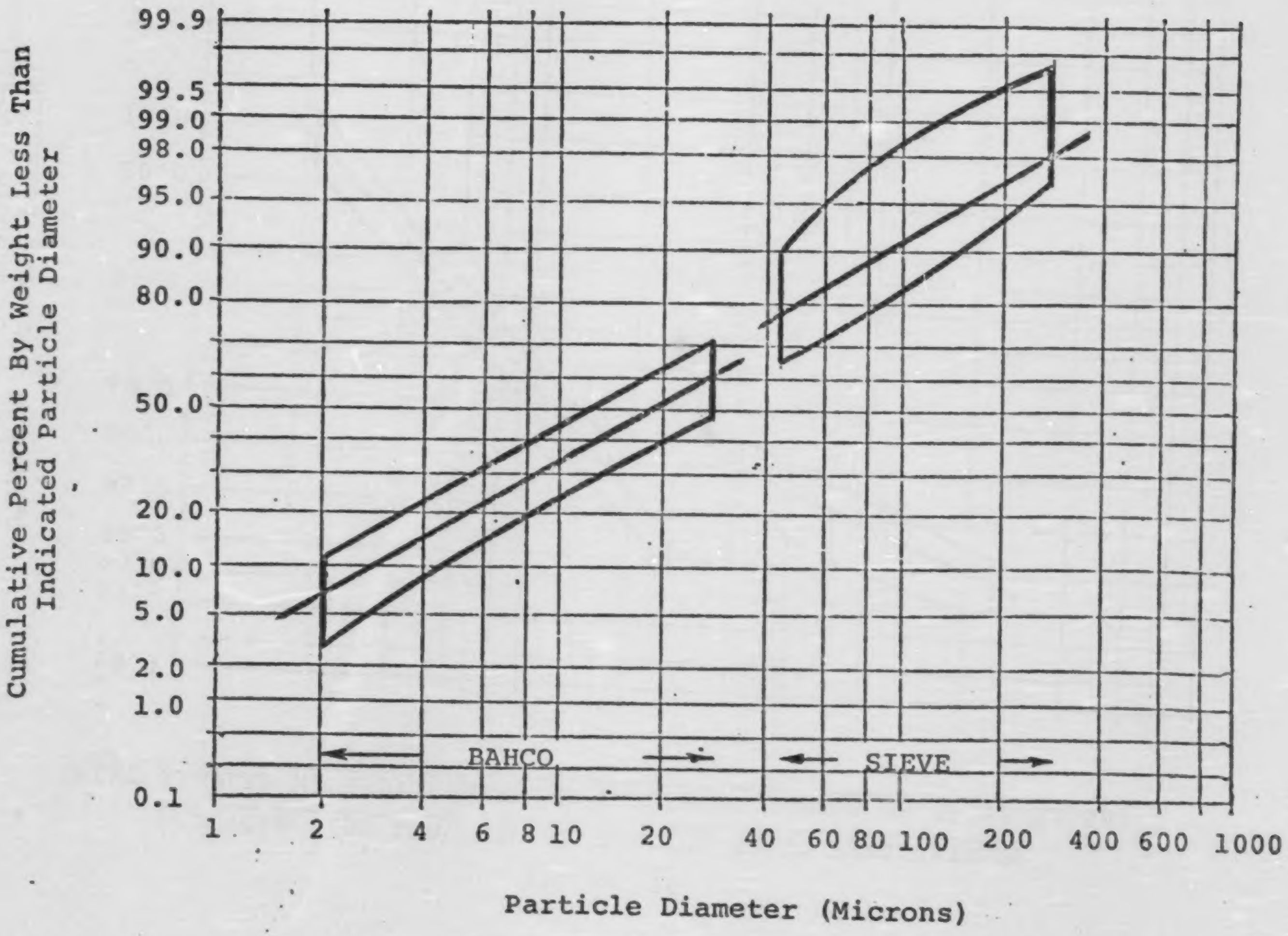

FIGURE 28

PARTICLE SIZE ANALYSES OF ELECTROSTATIC PRECIPITATOR INLET SAMPLES WITHOUT LIMESTONE INJECTION (TESTS 3A,4A,4B,5A,5B)

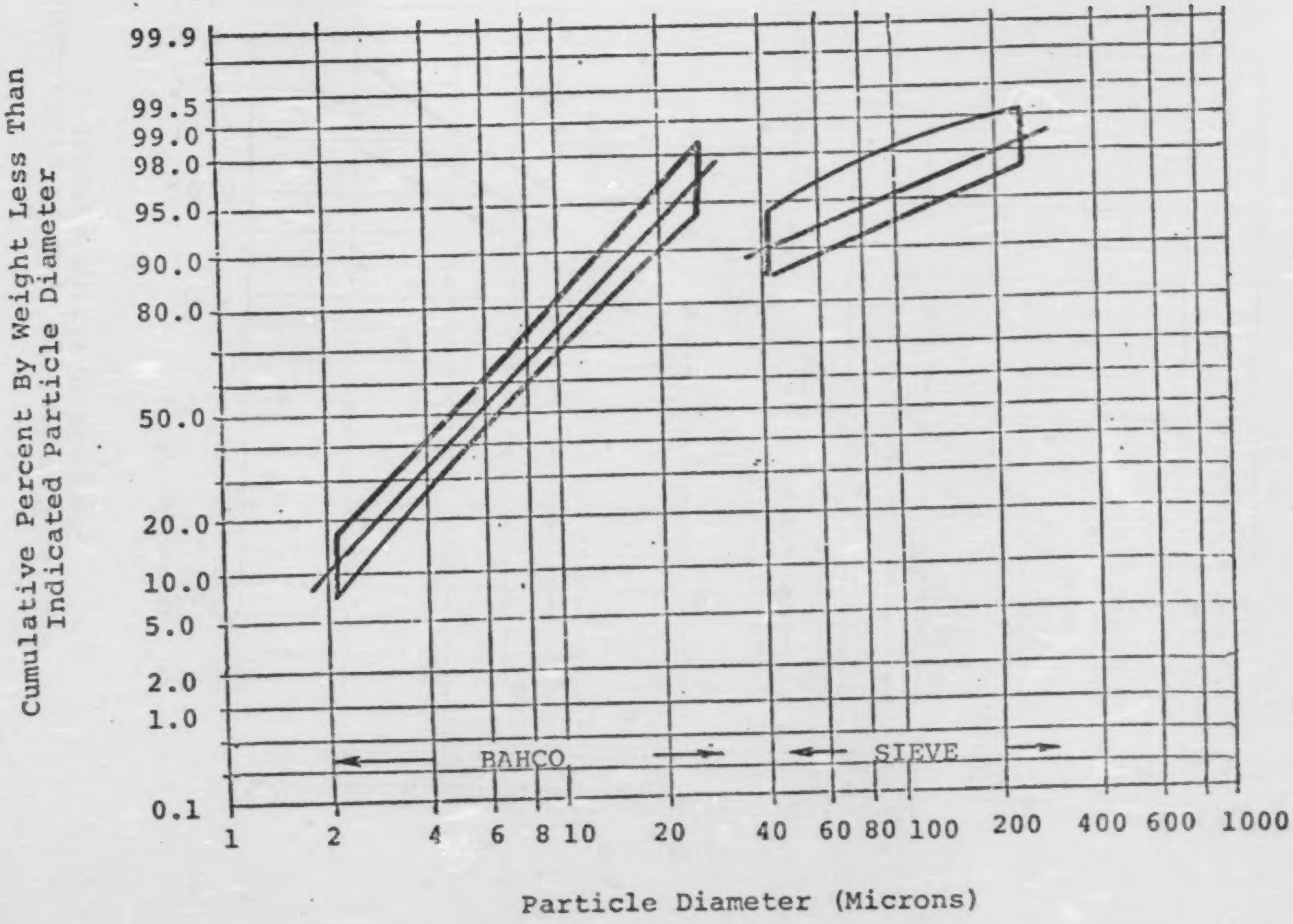

FIGURE 29

PARTICLE SIZE ANALYSES OF ELECTROSTATIC PRECIPITATOR

OUTLET SAMPLES WITHOUT LIMESTONE INJECTION (TESTS 2A,3A,3B,4B)

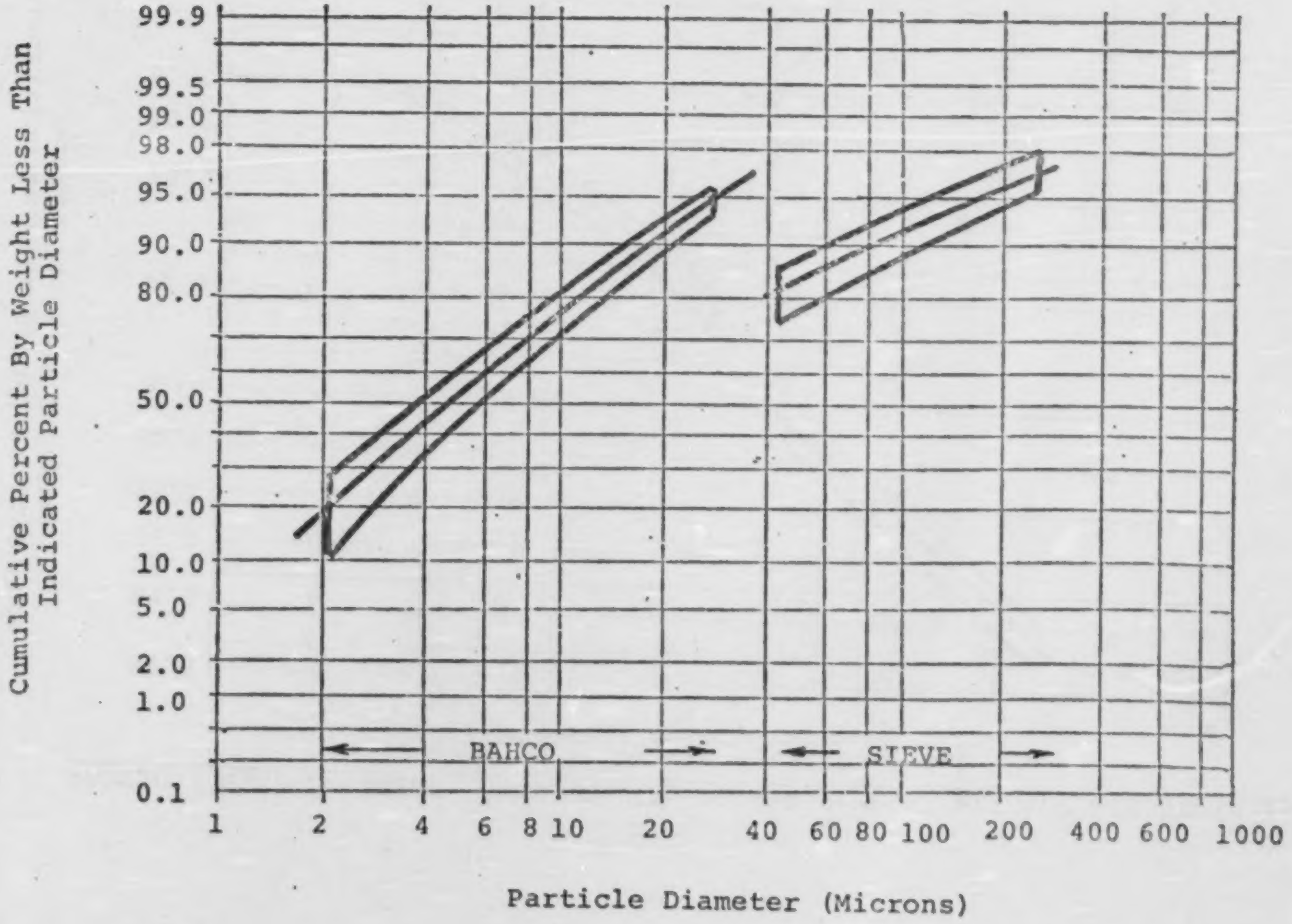

FIGURE 31

PARTICLE SIZE ANALYSES OF MECHANICAL HOPPER SAMPLES WITHOUT LIMESTONE INJECTION

(TESTS 1A,1B,2A,3A,3B,4A,4B,5A,5B)

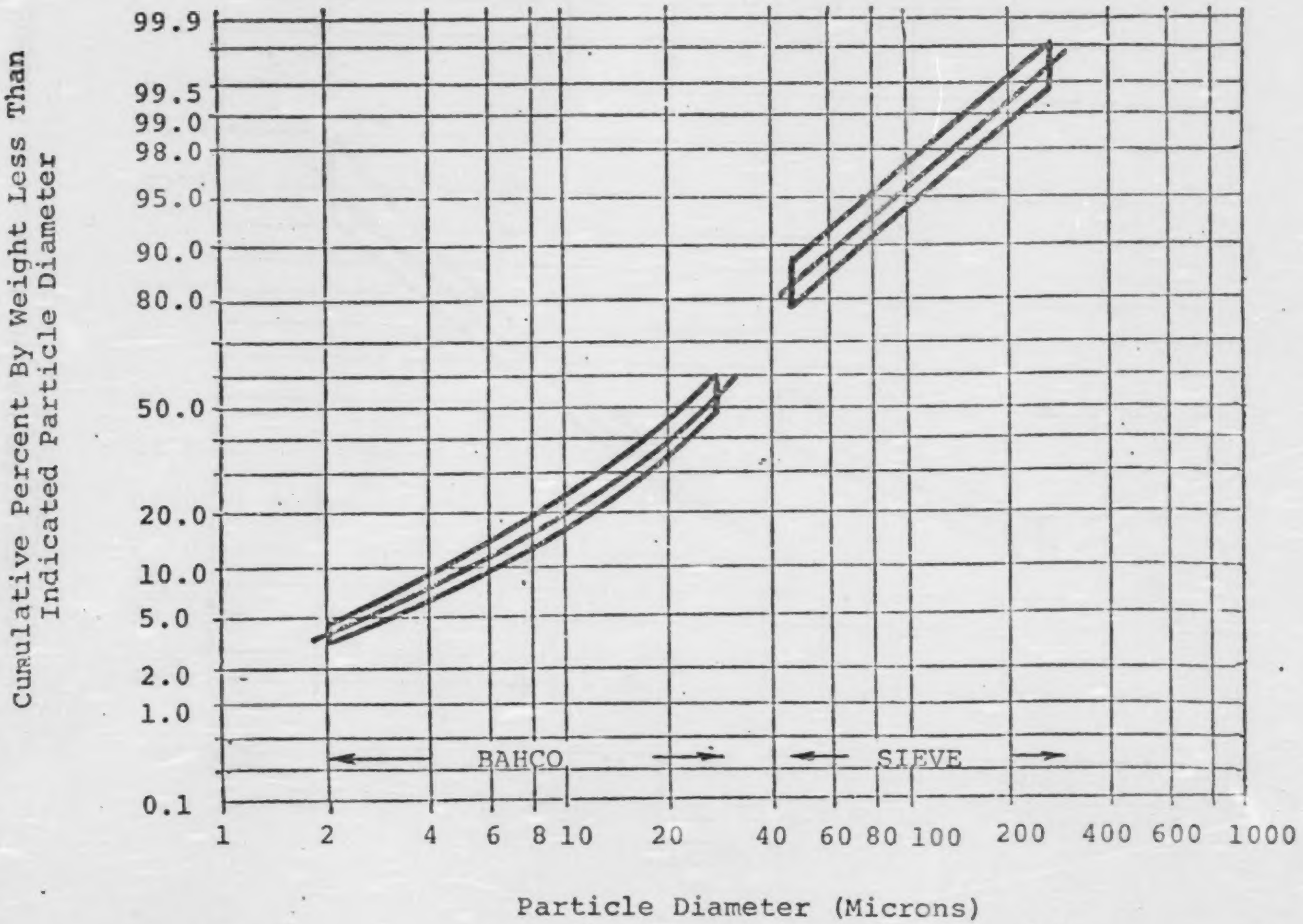

FIGURE 31

PARTICLE SIZE ANALYSES OF ELECTROSTATIC PRECIPITATOR HOPPER SAMPLES WITHOUT LIMESTONE INJECTION

(TESTS 1A,1B,2A,3A,4A,5A,5B)

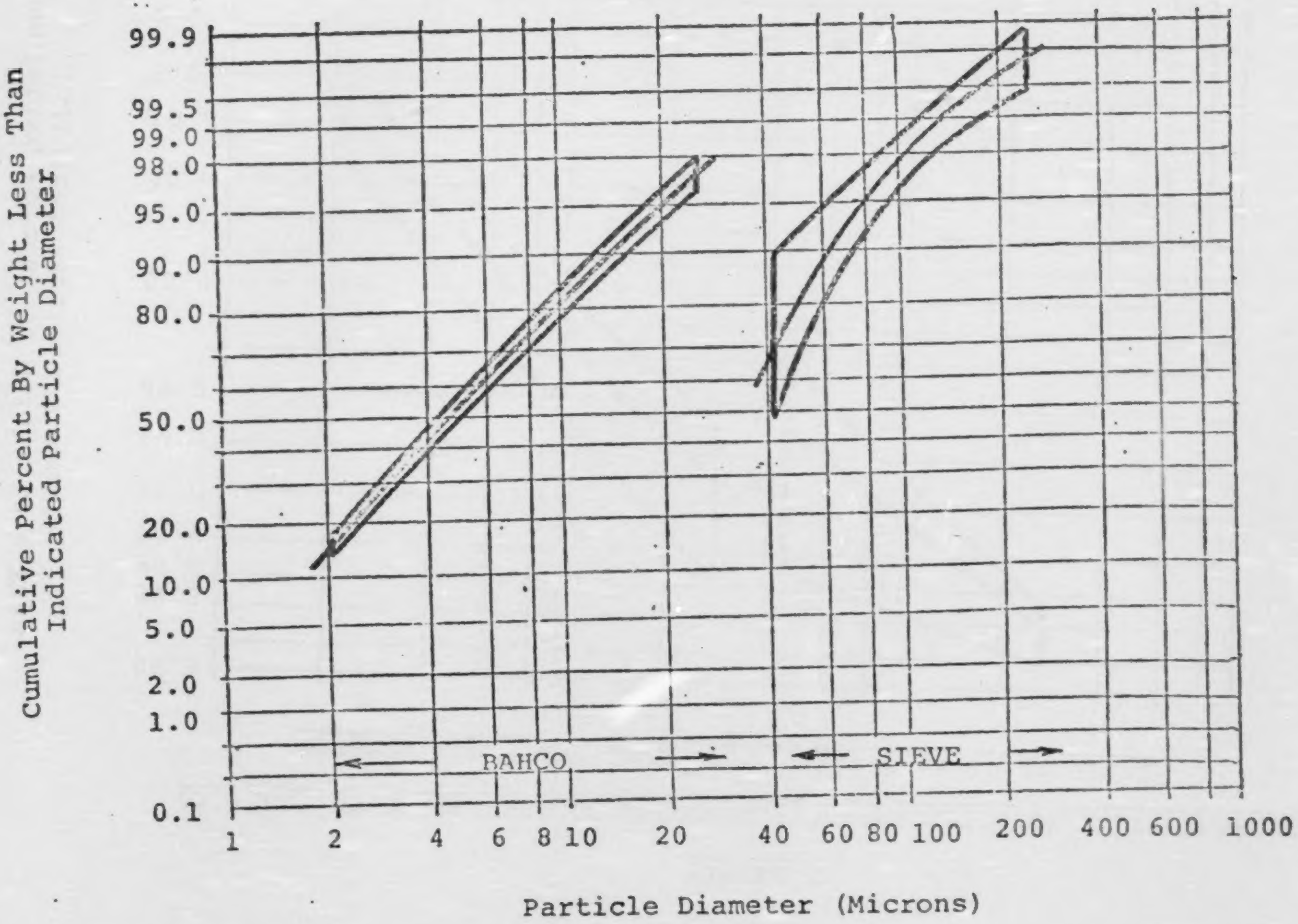

FIGURE 32

PARTICLE SIZE ANALYSES OF ELECTROSTATIC PRECIPITATOR INLET SAMPLES

WITHOUT LIMESTONE INJECTION (TESTS 16,19,20,21,22)

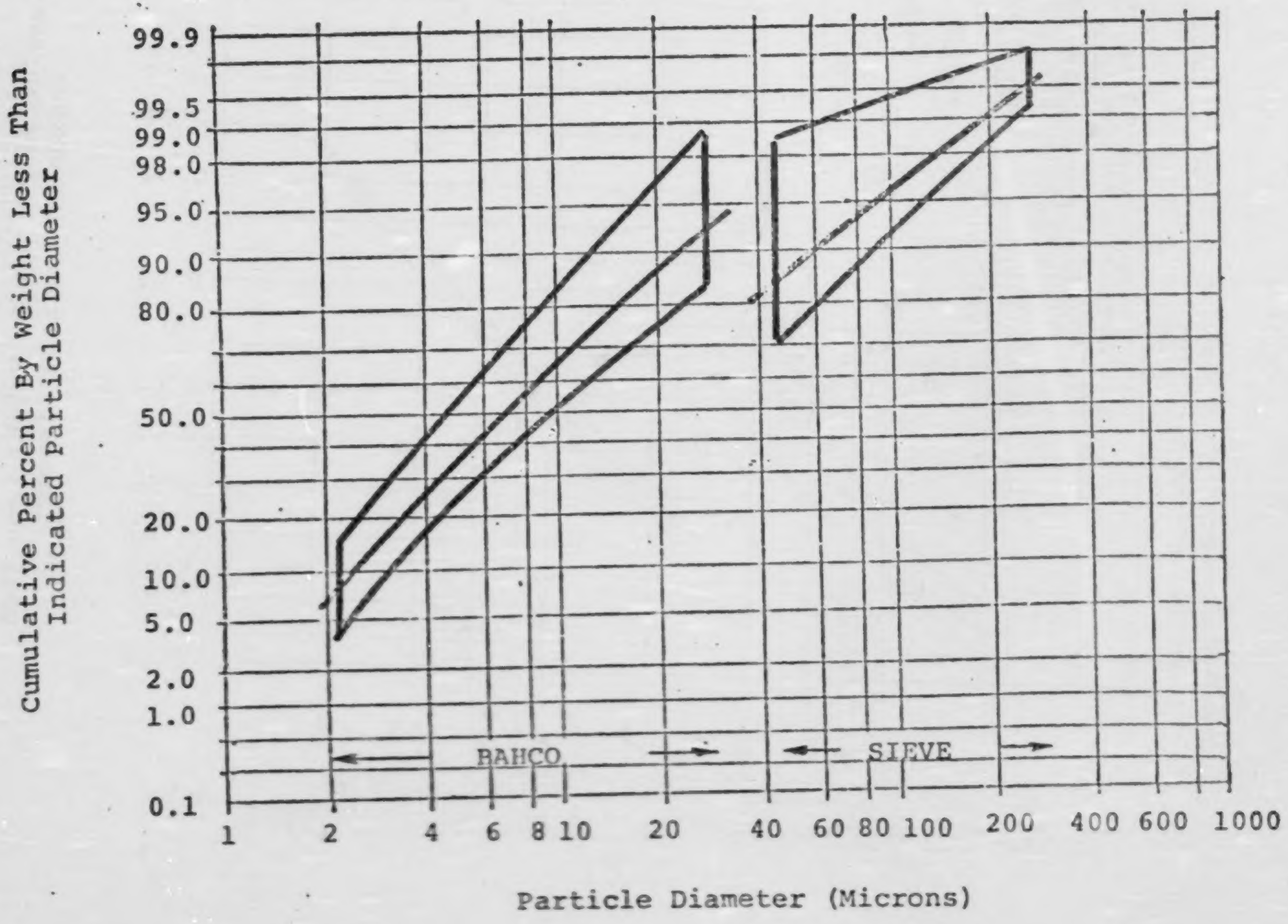

FIGURE 33

PARTICLE SIZE ANALYSES OF ELECTROSTATIC PRECIPITATOR HOPPER SAMPLES

WITHOUT LIMESTONE INJECTION (TESTS 16,21,22)

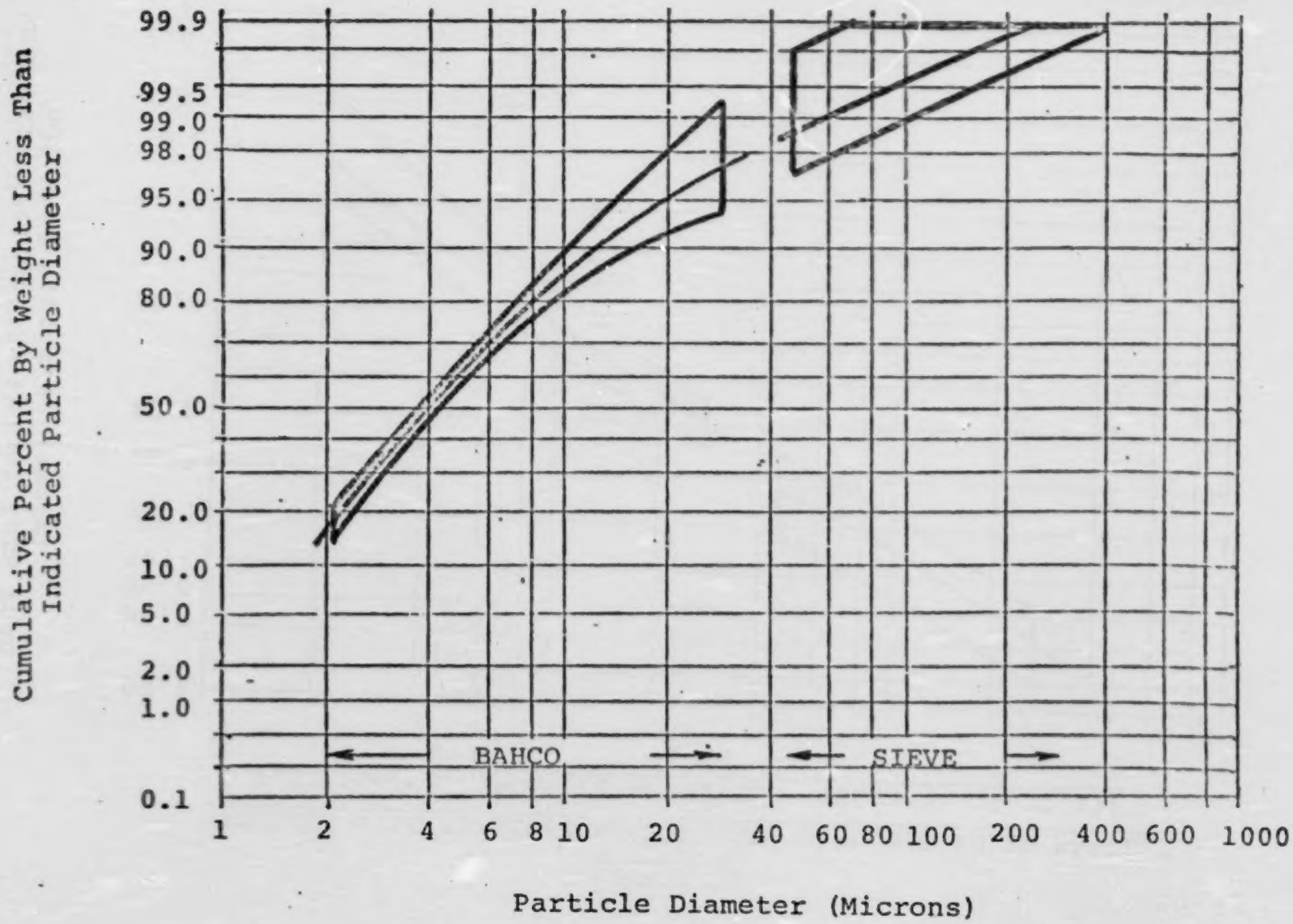

FIGURE 34

PARTICLE SIZE ANALYSES MECHANICAL COLLECTOR INLET SAMPLES WITH COARSE LIMESTONE INJECTION (TESTS 14,15,32,33)

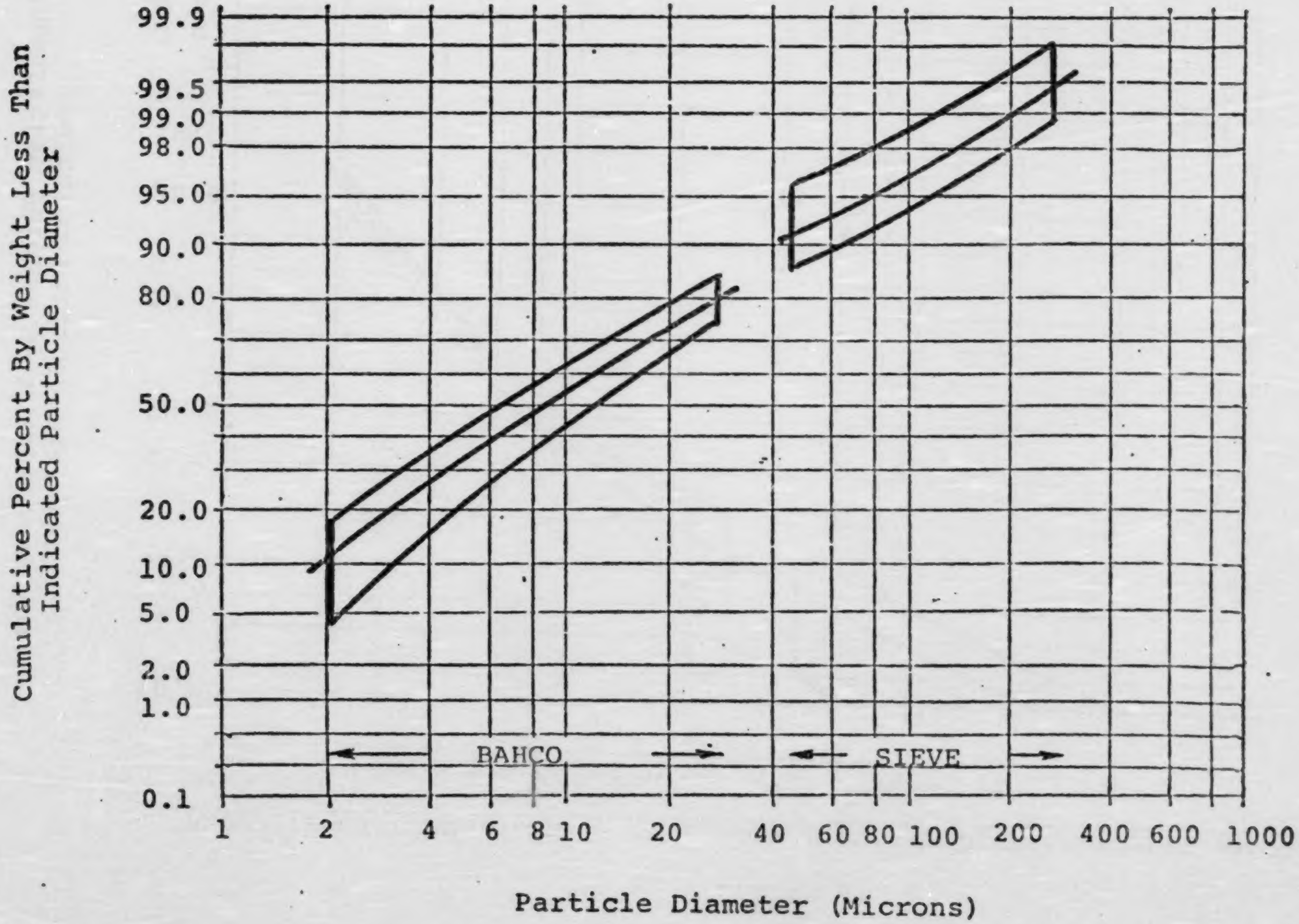

FIGURE 35

PARTICLE SIZE ANALYSES OF ELECTROSTATIC PRECIPITATOR INLET SAMPLES WITH COARSE LIMESTONE INJECTION (TESTS 10,11,14,15,25,32,33)

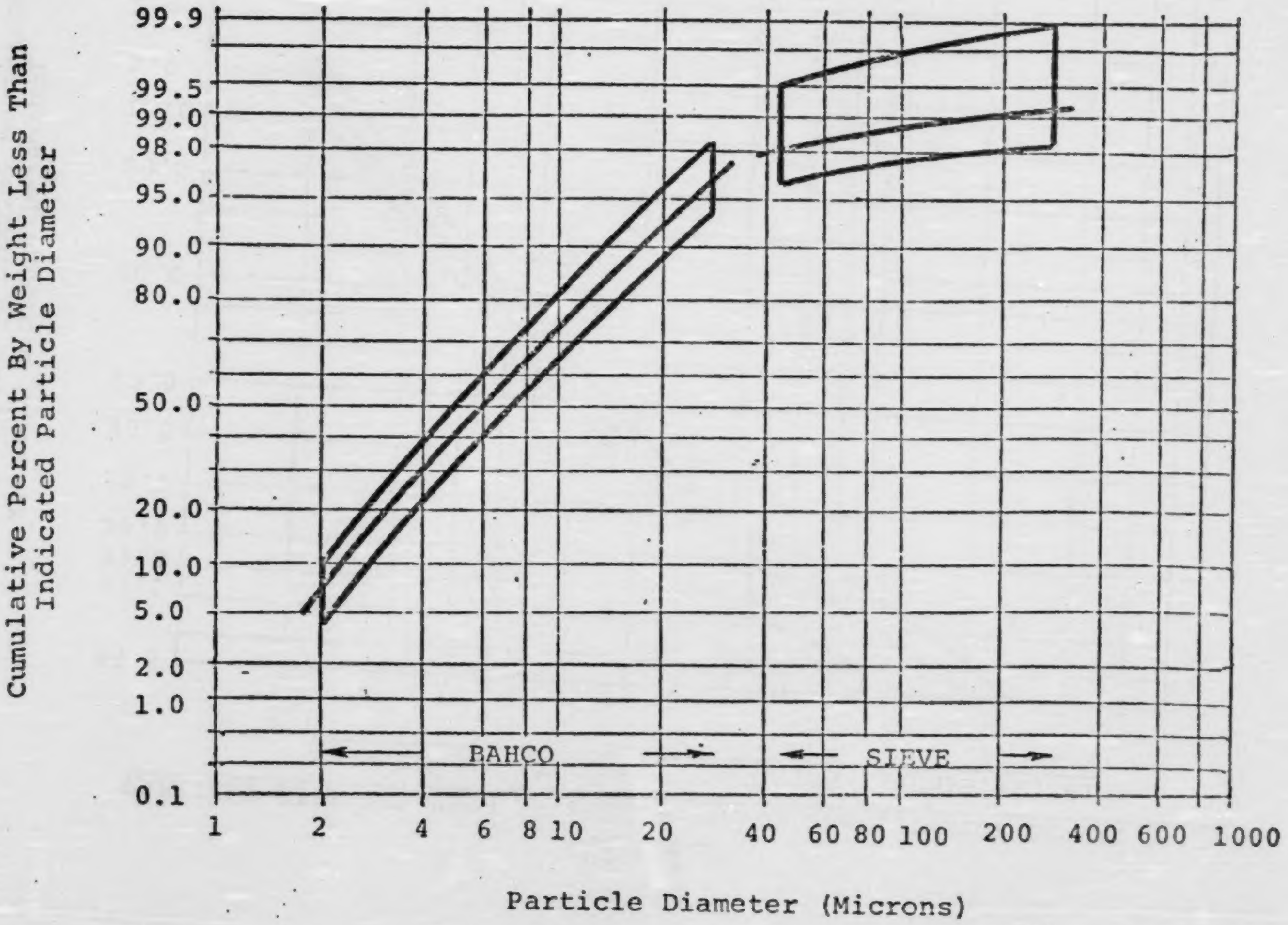

FIGURE 36

PARTICLE SIZE ANALYSIS OF ELECTROSTATIC PRECIPITATOR OUTLET SAMPLES WITH COARSE LIMESTONE INJECTION (TESTS 11,14)

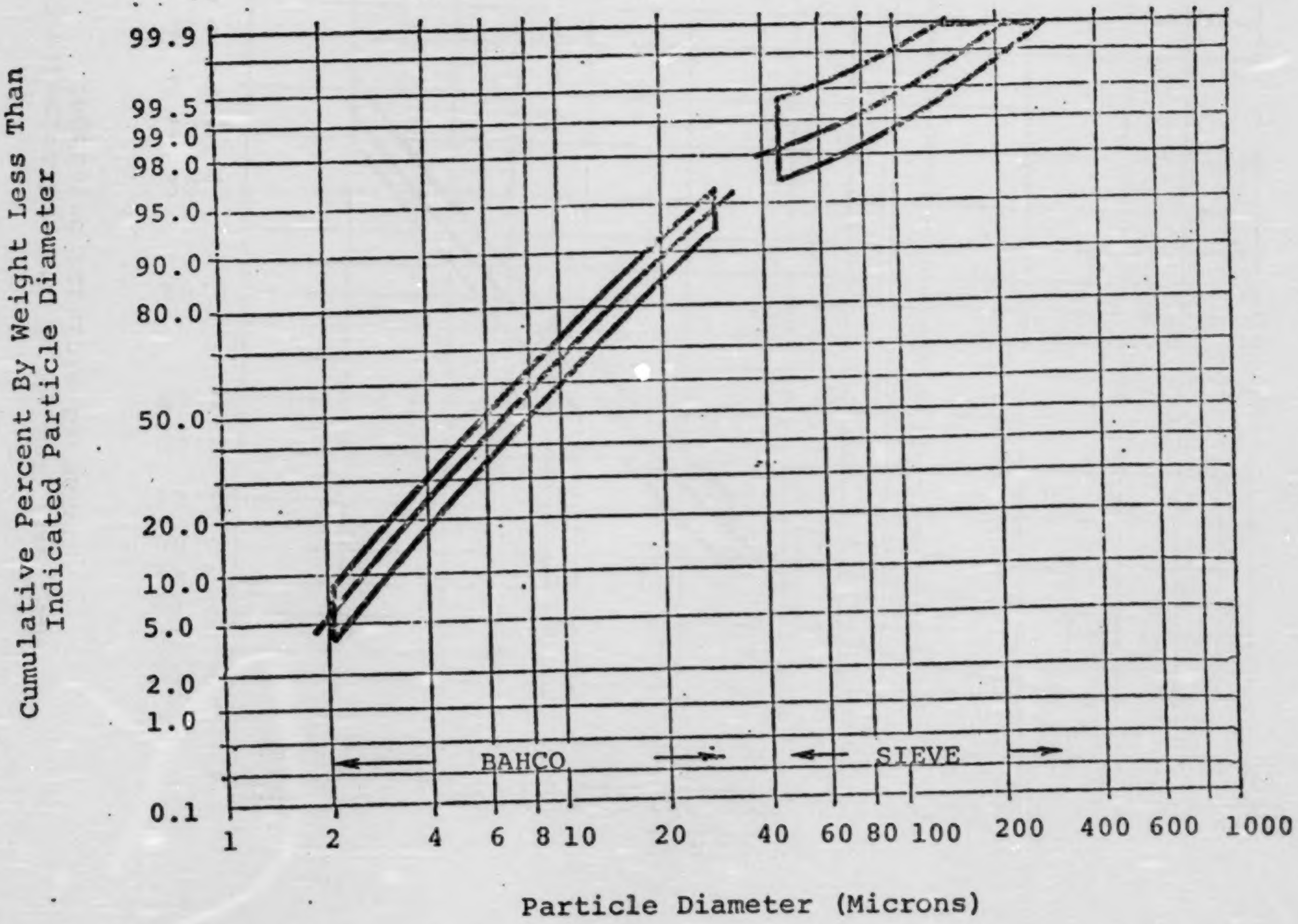

FIGURE 37

PARTICLE SIZE ANALYSES OF MECHANICAL COLLECTOR HOPPER SAMPLES WITH COARSE LIMESTONE INJECTION (TESTS 14,15,32,33)

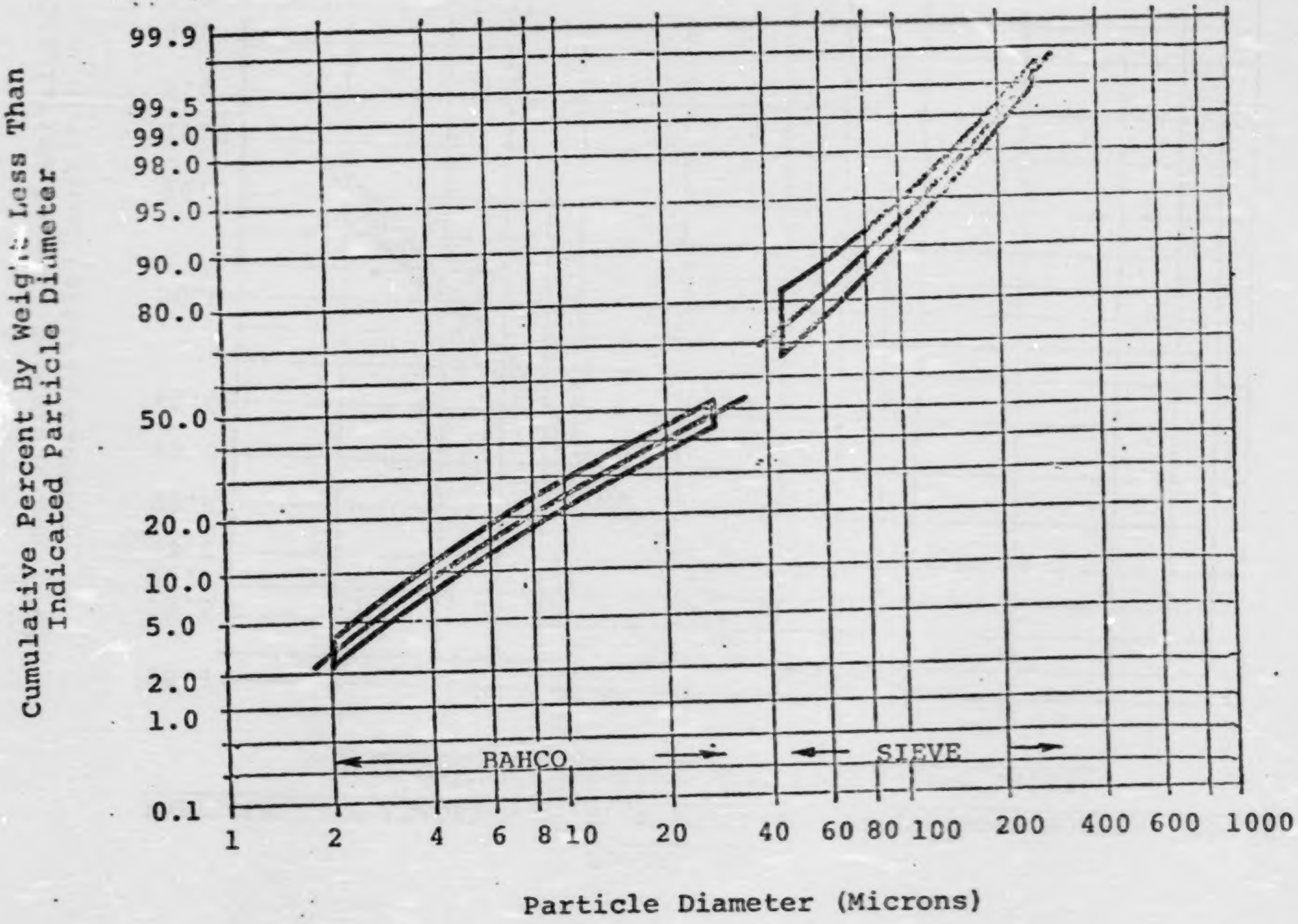

FIGURE 38

PARTICLE SIZE ANALYSES OF ELECTROSTATIC PRECIPITATOR HOPPER SAMPLES WITH COARSE LIMESTONE INJECTION (TESTS 14,15)

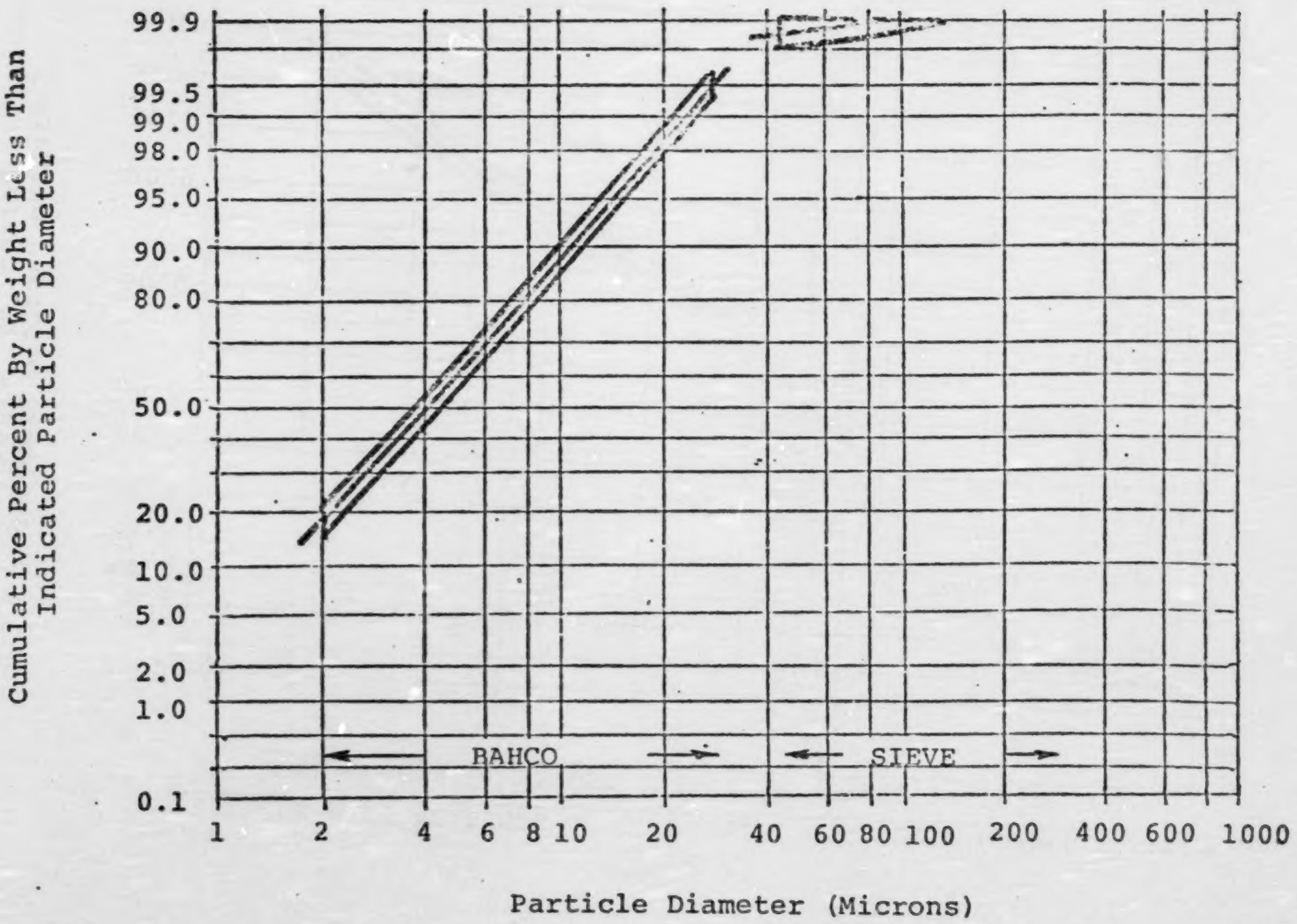

FIGURE 39

PARTICLE SIZE ANALYSES OF MECHANICAL COLLECTOR INLET SAMPLES WITH FINE LIMESTONE INJECTION (TESTS 2,3,5,6,8)

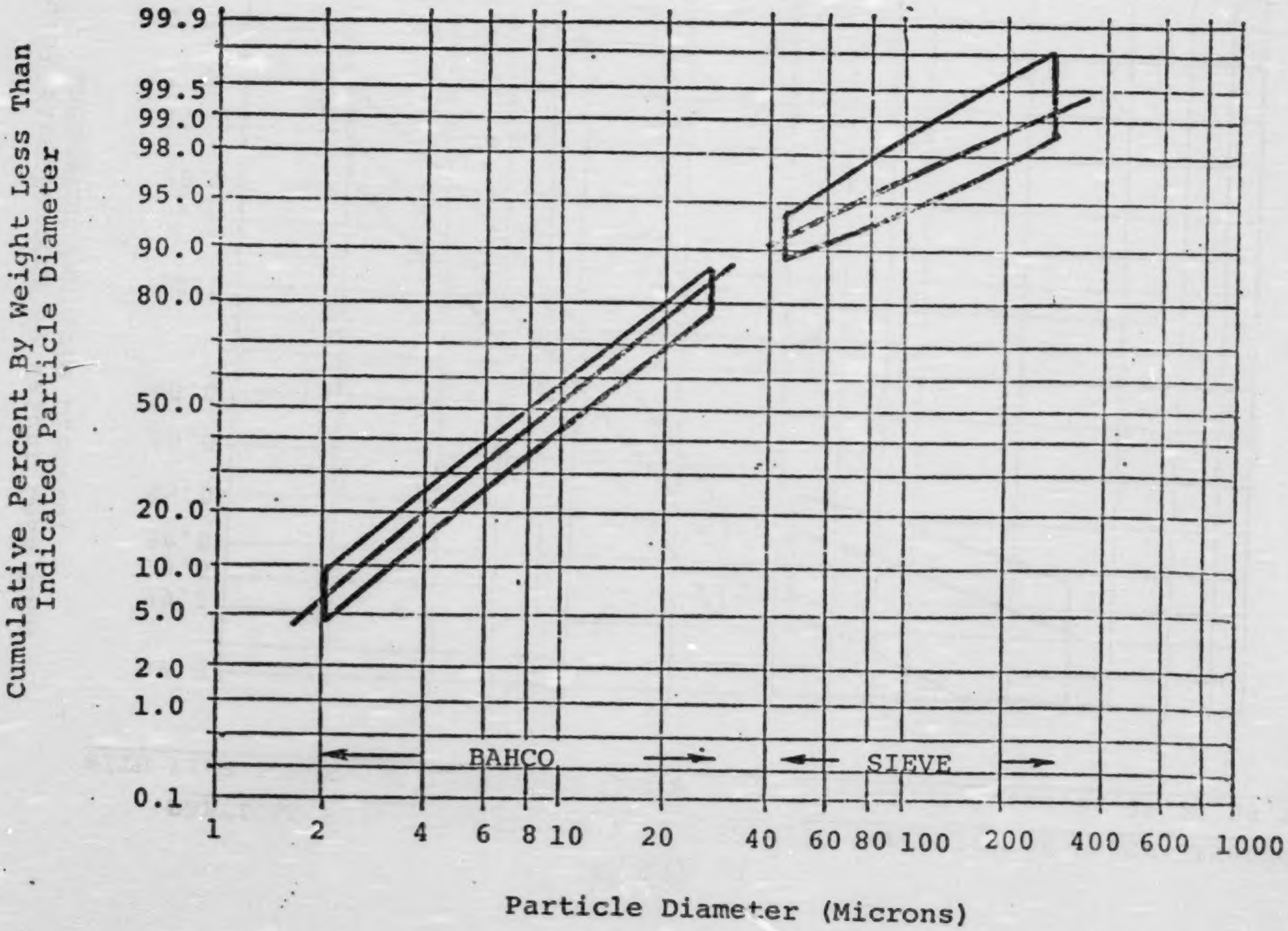

FIGURE 40

PARTICLE SIZE ANALYSES OF ELECTROSTATIC PRECIPITATOR INLET SAMPLES WITH FINE LIMESTONE INJECTION (TESTS 2,3,4,5,6,8,17,18,23,24,26,27,28,29,30)

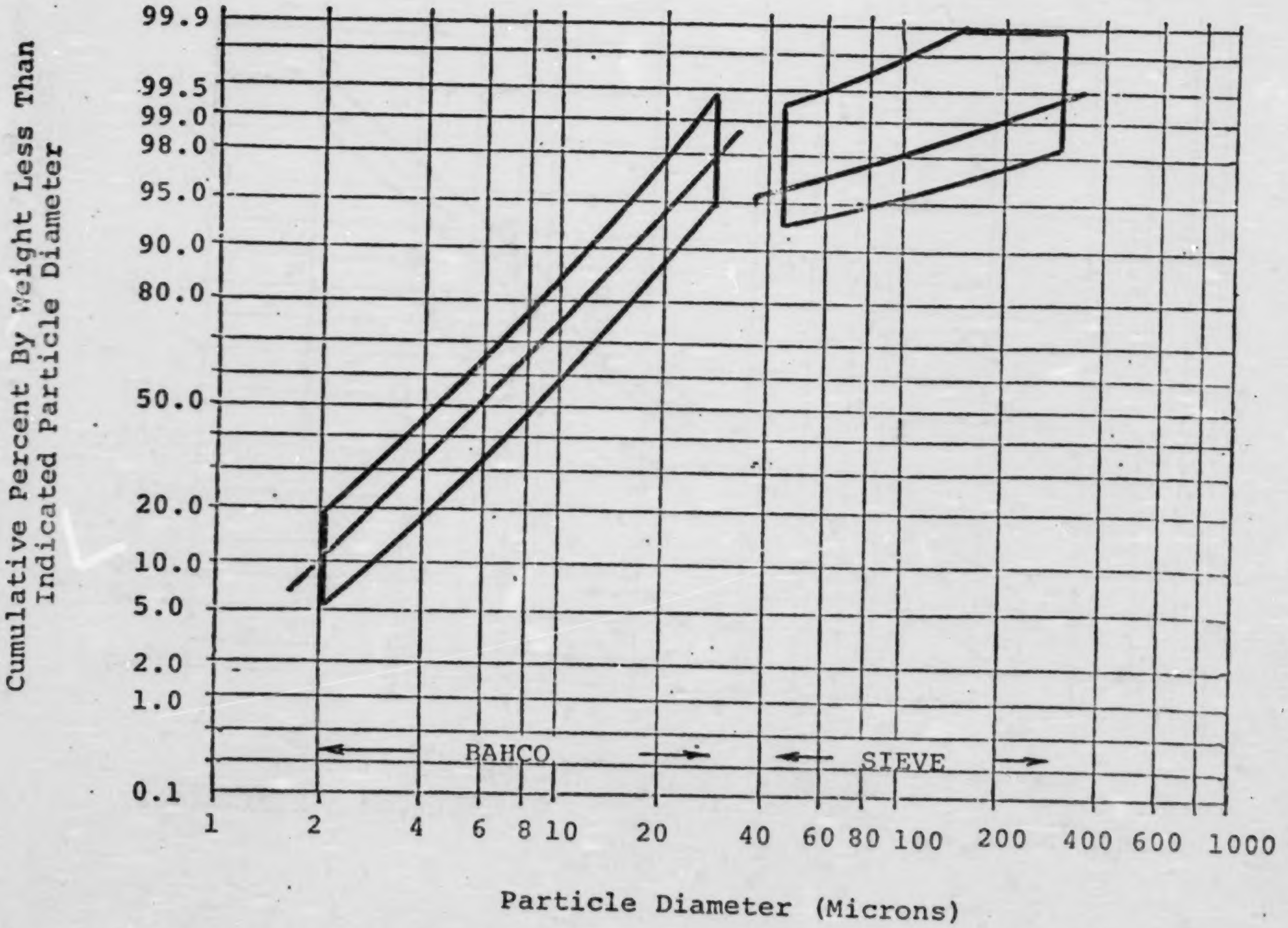

FIGURE 41

PARTICLE SIZE ANALYSES OF ELECTROSTATIC PRECIPITATOR OUTLET SAMPLES WITH FINE LIMESTONE INJECTION (TESTS 2,3,4,5,6,23,24,26)

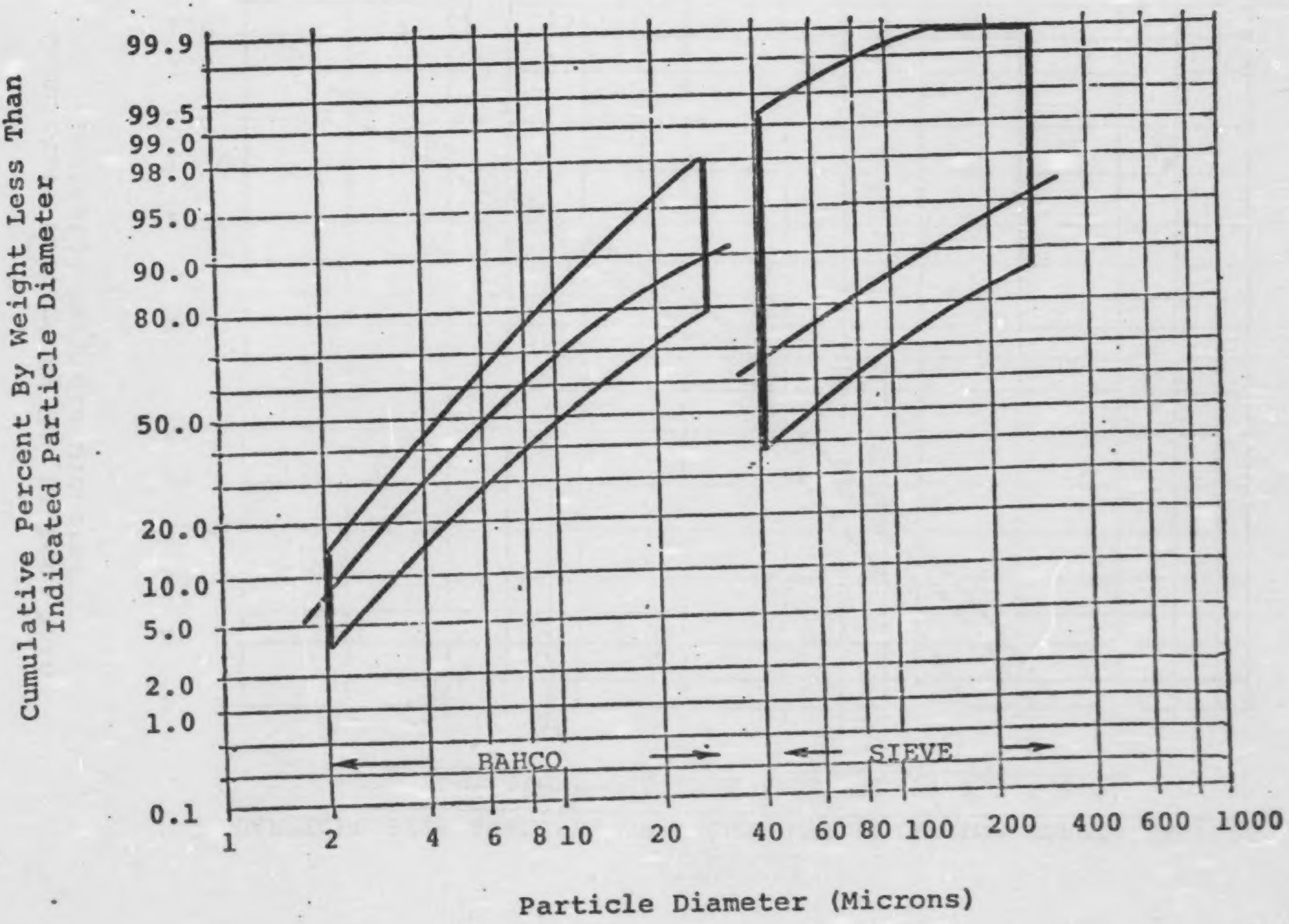

FIGURE 42

PARTICLE SIZE ANALYSES OF MECHANICAL COLLECTOR HOPPER SAMPLES

WITH FINE LIMESTONE INJECTION (TESTS 2,3,5,6,8)

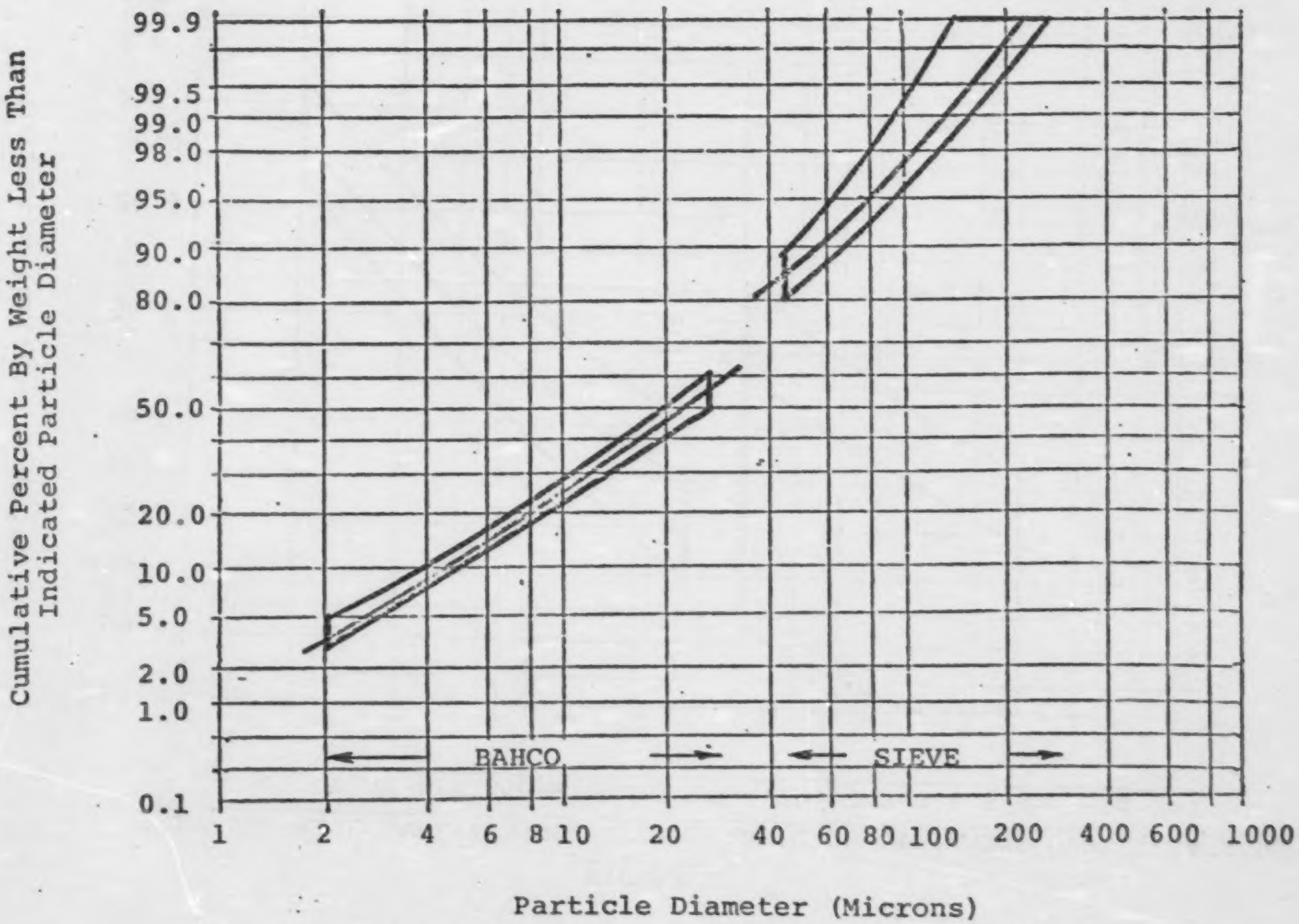

FIGURE 43

PARTICLE SIZE ANALYSES OF ELECTROSTATIC PRECIPITATOR HOPPER SAMPLES

WITH FINE LIMESTONE INJECTION (TESTS 17,18,23,24)

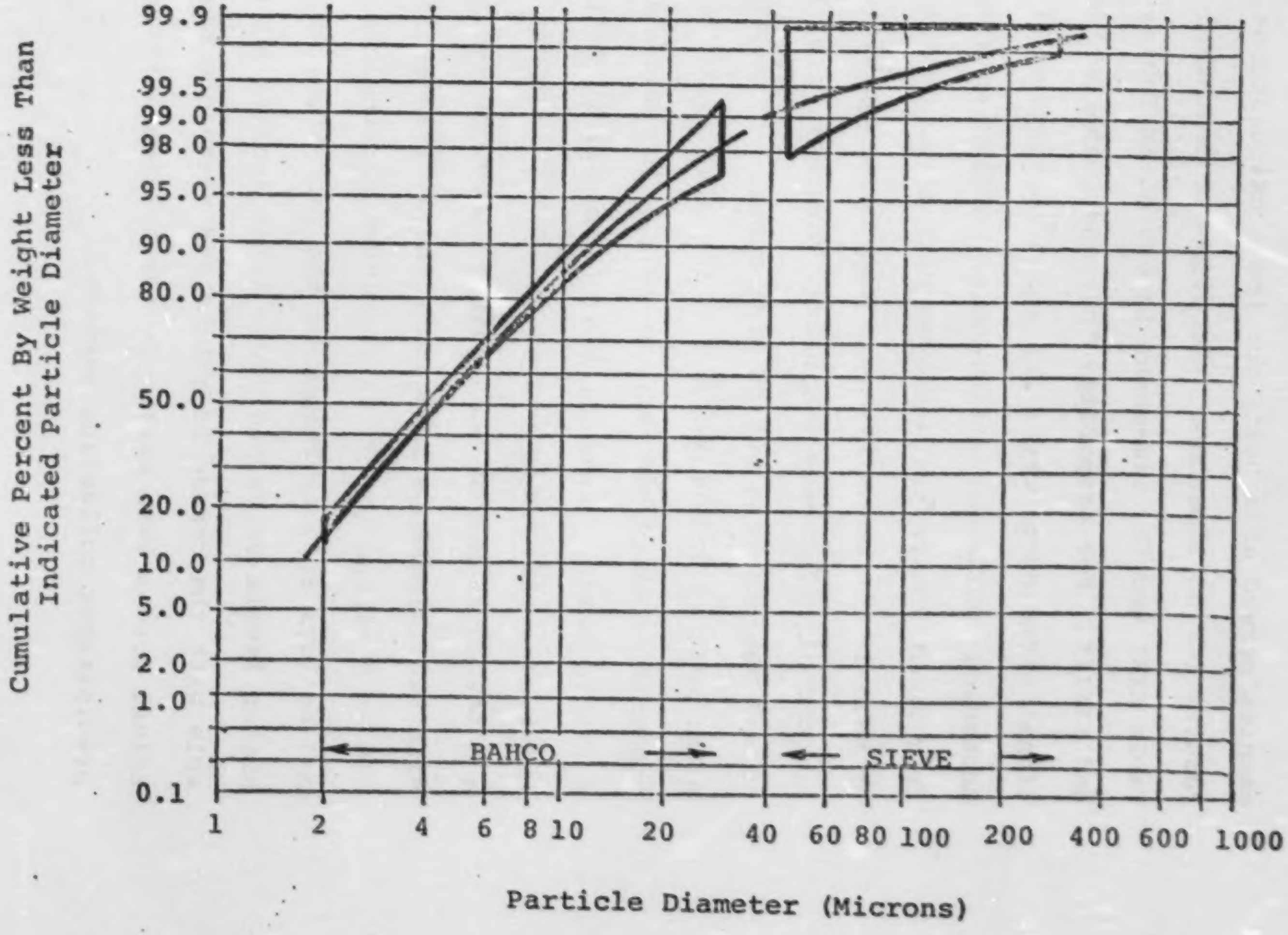

size distribution between inlet, outlet, and hopper catch samples served as a basis for these calculations. The results for no limestone injection are contained in Table XXXI and for limestone injection in Tables XXXII and XXXIII. For comparative purposes, the collector fractional efficiency curves are shown in Figures 44 and 45. Mechanical collector efficiencies on fly ash alone ranged from about 25% on the 5 micron size to 90 to 95% on greater than 25 microns. However, the electrostatic collector fractional efficiency was nearly constant, i.e. between 80 and 90% over the entire size range. In general, the mechanical efficiencies on fly ash plus additive reaction products is about the same as on fly ash alone or perhaps a little lower. However, the electrostatic collector fractional efficiency was about 90% on 5 micron material and 70% on 25 micron when coarse limestone was injected. With fine limestone injection, the efficiency varied from 65% on 5 micron to 25% on 25 micron particulate. This can be logically explained by the fact that, in general, higher levels of corona power input density were attainable with the coarse injection and therefore higher electrical forces were available for holding material on the precipitator collecting surface.

TABLE XXXI

FRACTIONAL EFFICIENCY OF DUST COLLECTORS - FLY ASH ONLY

(CES Test Series No. 1)

	MECHANICAL COLLECTOR FRACTION IN INTERVAL				ELECTROSTATIC PRECIPITATOR FRACTION IN INTERVAL				PERCENT FRACTIONAL EFFICIENCY[(1)]	
Micron Size Interval	Inlet	Outlet	Hopper	Hopper & Outlet	Inlet	Outlet	Hopper	Hopper & Outlet	Mechanical Collector	Electrostatic Precipitator
0-2	6.5	4.7	2.0	6.7	11.0	2.7	13.8	16.5	29.9	83.6
2-4	9.5	10.7	2.0	12.7	25.0	3.5	25.0	28.5	15.8	87.8
4-6	7.0	8.1	2.6	10.7	19.0	2.2	15.5	17.7	24.4	87.7
6-8	7.0	5.5	2.3	7.8	13.0	1.4	10.4	11.8	29.5	88.3
8-10	4.0	3.4	2.0	5.4	8.0	0.7	5.2	5.9	37.1	88.2
10-15	10.0	3.8	4.6	8.4	9.0	1.1	7.8	8.9	54.7	87.6
15-20	8.0	3.4	6.3	9.7	8.0	0.9	4.3	5.2	65.0	82.7
20-25	3.0	1.1	4.0	5.1	2.0	0.1	0.9	1.0	78.4	90.0
25-30	5.0	0.4	4.0	4.4	1.5	0.3	0.9	1.2	91.0	75.0
>30	40.0	1.5	27.6	29.1	3.5	0.7	2.6	3.3	92.3	78.8
	100.0	42.6	57.4	100.0	100.0	13.6	86.4	100.0		

(1) $\frac{\text{Hopper (100)}}{\text{Hopper + Outlet}}$

TABLE XXXII

FRACTIONAL EFFICIENCY OF DUST COLLECTORS - FINE LIMESTONE

	MECHANICAL COLLECTOR FRACTION IN INTERVAL				ELECTROSTATIC PRECIPITATOR FRACTION IN INTERVAL				PERCENT FRACTIONAL EFFICIENCY(1)	
Micron Size Interval	Inlet	Outlet	Hopper	Hopper & Outlet	Inlet	Outlet	Hopper	Hopper & Outlet	Mechanical Collector	Electrostatic Precipitator
0-2	6.5	4.3	1.7	6.0	10.0	2.9	11.1	16.5	28.4	79.3
2-4	13.5	8.4	3.1	11.5	23.0	8.6	19.2	27.8	27.0	69.1
4-6	12.0	8.0	3.7	11.7	18.0	6.9	13.2	20.1	31.6	65.7
6-8	11.0	6.7	2.8	9.5	15.0	4.6	6.2	10.8	29.5	57.4
8-10	9.0	3.6	2.3	5.9	8.0	3.1	3.1	6.2	39.0	50.0
10-15	13.0	5.8	6.2	12.0	11.0	3.8	4.9	8.7	51.7	56.3
15-20	12.0	4.0	5.7	9.7	9.0	1.9	2.2	4.1	58.8	53.6
20-25	3.0	0.9	1.1	1.9	2.0	1.3	0.3	1.6	58.0	18.8
25-30	4.0	0.9	5.0	5.9	2.0	1.4	0.5	1.9	84.9	26.3
>30	16.0	0.9	25.0	25.9	2.0	3.7	1.1	4.8	96.5	23.0
	100.0	43.4	56.6	100.0	100.0	38.2	61.8	100.0		

(1) $\frac{\text{Hopper (100)}}{\text{Hopper + Outlet}}$

TABLE XXXIII

FRACTIONAL EFFICIENCY OF DUST COLLECTORS - COARSE LIMESTONE

(CES Test Series No. 2)

	MECHANICAL COLLECTOR FRACTION IN INTERVAL				ELECTROSTATIC PRECIPITATOR FRACTION IN INTERVAL				PERCENT FRACTIONAL EFFICIENCY (1)	
Micron Size Interval	Inlet	Outlet	Hopper	Hopper & Outlet	Inlet	Outlet	Hopper	Hopper & Outlet	Mechanical Collector	Electrostatic Precipitator
0-2	11.0	3.4	1.8	5.2	7.0	0.6	14.2	14.8	34.6	95.9
2-4	17.0	11.0	2.8	13.8	23.0	2.4	28.4	30.8	20.3	92.3
4-6	11.0	10.3	3.6	13.9	21.0	1.9	19.6	21.5	25.9	91.3
6-8	9.0	6.8	2.1	8.9	14.0	1.6	9.8	11.4	23.6	86.1
8-10	6.0	4.4	2.1	6.5	9.0	1.0	4.6	5.6	32.2	82.2
10-15	11.0	5.3	4.1	9.4	11.0	1.4	8.0	9.4	43.5	88.8
15-20	7.0	3.4	4.1	7.5	7.0	1.0	2.7	3.7	54.7	73.0
20-25	3.0	0.5	1.5	2.0	1.0	0.1	0.3	0.4	75.0	75.0
25-30	5.0	1.5	3.1	4.6	3.0	0.4	1.1	1.5	67.5	73.3
>30	20.0	1.9	26.2	28.1	4.0	0.5	0.4	0.9	93.3	44.4
	100.0	48.5	51.5	100.0	10.9	89.1	100.0			

(1) $\frac{\text{Hopper (100)}}{\text{Hopper + Outlet}}$

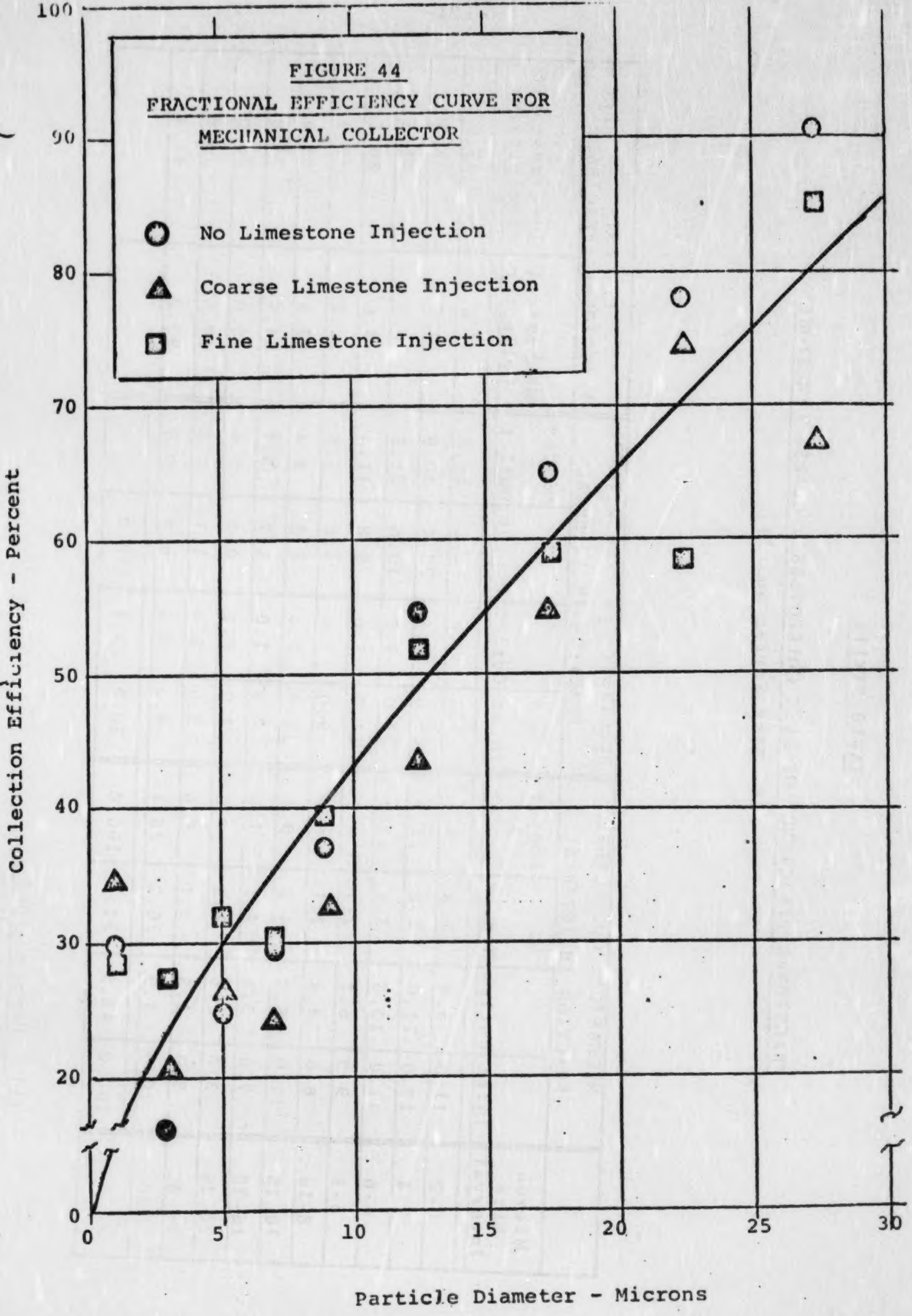

FIGURE 44
FRACTIONAL EFFICIENCY CURVE FOR MECHANICAL COLLECTOR

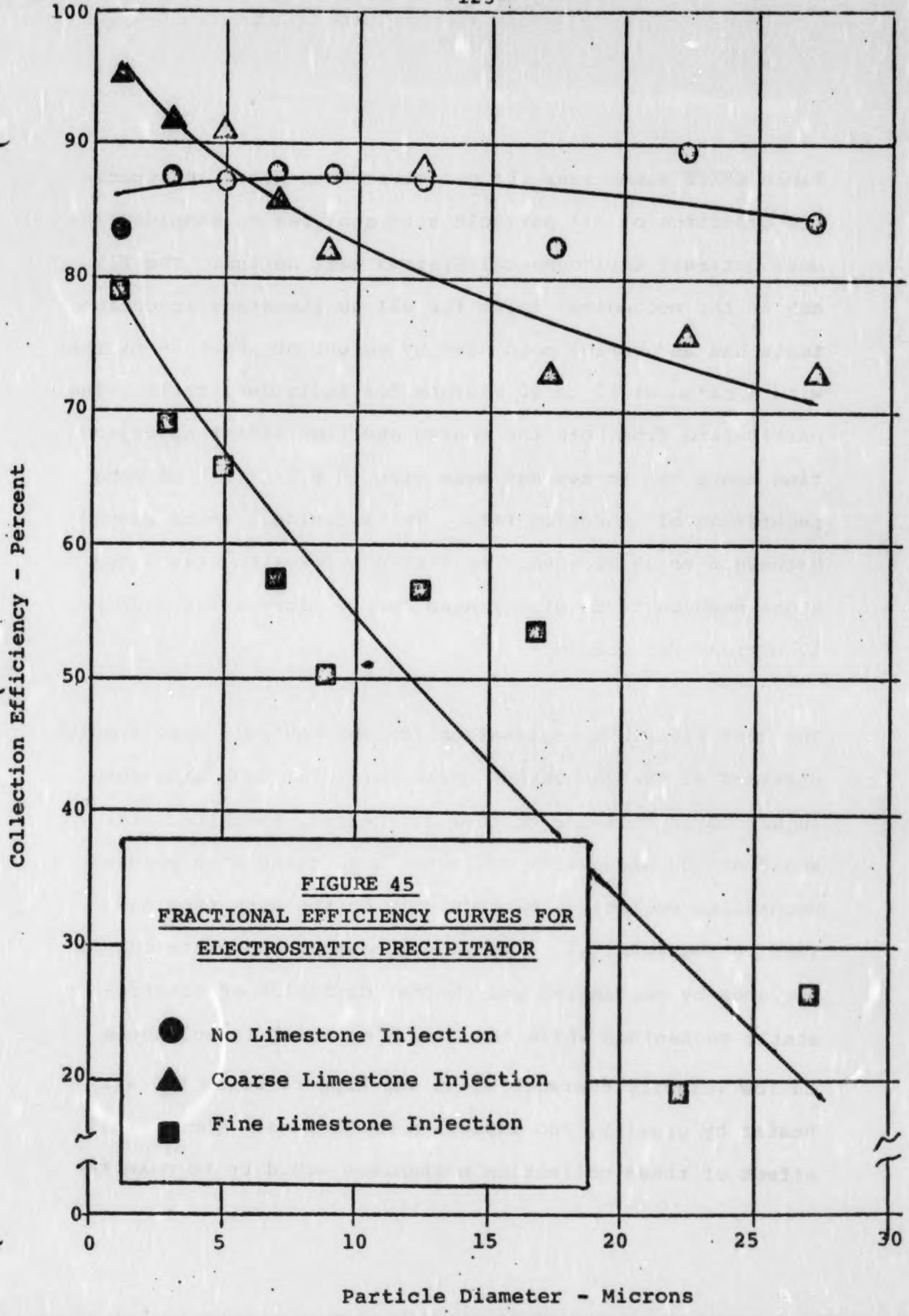

FIGURE 45

FRACTIONAL EFFICIENCY CURVES FOR ELECTROSTATIC PRECIPITATOR

Table XXXIV summarizes the geometric mean sizes and specific gravities of all particle size analyses on samples from both Cottrell Environmental Systems test series. The fly ash at the mechanical inlet for all no limestone injection tests had an average mean size by weight of about 19 microns with a range of 12 to 30 microns for individual tests. The particulate from both the coarse and fine limestone injection tests had an average mean size of 8.5 to 9.5 microns regardless of injection rate. The individual tests ranged between 6 to 13 microns. As stated before, the raw limestone mean particle size ranged from 6 microns for fine to 17 microns for coarse.

The most plausible explanation for the particle size results obtained at the mechanical collector inlet with limestone injection is that the boiler, air heater, ductwork, etc. ahead of the mechanical collector are acting as a primary mechanical collector, particularly on the very fine and very coarse material. The fine limestone can plate out on surfaces by mechanical and thermal diffusion or electrostatic mechanisms while the coarse material is collected in low velocity ductwork areas and hoppers below the air heater by gravity, and impaction mechanisms. The overall effect of these collection mechanisms would be to make the

TABLE XXXIV

SUMMARY OF PARTICLE SIZE ANALYSES ON SAMPLES FROM BOTH CES TEST SERIES

(From Figures 26 to 43)

Sample Point	Description	Test Numbers	Average Geometric Mean Size (μ)	Specific Gravity	Range of Geometric Mean Size For Individual Tests (μ)
Limestone Feeder	Coarse	14, 32, 33	17	2.55	15 - 20
Limestone Feeder	Fine	6, 8, 23, 24	6.0	2.54	5 - 7
MC Inlet	Fly Ash Only	1A&B, 3A, 4A&B, 5A&B	19	2.36	12 - 30
ESP Inlet	Fly Ash Only	1A&B, 3A, 4A&B, 5A&B	5.5	2.31	5 - 6.5
ESP Outlet	Fly Ash Only	2A, 3A&B, 4B	4.5	1.98	3.5 - 5.5
MC Hopper	Fly Ash Only	1A&B, 2A, 3A&B, 4A&B, 5A&B	28	2.32	24 - 33
ESP Hopper	Fly Ash Only	1A&B, 2A, 3A, 4A, 5A&B	4.6	2.04	4.2 - 5.2
ESP Inlet	Fly Ash Only	16, 19, 20, 21, 22	7.0	2.53	4.5 - 9
ESP Hopper	Fly Ash Only	16, 21, 22	4.0	2.30	3.8 - 4.3
MC Inlet	Fly Ash & Coarse Limestone Reaction Products	14, 15, 32, 33	8.5	2.69	6.2 - 13
ESP Inlet	Fly Ash & Coarse Limestone Reaction Products	10, 11, 14, 15, 25, 32, 33	6.0	2.67	5 - 7

TABLE XXXIV (Continued)

SUMMARY OF PARTICLE SIZE ANALYSES ON SAMPLES FROM BOTH CES TEST SERIES

(From Figures 26 to 43)

Sample Point	Description	Test Numbers	Average Geometric Mean Size (μ)	Specific Gravity	Range of Geometric Mean Size For Individual Tests (μ)
ESP Outlet	Fly Ash & Coarse Limestone Reaction Products	11, 14	6.6	3.05	5.8 - 8
MC Hopper	Fly Ash & Coarse Limestone Reaction Products	14, 15, 32, 33	30	2.85	26 - 40
ESP Hopper	Fly Ash & Coarse Limestone Reaction Products	14, 15	4.2	2.53	3.8 - 4.7
MC Inlet	Fly Ash & Fine Limestone Reaction Products	2, 3, 5, 6, 8	9.5	3.08	8 - 13
ESP Inlet	Fly Ash & Fine Limestone Reaction Products	2,3,4,5,6,8, 17,18,23,24, 26,27,28,29,30	5.8	2.78	4.5 - 8.5
ESP Outlet	Fly Ash & Fine Limestone Reaction Products	2, 3, 4, 5, 6, 23, 24, 26	6.5	2.09	4.5 - 11
MC Hopper	Fly Ash & Fine Limestone Reaction Products	2, 3, 5, 6, 8	23	2.71	20 - 27
ESP Hopper	Fly Ash & Fine Limestone Reaction Products	17, 18, 23, 24	4.1	2.63	3.9 - 4.3

particle size distribution at the mechanical collector inlet more uniform, and less dependent on the size distribution and amount of injected limestone. Other possibilities include agglomeration or attachment of fines to larger particles (fly ash) by impaction, ineffective dispersion of fines during injection, better calcination on the coarse material resulting in decreased size by carbon dioxide loss, and higher utilization of fines in reacting with sulfur oxides causing an increase in particle size of the reaction products.

The average particle loading at the mechanical outlet-precipitator inlet varies with limestone injection rate (see Figure 46) from about 1.5 grains/SCF with no limestone addition to about 4.0 grains/SCF with 16 tons/hour limestone feed into the boiler.

FIGURE 46

ELECTROSTATIC PRECIPITATOR PARTICULATE INLET LOADING AS A FUNCTION OF LIMESTONE FEEDRATE

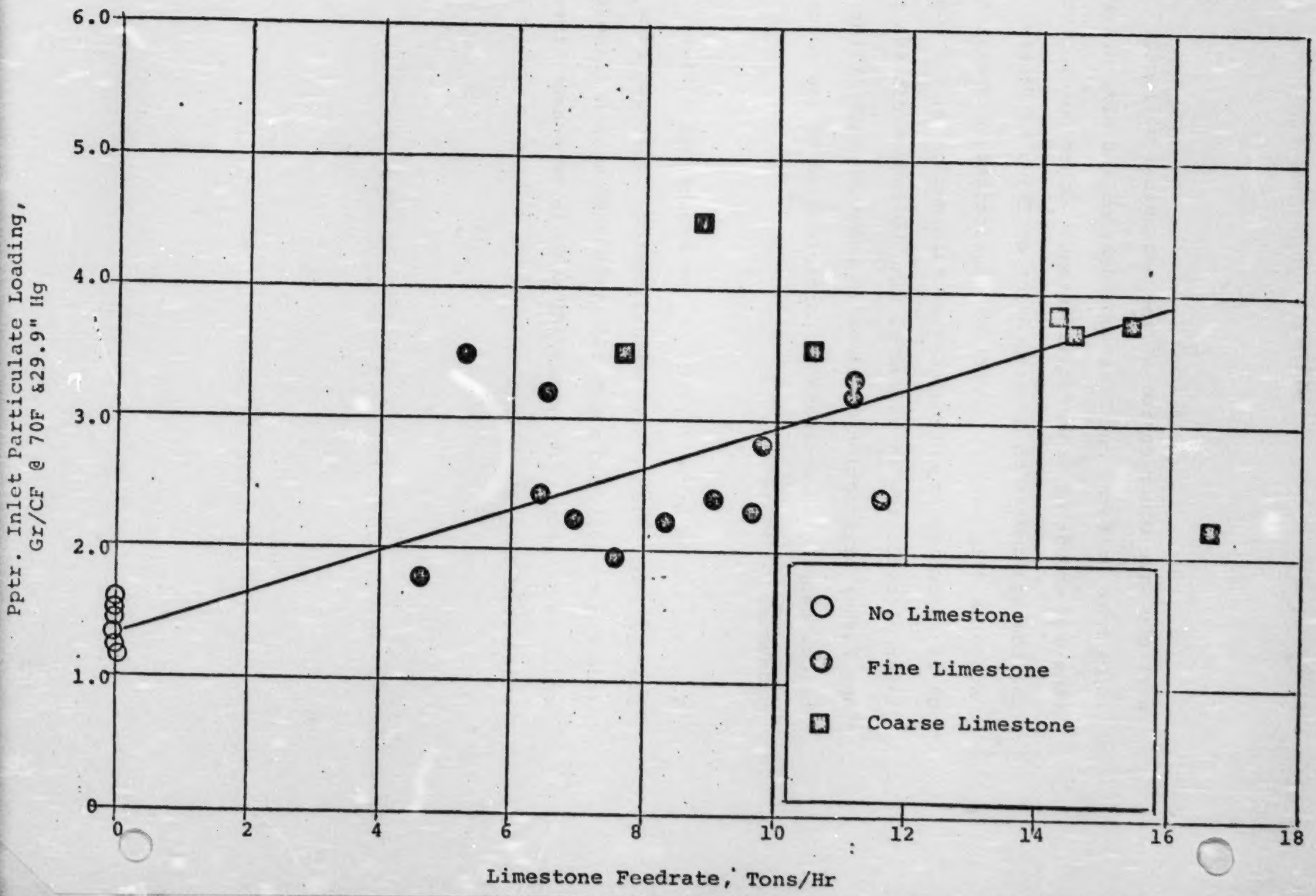

3. Discussion of Particle Resistivity Data

A. Correlation of In-Situ and Laboratory Resistivity Measurements

As discussed in an earlier section of the report, a fundamental parameter in electrostatic precipitation is the electrical resistivity of the particulate. Many industrial dusts are poor conductors and as a result inhibit the performance of precipitators. Generally, the critical value above which precipitation is deleteriously affected is somewhere between 10^{10} and 10^{11} ohm-cm.(6) The gas temperature and moisture content are the two main factors having the strongest influence on resistivity. Secondary agents present in some industrial gases, e.g. sulfur trioxide, can drastically change resistivity. It is this particular agent which appears to cause the differences in laboratory and in-situ resistivity of fly ash from coal fired boilers. (Sulfur trioxide cannot be simulated conveniently in the laboratory test gas.) Furthermore, the addition of large amounts of alkali material such as ground limestone to the boiler flue gas which removes the sulfur trioxide by chemical reaction is believed to result in degraded precipitation rates. An objective of the test program was to measure the effects of limestone injection on resistivity and precipitation rates.

In Figure 47, the in-situ resistivities obtained for coal firing only on full-scale boilers at Shawnee Station of TVA and a large midwest utility, and on a pilot scale combustor at Babcock and Wilcox Company Research Center are plotted as a function of gas temperature. Figure 48 displays in-situ resistivities obtained during limestone injection tests by the same organizations. The Shawnee data was obtained by Southern Research Institute(2) (see Table XXXV), K. J. McLean(5) (see Figure 49), and Cottrell Environmental Systems (see Tables XXIII through XXV). The midwest utility data was obtained by Research-Cottrell, Inc.(3) (see Table XXXVI). The pilot scale Babcock and Wilcox data(4) for coal firing is reproduced in Figure 50 and shown for comparison with full scale data as a dotted line polygon in Figure 47. Similarly, the Babcock and Wilcox limestone injection data is reproduced in Figures 51 through 53 and shown as a dotted line polygon in Figure 48.

Laboratory resistivity measurements obtained on precipitator inlet samples taken during the Cottrell Environmental Systems test series are shown in Figures 54 (without limestone injection) and 55 (with limestone injection). The in-situ measurements from Figures 47 and 48 are superimposed on this data as solid lined polygons. Note that although the data is scattered, due

FIGURE 47

IN-SITU RESISTIVITIES OBTAINED ON FULL-SCALE & PILOT SCALE PULVERIZED COAL-FIRING BOILERS WITHOUT LIMESTONE INJECTION

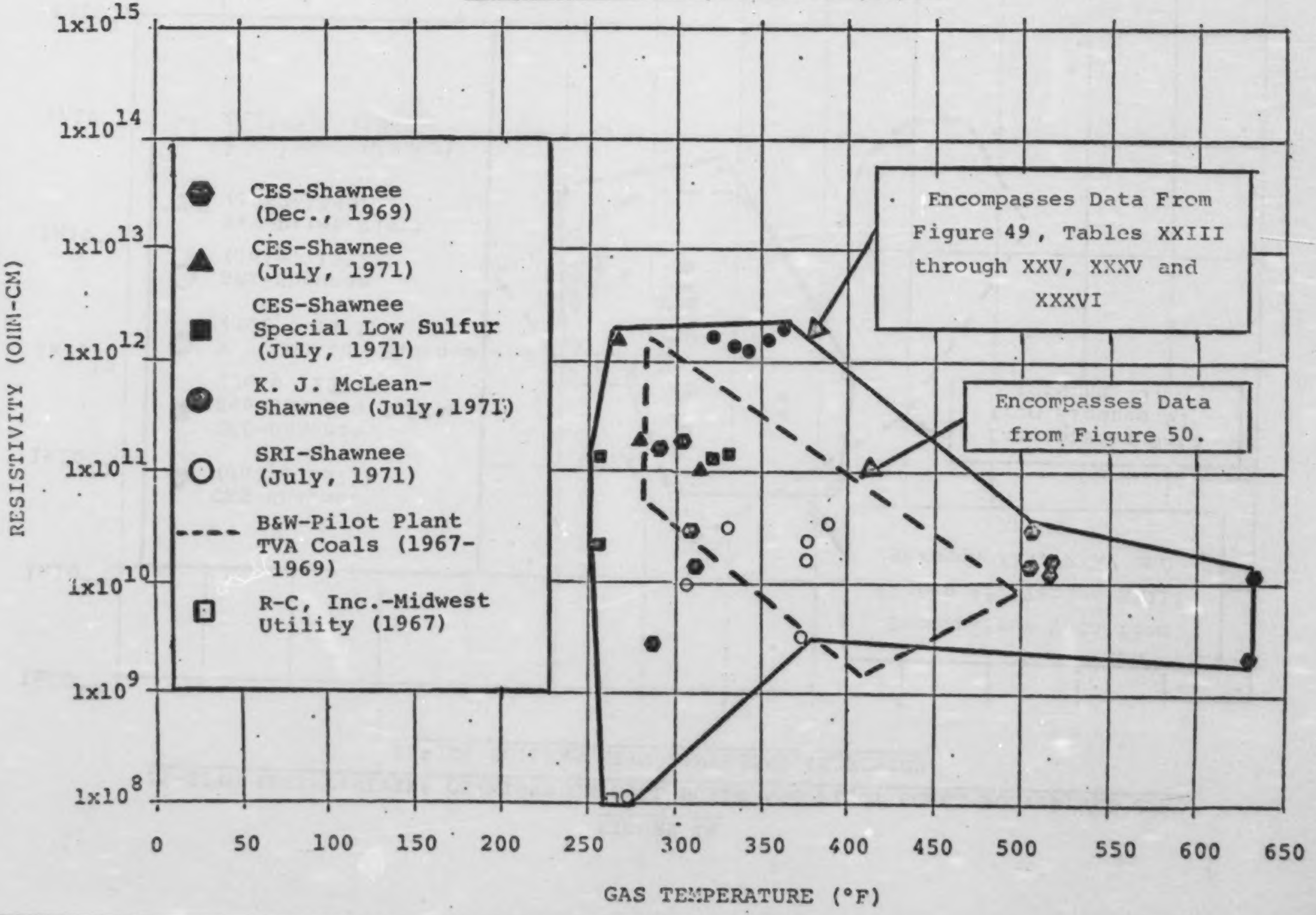

FIGURE 48

IN-SITU RESISTIVITIES OBTAINED ON FULL SCALE AND PILOT SCALE PULVERIZED COAL FIRING BOILERS WITH LIMESTONE INJECTION

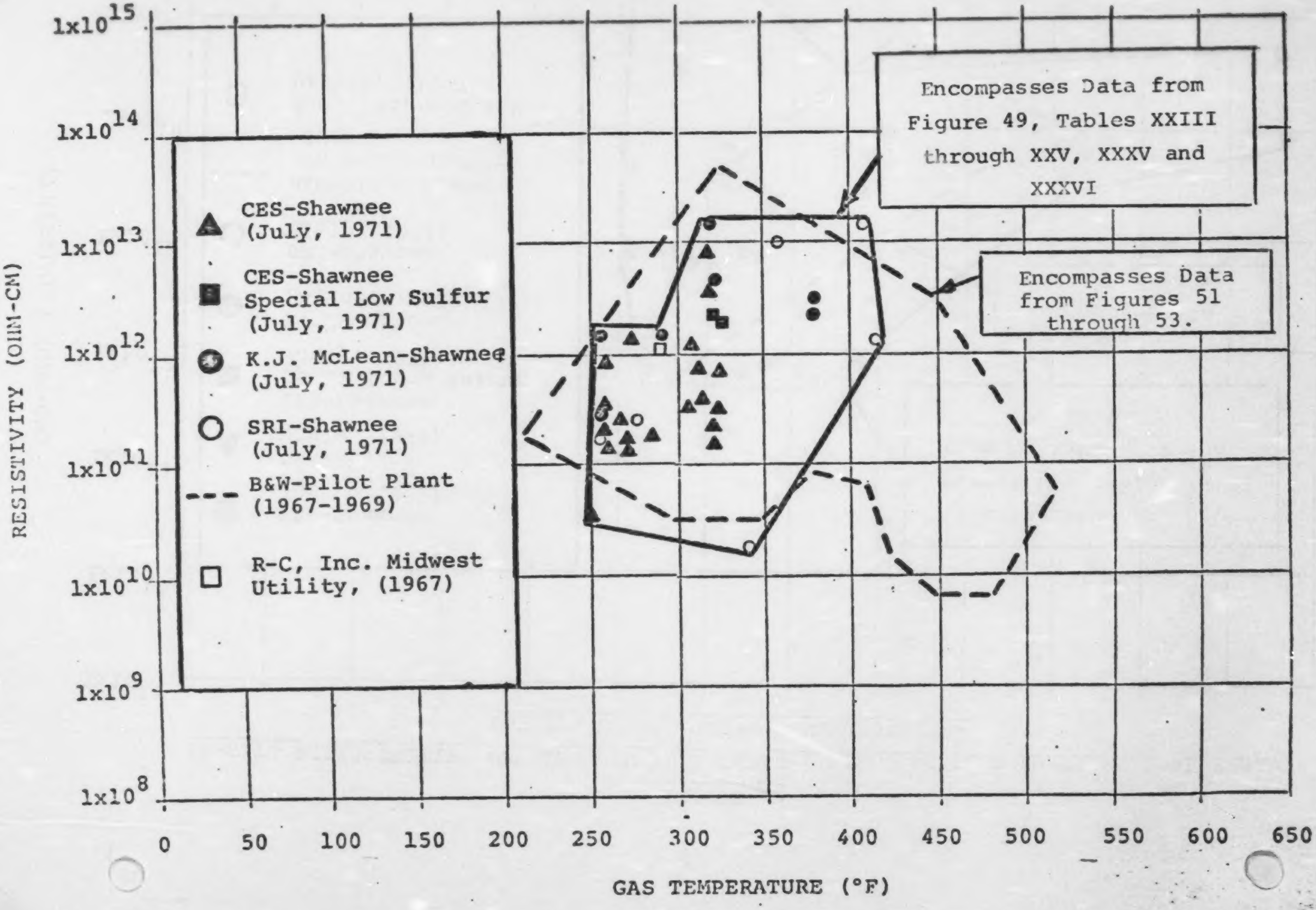

TABLE XXXV

IN-SITU RESISTIVITY DATA OBTAINED BY SOUTHERN RESEARCH INSTITUTE AT TVA SHAWNEE STATION, BOILER #10 DURING THE CES SECOND TEST SERIES

Date	Reported Injection Rate of $CaCO_3$, Lb./Min.	Temp., °F	Resistivity, ohm cm, at various electric fields					
			1.0 KV/cm	2.5 KV/cm	5.0 KV/cm	10.0 KV/cm	15.0 KV/cm	20.0 KV/cm
July 15	333	340	---	---	3.0×10^{10}	2.7×10^{10}	---	---
July 16	333	255	---	---	4.0×10^{11}	2.4×10^{11}	1.5×10^{11}	9.0×10^{10}
	333	273	---	---	4.5×10^{11}	4.5×10^{11}	4.5×10^{11}	4.5×10^{11}
July 21	167	407	---	---	1.3×10^{13}	1.7×10^{13}	2.3×10^{13}	2.6×10^{13}
	333	360	---	---	1.1×10^{13}	1.0×10^{13}	9.0×10^{12}	8.0×10^{12}
July 27	333	417	4.0×10^{11}	5.0×10^{11}	8.0×10^{11}	1.2×10^{12}	1.6×10^{12}	2.0×10^{12}

(a) With Limestone Injection

Date	Temp., °F	Resistivity, ohm cm, at various electric fields					
		1.0 KV/cm	2.5 KV/cm	5.0 KV/cm	10.0 KV/cm	15.0 KV/cm	20.0 KV/cm
July 15	375	2.3×10^{10}	1.4×10^{10}	8.0×10^{9}	5.0×10^{9}	---	---
	376	---	---	3.5×10^{10}	2.0×10^{10}	1.8×10^{10}	1.8×10^{10}
July 16	266	---	8.0×10^{10}	3.5×10^{10}	1.2×10^{8}	6.0×10^{7}	5.0×10^{7}
	273	---	---	2.3×10^{10}	$8.0\ 1\ 10^{7}$	---	---
	305	7.0×10^{10}	4.0×10^{10}	1.8×10^{10}	1.0×10^{10}	---	---
July 21	330	5.5×10^{10}	5.0×10^{10}	5.0×10^{10}	4.2×10^{10}	3.6×10^{10}	---
July 22	375	5.8×10^{10}	5.0×10^{10}	4.0×10^{10}	3.0×10^{10}	2.5×10^{10}	---
	385	8.0×10^{10}	7.0×10^{10}	6.0×10^{10}	4.6×10^{10}	3.8×10^{10}	3.0×10^{10}

(b) Without Limestone Injection

FIGURE 49

IN-SITU RESISTIVITY DATA OBTAINED BY K.J. McLEAN AT TVA SHAWNEE STATION, BOILER #10 DURING THE CES SECOND TEST SERIES

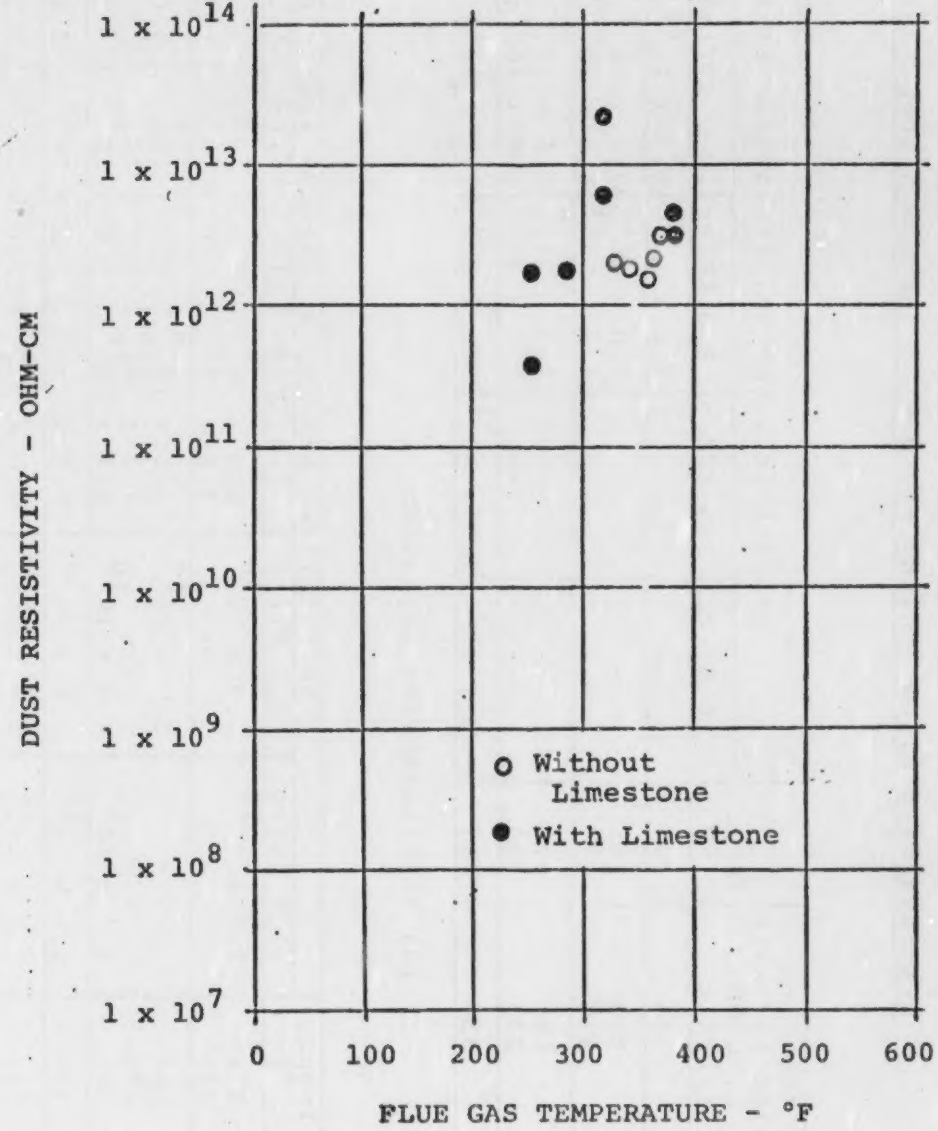

TABLE XXXVI

DATA SUMMARY - FULL SCALE DOLOMITE INJECTION TEST RESULTS OBTAINED BY RESEARCH-COTTRELL, INC. AT A LARGE MIDWEST UTILITY

Parameter	Boiler	
	Reheat	Superheat
Dolomite Injected-Tph	6	0
Coal Fired - Tph	60	65-70
Gas Vol. @ Pptr, ACFM	492,000	568,000
Gas Temp. @ Pptr. °F	287	270
SO_2 PPM by Volume	1,950	2,550
SO_3 PPM by Volume	Nil	17
Dust Concentrations (gr/SCFD)		
Mechanical Inlet	6.10	3.70
Precipitator Inlet	1.32	0.74
Precipitator Outlet	0.60	0.16
Efficiencies %		
Mechanical	78.3	80.0
Precipitator	55.0	78.8
Overall	90.2	95.8
In-Situ Resistivity - ohm-cm	1×10^{12}	1×10^{8}
Precipitation Rate - FPS	0.15	0.34

FIGURE 50

RESISTIVITY OF FLY ASH SAMPLES FROM VARIOUS COALS FIRED IN PILOT PLANT OF B&W

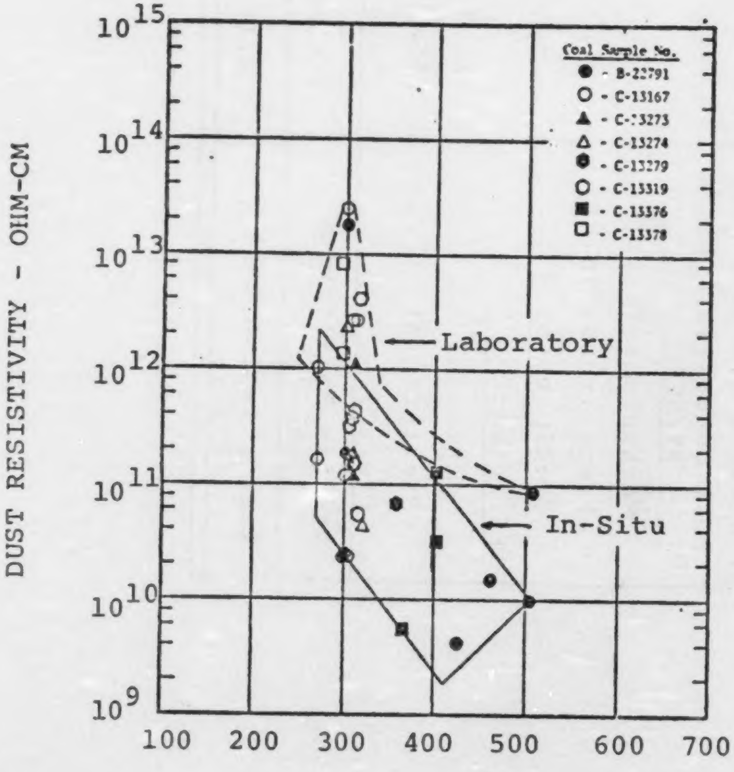

FIGURE 51

IN-SITU AND LABORATORY RESISTIVITIES FOR REACTED ADDITIVE-FLY ASH SAMPLES FROM B&W PILOT PLANT

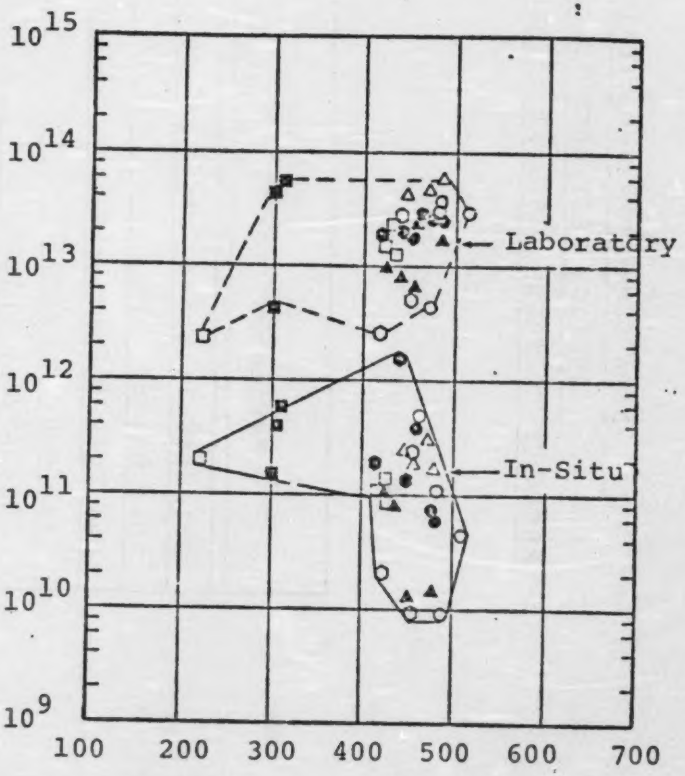

FIGURE 52

IN-SITU AND LABORATORY RESISTIVITIES FOR REACTED ADDITIVE-FLY ASH MIXTURES FROM B&W PILOT PLANT

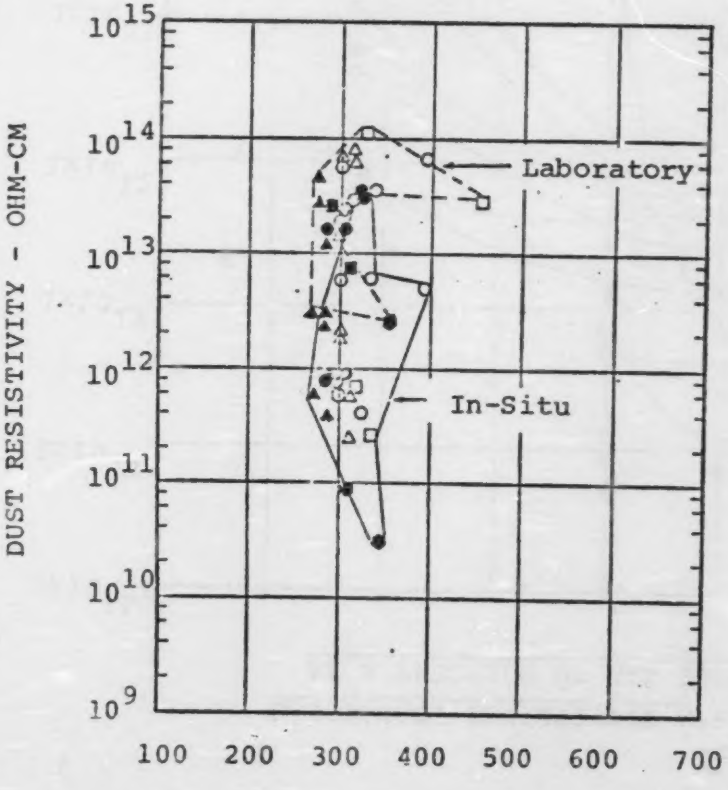

FIGURE 53

IN-SITU AND LABORATORY RESISTIVITIES FOR REACTED ADDITIVE-FLY ASH MIXTURES FROM B&W PILOT PLANT

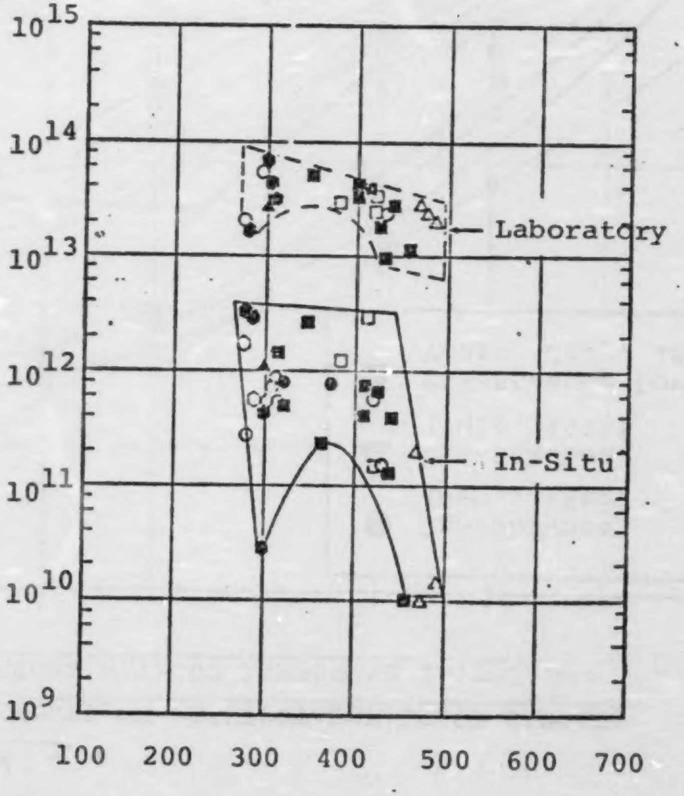

FIGURE 4

LABORATORY RESISTIVITY MEASUREMENTS ON PRECIPITATOR INLET SAMPLES AS A FUNCTION OF GAS TEMPERATURE WITHOUT LIMESTONE INJECTION

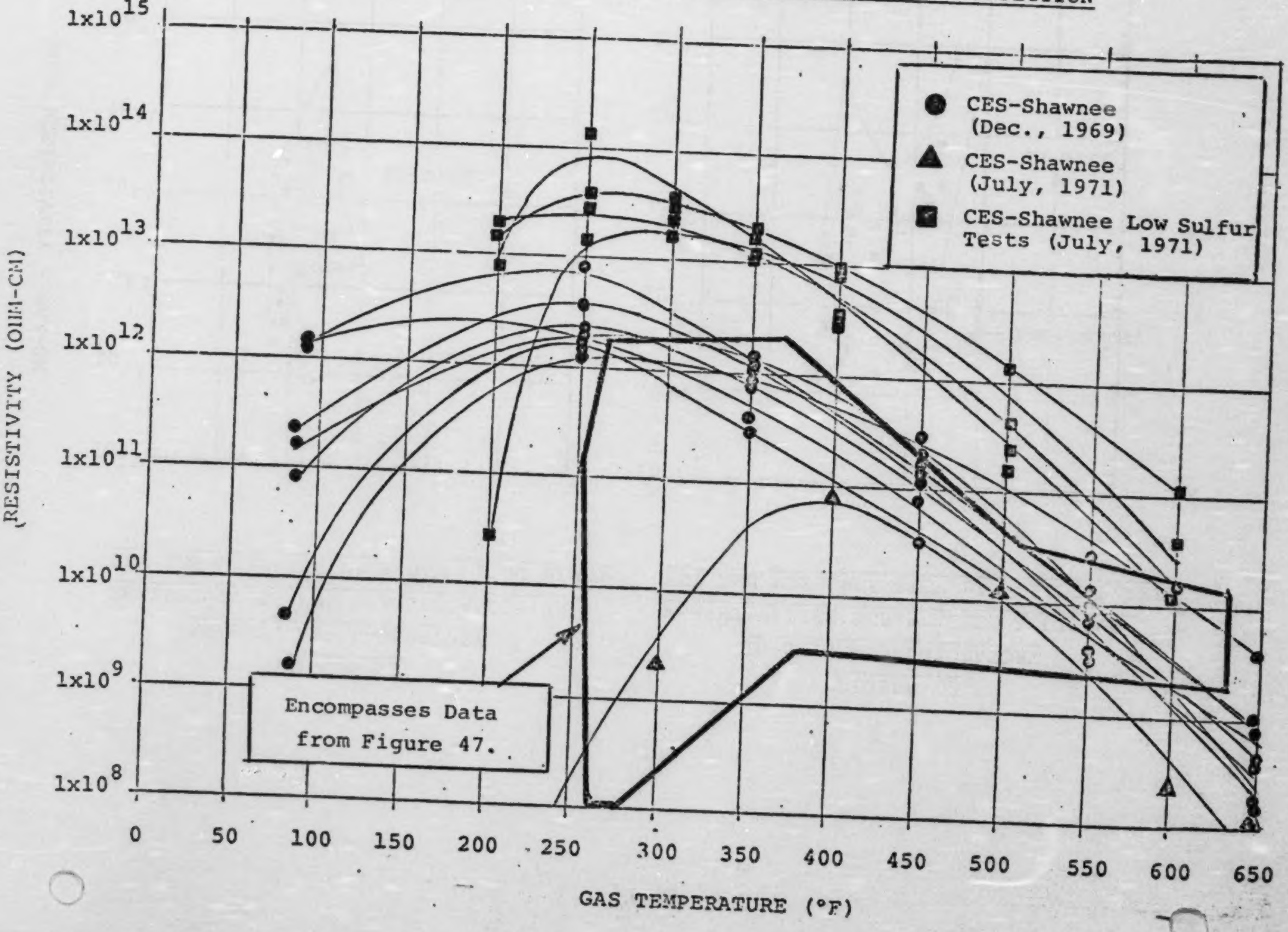

FIGURE 55

LABORATORY RESISTIVITY MEASUREMENTS ON PRECIPITATOR INLET SAMPLES AS A FUNCTION OF GAS TEMPERATURE WITH LIMESTONE INJECTION

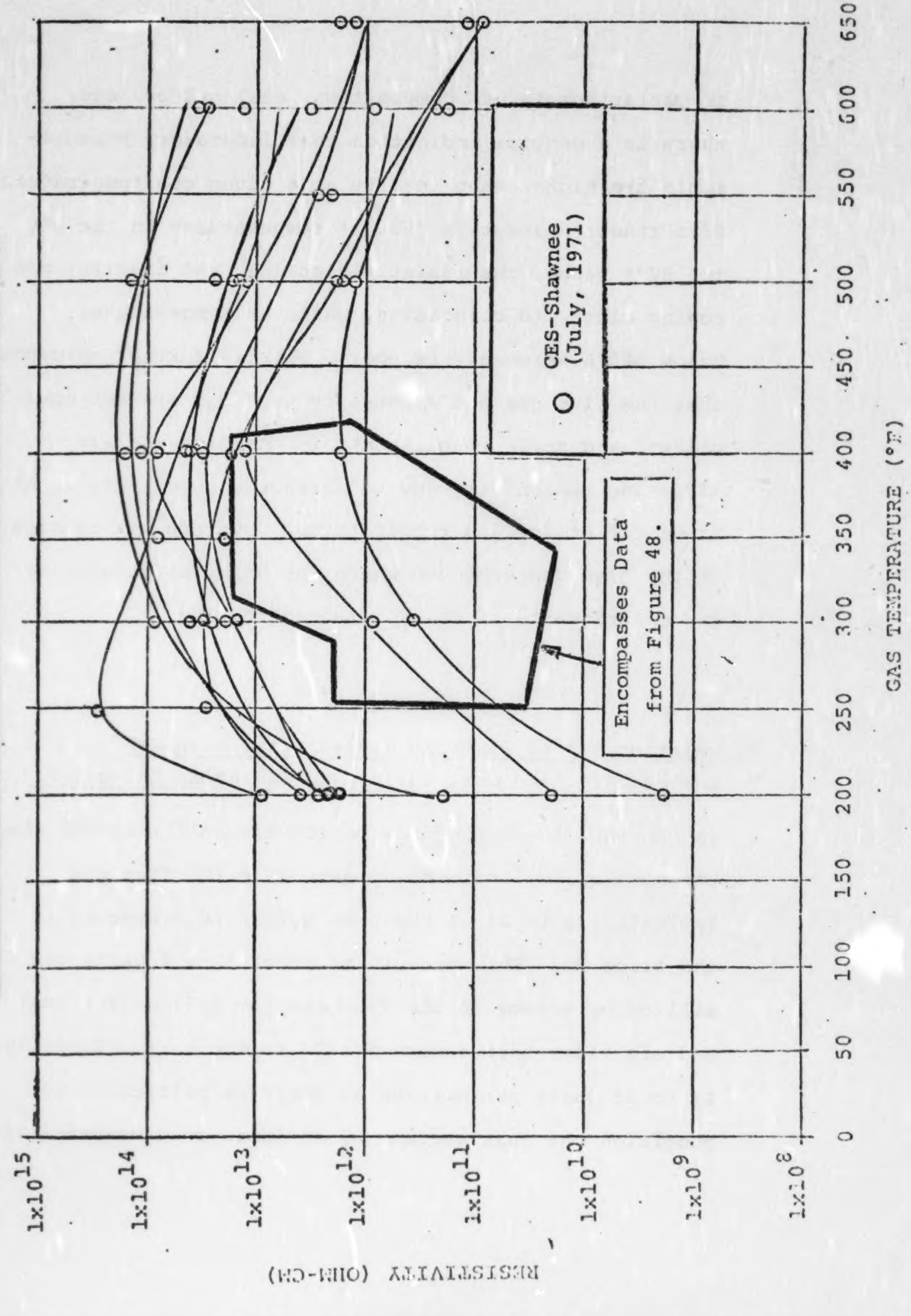

to variations in ash composition, coal sulfur, etc., there is a general indication that laboratory measurements are higher than in-situ at a given gas temperature. Of further interest is that at temperatures in the 550 to 650°F range, the resistivities (lab and in-situ) are coming closer to coinciding, while at temperatures below 500°F agreement is poor. This is further evidence that the flue gas and laboratory test gas are not equivalent, and trace constituents in the flue gas are affecting resistivity due to surface conductivity (most prevalent at low gas temperatures), but are not critical at the high temperatures where the bulk resistivity of the constituents of the ash is controlling.

B. Relationship of Particle Resistivity, Flue Gas Temperature, and Coal Sulfur (No Limestone Injection)

In general, the higher the percentage sulfur in the coal, the more sulfur trioxide appearing in the flue gas. Typically, 1 to 2% of the coal sulfur is converted to the trioxide. This amounts to about 3 to 6 parts per million by volume in the flue gas for 0.5% sulfur coal and six times this amount for 3% sulfur coal. Normally, 15 to 25 parts per million at 300°F is sufficient to condition the dust surface by sulfuric acid condensation giving resistivities in the 10^{10} ohm-cm range or lower. At lower temperatures, less amounts of sulfur trioxide are required and gas moisture content becomes more important. Conversely, at high temperatures, the bulk resistance of the material is controlling, and the coal sulfur and moisture are not critical. Figure 56 is a plot of particle resistivity as a function of flue gas temperature for a range of coal sulfur. The data were taken from Tables XXIII, XXXV, and XXXVI. The midwest utilities data are from unpublished Research-Cottrell, Inc. reports.(12,13) The criticality of coal sulfur and moisture on particle resistivity are graphically demonstrated in the lower temperature ranges (varies five orders of magnitude for 0.5 to 4.0% sulfur), while at the higher temperatures the effect is nearly independent of coal sulfur (varies about one order of magnitude).

C. Relationship of Particle Resistivity, Flue Gas Temperature, and Coal Sulfur (with Limestone Injection)

Normal expectation with a dry alkaline additive, such as limestone to the boiler or into flue gas, is a chemical reaction with the sulfur oxides formed, particularly the trioxide, resulting in a decreased conditioning effect

IN-SITU RESISTIVITY VS. TEMPERATURE RELATIONSHIP FOR VARIOUS COAL SULFURS (No Limestone Injection)

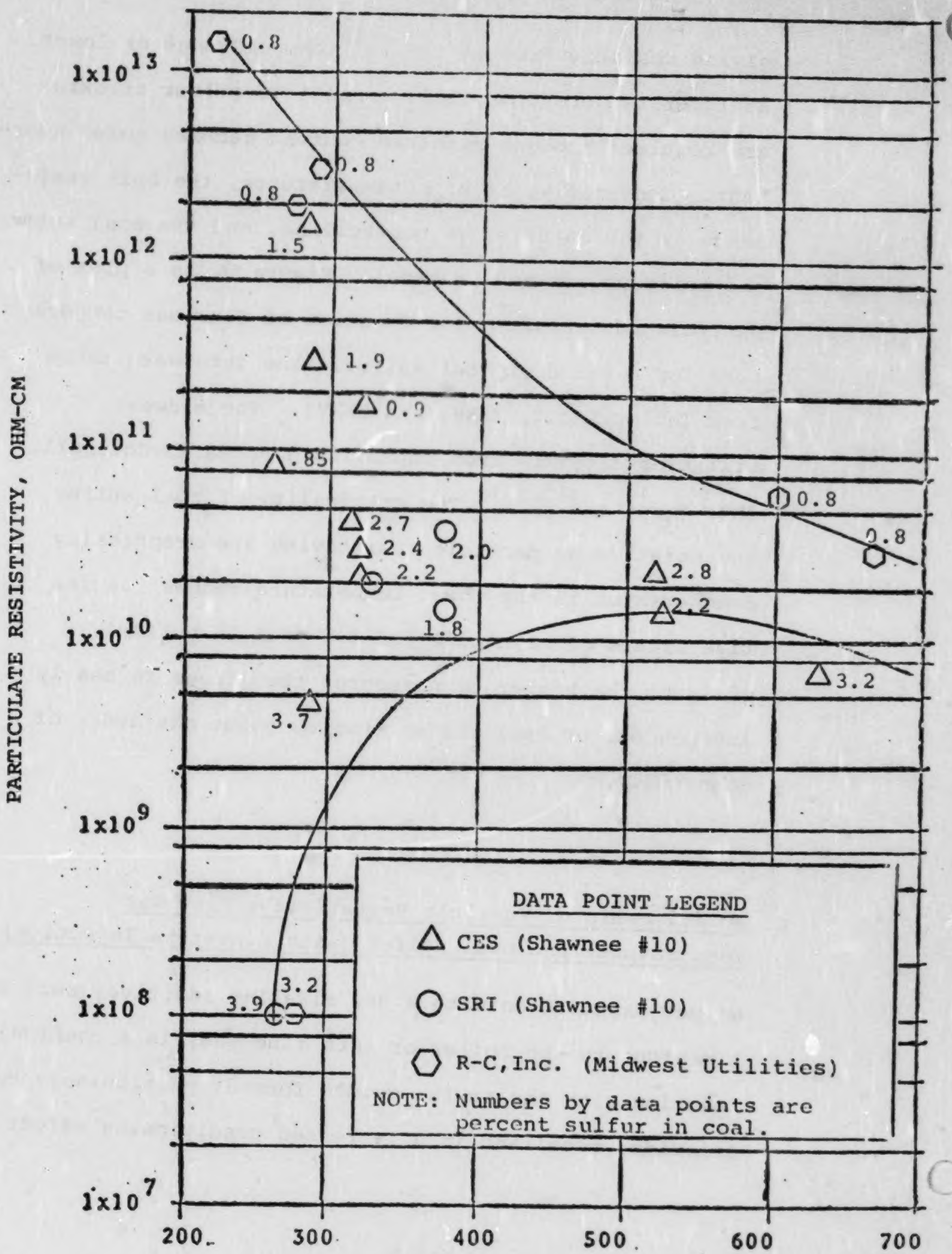

and a higher particulate resistivity. Consequently, the sulfur content of the coal will become relatively independent in its affect on resistivity. In Figure 57, the particulate resistivity is plotted as a function of flue gas temperature with the coal sulfur indicated for each data point. The data were taken from tables and reports as noted above. Of particular interest is the observation that coal sulfur appears to affect the resistivity in a random manner. Nevertheless, the data still shows the affect of low temperature surface conditioning on resistivity. Apparently, this is due mainly to the moisture in the gas plus a few parts per million of sulfur trioxide not removed by the limestone. (See Table 4.14 in Reference 4, and Tables 41 and 44 in Reference 2.)

D. Relationship Between Precipitation Rate Parameter and Particle Resistivity

In establishing the precipitation rate parameter of a dust, the most critical single parameter is the electrical resistivity. Figure 58 graphically demonstrates the degradation of the precipitation rate parameter with resistivity. Two solid line-curves, taken from the literature,(6, 7) are shown. Data points (Table XXXVII) from the Shawnee tests, and a large midwest utility, are plotted for comparison purposes. Verification of the

FIGURE 57

IN-SITU RESISTIVITY VS. TEMPERATURE RELATIONSHIP FOR VARIOUS COAL SULFURS
(With Limestone Injection)

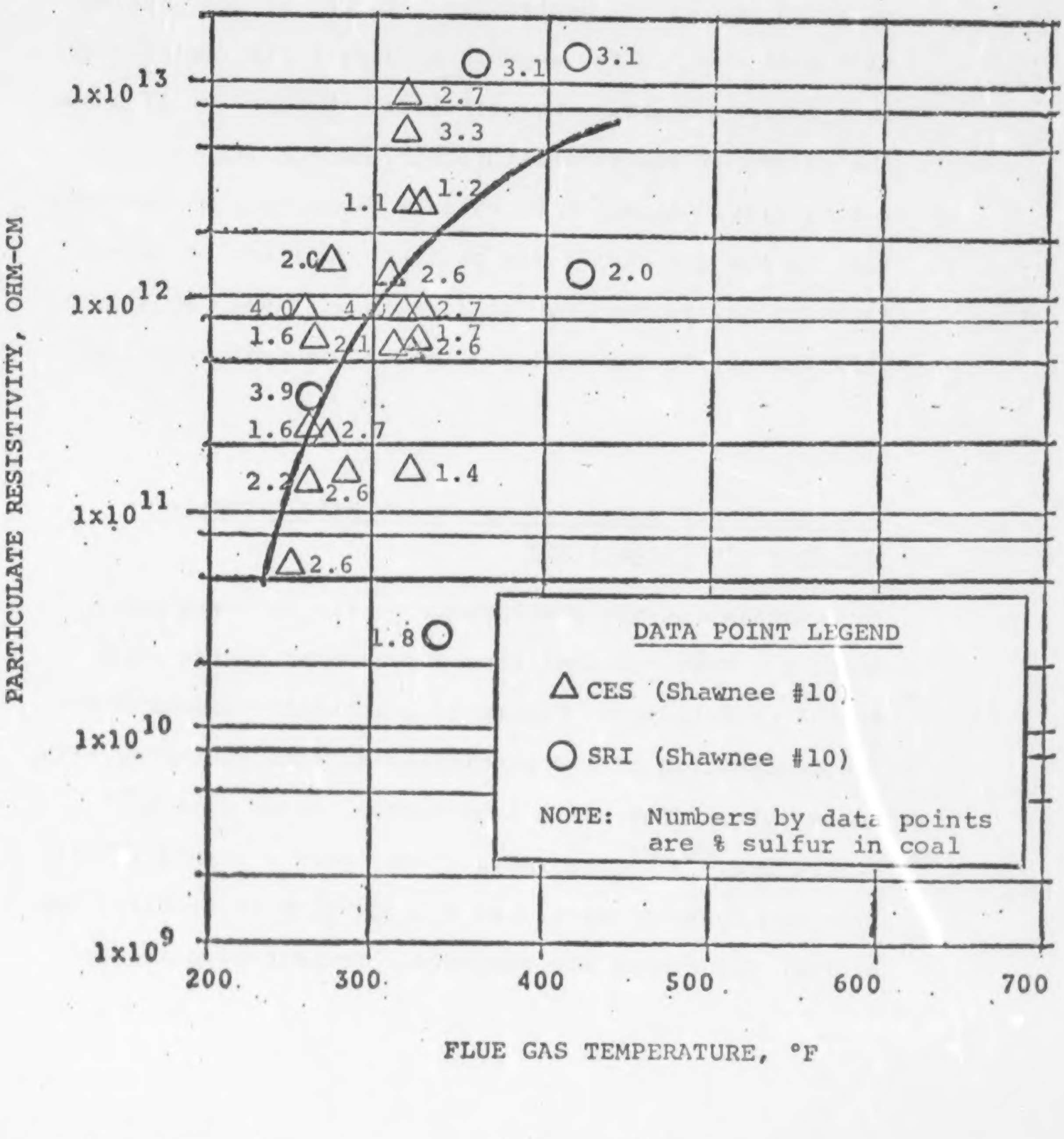

FIGURE 58

APPROXIMATE PRECIPITATION RATE PARAMETER VS. RESISTIVITY RELATIONSHIP WITHOUT AND WITH LIMESTONE INJECTION

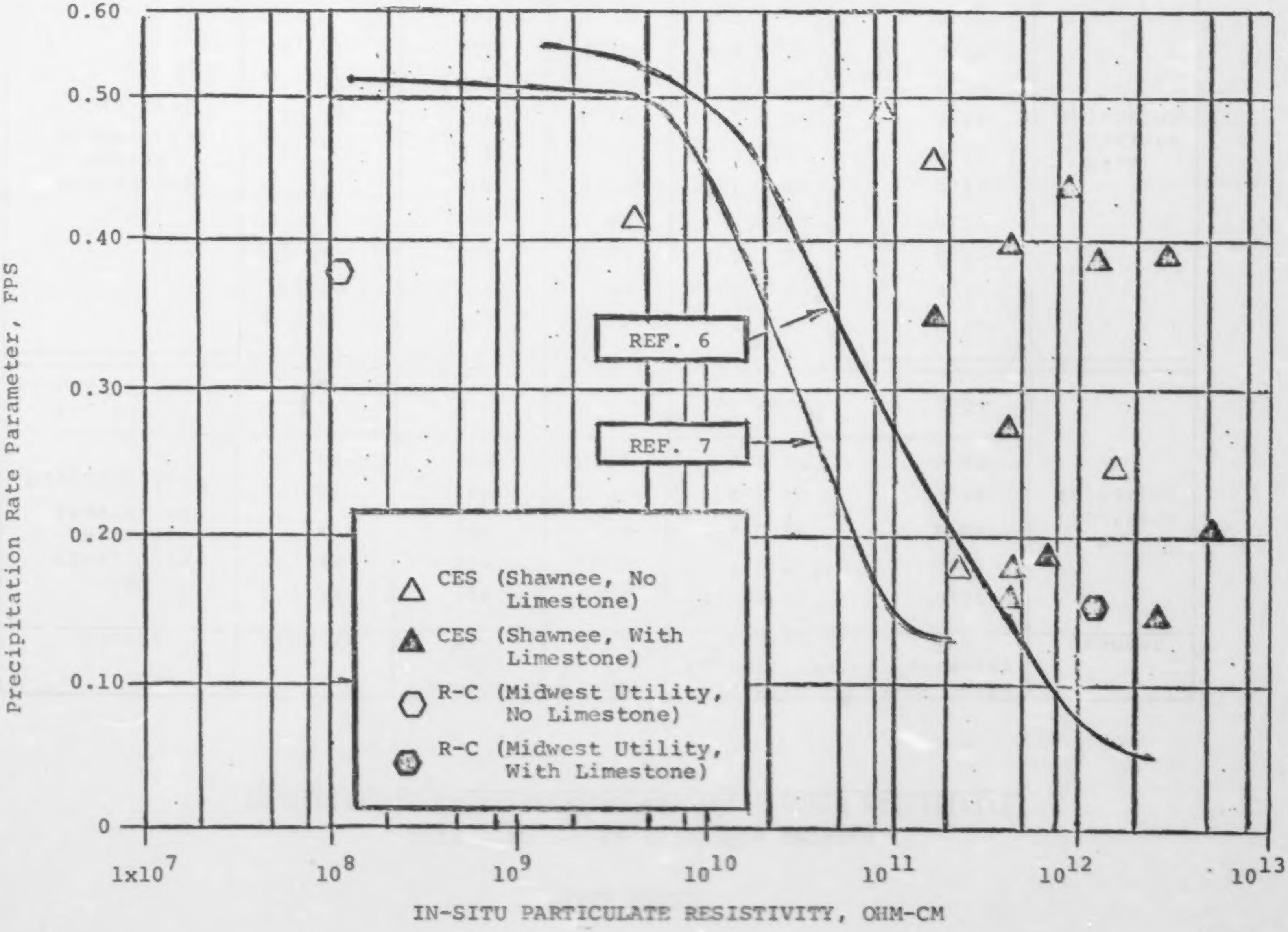

TABLE XXXVII

DATA USED FOR RELATIONSHIP BETWEEN PRECIPITATION RATE PARAMETER AND PARTICULATE RESISTIVITY

Source	Test No.	Flue Gas Temp. ^oF	Coal Sulfur %	In-Situ Resistivity ohm-cm	Pptn. Rate Parameter FPS	Comment
CES First Test Series Shawnee #10 December 1969	5A, 5B	300	3.22	4.8×10^{9}	0.42	No Limestone Injection
	3B, 4B	298	1.90	2.8×10^{11}	0.19	
	9, 16	275	1.54	1.6×10^{12}	0.26	
	19, 21	260	0.85	8.4×10^{10}	0.49	
	20, 22	326	0.90	1.8×10^{11}	0.47	
R-C, Inc. Midwest Utility	----	270	3.20	1.0×10^{8}	0.34	
CES Second Test Series Shawnee #10 July 1971	6, 14	322	2.66	7.3×10^{11}	0.18	With Limestone Injection
	10, 17	261	1.61	4.5×10^{11}	0.40	
	4, 11	323	1.53	4.1×10^{11}	0.16	
	8	285	2.59	1.9×10^{11}	0.35	
	2, 30	316	2.61	5.1×10^{12}	0.21	
	18, 26	318	2.20	4.0×10^{11}	0.17	
	23, 24	326	1.15	3.3×10^{12}	0.14	
	25, 27	271	1.87	1.3×10^{12}	0.38	
	28, 32	323	3.70	3.4×10^{12}	0.39	
	29	265	2.30	4.3×10^{11}	0.27	
	33	260	4.04	9.1×10^{11}	0.43	
R-C, Inc. Midwest Utility	----	287	3.20	1.2×10^{12}	0.15	

degradation noted above is indicated. However, the critical range of resistivity seems to be occurring between values of 10^{11} and 10^{13} ohm-cm. Obviously, more specific data are required to quantitatively establish the relationship between precipitation rate parameter and resistivity.

4. Discussion of Chemical Analyses Results

All the chemical analyses on particulate samples obtained during the test program were performed by TVA personnel at the Chattanooga, Tennessee Laboratory (see Tables XXVII through XXIX). A summary of the data used in the following discussion and correlations are contained in Table XXXVIII.

A. Relationship of Calcium Compounds at Electrostatic Precipitator Inlet with Limestone Feedrate

Since the dust collecting equipment is a combination mechanical-electrostatic unit, it is of interest to determine the affect on the dust chemical composition at the precipitator inlet caused by the mechanical collector for no, coarse, and fine limestone injection. One basis for doing this is to correlate the total amount of

TABLE XXXVIII

SUMMARY OF DATA USED IN SECTION ON CHEMICAL ANALYSES (PPS.147-153)

Test No.	% CaO MC Inlet	% CaO ESP Inlet	Ratio CaO/S ESP Inlet	CaO At ESP Inlet (Tons/Hr)	(1) Gas Temp.	Precipitation Rate Parameter W(FPS)	Limestone Feedrate (tons/hr)	(2) Type Limestone	Particle Resistivity Ohm-Cm (3)
2	30.8	28.6	4.1	0.48	H	0.24	7.55	F	1.2×10^{12}
6	33.0	30.0	4.9	0.64	H	0.03	11.60	F	5.6×10^{11}
8	33.3	31.4	4.4	0.91	L	0.35	11.15	F	1.6×10^{11}
9	--	4.5	3.0	0.05	L	0.34	0	-	3.8×10^{11}
10	--	23.5	3.8	0.43	L	0.43	16.75	C	6.7×10^{11}
11	--	31.6	6.4	1.03	H	0.26	15.25	C	6.5×10^{11}
14	35.6	33.9	6.0	1.19	H	0.33	14.10	C	8.9×10^{11}
15	36.7	34.7	5.3	1.08	L	0.29	14.45	C	1.4×10^{11}
18	--	33.6	7.0	0.69	H	0.17	9.15	F	5.6×10^{11}
19	--	1.4	3.5	0.04	L	0.41	0	-	2.8×10^{11}
20	--	2.2	3.7	0.08	H	0.58	0	-	1.8×10^{11}
21	--	1.1	2.7	0.02	L	0.44	0	-	1.4×10^{11}
22	--	5.6	7.0	0.13	H	0.36	0	-	1.8×10^{11}
23	--	5.9	5.4	0.14	H	0.13	1.84	F	3.7×10^{12}
24	--	18.8	8.9	0.47	H	0.15	3.45	F	2.9×10^{12}
25	--	26.0	4.8	0.80	L	0.50	10.55	C	1.4×10^{12}
26	--	30.8	6.2	0.59	H	0.17	7.05	F	2.4×10^{11}
27	--	28.8	7.4	0.60	L	0.26	6.45	F	1.5×10^{11}
28	--	38.6	9.9	1.12	H	0.29	11.15	F	5.9×10^{12}
29	--	28.8	7.4	0.78	L	0.27	6.25	F	4.3×10^{11}
30	--	27.2	6.5	0.84	H	0.18	6.30	F	9.0×10^{12}
32	27.7	27.7	4.1	1.11	H	0.48	8.50	C	8.3×10^{11}
33	25.5	26.3	4.5	0.75	L	0.43	7.85	C	9.1×10^{11}

(1) H = 290 to 320°F
(1) L = 240 to 260°F

(2) F = 50% by weight less than 6 microns
(2) C = 50% by weight less than 17 microns
(3) In-Situ at Precipitator Inlet

calcium reported as calcium oxide, as a function of the amount and particle size of the limestone fed into the boiler. Using the measured inlet grain loadings and gas volumes at the precipitator inlet, a rate in tons/hour of calcium oxide was calculated from the sample analyses. These were then plotted as a function of limestone feedrate in tons/hour in Figure 59. As expected, the amount of calcium compounds found at the precipitator inlet is a function of feedrate. Unexpected is the randomness of the data points with respect to particle size of the limestone. A regression analysis of Table XXXVIII data (22 sets) using the form of equation 21, where:

Y = Calcium oxide at precipitator inlet, tons/hour
X = Limestone feedrate to boiler, tons/hour

was performed. The data point from Test 10 was discarded, since it appears completely alien to the other test data points and there is no convenient way of determining whether it is bad or a real point. The following result was obtained:

$$Y = 0.12 + 0.071X \tag{38}$$

Correlation Coefficient = 0.91

F - Ratio Test Statistic = 99

Figure 59

CALCIUM OXIDE AT ELECTROSTATIC INLET AS A FUNCTION OF LIMESTONE FEEDRATE TO THE BOILER

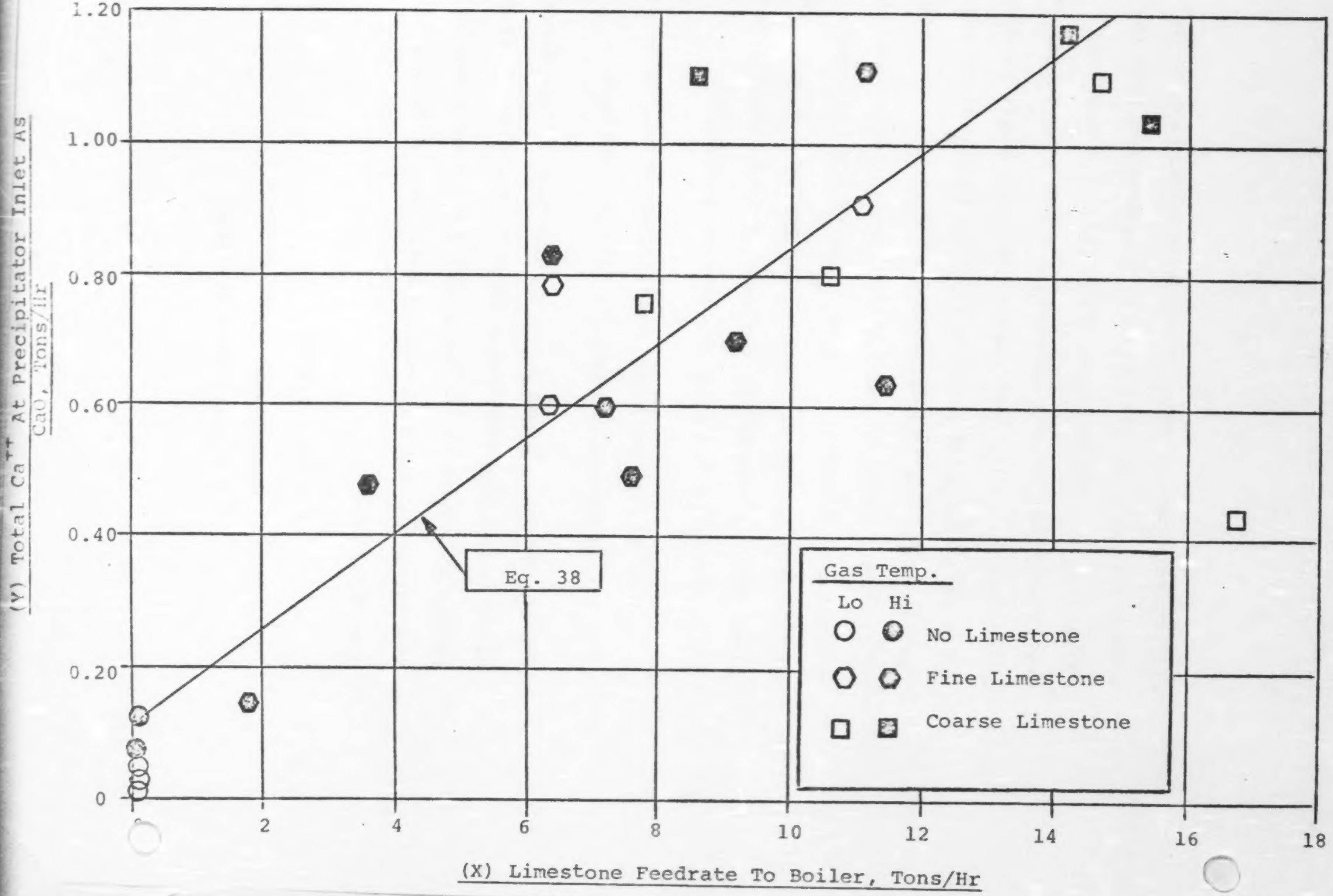

This equation is limited to limestone feedrates in the range of 0 to 15 tons/hour.

The conclusions are that the amount of calcium oxide found at the precipitator inlet is significantly related to the feedrate in a linear manner, and neither the particle size of the limestone or the flue gas temperature at the dust collecting system is significant.

B. Examination of Particle Resistivity at the Precipitator Inlet as a Function of Calcium Oxide/ Sulfur Ratio for High and Low Temperature Flue Gas

In Figure 60, the in-situ particle resistivity at the precipitator inlet has been plotted as a function of the CaO/S ratio in the particulate. The high and low flue gas temperature ranges are indicated separately. There appears to be no obvious correlation. However, in general, the lower gas temperature data seem, on the average, to result in a lower particle resistivity for the same CaO/S ratio. Nevertheless, it is concluded that while no significant trends are obvious in Figure 60 relative to resistivity and CaO/S content of the particulate, this could suggest that under the conditions tested, stoichiometry has little or no effect on resistivity.

Generally, the bulk chemical composition of the parti-

Figure 60

PARTICLE RESISTIVITY AS A FUNCTION OF THE CaO/S RATIO AT THE PRECIPITATOR INLET

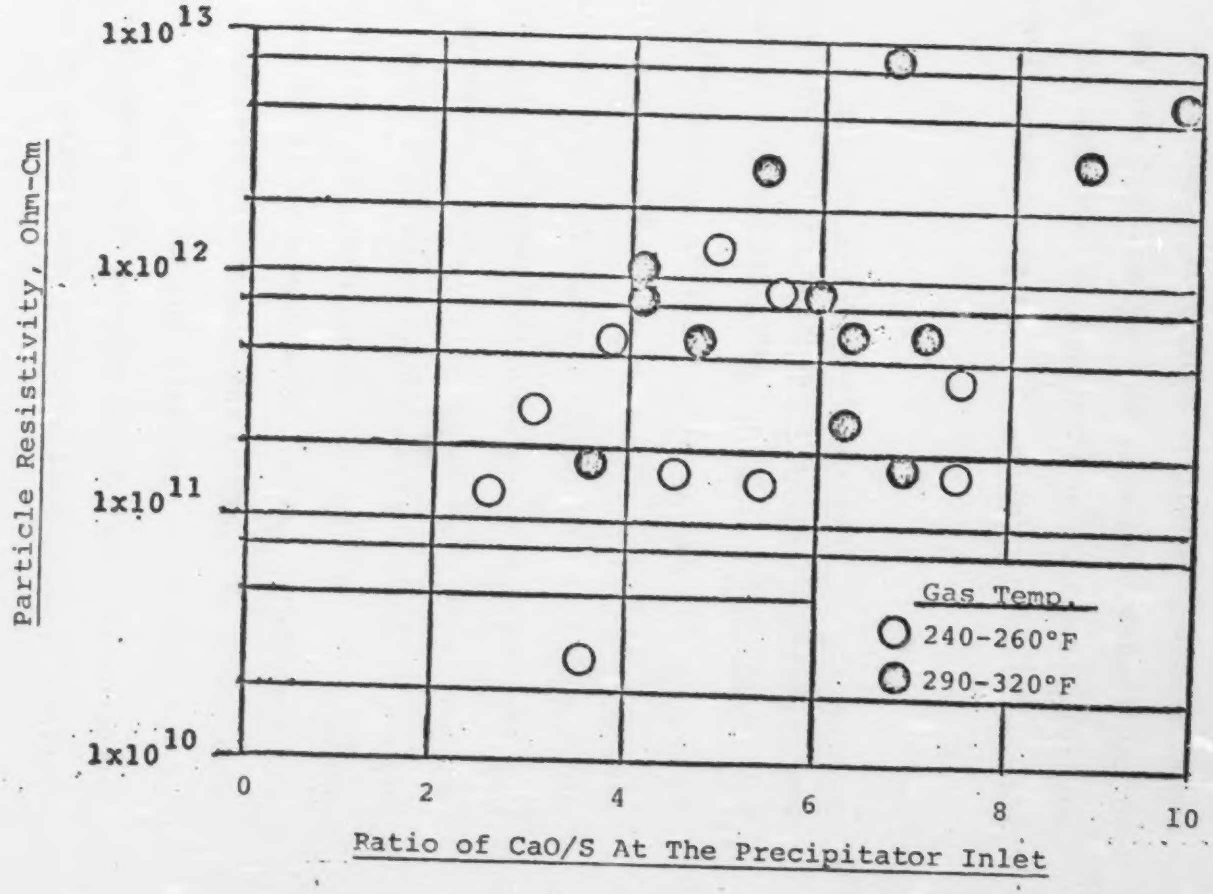

culate and the performance of the precipitator elude correlation. An extensive research program into the chemical composition and physical nature of the particle surface is required.

5. Review of Optical Sensor Data

A proprietary Research-Cottrell, Inc. optical sensing instrument to determine dust concentrations was installed on the "B" side of Boiler #10 at Shawnee Station (see Figures 14 and 15). A simplified system diagram is shown in Figure 61. After standardizing with clean gas in measuring path and use of slope and intercept controls, the dust and reference signals are equal and of opposite polarity under a wide range of light source intensities when measuring path is clean.

$$E_A = -E_B \qquad (39)$$

With dirty gas, E_A decreases with increasing particle concentration and $-E_B$ remains constant.

Summing amplifier adds signals E_A and $-E_B$ and multiplies sum by its gain Gc to provide amplified difference signal to recorder.

FIGURE 61

SIMPLIFIED SYSTEM DIAGRAM OF THE
RESEARCH-COTTRELL, INC. PROPRIETARY OPTICAL SENSOR

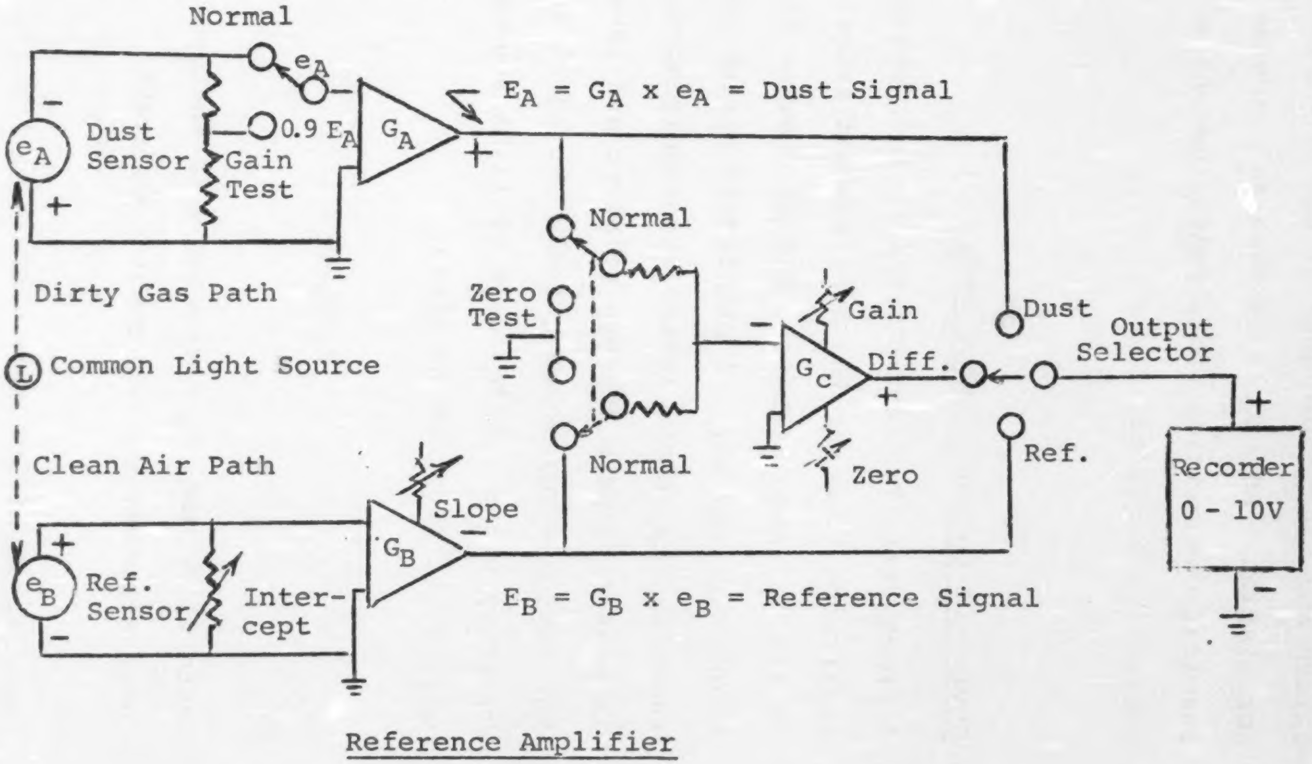
Normal
e_A
$E_A = G_A \times e_A$ = Dust Signal
e_A
Dust Sensor
0.9 E_A
Gain Test
G_A
Normal
Dirty Gas Path
Zero Test
Gain
Dust
Output Selector
L Common Light Source
G_C
Diff.
Normal
Zero
Ref.
Clean Air Path
Slope
Recorder 0 - 10V
G_B
e_B
Ref. Sensor
Inter- cept
$E_B = G_B \times e_B$ = Reference Signal
Reference Amplifier

$$\text{Recorder Reading} = Gc \quad E_A + (-E_B) \qquad (40)$$

After an installation has been standardized, the reference signal $-E_B$ is equal to the maximum difference signal for that installation. For 0-5 Ringleman calibration, full scale recorder voltage = $(Gc)(-E_B)$. Maximum summing amplifier output is limited to about 13 volts.

The instrument was operative during the first CES and second TVA test series. Component failure (signal amplifier) during the second CES test series aborted further use of the instrument. Since all TVA tests were conducted on the "A" side, the correlation of nearly all the dust loadings with optical readout data are only qualitative. (Assumes comparable performance of the "A" and "B" side precipitators.) Table XXXIX summarizes data taken from the recorder charts during the first CES test series and the second TVA test series. A plot of the results (Figure 62) shows a fair correlation between the recorder chart reading (millivolts) and the precipitator outlet loading (grains/SCF). A critical consideration noted in the use of the optical sensor was the necessity for cleaning the lenses of the monitor periodically (at least daily). This requirement is evidenced by the two separate curves shown in Figure 62.

TABLE XXXIX

DATA TAKEN FROM THE OPTICAL SENSOR RECORDER CHARTS

Test No.	Chart Reading (Millivolts)	ESP Outlet Loading (gr/SCF)	Type Firing	Condition of Optical Sensor Lenses	Lime-stone Addition Rate (1)
1A(CES)	1.8	0.036	Coal	Dirty	0
2A	2.8	0.321	↓	↓	↓
5A	2.5	0.112	↓	↓	↓
3B	3.7	0.227	↓	↓	↓
4B	3.7	0.328	↓	↓	↓
5B	2.7	0.045	↓	↓	↓
38 (TVA)	3.1	0.270	Coal + Additive	↓	Medium
39	3.7	0.416	↓	↓	High
40	3.0	0.207	Coal	↓	0
42	2.9	0.126	↓	↓	0
43	3.5	0.263	Coal + Additive	↓	Medium
44	4.0	0.319	↓	↓	High
46	2.8	0.080	Coal	↓	0
47	3.3	0.313	Coal + Additive	↓	Medium
48	3.6	0.329	↓	↓	High
50	1.9	0.099	Coal	↓	0
51	2.6	0.146	Coal + Additive	↓	Medium
52	3.2	0.228	↓	↓	High
54	1.1	0.49	Coal	Clean	0
55	2.4	0.362	Coal + Additive	↓	Low
56	2.3	0.333	↓	↓	Low
58	1.6	0.087	Coal	↓	0
59	2.0	0.246	Coal + Additive	↓	Low
60	2.1	0.278	↓	↓	Low
61	1.2	0.097	Coal	↓	0
62	1.9	0.243	Coal + Additive	↓	Low
64	1.4	0.094	Coal	↓	0
65	2.4	0.363	Coal + Additive	↓	Medium
66	3.1	0.418	↓	↓	High
68	1.6	0.211	Coal	↓	0
69	2.2	0.319	Coal + Additive	↓	Low
70	2.6	0.352	↓	↓	Medium
72	2.3	0.129	Coal	Dirty	0
73	2.9	0.162	Coal + Additive		Low
74	4.0	0.213	↓		Medium

(1) Low = 1 to 3.5 tons/hour
Medium = 4.5 to 5.5 tons/hour
High = 9 to 10 tons/hour

FIGURE 62

DATA OBTAINED ON PARTICULATE LOADING USING AN OPTICAL MONITOR

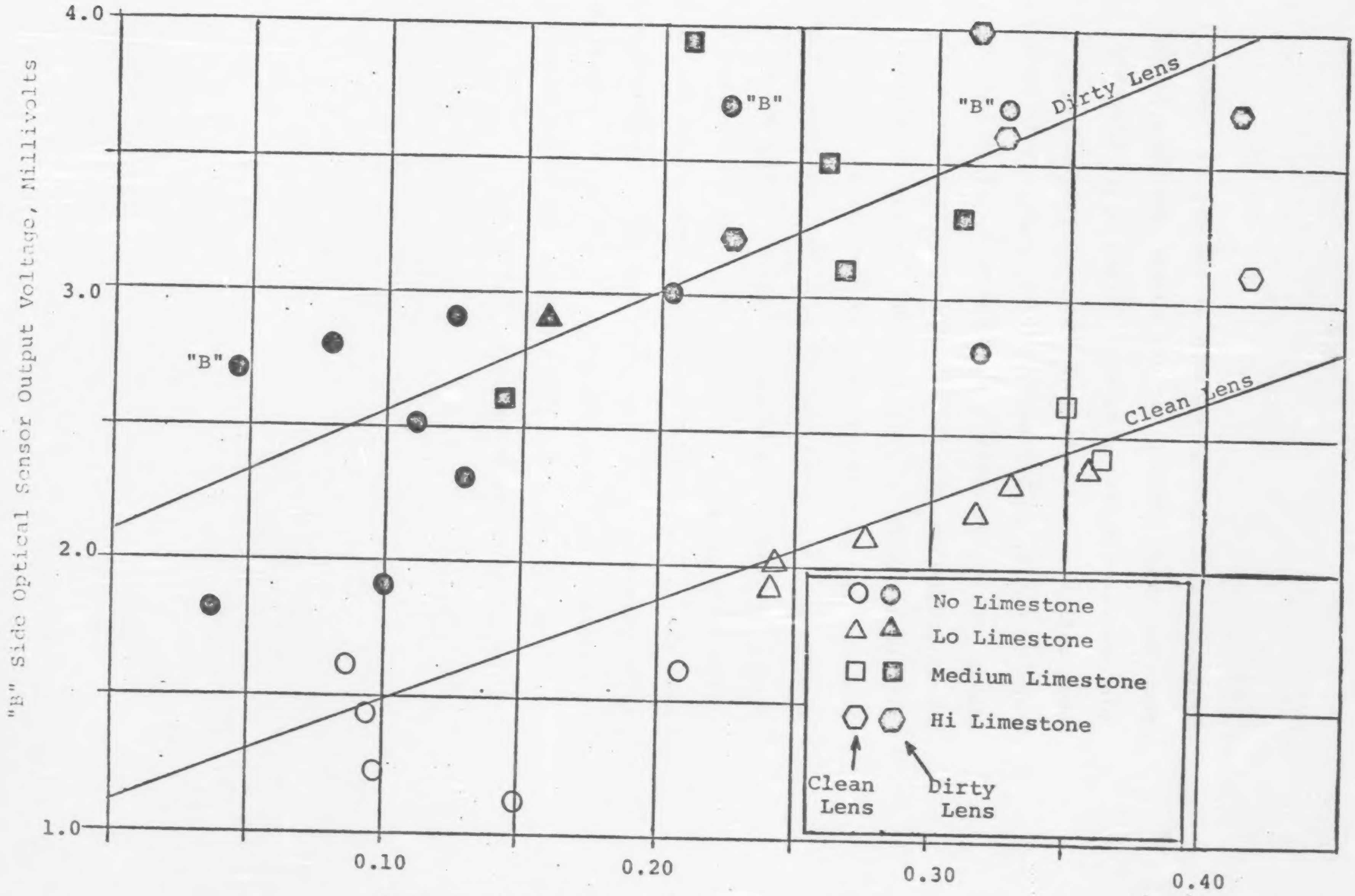

Figure 63 is a typical section of the optical sensor recorder chart showing various boiler and dust collector operating modes, e.g. coal firing only, response when additive is started and stopped, precipitator rapping puffs, boiler soot blowing, etc. This particular section of chart covers the time period beginning about 8:30AM on July 1, 1970 and running continuously til about 3:00PM on July 3, 1970. During this time period, TVA was running tests 37 through 44 from their second test series on the "A" side precipitator. Pertinent operating conditions are noted on the chart (Figure 63, pages 159 through 165). As can be seen on this chart, the optical sensor provides a good qualitative indication of boiler and dust collecting equipment operation. However, additional refinements and evaluation are necessary for its modification into a quantitative particulate monitoring instrument.

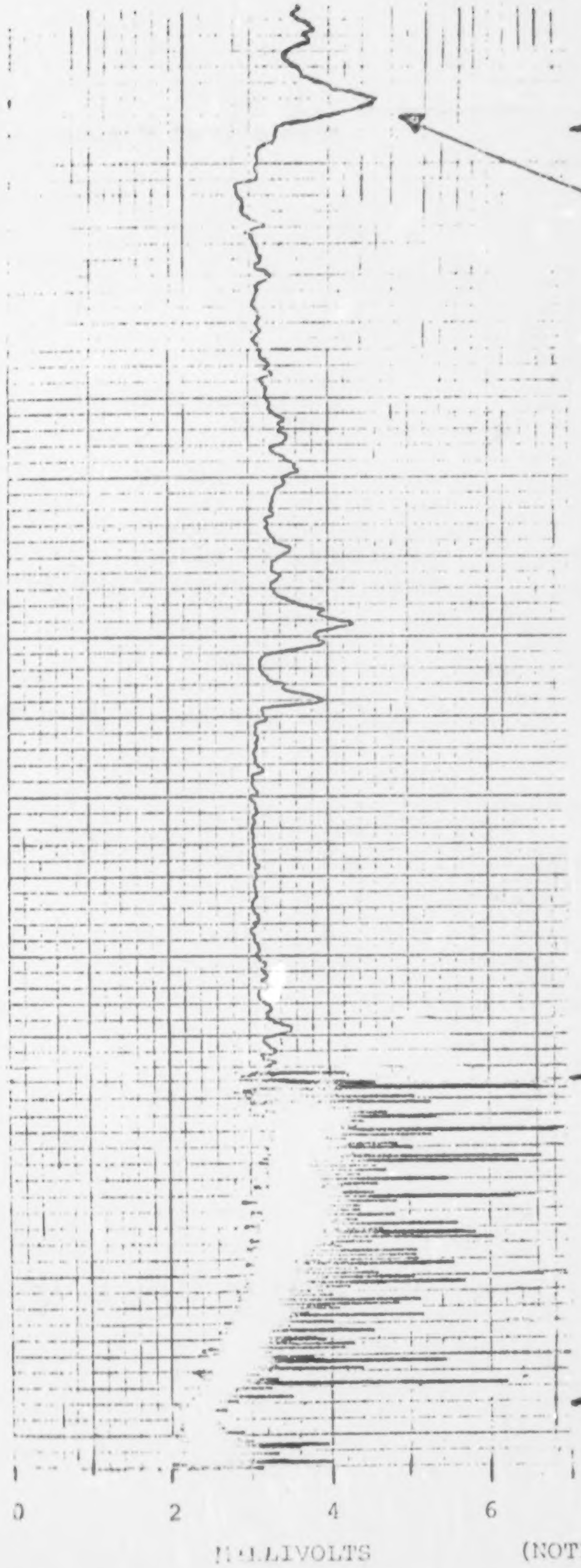

10:43 AM

Peaks are rapping losses from third section of precipitator.

FIGURE 63

TYPICAL OPTICAL SENSOR CHART ON SHAWNEE #10 BOILER ("B" SIDE) WITH AND WITHOUT LIMESTONE INJECTION

10:40 AM
Chart Speed = 2"/Minute

Boiler Load = 143 MW
Coal Ash = 18.3%
Coal Sulfur = 2.7%
Pptr. Eff. = 85.8%
Pptr. Outlet Loading = 0.27 gr/SCF

8:40 AM (July 1, 1970)
Start - Chart Speed = 1"/Hour

Limestone Feed Rate = 5.5 Tons/Hou

(NOTE: 0 to 10 millivolts equivalent to 0 to 5 Rincelmann)

2 of 7

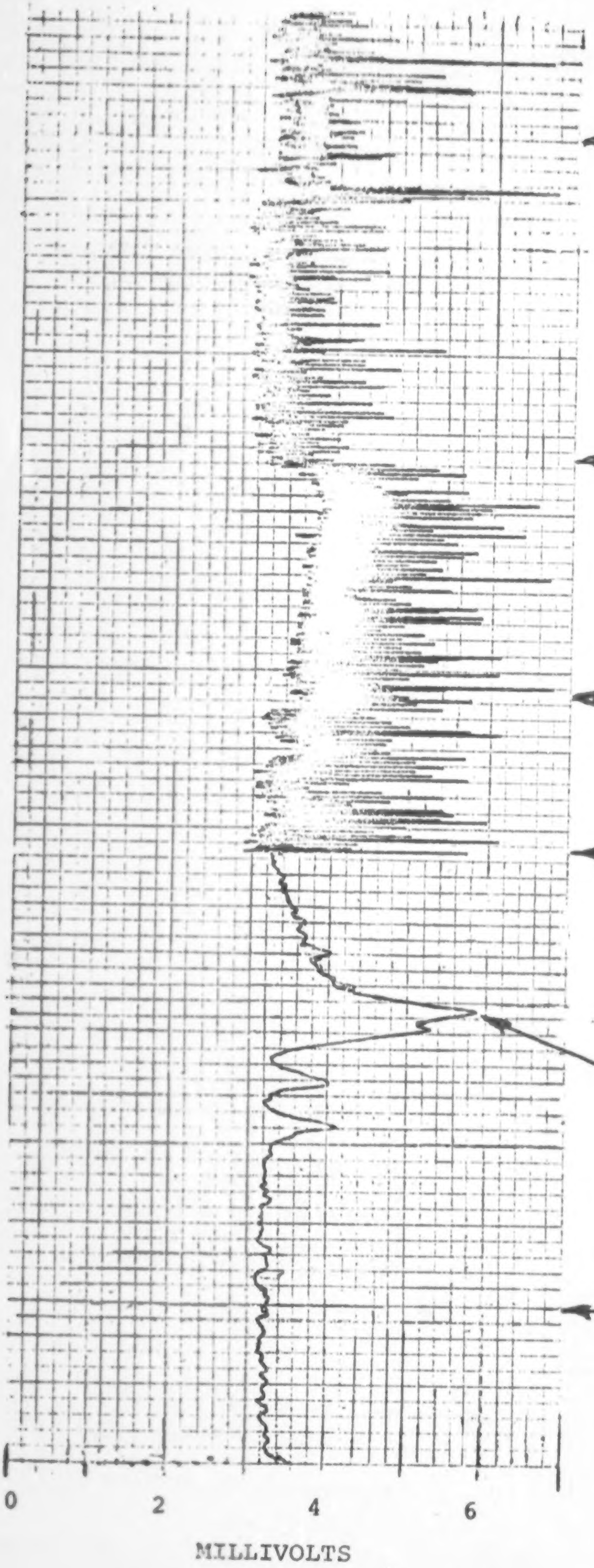

3:20 PM
Normal Coal Firing

Limestone Feed Off
1:20 PM

Boiler Load = 144 MW
Coal Ash = 15.4%
Coal Sulfur = 3.0%
Pptr. Eff. = 78.2%
Pptr. Outlet Loading = 0.42 gr/SCF

11:45 AM

Limestone Feed Rate = 10.0 tons/hour

10:45½ AM
Chart Speed = 1"/hour

Rapping Loss

10:44 AM (July 1, 1970)

3 of 7

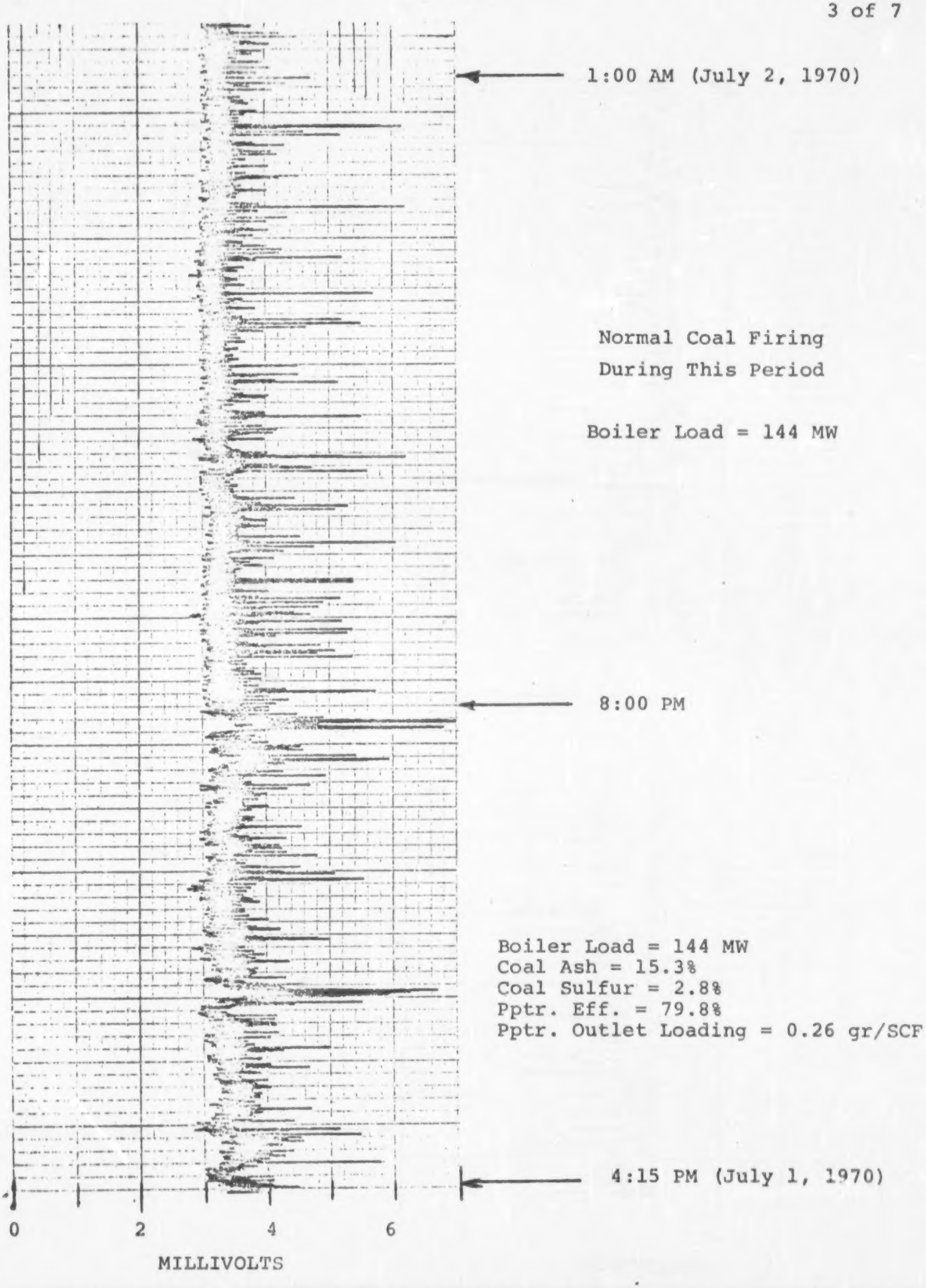
1:00 AM (July 2, 1970)
Normal Coal Firing
During This Period
Boiler Load = 144 MW
8:00 PM
Boiler Load = 144 MW
Coal Ash = 15.3%
Coal Sulfur = 2.8%
Pptr. Eff. = 79.8%
Pptr. Outlet Loading = 0.26 gr/SCF
4:15 PM (July 1, 1970)
0
2
4
6
MILLIVOLTS

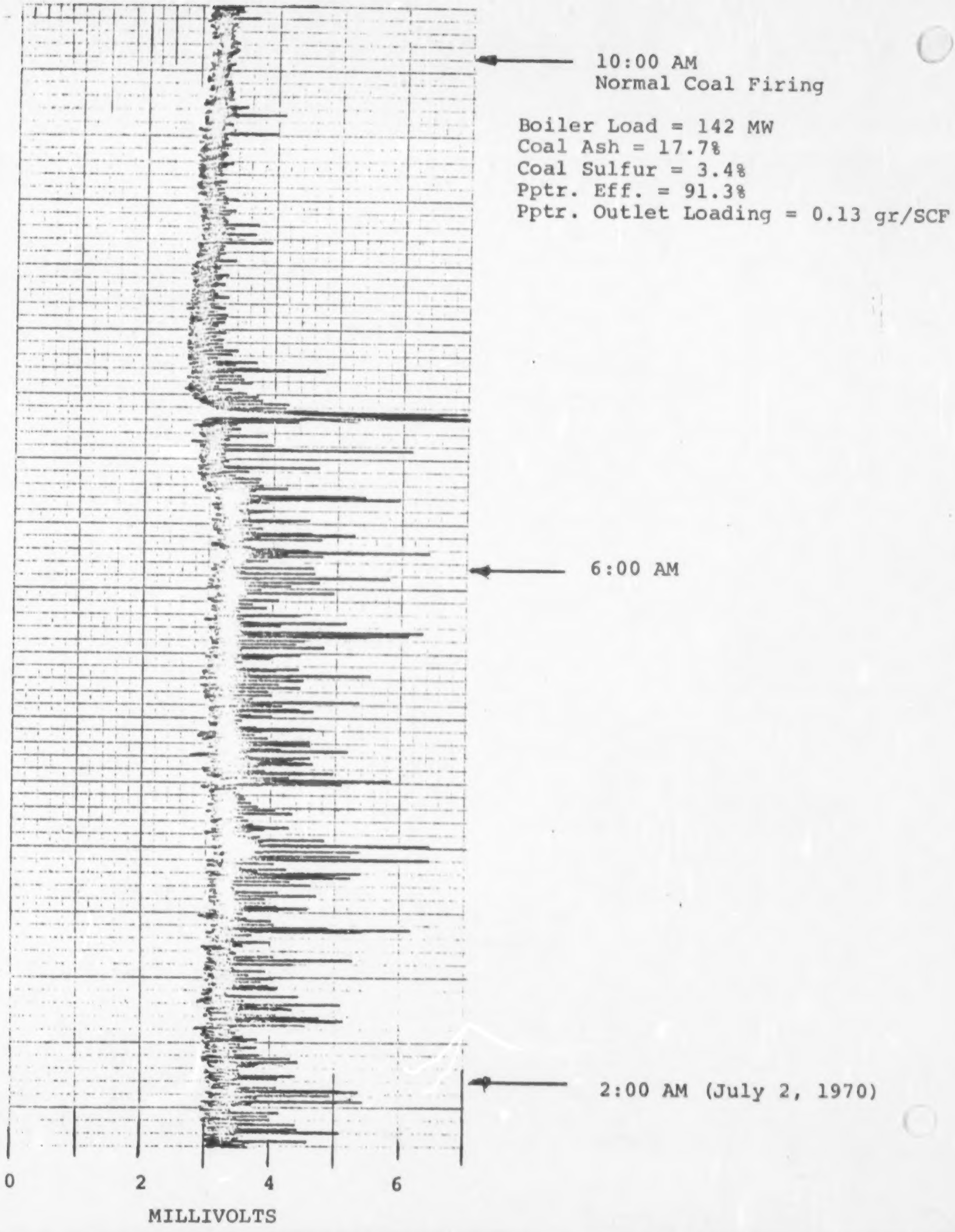

Boiler Load = 142 MW
Coal Ash = 17.7%
Coal Sulfur = 3.4%
Pptr. Eff. = 91.3%
Pptr. Outlet Loading = 0.13 gr/SCF

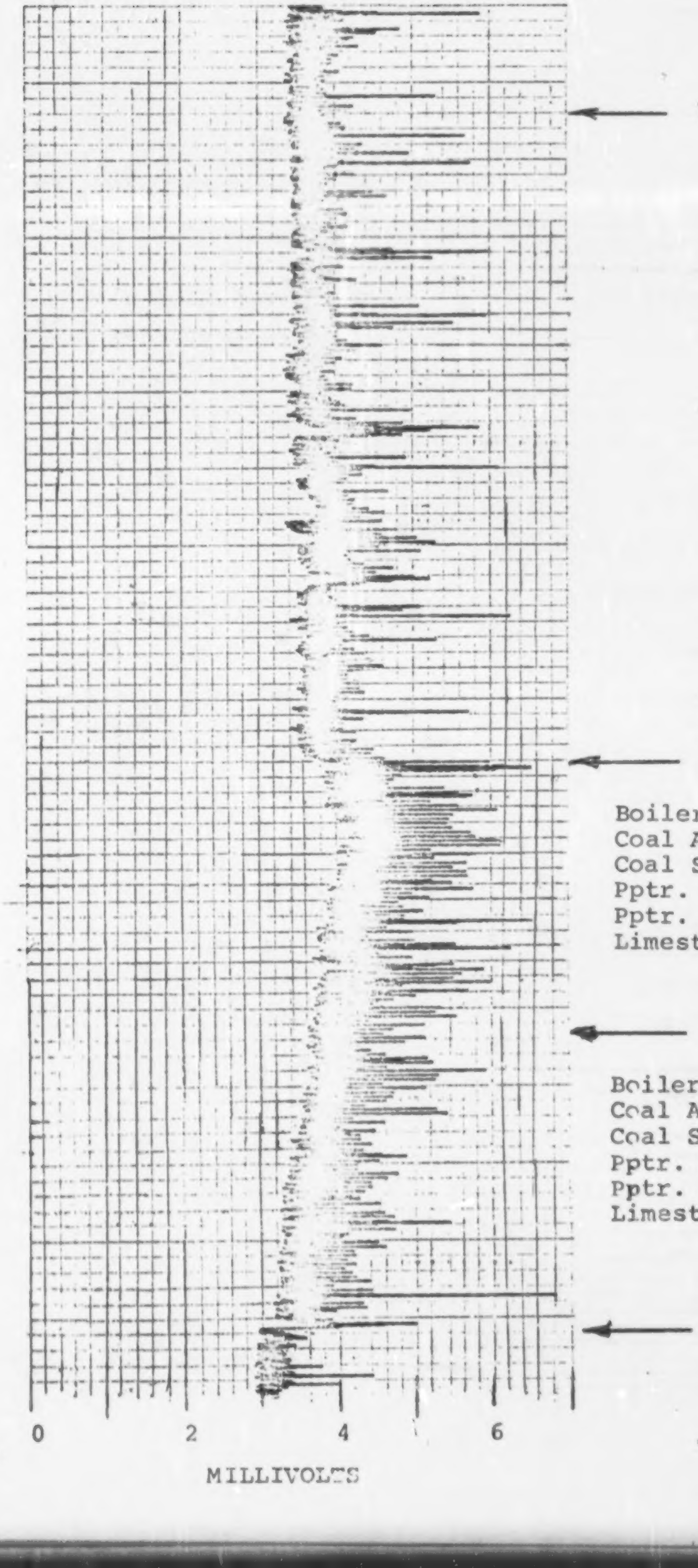

7:00 PM

Normal Coal Firing
During This Period

Limestone Feed Off
2:40 PM

Boiler Load = 144 MW
Coal Ash = 15.9%
Coal Sulfur = 2.7%
Pptr. Eff. = 85.3%
Pptr. Outlet Loading = 0.32 gr/SCF
Limestone Feed Rate = 9.5 Tons/Hour

12:50 PM

Boiler Load = 143 MW
Coal Ash = 16.1%
Coal Sulfur = 3.0%
Pptr. Eff. = 82.7%
Pptr. Outlet Loading = 0.26 gr/SCF
Limestone Feed Rate = 4.5 Tons/Hour

10:55 AM (July 2, 1970)

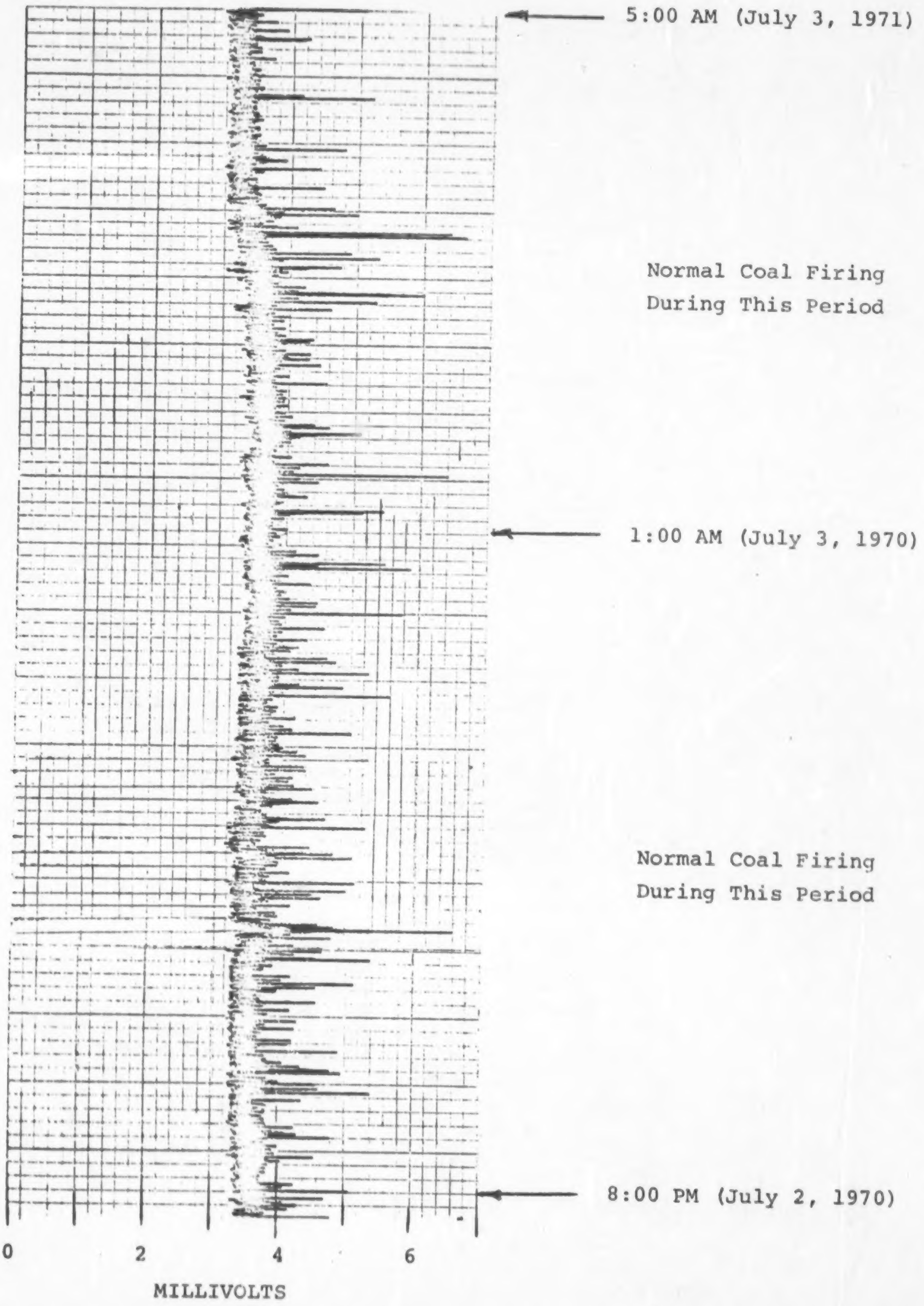
5:00 AM (July 3, 1971)
Normal Coal Firing During This Period
1:00 AM (July 3, 1970)
Normal Coal Firing During This Period
8:00 PM (July 2, 1970)
0
2
4
6
MILLIVOLTS

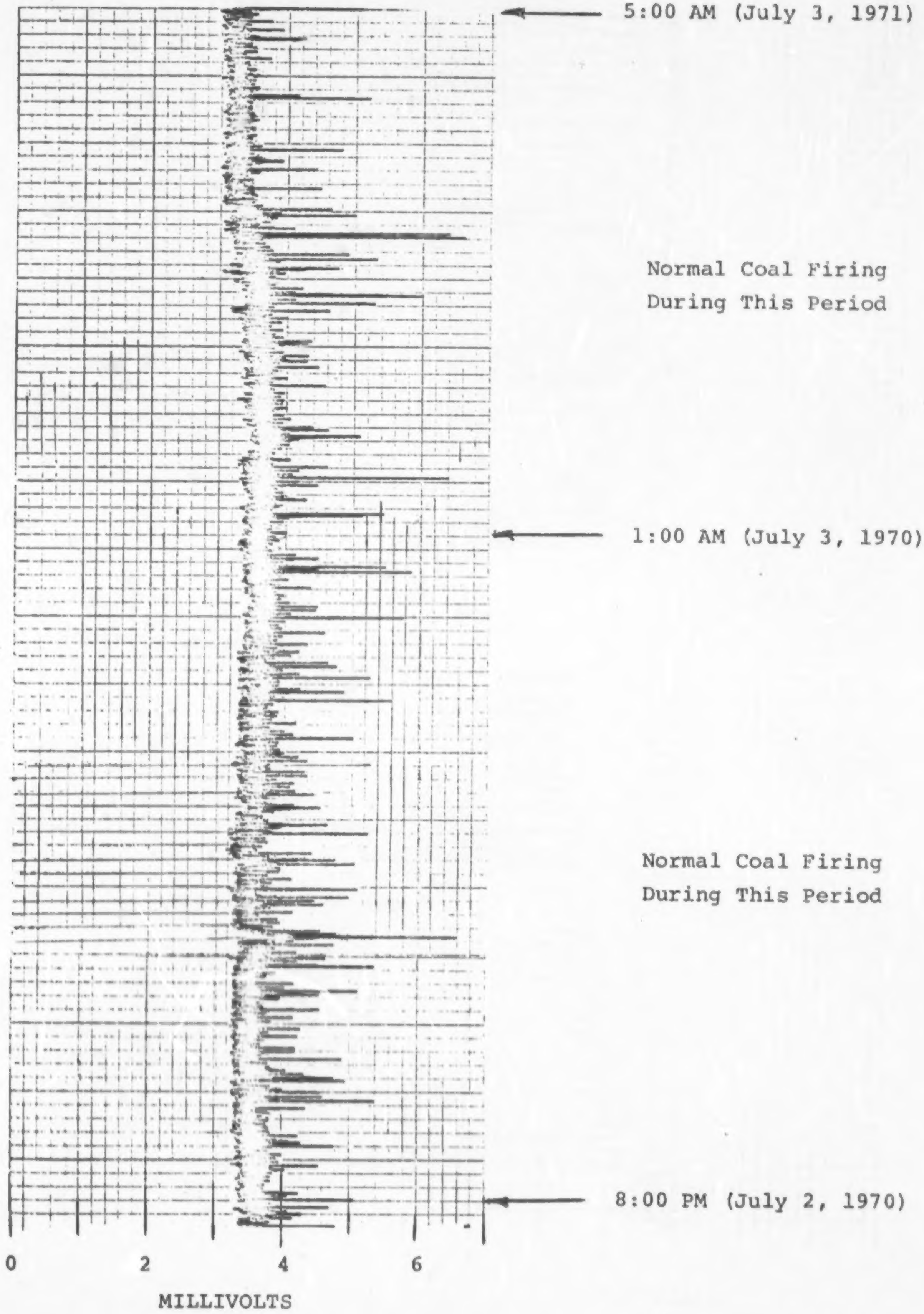
5:00 AM (July 3, 1971)
Normal Coal Firing During This Period
1:00 AM (July 3, 1970)
Normal Coal Firing During This Period
8:00 PM (July 2, 1970)
0
2
4
6
MILLIVOLTS

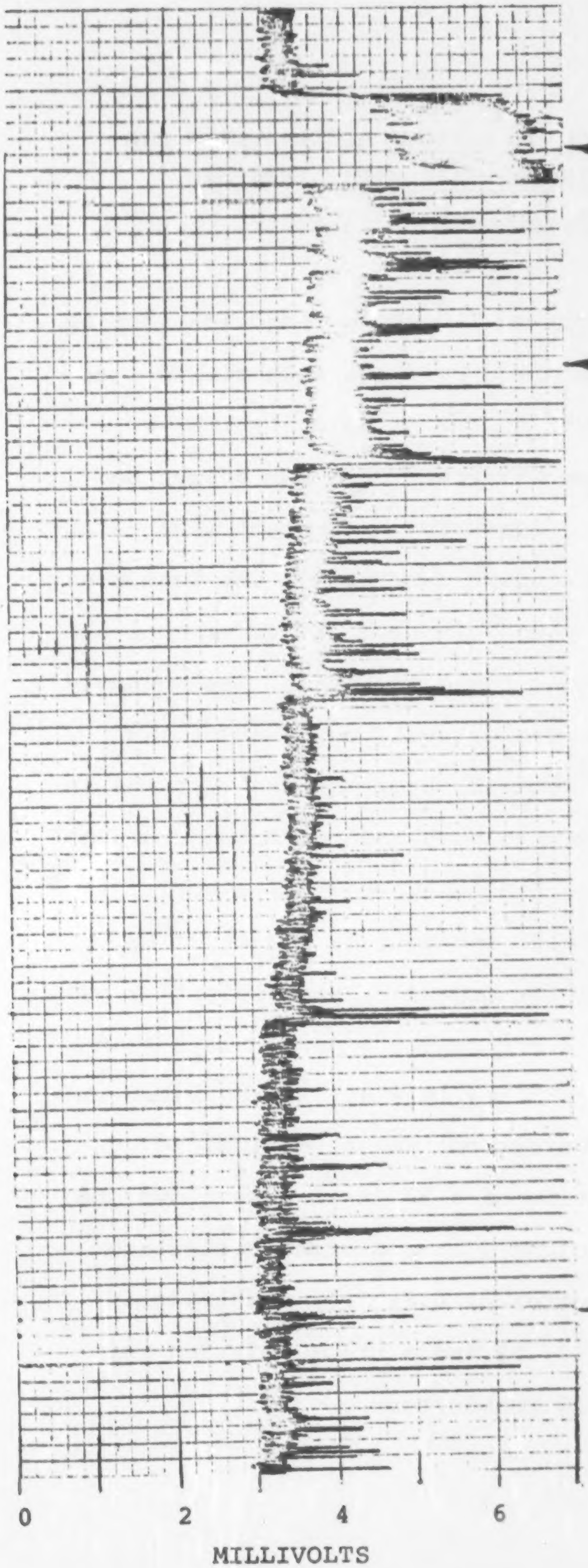

Boiler Soot Blowing

12:00 PM

Normal Coal Firing
During This Period

6:00 AM (July 3, 1970)

VII. TECHNO-ECONOMIC EVALUATION OF VARIOUS ALTERNATIVES FOR MAINTAINING THE STACK EMISSION RATE WITH LIMESTONE INJECTION EQUIVALENT TO A BASELINE CONDITION OF NO LIMESTONE INJECTION

The baseline conditions for no limestone injection used in this evaluation were determined by first selecting a coal having between 2.5 and 3.5% sulfur as being typical of that burned at the Shawnee Station. Then the boiler and electrostatic precipitator operating parameters were established by averaging test results obtained by the Tennessee Valley Authority in 1970 when this type of sulfur coal was fired. (Table XL summarizes these results.) The mechanical collector performance was established by averaging test results obtained by Cottrell Environmental Systems in 1969. (Table V.) The average baseline conditions obtained in this manner for Shawnee Station were - (1) a boiler burning 2.8% sulfur and 15.5% ash coal at a rate of 63.3 tons/hour, resulting in a 141 megawatt load and a flue gas volume of 570,000 cfm at 309°F having a particulate loading of 3.32 grains/SCF (70°F and 29.9"Hg) at the inlet to the particulate collection system; (2) a particulate collection system consisting of a 57.4% efficient cyclone followed by a 91.3% efficient electrostatic precipitator (precipitation rate parameter of 0.39 FPS) resulting in an overall efficiency of 96.3% and a stack emission rate of 0.122 grains/SCF or 412 pounds/hour.

TABLE XL

SUMMARY OF 1970 TVA TEST RESULTS USED IN ESTABLISHING BASELINE BOILER AND PARTICULATE COLLECTOR OPERATING PARAMETERS FOR NO-LIMESTONE INJECTION

(1) Test No.	ESP Particulate Loading (gr/scf)		ESP Efficiency (%)	Flue Gas Temp. (°F.)	Gas Volume (ACFMx10^{-3})	(2) Coal Analysis(%)		Pptn. Rate Parameter (FPS)	Boiler Load (MW)	Coal Firing Rate (tons/hr)
	Inlet	Outlet				Sulfur	Ash			
42	1.446	0.126	91.3	316	306	3.4	17.7	0.41	142	64.0
46	1.392	0.102	92.6	306	295	2.7	17.1	0.43	142	64.0
50	1.559	0.099	93.7	307	289	2.7	14.0	0.37	142	64.0
54	1.465	0.149	89.8	310	285	2.7	13.7	0.36	140	62.5
58	1.737	0.087	94.9	304	279	2.8	14.0	0.46	142	64.0
61	1.119	0.097	91.6	304	302	2.6	13.8	0.42	141	63.0
64	1.449	0.094	93.4	310	294	3.1	14.2	0.44	142	64.0
68	1.463	0.214	85.6	309	287	2.5	14.8	0.31	140	62.5
72	1.119	0.129	88.5	311	227	2.5	20.2	0.27	139	62.0
Avg.	1.416	0.122	91.3	309	285	2.8	15.5	0.39	141	63.3

(1) Tests run with no limestone injection and a precipitator sparking rate of about 150/min.

(2) Tests with coal sulfur between 2.5 and 3.5%.

For purposes of this evaluation, an injection stoichiometry of 2.0 moles of CaO/mole S in the coal was established.

Using the baseline condition of 63.3 tons/hour of 2.8% sulfur coal, a limestone injection rate of 11.1 tons/hour was calculated.

Five basic alternatives were considered in the techno-economic evaluation, i.e. size modification of the presently installed dust collecting system, use of a "hot" electrostatic precipitator, gas cooling ahead of the dust collecting system, gas conditioning ahead of the dust collecting system, and type of electrical energization for the precipitator.

1. Size Modification of the Presently Installed Dust Collecting System

   Examination of the performance data of the mechanical collector without and with coarse or fine limestone injection shows no significant differences, i.e. the removal efficiency was essentially unaffected, ranging on the average between 50 and 60% removal. However, the particulate loading at the mechanical inlet and outlet will vary with the coal ash content and amount of additive injection. The mechanical outlet-electrostatic inlet loading, as a function of limestone feedrate, has been shown previously in Figure 46. The performance of the precipitator is significantly affected by the particle size of the limestone injected (Table XXX) with the coarse giving the higher precipitation rate parameter. Accordingly, the overall efficiency and the resulting emission rate from the stack will be a significant function of the electrostatic precipitator performance and inlet particulate loading only. For purposes of comparing required size modifications for the baseline no injection, and the coarse or fine limestone injection cases, it has been assumed that the precipitation rate parameter is unaffected in the 290 to 310°F flue gas temperature range. Using data contained in Figures 19 or 46, and Tables XXX or XL, a precipitator size modification and cost evaluation has been made for the presently installed dust collecting system. Results are summarized in Table XLI.

The estimated precipitator capital cost (installed) of $\$5.25/ft^2$ of collecting plate area includes the base precipitator flange to flange, support steel, insulation, foundations, and labor to supervise and install the precipitator. It does not include the ash handling

TABLE XLI

SUMMARY OF ELECTROSTATIC PRECIPITATOR SIZE MODIFICATIONS AND COSTS FOR THE PRESENTLY INSTALLED DUST COLLECTING SYSTEM REQUIRED TO MAINTAIN A STACK EMISSION RATE EQUIVALENT TO BASELINE NO-LIMESTONE INJECTION

(ESP Follows MC)

Condition	Baseline No Limestone Injection	Coarse Limestone Injection	Fine Limestone Injection
Flue Gas Temperature, °F.	309	309	309
Sulfur Feed Rate, tons/hr (1)	1.77	1.77	1.77
Limestone Feed Rate, tons/hr	0	11.1	11.1
Injection Stoichiometry, moles CaO/mole S	0	2	2
Gas Volume, ACFM	570,000	570,000	570,000
Pptr. Inlet Loading, gr/cf (2) @ 70F & 29.9"Hg	1.416	3.10	3.10
Pptr. Outlet Loading, gr/cf @ 70F & 29.9"Hg	0.122	0.122	0.122
Pptr. Efficiency, %	91.3	96.1	96.1
Power Density, KW/1000 ft^2 (3)	0.70	0.23	0.15
Precipitation Rate, FPS (4)	0.39	0.36	0.16
Precipitator Area, Ft^2	59,400	85,800	193,000
Pptr. Size Factor X Base Size	1.0	1.45	3.25
Pptr. Capital Cost (Installed) (5) $/KW	2.21	3.21	7.20

(1) Based on 63.3 tons/hr of coal @ 2.8% sulfur.

(2) Taken from Figure 46 or Table XL.

(3) Taken from Figure 19 or Table XXX.

(4) Taken from Table XL or XXX.

(5) Based on a boiler load of 141 megawatts and precipitator capital cost (installed) as defined in the text. ($5.25/$ft^2$ collecting plate area).

system and any mark-up for profit which can vary widely, depending upon the vendor.

2. Installation of a "Hot" Precipitator

The use of a straight "hot" precipitator at 600°F (air heater inlet gas temperature) would eliminate the dust resistivity problem and, whether limestone is injected or not, the precipitation rate parameter would be constant, e.g. in the range of 0.3 FPS.

Theoretical considerations show the precipitation rate parameter is a function of particle size. However, practical experience has shown that this does not become important until the size approaches the submicron range. Therefore the injection of coarse or fine limestone which had little material in this range will not affect the precipitation rate parameter substantially.

Adjusting the baseline gas volume to 600°F and eliminating the mechanical collector (assume 57.4% efficient on fly ash and 55% efficient on fly ash plus limestone reaction products), the new precipitator inlet gas volume and particulate loadings would be 788,000 ACFM and 3.32 grains/SCF for no injection, and 6.88 grains/SCF for 2X stoichiometric injection. On the basis of the above assumptions, a "hot" precipitator has been sized and costed that would reduce particulate emissions to 0.122 grains/SCF. Results are summarized in Table XLII.

TABLE XLII

SUMMARY OF THE "HOT" PRECIPITATOR SIZING AND COSTING FOR SHAWNEE STATION BOILER #10 WITH AND WITHOUT LIMESTONE INJECTION

(Straight Precipitator)

Condition	No Limestone Injection	Coarse or Fine Limestone Injection
Flue Gas Temperature, °F.	600	600
Sulfur Feed Rate, tons/hr	1.77	1.77
Limestone Feed Rate, tons/hr	0	11.1
Injection Stoichiometry, moles CaO/mole S	0	2
Gas Volume, ACFM	788,000	788,000
Pptr. Inlet Loading, gr/cf @ 70F & 29.9"Hg	3.32	6.88
Pptr. Outlet Loading, gr/cf @ 70F & 29.9"Hg	0.122	0.122
Precipitator Efficiency, %	96.3	98.2
Precipitator Rate, FPS	0.30	0.30
Precipitator Area, Ft^2	144,500	176,000
Precipitator Capital Cost (1) (installed), $/KW	5.85	7.10

(1) Based on a boiler load of 141 megawatts and precipitator capital cost (installed) of $5.70/ft^2 collecting plate area.

3. Gas Cooling Ahead of the Dust Collecting System

With an alkaline additive injected into the gas stream which removes most of the sulfur trioxide by chemical reaction, it is possible to design a dust collecting system to operate at about 250°F without danger of corrosion due to sulfuric acid condensation. Since the present system, normally operates about 300°F, it would be necessary to cool the gas about 50°F. This could be accomplished by the addition of more heat transfer surface or possibly by injection of atomized water with the added benefit of moisture conditioning. Table XLIII summarizes results of an evaluation using gas cooling ahead of the dust collecting system.

4. Gas Conditioning Ahead of the Dust Collecting System

The use of conditioning agents, such as sulfur trioxide (sulfuric acid), to reduce dust resistivity and improve precipitator performance is well known. However, with the addition of large amounts of alkali, the conditioning affect may be cancelled. Nevertheless, if the additive surface has been sulfated ahead of the conditioning injection point, it may still be possible to improve precipitator performance by sulfur trioxide addition. On this basis, and assuming the precipitation rate with coarse or fine limestone injection will be improved to the no limestone level, a size and cost of a precipitator for limestone injection has been determined.

TABLE XLIII

SUMMARY OF GAS COOLING AS AN OPTION FOR COARSE OR FINE LIMESTONE INJECTION

Condition	Coarse Limestone Injection	Fine Limestone Injection
Flue Gas Temperature, °F	250	250
Sulfur Feed Rate, Tons/Hour	1.77	1.77
Limestone Feed Rate, Tons/Hour	11.1	11.1
Injection Stoichiometry, Moles CaO/Mole S	2	2
Gas Volume, ACFM	526,000	526,000
Pptr. Inlet Loading, gr/cf @ 70°F & 29.9"Hg	3.10	3.10
Pptr. Outlet Loading, gr/cf @ 70°F & 29.9"Hg	0.122	0.122
Precipitator Efficiency, %	96.1	96.1
Power Density, KW/1000 Ft^2	0.51	0.30
Precipitation Rate, FPS	0.41	0.31
Precipitation Area, Ft^2	69,300	92,300
Pptr. Capital Cost (Installed)(1) $/KW	2.58	3.44

(1) Based on a boiler load of 141 megawatts and precipitator capital cost (installed) of $5.25/$ft^2$ collecting plate area.

At 309°F, with a precipitation rate of 0.39 FPS and a required efficiency of 96.1% for 570,000 ACFM, the collecting area is 70,000 ft^2. The precipitator capital cost (installed) per kilowatt generated is $2.94.

5. Electrical Energization of the Precipitator

Basically the precipitator electrical system consists of the electrical load (precipitator), the power conversion equipment (high voltage power supply), and the power control equipment (low voltage control). Single stage industrial gas-cleaning precipitators are generally energized by H-V direct current which is derived from commercial alternating current power supply lines. Power conversion is accomplished in the H-V power supply by means of A-C voltage transformation and H-V rectification, usually without ripple filtering. Precipitator energization is controlled by the L-V control which regulates electrical input to the H-V power supply. The combination of a H-V power supply and its associated L-V control is commonly called an electrical set. Most large precipitators are internally subdivided to provide a number of isolated electrical sections or collecting zones. These precipitator subdivisions are made longitudinally, transversely, or in a longitudinal/

transverse arrangement in relation to precipitator gas flow stream. Each section or collecting zone represents a discrete electrical load requiring an electrical set for energization.

A single stage precipitator is essentially a gaseous electrical discharge device which in most cases is operated at pressures close to atmospheric and temperatures ranging from ambient to several hundred degrees. As such it has a non-linear voltage-current characteristic with discontinuities as illustrated in Figure 64. Except for insulator leakage, negligible current flows until sufficient voltage exists between the discharge electrode and the collecting electrode to initiate a corona discharge. (corona starting voltage) Increasing the voltage above the corona start point causes precipitator current to rise sharply until the voltage becomes sufficiently high to cause random, momentary spark-over "snaps" between the discharge electrode and the collecting surface. (sparking region) At this point the gaseous discharge is highly unstable and can readily transfer from the sparking mode to the power arc mode. The power arc mode is characterized by sustained low voltage and heavy currents which are limited only by the power supply system impedance.

FIGURE 64

TYPICAL PRECIPITATOR VOLTAGE VS CURRENT CHARACTERISTIC

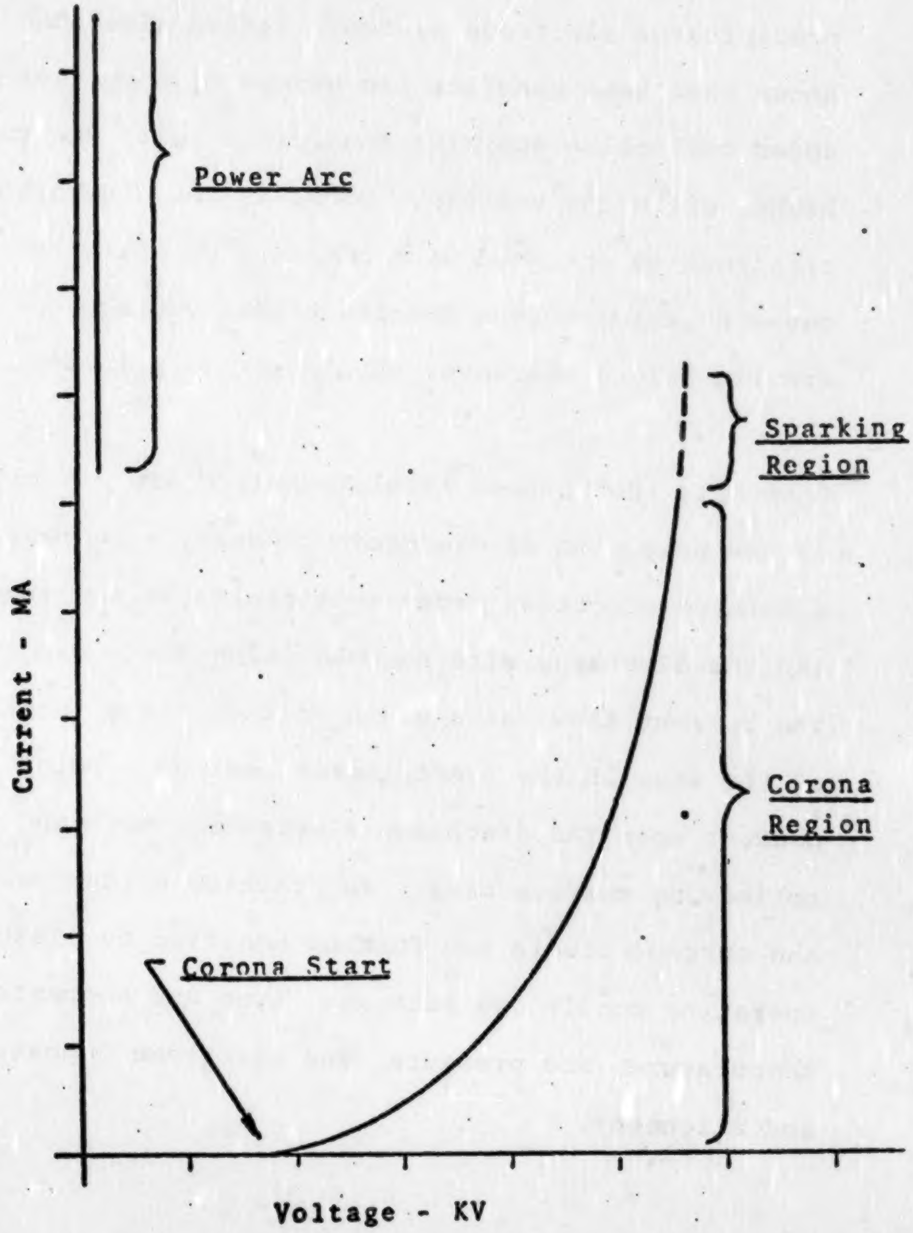

The corona region just prior to and slightly into the sparking region is the useful portion of the precipitator voltage-current characteristic for particulate collection. Fundamental research has shown that precipitator performance is initially dependent upon maintaining the highest possible voltage on the precipitator electrode system. It has also been shown that some benefits are gained by operation under controlled sparking conditions again due to higher operating voltage. Normally the discharge electrode is operated with negative polarity because negative corona permits higher voltage operation before sparkover than positive polarity.

Basically the voltage levels required are a function of the precipitator electrode geometry - including discharge electrode cross-sectional size and shape and the discharge wire to collecting surface spacing. The current flow, at a given voltage, is a function of the size of the precipitator section - being dependent upon the discharge electrode length and collecting surface area. In practice, corona voltage and current levels are further modified by plant operating conditions such as: type and concentration, temperature, and pressure; and electrode deposits and alignment.

Actual precipitator electrode configurations are selected to permit stable corona conditions and relatively high sparking voltages in addition to practical considerations of durability and economy. Since sparking voltage is generally governed by the closest discharge electrode to collecting electrode spacing, it has been found that electrical sectionalization of a large precipitator permits higher operating voltages and reduces dust loss due to an individual sparkover. Differences in particulate concentration throughout the precipitator also affect the corona and sparking characteristics. Thus, sectionalization permits each treating zone to be energized more closely to ideal levels for the particular zone.

Back corona is a description term applied to a very undesirable gaseous discharge phenomena which occurs in precipitators treating particulate matter having resistivities greater than $\sim 10^{10}$ ohm-cm. Under this condition, a corona discharge occurs on the dust layer on the collecting electrode as well as the discharge electrode.

With negative polarity, the typical electrical characteristic of the precipitator is drastically altered by back corona. The sparkover voltage for the precipitator is lowered to 50% or less than normal and a stable heavy-current, low-voltage discharge can occur. In this latter case, rated current flows at perhaps 30% or less of the voltage normally associated with the electrode structure. Needless to say, particulate collection falls far below design with back corona because of the low interelectrode voltage. Normal corona on the discharge electrodes appears as sharply defined tufts of light which lie along straight lines, formed by the wires. The back corona appears as more diffuse tufts of light randomly spread over the collecting electrode area.

Traditionally, back corona problems have been alleviated by: reducing particulate resistivity by process change; use of conditioning agents; and increased precipitator sectionalization. It has been found that back corona conditions can also be solved by controlling the voltage wave shape. This is possible since a time factor, quite analogous to that of a capacitor, is involved in the establishment of back corona. Thus, use of impulse voltages provides means to raise spark-over and peak operating voltage under back corona conditions.

Radar type pulse systems which provide sharply rising voltage pulses have been experimentally applied and found advantageous in high-resistivity problem areas. However their commercial application has so far been precluded by: general lack of understanding, economy, apparatus complexity, and certain electrical component deficiencies.

As previously mentioned, large precipitators are normally subdivided into discrete electrical sections. Figure 65(a) shows typical precipitator energization arrangements for a sectionalized precipitator. The Figure 65(b) arrangement is often beneficial since gas inlet sections tend to operate at lower corona power levels (high voltage, low current, heavy sparking) as compared to gas outlet sections. Half wave energization does have the disadvantage that dissimilar sections cannot be properly energized - the energization level is limited by the power section. Also it has been found in certain high-power electrical set arrangements (50KW or larger sets) that a spark transient disturbance in one HW section can cause magnetic circuit unbalance which unduly prolong the disturbance.

FIGURE 65

TYPICAL PRECIPITATOR ENERGIZATION ARRANGEMENTS

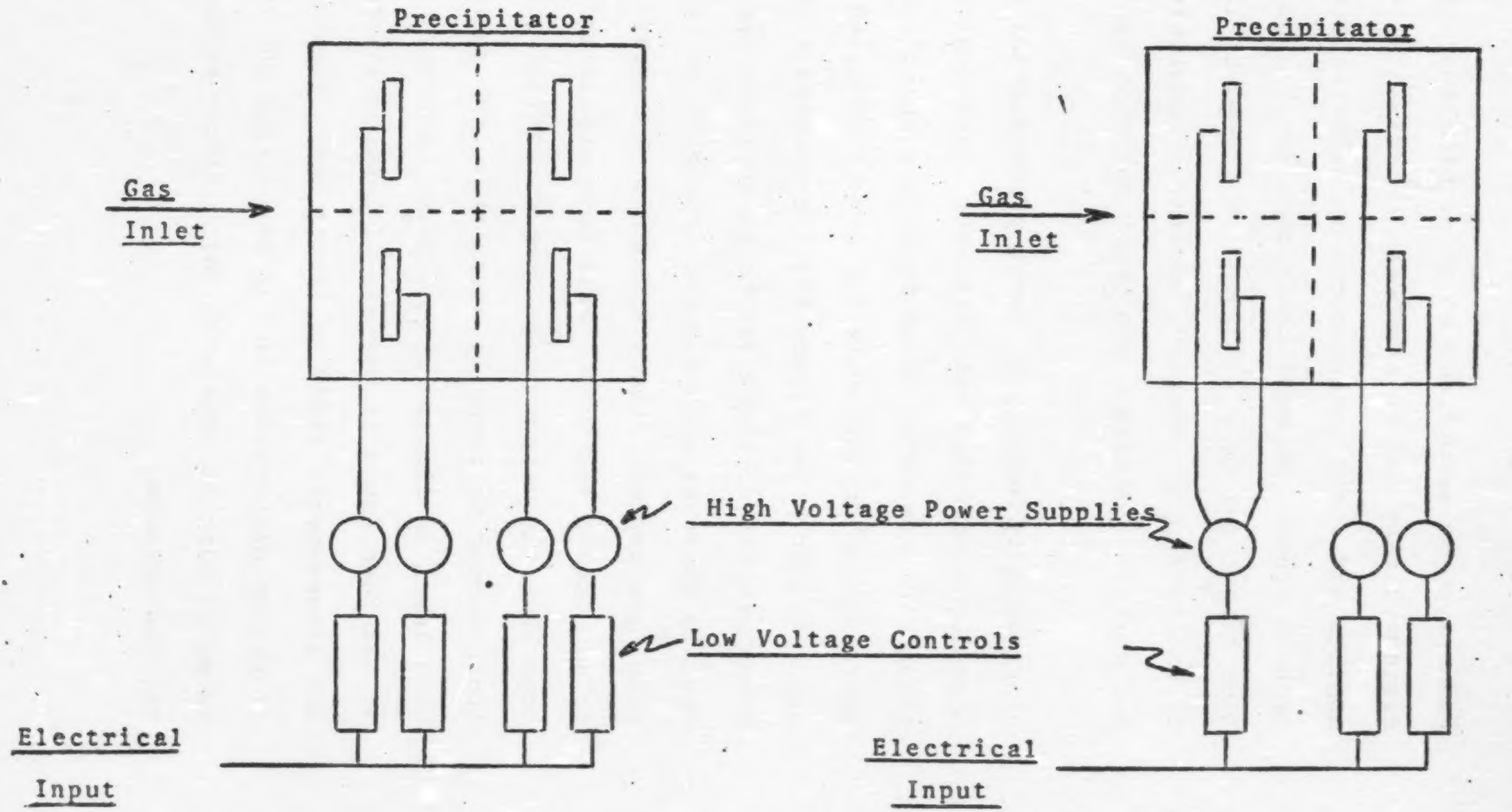
Precipitator
Gas
Inlet
High Voltage Power Supplies
Low Voltage Controls
Electrical
Input
Precipitator
Gas
Inlet
Electrical
Input

Figure 65(a)

All Sections Full-Wave

Figure 65(b)

Half-Wave Inlet Sections

Full-Wave Outlet Sections

During the present test program, all precipitator sections were energized full wave. Possible performance improvement might be achieved by more sectionalization, half wave or pulse energization. Additional testing is required to establish this.

VIII. RECOMMENDATIONS

Although the use of dry limestone injection into the boiler hot gases, as a means of significantly reducing sulfur oxide emissions, appears to be only a stop gap measure useful in existing power plant boilers, the deleterious affects on electrostatic precipitator performance are analogous to those experienced when burning low sulfur coals, particularly the sub-bituminous western coals. In view of this more general problem, it is recommended that further experimental work be performed.

1. The present test program has clearly shown the affect of corona input power density on the precipitation rate parameter. The most critical variable that determines corona power is the particulate resistivity. There are basically four ways of combating high resistivity, i.e. use of a large precipitator, use of some form of conditioning such as moisture, ammonia, sulfur trioxide, etc., control the flue gas temperature entering the precipitator, or change the voltage waveform of electrical energization and/or increase sectionalization. The first three have been the subject of numerous investigations, however, the latter, although known to be effective, has never been really investigated using a carefully planned experimental program. Accordingly, it is recommended that this be done using fullwave, half-

wave and pulse energization along with variations in sectionalization.

2. The fact that precipitator performance during the special low sulfur coal tests of this program was as good or better than when firing the higher sulfur coals points out the need for establishing additional means other than coal sulfur for predicting expected performance. Recent experimental work by the Bureau of Mines(14) has correlated the ratio of $\frac{MgO + CaO}{Na_2O + SO_3}$ in the ash to resistivity. Also, the Na_2O of the ash alone appears to be significant.

It is recommended that experimental work relating precipitator performance to coal ash and fly ash chemical constituents be performed.

3. Recent state particulate emission codes are establishing stack opacity as a means of determining compliance. Therefore, it is recommended that further work in quantifying an optical sensor, such as the Research-Cottrell instrument, be undertaken.

BIBLIOGRAPHY

(1) Tennessee Valley Authority, Results Report No. 54, "Electrostatic Flyash Collector Performance Test, Shawnee Steam Plant Unit 10", July 9 - August 6, 1969.

Tennessee Valley Authority, Results Report No. 62, "Electrostatic Flyash Collector Performance with Limestone Injection, Shawnee Steam Plant Unit 10", June 9 - July 15, 1970.

(2) Southern Research Institute, Final Report to EPA, Office of Air Programs, Contract CPA70-149, "A Study of Resistivity and Conditioning of Fly Ash", PP 84-96.

(3) Walker, A. B., "Effects of Desulfurization Dry Additives on the Design of Coal-Fired Boiler Particulate Emission Control Systems", paper presented at the 73rd Annual General Meeting of the CIM, Quebec City, April 1971.

(4) Attig, R. C. and Sedor, P., "Additive Injection for Sulfur Dioxide Control - A Pilot Plant Study", B&W Research Center Report 5960, PHS Contract No. 86-67-127.

(5) McLean, Kenneth J., "An Evaluation of the Kevatron Model 223 Electrostatic Precipitator Analyser", July, 1971.

(6) White, H. J. "Industrial Electrostatic Precipitation" Addison Wesley, 1963, LC No. 62-18240.

(7) Sproull, W. T., "Laboratory Performance of a Special Two-Stage Precipitator for Collecting High Resistivity Dust and Fume", American Chemical Society, New York, N. Y., September 1954.

(8) Busby, H. G. T., "Efficiency of Electrostatic Precipitators as Affected by the Properties and Combustion of Coal", Journal of the Institute of Fuel, May, 1963.

(9) Lowe, H. J., et al, "The Precipitation of Difficult Dusts", Institute of Electrical Engineers, Colloquium on Electrostatic Precipitators, February, 1965.

(10) Robinson, M. and Brown, R. F., Letter to the Editors, "Electrically Supported Liquid Columns in High-Pressure Electrostatic Precipitators", Atmospheric Environment, Volume 5, PP. 895-896, 1971.

(11) Southern Research Institute, "A Manual of Electrostatic Precipitator Technology, Part I - Fundementals and Part II - Application Areas", prepared for the NAPCA under Contract CPA-22-69-73, August 25, 1970.

(12) Shepard, J. C., "Field Resistivity Measurements at a Midwest Utility Burning Low Sulfur Coal" (unpublished Research-Cottrell, Inc. report, August, 1972).

(13) Pfoutz, B. D., "Precipitator Performance and Sulfur Emission from Pulverized Coal Fired Boilers with Dolomite Injection" (unpublished Research-Cottrell, Inc. report, June, 1967).

(14) Selle, S. J., Tufte, P. H., and Gronhovd, G. H., "A Study of the Electrical Resistivity of Fly Ashes From Low-Sulfur Western Coals Using Various Methods", Bureau of Mines, U.S. Department of the Interior, Grand Forks, N.D., Paper #72-107, 65th Annual Meeting APCA, Miami Beach, Florida, June, 1972.